Development and Demise of *Plasmodium* Liver Stage Parasites

The Hunt for a Genetically Attenuated Malaria Vaccine

Ivo Ploemen

Cover design: Pien de Meijer www.spiensel.nl
Printed by:
ISBN:

The research described in this thesis was performed within the framework of Top Institute Pharma (Netherlands) project T4-102 and T4-501.

Development and Demise of *Plasmodium* Liver Stage Parasites

The Hunt for a Genetically Attenuated Malaria Vaccine

Proefschrift

ter verkrijging van de graad doctor
aan de Radboud Universiteit Nijmegen
op gezag van de rector magnificus prof. mr. S.C.J.J Kortmann,
volgens besluit van college van decanen
in het openbaar te verdedigen op maandag 10 juni 2013
om 15:30 uur precies

door

Ivo Henri Johannes Ploemen

geboren op 2 Februari 1984
te Heerlen

Promotor:
Prof. dr. R. W. Sauerwein

Copromotor:
Dr. C. J. Janse (LUMC, Leiden)

Manuscriptcommissie:
Prof. dr. I.J.M de Vries (voorzitter)
Prof. dr. P. W. M. Hermans
Dr. C.H Kocken (BPRC, Rijswijk)

Contents

Chapter 1

General Introduction

Malaria

More than 40 percent of the world's population is at risk of exposure to malaria. An estimated 250-450 million clinical cases of malaria occur annually, resulting in a death toll of 655.000 to 1.200.000 [1,2]. Besides morbidity and mortality, the social and economic burden of malaria, specifically in underdeveloped countries, remains enormous [3]. Malaria forms one of the most dreadful global health problems.

Malaria is caused by the protozoan parasite of the genus *Plasmodia* which is transmitted to humans by the bite of infected *Anopheles* mosquitoes. There are five malaria species known to infect man: *P. falciparum*, *P. vivax*, *P. ovale*, *P. malariae* and *P. knowelsi* [4,5], all of which have a distinct global distribution and clinical outcome. *P. falciparum* is the most prevalent malaria species and is by far responsible for most of the malaria associated severe disease and mortality. Over 90% of malaria morbidity and mortality is restricted to Sub-Saharan Africa, where especially young children and pregnant women are most vulnerable [6].

Life Cycle

More than 200 *Plasmodium* species have been described, which can infect mammalian, avian and reptilian hosts [7]. Here we focus on *P. falciparum* for the human host and the murine *P. berghei* and *P. yoelii,* with particular emphasis on the sporozoite and liver stage. The following outline of the parasite's life cycle contains an in-depth description (mainly based on *P. berghei* studies) of the sporozoite and liver stage biology (depicted in Figure 1).

For its survival and procreation, the *Plasmodium* parasite is dependent on two hosts; the definitive host, which is the female *Anopheles* mosquito, and a mammalian host. *Plasmodium* parasites enter the mammalian body by the bite of an infected *Anopheles* mosquito. The mosquito probes the skin for a blood meal and either imbibes from a pool of blood generated by capillary damage or by directly cannulating from a subcutaneous blood vessel [8]. To prevent the blood from coagulating, saliva is deposited [9] containing up to a few hundred sporozoites. The sporozoites now start an active gliding locomotion of 4 μm/s leaving a trail of circum-sporozoite-protein (CSP) and enter the blood stream by breaking the endothelial barrier [10]. Alternatively, around 20% of the sporozoites enter a lymphatic vessel and are drained to a lymph node where most are internalized inside dendritic cells, and some can (partially) develop into exoerythrocytic forms [11]. Sporozoites that reach the blood

vessel rapidly travel to the liver. It is unknown how the sporozoites exactly select and recognize the liver as the preferred organ for further development. Possibly a family of liver specific highly sulfated heparan sulfate proteoclycans (HSPGs) play a role. In the liver the sporozoites glide alongside and adhere to the sinusodial epithelium before entering a Kupffer cell and crossing into the space of Disse [12]. Sporozoites can enter a host cell in two distinct ways. Firstly, they can disrupt the host cell membrane and migrate through the cells, a feature used by the sporozoite in the skin, the Kupffer cells and hepatocytes, leaving the latter in a state of necrosis [13,14,15]. Alternatively, the sporozoite can invade a hepatocyte by invagination of the host cell membrane forming a so called parasitophorous vacuole (PV). The HSPGs appear to play an essential role in guiding the sporozoite from its migration mode of cell entry into its invasion mode. It is unclear how sporozoites precisely switch mode. Proteins like P52 and P36 seem to be essential in host cell invasion and the formation of a PVM [16,17,18,19]. By forming the PV with a parasitophorous vacuole membrane (PVM), the sporozoite creates a homeostatic environment and shields itself from the interior of the hepatocyte. The proper formation and subsequent modification of the PV and PVM are considered essential for development and survival of the intrahepatic parasites [20]. At very low frequencies however, *Plasmodium* can develop in the nucleus of the hepatocyte, in the absence of an apparent PVM [21,22]. These parasites are thought to enter the cell through migration, and start nuclear replication following an arrest inside the hepatocyte nucleus, thereby using the nuclear envelope as a surrogate for the PVM. Nonetheless, contrary to the parasites residing in the cytosol, these intranuclear parasites seem unable to fully develop into blood stage parasites [22].

Besides an extensive manipulation of the hepatocyte, allowing for parasite growth and an uptake of host nutrients, the invaded sporozoite prohibits the infected hepatocyte to undergo a programmed cell death [12]. The invaded sporozoite undergoes nuclear replication and in a period of days (e.g 48-52 hours for *P. berghei* and 5-7 days for *P. falciparum)* the sporozoites fully develop into mature liver schizonts. These mature liver schizonts contain tens of thousands of infectious merozoites, which are released into the bloodstream as merosomes, each containing 100-200 merozoites [23]. Merosomes bud from the infected hepatocyte, exit the liver, survive the subsequent passage through the right heart and accumulate in the lungs. Here the merosomes burst in the pulmonary capillaries with the subsequent liberation of merozoites into the bloodstream. These merozoites now invade erythrocytes thereby entering the blood stage of the *Plasmodium* life cycle.

In the blood stage, parasites rapidly multiply and invade new erythrocytes. A small proportion of the blood stage parasites undergoes sexual differentiation and matures into male or female gametocytes. These gametocytes may be taken up in the blood meal of a new mosquito, where in the female mosquito midgut male and female gamets fuse to form an ookinete.

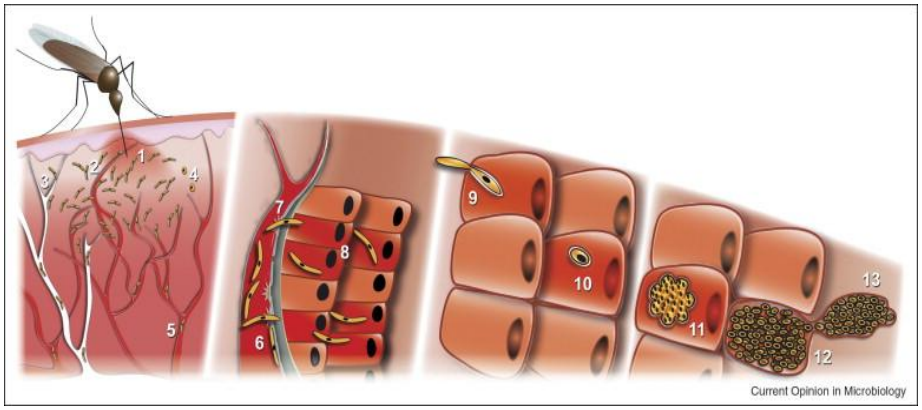

Figure 1: *Plasmodium* sporozoite and liver stage biology.
Sporozoites are injected by a female Anopheles mosquito (1). They start migrating through the dermis (2) and enter the blood capillary (2), the lymphatic system (3), or they start (incomplete) development in the skin (4). Once inside the blood vessel, sporozoites are rapidly distributed through the blood circulation (5). In the liver, sporozoites adhere to the endothelial cells (6) and cross the sinusoidal barrier by transmigrating through Kupffer cells (7). The parasites now actively traverse through a number of hepatocytes (8), before invading a final hepatocyte by the formation of a PV (9). Inside the PV, sporozoites rapidly transform into round early liver stages (10). Intrahepatic parasites commence cell division resulting in merozoite formation in a process called schizogony (11). Infectious merozoites are released as membrane-shielded merosomes (12), which are transported away (13) and eventually rupture in the lung microvasculature. (Reprinted from [49] with permission of Elsevier)

After invasion of the midgut wall these ookinetes form oocyst. Inside the oocyst, sporozoites are formed and when the oocyst bursts after a number of days, the sporozoites migrate through the hemacoel to the salivary glands. The infectious sporozoites can re-infect another host after the mosquito takes a blood meal thereby completing the *Plasmodium* life cycle.

The fight against malaria: Rationale for a pre-erythrocytic malaria vaccine

There are many ways in which malaria and its disease burden can be combated.

Vector control is a primary intervention for the reduction of malaria transmission. While impregnated bednets and indoor spraying are effective there is an increasing resistance of mosquitoes to insecticides, particularly in Africa [2]. Resistance has also been observed to the currently available anti-malarial drugs [24], and at present new drugs in advanced stages of development are scarce [24]. An effective malaria vaccine is needed to support malaria control and eradication.

In this thesis we focus on the development of a pre-erythrocytic malaria vaccine, effective against the parasite's sporozoite and liver stage. Vaccines directed against the parasite's liver stage might have some theoretical advantages over vaccines directed against the pathogenic erythrocytic stage. Firstly, in the liver stage the number of parasites and infected host cells is low compared to erythrocytic stages. Moreover, the liver stage is clinically silent and as such, provides a relatively large time window for an effective immune response against the parasites [25,26]. Vaccines directed against the erythrocytic stage have a much shorter time window to act. Finally, antigenic polymorphisms might be limited during the liver stage [26,27].

To date, the most advanced vaccine candidate is a subunit vaccine based on the immunogenicity of the sporozoite and early liver stage CSP, GlaxosmithKline's RTS,S. It is currently in phase III clinical development and has shown 30-50% clinical protection in a number of clinical trials [28,29,30]. While promising, a pre-erythrocytic vaccine with a (much) higher protective efficacy would be preferred. The Malaria Vaccine Technology Roadmap has set ambitious goals, aiming to develop and license a malaria vaccine with more than 80% protective efficacy against clinical disease that lasts longer than four years, by the year 2025 [31].

Attenuated sporozoites: a promising vaccine approach.

The identification of CSP as potential vaccine candidate followed the observation by Ruth Nussenzweig over 40 years ago, that immunization of mice with live irradiated sporozoites resulted in protection from a sporozoite challenge [32,33]. This whole organism vaccine approach with irradiated sporozoites, from now on referred to as Radiation Attenuated Sporozoites (RAS), held promise and the bite of human volunteers by 1000 *P. falciparum* infected, irradiated *Anopheles stephensi* mosquitoes protected from subsequent challenge [34]. The >80 % protection achieved in these human volunteers was much higher than the 30-50 % protection achieved by immunization with RTS,S and can potentially meet the goals set by The Malaria

Vaccine Technology Roadmap [32].

While promising, several issues have been raised with respect to the safety of RAS immunization. First under-radiated sporozoites are able to complete liver stage development and cause a blood-stage parasitemia. Second, over-radiation inactivates sporozoites by limiting the efficiency to invade hepatocytes and transform into liver stage parasites, resulting in poor protection against malaria [35]. Based on the success of RAS immunizations, several distinct whole sporozoite vaccine approaches have been pursued. Using the DNA sequence-specific alkylating agent centamycin, sporozoites were chemically attenuated (CAS) which were then used to efficaciously immunize mice [36,37]. However, much like for RAS a major theoretical disadvantage of this immunization protocol is formed by the need for a correct dose of centamycin to obtain adequate attenuation. Another sporozoite vaccine approach consists of the inoculation of life sporozoites concomitantly with the anti-malarial drug chloroquine (CQ). Chloroquine is a potent malaria schizonticide that efficiently eliminates erythrocytic parasites. Immunization of mice with sporozoites under chemoprofylactic coverage (CPS) protects against a subsequent sporozoite challenge [38,39]. More importantly, in men, CPS immunization leads to protection in more than 90% of the volunteers [40] for a period of up to 28 months [41]. Despite this unambiguous success, it might be difficult to translate the CPS approach to the field. Following CPS immunization, blood stage parasites are formed and the clearance of these parasites is reliant on the effect of chloroquine. The absence of the onset of a pathogenic blood stage infection is therefore dependant on the (pharmacokinetic) uptake and metabolism of chloroquine presenting obvious potential safety risks.

An immunization approach that does not rely on the external attenuation of sporozoites or the metabolic killing of parasites is the Genetically Attenuated Parasite (GAP) approach. Through targeted deletion of genes or a combination of genes, live sporozoites are made to arrest in the liver. These parasites form a homogenous mutant population and are therefore not troubled with the restrictions of RAS, CAS and CPS.

Genetically attenuated parasites

The GAP approach started with the nearly simultaneous observation by independent laboratories that mutant parasites, deleted of a specific gene, arrested specifically in the liver stage [17,42]. A number of GAP with distinct gene deletions have been

described which, following immunization protected mice against challenge. Most GAP, including *Δp52, Δp36, Δuis3* and *Δuis4* mutant parasites arrest at early liver stage and are likely involved in the formation or maintenance of the PVM [17,42,43]. Other gene deletion mutants like *P. berghei Δslarp*, and its *P. yoelii* orthologue *Δsap1* are involved in the (post-)transcriptional regulation of sporozoites and early liver stages [44,45,46]. The *Δfabb/f* parasite arrests in late liver stage, due to a defect in the type II fatty acid synthesis pathway [47].

Despite the apparent abundance of GAP vaccine candidates it has been difficult to directly translate findings in mice and generate a safe and protective GAP in *P. falciparum*. For instance, unequivocal orthologs for the two rodent *uis*-genes are absent in the *P. falciparum* genome (www.PlasmoDB.org). Moreover, the developmental arrest of *Δp52* and the *Δp36* parasites was incomplete and low numbers of parasites maturated in the liver, resulting in a blood stage infection in mice [17,18].

Requisites for an effective and safe GAP vaccine

Ultimately, immunization with GAP has to be safe and lead to protection against challenge. Moreover, sporozoites have to be administered in a manner suitable for human immunization (e.g not by mosquito bite or by intravenous injection). These criteria are schematically visualized in Figure 2.

The first challenge will be to generate a safe GAP candidate (Figure 2, Challenge I). Some (murine) GAPs, like *Δp52* partially develop into infectious merozoites in the liver and cause a blood stage infection. While GAPs based on the deletion of one individual gene, might not be fully safe (i.e lead to breakthrough blood stage infection), a GAP consisting of multiple gene deletions might be. At present, only the *Δslarp/Δsap1* mutant parasites completely arrest in the liver of murine *P. berghei* and *P. yoelii* and a clear orthologue of the gene is present in *P. falciparum*. The *Δslarp* GAP is therefore a potential safe candidate for a GAP vaccine. However, there is controversy over the protective efficacy of these *Δslarp/Δsap1* parasites upon immunization [44,45,46]. Immunization of mice with *P. berghei Δslarp* did not confer sterile long lasting protection, contrary to immunization with *P. yoelii Δsap1*. In order to find a GAP that completely arrests in the liver stage and following immunization, confers long-lasting protection, one can i) combine known GAP candidates to one multiple attenuated GAP or ii) pursue new GAP candidates.

Here, we pursue new GAP candidates by selecting genes based on their high protein expression profiles in the sporozoite stage. Supposedly, these genes have a function in the (early) liver stage. The high efficiency of the transfection technology in the *P. berghei* model allows for a fast screening of potential GAP candidates. Once protective efficacy and GAP safety have been assessed in the *P. berghei* model a *P. falciparum* GAP consisting of the orthologue gene deletions can subsequently be generated.

The effective delivery of GAP sporozoites for human immunization forms a next great obstacle in the clinial development of a GAP vaccine. Firstly, immunization with dead sporozoites is ineffective and has to be performed with live sporozoites that can be preserved (Figure 2, Challenge II). In fact, for long the production of any whole sporozoite vaccine was not considered feasible based on mainly logistic reasons. It requires a standardized isolation, purification and (cryo-)preservation of parasites from mosquito salivary glands [50]. Specifically Sanaria Inc. (http://www.sanaria.com), a company devoted to the generation of a whole sporozoite vaccine, has taken a lead and made much progress in tackling the problems associated with the production and the cryopreservation of a sporozoite vaccine [48]. Secondly, irrespective of the whole sporozoite vaccine approach (e.g CPS, RAS or GAP), live sporozoites need to be effectively administered by needle and syringe (Figure 2, Challenge III). While the immunization of mice with life sporozoites have thus far almost exclusively been performed by intravenous injection, nearly all human immunizations have been performed by infected mosquito bite. Intravenous injection of sporozoites and immunization by infectious mosquito bite are not preferred/feasible for immunization of large groups of people in Sub-Saharan Africa. Besides the generation of a safe and protective GAP it is therefore crucial to understand and optimize the route of sporozoite administration for further clinical vaccine development.

It is essential to have the correct tools so that both the safety of GAP candidates (i.e absence of development into blood stage) and the fate of sporozoites subsequent to injection can be assessed. At the start of this thesis, a quantitative analysis of the liver stage of *Plasmodium* parasites was hampered by time consuming techniques like qRT-PCR and RNA hybridization or microscopy, which is often prone to a large variation between observers . Low levels of parasite liver infection *in vivo* in laboratory animals and *in vitro* in cultured hepatocytes further complicated the quantification.

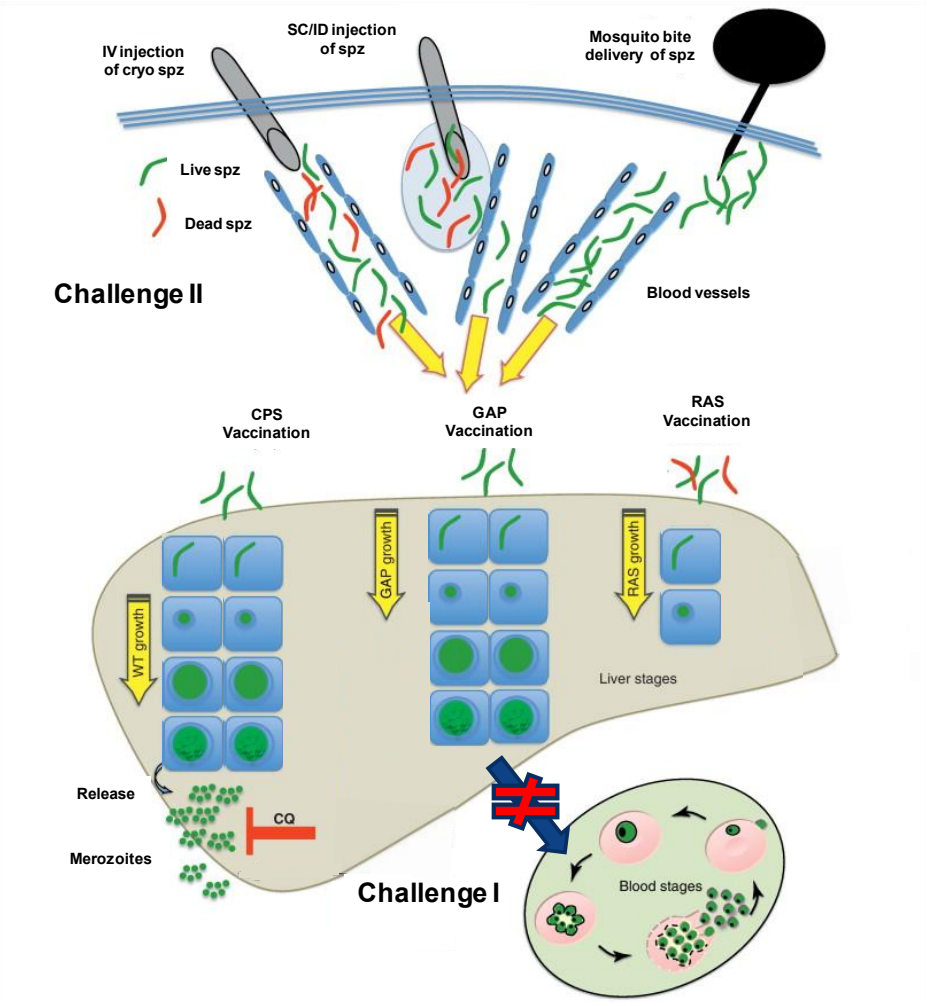

Figure 2: Challenges of whole sporozoite vaccination.
Schematic of challenges that need to be overcome for the generation of a whole sporozoite malaria vaccine. GAP parasites have to be safe, indicating that they must fully arrest in the liver stage and not develop into the pathogenic blood stage **(Challenge I)**. Secondly, the sporozoites need to be purified and cryopreserved so that they can be administered by needle and syringe **(Challenge II)**. A large percentage of the sporozoites might not be viable after cryopreservation. A third challenge **(Challenge III)** will be to administer the sporozoites by needle and syringe so that the sporozoites enter the circulation. Irrespective of the whole sporozoite vaccine approach (e.g CPS, RAS or GAP) parasites will need to be cryopreserved and administered by needle and syringe. (Adapted from [50] with permission of Elsevier).

Aims

At the outset, this thesis aims to develop the tools for the simple and sensitive quantification of liver stage parasites in a murine model. These tools are instrumental in the quest for a GAP vaccine approach that meets the requisites for further clinical development.

The first objective is to develop and characterize a GAP that fully arrests in the liver stage and induces long-lived protection in the murine *P. berghei* model. The quantification of liver stage parasites will be a practical tool in the assessment of murine GAP safety. Once safe and fully protective, a *P. falciparum* GAP consisting of the orthologue gene deletions can be considered to serve as a pre-erythrocytic malaria vaccine candidate in humans.

The second objective is to decipher the role of the route of sporozoite immunization (e.g intravenous or intradermal) on the protective outcome. We further aim to optimize the administration of sporozoites in a *P. berghei* model to improve the levels of conferred protection. These results can possibly be used to advance the current knowledge of the efficient administration of sporozoites, essential for further clinical vaccine development of an attenuated *P. falciparum* sporozoite vaccine.

Thesis outline

The work described in this thesis can be grouped into three sections.

Section 1. Characterization and evaluation of luciferase expressing parasites in the *P. berghei* liver stage.

In this section we characterize and evaluate the use of luciferase expressing parasites for the real-time *in vivo* and *in vitro* imaging of parasite liver load. In **Chapter 2** we report the use of a transgenic *P. berghei* parasite, *Pb*GFP-Luc$_{con}$, expressing the bioluminescent reporter protein luciferase to visualize and quantify parasite development in liver cells both in culture and in live mice using real-time luminescence imaging. In **Chapter 3** we describe the use of these *Pb*GFP-Luc$_{con}$ parasites for the evaluation of immunity against malaria.

Section 2. Assessment of GAP attenuation and protective efficacy.

In this section we explore different GAP vaccine candidates for their level of attenuation and protective efficacy. For this, we use the luminescent *P. berghei* parasites characterized in section 1. **Chapter 4** describes the lack of complete

attenuation of two leading GAP, *Δp52+p36* and *Δfabb/f* parasites. In **Chapter 5** we study the phenotype of developing intrahepatic *Δp52+p36 P. berghei* parasites and describe a non-conventional pathway, by which these parasites are capable of maturing into asexual parasites. **Chapter 6** describes the generation and characterization of a new GAP vaccine candidate, *Δb9*. Moreover, it reports on the safety and the protective efficacy of a multiple attenuated GAP, *Δb9Δslarp*.

Section 3. Inoculation of whole sporozoites.

In this section we focus on the route of sporozoite inoculation and its effect on protective efficacy. These studies are important in the light of a potential future human whole sporozoite vaccine. In **Chapter 7** we study the protective efficacy of intradermal (ID) and intravenous (IV) RAS and CPS sporozoite immunization and its relation to the parasite liver load following either route. Moreover we assess both the humoral and cellular immune responses in ID and IV immunized mice. In **Chapter 8** we explore alternative routes of sporozoite administration to increase efficiency of liver infection. By a stepwise selection process we study the effects of route of administration, number of injections and location and volume of sporozoite injection on subsequent parasite liver load.

In conclusion, we will summarize and discuss the data from the above sections in **Chapter 9**.

References

1. Murray CJ, Rosenfeld LC, Lim SS, Andrews KG, Foreman KJ, et al. (2012) Global malaria mortality between 1980 and 2010: a systematic analysis. Lancet 379: 413-431.
2. WHO (2011) World Malaria Report. (http://www.who.int/malaria/world_malaria_report_2011/9789241564403_eng.pdf)
3. Sachs J, Malaney P (2002) The economic and social burden of malaria. Nature 415: 680-685.
4. Cox-Singh J, Davis TM, Lee KS, Shamsul SS, Matusop A, et al. (2008) Plasmodium knowlesi malaria in humans is widely distributed and potentially life threatening. Clin Infect Dis 46: 165-171.
5. Baird JK (2009) Malaria zoonoses. Travel Med Infect Dis 7: 269-277.
6. Breman JG, Alilio MS, Mills A (2004) Conquering the intolerable burden of malaria: what's new, what's needed: a summary. Am J Trop Med Hyg 71: 1-15.
7. Perkins SL, Austin CC (2009) Four new species of Plasmodium from New Guinea lizards: integrating morphology and molecules. J Parasitol 95: 424-433.
8. Frevert U (2004) Sneaking in through the back entrance: the biology of malaria liver stages. Trends Parasitol 20: 417-424.
9. Beier JC (1998) Malaria parasite development in mosquitoes. Annu Rev Entomol 43: 519-543.
10. Amino R, Thiberge S, Blazquez S, Baldacci P, Renaud O, et al. (2007) Imaging malaria sporozoites in the dermis of the mammalian host. Nat Protoc 2: 1705-1712.
11. Amino R, Thiberge S, Martin B, Celli S, Shorte S, et al. (2006) Quantitative imaging of Plasmodium

transmission from mosquito to mammal. Nat Med 12: 220-224.
12. Vaughan AM, Aly AS, Kappe SH (2008) Malaria parasite pre-erythrocytic stage infection: gliding and hiding. Cell Host Microbe 4: 209-218.
13. Amino R, Giovannini D, Thiberge S, Gueirard P, Boisson B, et al. (2008) Host cell traversal is important for progression of the malaria parasite through the dermis to the liver. Cell Host Microbe 3: 88-96.
14. Frevert U, Engelmann S, Zougbede S, Stange J, Ng B, et al. (2005) Intravital observation of Plasmodium berghei sporozoite infection of the liver. PLoS Biol 3: e192.
15. Mota MM, Pradel G, Vanderberg JP, Hafalla JC, Frevert U, et al. (2001) Migration of Plasmodium sporozoites through cells before infection. Science 291: 141-144.
16. Ishino T, Chinzei Y, Yuda M (2005) Two proteins with 6-cys motifs are required for malarial parasites to commit to infection of the hepatocyte. Mol Microbiol 58: 1264-1275.
17. van Dijk MR, Douradinha B, Franke-Fayard B, Heussler V, van Dooren MW, et al. (2005) Genetically attenuated, P36p-deficient malarial sporozoites induce protective immunity and apoptosis of infected liver cells. Proc Natl Acad Sci U S A 102: 12194-12199.
18. Labaied M, Harupa A, Dumpit RF, Coppens I, Mikolajczak SA, et al. (2007) Plasmodium yoelii sporozoites with simultaneous deletion of P52 and P36 are completely attenuated and confer sterile immunity against infection. Infect Immun 75: 3758-3768.
19. VanBuskirk KM, O'Neill MT, De La Vega P, Maier AG, Krzych U, et al. (2009) Preerythrocytic, live-attenuated Plasmodium falciparum vaccine candidates by design. Proc Natl Acad Sci U S A 106: 13004-13009.
20. Vera IM, Beatty WL, Sinnis P, Kim K (2011) Plasmodium protease ROM1 is important for proper formation of the parasitophorous vacuole. PLoS Pathog 7: e1002197.
21. Meis JF, Hollingdale MR, Verhave JP, Aikawa M (1984) Intranuclear localization of Plasmodium berghei sporozoites. Cell Biol Int Rep 8: 1016.
22. Silvie O, Greco C, Franetich JF, Dubart-Kupperschmitt A, Hannoun L, et al. (2006) Expression of human CD81 differently affects host cell susceptibility to malaria sporozoites depending on the Plasmodium species. Cell Microbiol 8: 1134-1146.
23. WHO (2011) Guidelines for the treatment of malaria.
24. Mendis K, Rietveld A, Warsame M, Bosman A, Greenwood B, et al. (2009) From malaria control to eradication: The WHO perspective. Trop Med Int Health 14: 802-809.
25. Crompton PD, Pierce SK, Miller LH (2010) Advances and challenges in malaria vaccine development. J Clin Invest 120: 4168-4178.
26. Vaughan AM, Wang R, Kappe SH (2010) Genetically engineered, attenuated whole-cell vaccine approaches for malaria. Hum Vaccin 6: 107-113.
27. Takala SL, Plowe CV (2009) Genetic diversity and malaria vaccine design, testing and efficacy: preventing and overcoming 'vaccine resistant malaria'. Parasite Immunol 31: 560-573.
28. Sacarlal J, Aide P, Aponte JJ, Renom M, Leach A, et al. (2009) Long-term safety and efficacy of the RTS,S/AS02A malaria vaccine in Mozambican children. J Infect Dis 200: 329-336.
29. Bejon P, Lusingu J, Olotu A, Leach A, Lievens M, et al. (2008) Efficacy of RTS,S/AS01E vaccine against malaria in children 5 to 17 months of age. N Engl J Med 359: 2521-2532.
30. Agnandji ST, Lell B, Soulanoudjingar SS, Fernandes JF, Abossolo BP, et al. (2011) First results of phase 3 trial of RTS,S/AS01 malaria vaccine in African children. N Engl J Med 365: 1863-1875.
31. (2006) Malaria Vaccine Technology Roadmap
32. Nussenzweig RS, Vanderberg J, Most H, Orton C (1967) Protective immunity produced by the injection of x-irradiated sporozoites of plasmodium berghei. Nature 216: 160-162.
33. Nussenzweig V, Nussenzweig RS (1986) Development of a sporozoite malaria vaccine. Am J Trop Med Hyg 35: 678-688.
34. Hoffman SL, Goh LM, Luke TC, Schneider I, Le TP, et al. (2002) Protection of humans against malaria by immunization with radiation-attenuated Plasmodium falciparum sporozoites. J Infect Dis 185: 1155-1164.
35. Silvie O, Semblat JP, Franetich JF, Hannoun L, Eling W, et al. (2002) Effects of irradiation on Plasmodium falciparum sporozoite hepatic development: implications for the design of pre-erythrocytic malaria vaccines. Parasite Immunol 24: 221-223.
36. Purcell LA, Yanow SK, Lee M, Spithill TW, Rodriguez A (2008) Chemical attenuation of Plasmodium berghei sporozoites induces sterile immunity in mice. Infect Immun 76: 1193-1199.

37. Purcell LA, Wong KA, Yanow SK, Lee M, Spithill TW, et al. (2008) Chemically attenuated Plasmodium sporozoites induce specific immune responses, sterile immunity and cross-protection against heterologous challenge. Vaccine 26: 4880-4884.
38. Belnoue E, Costa FT, Frankenberg T, Vigario AM, Voza T, et al. (2004) Protective T cell immunity against malaria liver stage after vaccination with live sporozoites under chloroquine treatment. J Immunol 172: 2487-2495.
39. Belnoue E, Voza T, Costa FT, Gruner AC, Mauduit M, et al. (2008) Vaccination with live Plasmodium yoelii blood stage parasites under chloroquine cover induces cross-stage immunity against malaria liver stage. J Immunol 181: 8552-8558.
40. Roestenberg M, McCall M, Hopman J, Wiersma J, Luty AJ, et al. (2009) Protection against a malaria challenge by sporozoite inoculation. N Engl J Med 361: 468-477.
41. Roestenberg M, Teirlinck AC, McCall MB, Teelen K, Makamdop KN, et al. (2011) Long-term protection against malaria after experimental sporozoite inoculation: an open-label follow-up study. Lancet 377: 1770-1776.
42. Mueller AK, Labaied M, Kappe SH, Matuschewski K (2005) Genetically modified Plasmodium parasites as a protective experimental malaria vaccine. Nature 433: 164-167.
43. Mueller AK, Camargo N, Kaiser K, Andorfer C, Frevert U, et al. (2005) Plasmodium liver stage developmental arrest by depletion of a protein at the parasite-host interface. Proc Natl Acad Sci U S A 102: 3022-3027.
44. Silvie O, Goetz K, Matuschewski K (2008) A sporozoite asparagine-rich protein controls initiation of Plasmodium liver stage development. PLoS Pathog 4: e1000086.
45. Aly AS, Mikolajczak SA, Rivera HS, Camargo N, Jacobs-Lorena V, et al. (2008) Targeted deletion of SAP1 abolishes the expression of infectivity factors necessary for successful malaria parasite liver infection. Mol Microbiol 69: 152-163.
46. Aly AS, Lindner SE, MacKellar DC, Peng X, Kappe SH (2011) SAP1 is a critical post-transcriptional regulator of infectivity in malaria parasite sporozoite stages. Mol Microbiol 79: 929-939.
47. Vaughan AM, O'Neill MT, Tarun AS, Camargo N, Phuong TM, et al. (2009) Type II fatty acid synthesis is essential only for malaria parasite late liver stage development. Cell Microbiol 11: 506-520.
48. Hoffman SL, Billingsley PF, James E, Richman A, Loyevsky M, et al. (2010) Development of a metabolically active, non-replicating sporozoite vaccine to prevent Plasmodium falciparum malaria. Hum Vaccin 6: 97-106.
49. Silvie O, Mota MM, Matuschewski K, Prudencio M (2008) Interactions of the malaria parasite and its mammalian host. Curr Opin Microbiol 11: 352-359.
50. Butler NS, Vaughan AM, Harty JT, Kappe SH (2012) Whole parasite vaccination approaches for prevention of malaria infection. Trends Immunol.

Chapter 2

Visualisation and quantitative analysis of the rodent malaria liver stage by real time imaging.

Ivo Ploemen*, Miguel Prudêncio*, Bruno Douradinha, Jai Ramesa, Jannik Fonager, Geert-Jan van Gemert, Adrian Luty, Cornelus Hermsen, Robert Sauerwein, Fernanda Baptista, Maria Mota, Andrew Waters, Ivo Que, Clemens Lowik, Shahid Khan, Chris Janse, Blandine Franke-Fayard

**these authors contributed equally*

PLoS ONE. 2009 Nov 18;4(11):e7881

Abstract

The quantitative analysis of *Plasmodium* development in the liver in laboratory animals in cultured cells is hampered by low parasite infection rates and the complicated methods required to monitor intracellular development. As a consequence, this important phase of the parasite's life cycle has been poorly studied compared to blood stages, for example in screening anti-malarial drugs. Here we report the use of a transgenic *P. berghei* parasite, *Pb*GFP-Luc$_{con}$, expressing the bioluminescent reporter protein luciferase to visualize and quantify parasite development in liver cells both in culture and in live mice using real-time luminescence imaging. The reporter-parasite based quantification in cultured hepatocytes by real-time imaging or using a microplate reader correlates very well with established quantitative RT-PCR methods. For the first time the liver stage of *Plasmodium* is visualized in whole bodies of live mice and we were able to discriminate as few as 1–5 infected hepatocytes per liver in mice using 2D-imaging and to identify individual infected hepatocytes by 3D-imaging. The analysis of liver infections by whole body imaging shows a good correlation with quantitative RT-PCR analysis of extracted livers. The luminescence-based analysis of the effects of various drugs on *in vitro* hepatocyte infection shows that this method can effectively be used for *in vitro* screening of compounds targeting *Plasmodium* liver stages. Furthermore, by analysing the effect of primaquine and tafenoquine *in vivo* we demonstrate the applicability of real-time imaging to assess parasite drug sensitivity in the liver. The simplicity and speed of quantitative analysis of liver stage development by real-time imaging compared to the PCR methodologies, as well as the possibility to analyse liver development in live mice without surgery, opens up new possibilities for research on *Plasmodium* liver infections and for validating the effect of drugs and vaccines on the liver stage of *Plasmodium*.

Introduction

Malaria remains a major cause of global morbidity and mortality. New anti-malarial drugs are urgently needed, especially with the increase in drug resistant parasites and the lack of effective vaccines and vector control measures [1–4]. The main site for intracellular development of human and rodent *Plasmodium* sporozoites after they are injected by an infected mosquito is the liver. This stage of the parasite's development is clinically silent and therefore regarded as an ideal point of intervention for prophylactic or vaccine strategies [5–7]. The liver stage of *Plasmodium*'s life cycle has also received particular attention in the context of *P. vivax*, the second most important agent of human malaria, which can generate cryptic forms called hypnozoites that persist in the liver for long periods of time [8–10]. These dormant forms of the parasite are responsible for what is termed relapsing malaria, which may occur following latent periods of months or even years without new infection [10-11]. In comparison with drugs that kill blood stage parasites, only a limited number of drugs exist that act on liver stages; most notable amongst these are primaquine, atovaquone and tafenoquine [12-13], and only primaquine [14-15] has been shown to act on the hypnozoite stage of *P. vivax* [14-15]. Clearly, the development of new inhibitors/drugs against the malaria liver stage would target an important and under-exploited site of intervention [1,16].

Quantitative analysis of liver stage *Plasmodium* development both *in vivo* in laboratory rodents and *in vitro* in cultured liver cells is hampered by the low levels of parasite infection and by the complicated methods required to monitor parasite development. As a consequence, the development of novel and efficient methods for analysing/screening the effect of drugs and small molecule inhibitors on the parasite's intracellular growth in the liver lags well behind the more rapid developments being made in the automated drug/inhibitor screening assays for blood stage parasites [17–20]. Currently, one of the standard ways to assess drug efficacy against liver stages is to monitor *in vitro* liver stage development by quantitative RT-PCR (qRT-PCR) methods [21-25] that are time consuming and expensive. Other studies have involved direct quantification and viability of parasite development by microscopy [26,27], RNA hybridization [28], or infrared fluorescence scanning system However, these methods are not only prone to large variations between observers but are also time consuming given the very low infection rates (generally less than 2%) observed in cultured hepatocytes [29]. Moreover, simple and efficient methods for analysing *in vivo* liver stage development in small laboratory animals are completely absent. The

recent generation of new transgenic rodent malaria parasites expressing fluorescent reporter proteins has enabled an intimate analysis of *Plasmodium* sporozoites interacting with host hepatocytes during invasion and subsequent development inside hepatocytes, both *in vitro* and *in vivo* [30-34]. Recently, GFP-expressing parasites have been used in conjunction with flow cytometry to provide quantitative information on the parasites development in hepatic cells [35]. However, the use of fluorescent parasites in *in vivo* analysis of *Plasmodium* liver stage development requires complex surgery and when such parasites are used in conjunction with flow cytometry, their usefulness is presently restricted to *in vitr*o and *ex vivo* analyses.

We have previously reported the use of transgenic *P. berghei* parasites expressing the bioluminescent reporter protein, luciferase, to examine the distribution and development of sequestering blood stage parasites in live animals using real-time imaging [36-37]. Recently, we have also shown the effectiveness of such bioluminescent reporter parasites in simple and sensitive microplate reader assays for screening of drugs against blood stage parasites both *in vitro* and *in vivo* in rodents [19]. For these assays we generated a transgenic *P. berghei* parasite line that expresses a luciferase-GFP fusion protein and is free of a drug-selectable-marker [38]. In the study described here, we utilised the luminescent properties of this reporter parasite, *Pb*GFP-Luc$_{con}$, to analyse liver stage development by real-time imaging both in cultured hepatocytes and within the liver of living mice. We established that the changes in bioluminescence are directly proportional to the level of hepatocyte infection *in vitro* and *in vivo*, determined by comparison with standard qRT-PCR methodologies. As the liver parasite infection progresses real-time *in vivo* imaging allows the identification of individual infected hepatocytes in living animals. We demonstrated the application of the technique for the *in vitro* screening of compounds targeting the liver stage and the use of real-time imaging to determine *in vivo* drug sensitivity of liver stages through analysis of the effect of primaquine. Importantly, bioluminescence imaging also allows the course of an infection to be monitored, both throughout liver stage parasite development and in the blood stage of infection without sacrificing the animal, and therefore, can greatly reduce the number of experimental animals required to determine drug sensitivity. Since bioluminescence imaging is relatively simple to execute, the use of the methodologies described in this paper will greatly simplify the analysis of drug toxicity and small molecule inhibition on liver stage parasite growth.

Material and Methods

Experimental animals

Female C57BL/6 and Swiss CD1 mice, 6–8 weeks old (Charles River), weighing 20 to 35 g at the time of primary infection and female Wistar rats (Harlan; 175–200 g) were used. All studies in which animals were involved have been performed according to the regulations of the Dutch "Animal On Experimentation act" and the European guidelines 86/609/EEG.

Transgenic parasite line

The transgenic *P. berghei* line 676m1cl1 line (*Pb*GFP-Luc$_{con}$) has been used in this study (mutant RMgm-29 in www.pberghei.eu). It expresses a fusion GFP (mutant 3) and firefly luciferase (LucIAV) and has been generated in the reference clone of ANKA strain cl15cy1 [38]. Parasites of line 676m1cl1 contain the *Pb*GFP-Luc gene fusion stably integrated as a single copy gene by double cross over recombination into the 230p locus and the reporter gene is under control of the constitutive eef1α promoter [39]. This line has been selected by FACS-sorting of GFP-expressing parasites and therefore does not contain a drug-selectable marker. This line can be obtained from the Malaria Research and Reference Reagent Resource Center, MR4 (www.malaria.mr4.org).

Collection of sporozoites

Anopheles stephensi mosquitoes were infected by feeding on infected mice using standard methods of mosquito infection. On day 21–28 after infection, the salivary glands of the mosquitoes were collected by hand-dissection. Salivary glands were collected in DMEM (Dulbecco's Modified Eagle Medium from GIBCO) and homogenized in a home-made glass grinder. The free sporozoites were counted in a Bürker-Türk counting chamber using phase-contrast microscopy.

Sporozoites traversal and gliding

Traversal assays were performed as described previously [40]. Briefly, Huh7 cells were plated in 24 well plates (10^4 cells/ml) and an equivalent number of sporozoites was added to the wells with the addition of FITC labeled dextran (Invitrogen, NL). No sporozoites were added to the negative control wells that were used as threshold for the FACS analysis. FACS analysis was performed on 25 000 cells per well (wells were prepared in triplicate) using a FACScalibur flowcytometer (Becton Dickinson, NL).

Gliding assays were performed in precoated (3D11, 10 ug/ml) Labtek slides (Nunc, NL) and 2×10^4 sporozoites were added. After 30 minutes of incubation at 37°C sporozoites were fixed with 4% PFA and after washing with PBS, the sporozoites and the trails ('gliding circles') were stained with 3D11-Alexa 488 conjugated antibody (Dylight 488 antibody labelling kit; Thermo Scientific, NL). Slides were mounted with Fluoromount-G (SouthernBiotech, NL) and 'gliding circles' were analyzed using a Leica DMR fluorescence microscope at ×1000 magnification.

In vitro development of liver stages in hepatocyte cultures

To measure the luciferase activity of liver stages in HepG2 cells, a total of 2×10^4 to 1.5×10^5 sporozoites were added to monolayers of 2×10^5 HepG2 cells (1 ml/well in 24 well plates) as described previously [41]. Cells were prepared in quadruplet wells. In several assays, Cytochalasin D (Sigma, NL) was added to the cells at a concentration of 10 µg/ml prior to addition of the sporozoites as described [42]. At different time points after invasion, 100 µl of cells were collected, transferred to 96-well plates and processed for imaging with the Lumina system (see below). Four hundred µl of the remaining cells were harvested and lysed with either 200 µl of RLT buffer (RNA easy kit, Quiagen, NL) or 200 µl of cell culture lysis reagent obtained from the Promega Luciferase Assay System Kit® (Promega, NL) and stored at −80°C until further analysis by qRT-PCR or bioluminescence with a microplate reader(see below). To measure the luciferase activity of liver stages in Huh7 cells a total of 5×10^3 to 7×10^4 sporozoites were added to triplicate wells containing monolayers of 7×10^4 Huh7 cells (400 µl/well in 24 well plates) as previously described [35]. At different time points after sporozoite addition, cells were harvested and lysed with either 150 µl of qRT-PCR buffer (RNA easy kit, Quiagen, NL) or 100 µl of cell culture lysis reagent obtained from the Promega Luciferase Assay System Kit® (Promega, PT). Samples in Promega lysis buffer were either stored at −80°C or processed immediately to measure luminescence intensity with the Lumina system (see below) or bioluminescence analysis by microplate reader (see below) and qRT-PCR samples were stored at −80°C until further analysis by qRT-PCR analysis (see below).

Real-time measurements of bioluminescence of *in vitro* cultured liver stages using the Lumina system

The *in vivo* imaging system Lumina (Caliper Life Sciences, USA) was used to measure luciferase activity of infected HepG2 and Huh7 cells. Imaging data were analysed using the Living Image® 3.0 software (Caliper Life Sciences, USA). For the infected HepG2 cells, 100 µl of Assay Substrate (Promega Luciferase Assay System Kit®) were added to 100 µl of hepatocyte cultures collected in 96-well plates (see above) and bioluminescence images were acquired with a 12,5 cm field of view (FOV), medium binning factor and an exposure time of 1 to 3 minutes. For infected Huh7 cells, 70 µl of Luciferase Assay Substrate (Promega Luciferase Assay System Kit®) were added to 20 µl of lysed hepatocyte cultures in black 96-well plates. Bioluminescence images were acquired with a 12,5 cm FOV, medium binning factor and an exposure time of 5 minutes.

Bioluminescence measurements of *in vitro* cultured liver stages using a microplate reader (luminometer)

For infected HepG2 cells, 100 µl of Luciferase Assay Substrate (Promega Luciferase Assay System Kit®) were added to 10 µl of lysed parasite samples in 96-well plates. Luminescence spectra of the samples were measured using a microplate reader (Wallac 1420 multilabel counter, PerkinElmer, NL) and the light reaction of each well was measured for 10 s. Measurements of luciferase activity are expressed as relative luminescence units (RLU). For

infected Huh7 cells, 75 µl of Luciferase Assay Substrate (Promega Luciferase Assay System Kit®) were added to 15 µl of lysed parasite samples in white 96-well plates. Luminescence intensity of the samples was measured using a microplate reader (Tecan, CH) and the light reaction of each well was measured for 5 seconds. Measurements of luciferase activity are expressed as relative luminescence units (RLU).

In vivo development of liver stages in mice

Mice were inoculated with sporozoites by i.v. injection of 1×10^3, 1×10^4, 5×10^4 or 1×10^5 purified sporozoites or by mosquito bite (5–10 infected mosquitoes per mouse) at day 20–22 after the infectious blood meal. Blood stage infections were monitored by analysis of Giemsa-stained blood smears of tail blood collected on day 4–10 after inoculation of sporozoites or infection by mosquito bite.

Real-time *in vivo* imaging of liver stage development in whole bodies of live mice or in dissected livers

Luciferase activity in animals was visualized through imaging of whole bodies or of dissected livers using the *in vivo* Imaging System (IVIS 100 and Spectrum; Caliper Life Sciences, USA) as described in Franke-Fayard *et al.* [37]. Animals were anesthetized using the isofluorane-anesthesia system (XGI-8, Caliper Life Sciences, USA), their belly was shaved and D-luciferin dissolved in PBS (100 mg/kg; Synchem Laborgemeinschaft OHG, Germany) was injected subcutaneously (in the neck). Animals were kept anesthetized during the measurements, which were performed within 3 to 5 minutes after the injection of D-luciferin. Bioluminescence imaging was acquired with a 10 cm FOV, medium binning factor and an exposure time of 10 to 180 seconds. Luciferase activity in individual livers was visualized in whole organs dissected 44 h after sporozoite injection or mosquito bite. Livers were obtained by dissection of animals 2 to 3 min after a second intravenous injection of D-luciferin (in the tail vein; 100 mg/kg). Livers were placed in Petri-dishes or on black tape to minimize light interference from plastic Petri-dishes. Dissected livers were imaged with a 10 cm FOV, medium binning factor and an exposure time of 60 to 180 seconds. Imaging data were analysed using the Living Image® 3.0 (Caliper Life Sciences, USA) software. Quantitative analysis of bioluminescence of whole bodies or dissected livers was performed by measuring the luminescence signal intensity using the ROI settings of the Living Image® 3.0 software. The ROI was set to measure either the abdominal area at the location of the liver for whole body imaging or the complete livers in the case of dissected livers. ROI measurements are expressed in total flux of photons.

For the 3D imaging of luciferase activity in live mice, the *in vivo* imaging system IVIS® 3D (Caliper Life Sciences, USA) was used as described [43-45]. The IVIS® 3D performs rotational axis imaging of the bioluminescent light sources within a living animal. The IVIS 3D acquires eight imaging views about the longitudinal axis of the animal at 3 different wavelengths: 580, 600 and 620 nm. At each angle view, the animal height or surface topography is determined and stitched together to generate the whole 3D map of the animal. The 3D diffuse tomography software (Living Image ™) is used to reconstruct the eight bioluminescent images resulting in

data on *in vivo* source brightness, location, and size of the infection. Exposure time was of 60 seconds for each angle of measurements. A digital female mouse atlas was overlaid onto the 3D diffuse tomography reconstruction to obtain anatomical reference points. This feature is included in the Living Image Software 3D Analysis Package. The liver was removed from the 3D reconstruction of the mouse organs to better visualize the bioluminescence signals.

Analysis of *in vitro* development of liver stages in hepatocyte cultures and in extracted livers by qRT-PCR

RNA was extracted from hepatocyte culture samples collected in 200 µl (HepG2) or 150 µl (Huh7) of qRT-PCR buffer (see above) with Quiagen's MicroRNeasy kit following the manufacturer's instructions. The transcriptor first-strand cDNA synthesis kit (Roche) was used according to the manufacturer's recommendations to make single-stranded cDNA. RNA was extracted from livers collected at 44 h after infection and homogenized in RLT buffer (DNA/RNA Quiagen extraction kit) supplemented with 0,07% β-mercaptoethanol and stored at −80°C till qRT-PCR analysis. The RNA samples were further processed as described above for the samples of the hepatocyte cultures.

Real-time PCR analysis of specific *P. berghei* parasite 18S rRNA and β actin mouse (HepG2 invasion) or Hypoxanthine Guanine Phosphoribosyl Transferase (HPRT; Huh7 invasion and whole infected livers) housekeeping genes was done according to [21,35]. Standardization was done by multiplying the value of each sample with a correction factor. This correction factor is the maximum value for the housekeeping genes found for all samples divided by the value of this gene obtained for the sample).

Analysis of drug-inhibition of *in vitro* liver stage development

For the analysis of inhibition of *in vitro* liver stage development by drugs, 3×10^4 sporozoites were added to monolayers of 7×10^4 Huh7 cells (400 µl/well) in 24 well plates as described above. Five drugs that are known to inhibit liver stage development were used to test the drug susceptibility: primaquine (primaquine diphosphate 98%, Aldrich, NL); tafenoquine (GlaxoSmithKline, UK); genistein [25]; lopinavir [24] and saquionovir [24]). Primaquine was dissolved in water to a final stock solution of 100 µM and serial dilutions with complete culture medium were prepared ranging from 1 µM to 100 µM. Tafenoquine was dissolved in ethanol to a final stock concentration of 100 µM and serial dilutions were prepared ranging from 0,3 to 30 µM. Genistein, lopinavir and saquinavir were dissolved in water to a final stock concentration of 100 µM, 100 µM and 25 µM, respectively. Serial dilutions with complete culture medium were prepared, ranging from 10 to 100 µM for genistein and 2,5 to 40 µM for lopinavir and saquinovir. Huh7 cells were incubated with different concentrations of the drugs in triplicate wells by replacing the culture medium with drug-containing medium prior to sporozoite addition. Forty-six hours after adding the sporozoites, the infected Huh7 cells were harvested and lysed with 100 µl of cell culture lysis reagent obtained from the Promega Luciferase Assay System Kit®. Seventy-five µl of Luciferase Assay Substrate (Promega Luciferase Assay System Kit®) were added to 15 µl of lysed parasite samples in white 96-well

plates. Luminescence spectra of the samples were measured using a microplate reader (Tecan, CH) and the light reaction of a sample of each well is measured for 5 seconds. Measurements of luciferase activity are expressed as relative luminescence units (RLU).

Analysis of the inhibition of *in vivo* liver stage development by primaquine and tafenoquine

Mice were treated with primaquine (primaquine diphosphate 98%, Aldrich, NL) and tafenoquine (GlaxoSmithKline, UK) once at day −1, twice on the day of infection (day 0; 5 hours before and after infection) and once the following day (day +1; 19 h and 29 h after infection). Both primaquine and tafenoquine were dissolved in distilled water and administered subcutaneously with concentrations ranging from 1–40 mg/kg body weight and 10 and 20 mg/kg body weight respectively. Mice were infected at day 0 by the bite of 5–10 mosquitoes, as described above. *In vivo* imaging was performed at 44 hours after infection as described above. At day 6 – 9 after infection, the same mice were analysed for blood stage infections by determination of the course of parasitemia in Giemsa stained thin blood films of tail blood.

Growth inhibitory curves and statistical analysis

The two tailed analysis using the Spearman's rho test of the SPSS 16 software (SPSS Inc., USA) was used for statistical analysis. Correlation coefficients were determined using the two-tailed Spearman's rho test for non-parametric analysis of small data set. qRT-PCR curves were drawn using the GraphPad Prism software (GraphPad Prism, Inc., US). p values were calculated using the same GraphPad Prism software. The non-linear regression function for sigmoidal dose-response (variable slope) of the GraphPad Prism software was used to calculate the (best-fit) effective concentration (EC_{50}) values.

Results

Analysis of *Pb*GFP-Luc$_{con}$ liver stage development *in vitro*

For the analysis of liver stage development we used a transgenic *P. berghei* parasite, *Pb*GFP-Luc$_{con}$ (line 676m1cl1), which expresses a reporter fusion gene of gfp and luciferase, stably integrated in the 230p locus (PB000423.03.0) of the *P. berghei* genome. *Pb*GFP-Luc$_{con}$ parasites do not contain a drug-resistance marker as they were selected by FACS sorting of transfected GFP-positive blood stages immediately after the transfection procedure [38]. The gfp-luciferase transgene in *Pb*GFP-Luc$_{con}$ is under the control of the *P. berghei eef1a* promoter. Through the analysis of GFP expression we have previously demonstrated that the *eef1a* promoter drives constitutive and strong gene expression in all life cycle stages, including liver stage parasites [39]. The blood and mosquito stages of *Pb*GFP-Luc$_{con}$ show similar growth characteristics as those of the parent reference line, cl15cy1 of *P. berghei* ANKA

(data not shown). Analysis of sporozoite motility, cell traversal and *in vitro* and *in vivo* infectivity demonstrated that all features of *Pb*GFP-Luc$_{con}$ sporozoites were comparable to those of wildtype sporozoites (Figure S1).

To determine the timing and level of luciferase expression of *Pb*GFP-Luc$_{con}$ throughout development of liver stages *in vitro*, two hepatoma cell lines, HepG2 and Huh7, were infected with different numbers of sporozoites, ranging from 5×10^3 to 1.5×10^5, in 24-well plates. The time course of luciferase expression during the first 48 hours of development is shown in Figures 1A&B and S2A&B. The luminescence intensity (luciferase activity) was measured by (a) direct imaging of the culture plates of live or lysed cells using the Lumina system (the luminescence intensity expressed as photons per second) or by (b) analysis of lysed cell samples in a microplate reader (luminescence intensity expressed as Relative Light Units, RLU). Both methods show a strong increase in luciferase activity throughout the 48 h period during which the invaded sporozoites develop into liver schizonts. The increase in reporter protein expression during trophozoite and schizont development is expected as a similar increase in *eef1a* based expression of luciferase or GFP is observed in blood stage trophozoites and schizonts [19,36]. Uninfected control cells showed low photon counts and luminescence values are significantly lower than those of infected cells at any of the time points assessed. The mean photon counts were 3×10^6 p/s (sd 2×10^6) and 5×10^4 p/s (sd 1×10^3) and the mean RLU values were 56 (sd 17) and 30 (sd 15) for HepG2 and Huh7 cells respectively. Sporozoites contain low levels of the GFP-Luciferase protein as shown by analysis of GFP expression by fluorescence-microscopy (data not shown) and therefore low bioluminescence levels at 4–5 h might be derived from invaded sporozoites. A strong increase in luminescence values is observed after 24–30 h which correlates with the development of the liver trophozoite into the schizont stage. For further quantitative analyses of liver stage development we compared luminescence levels of samples taken at time points between 30 and 48 h after sporozoite incubation.

Luminescence intensities at 30 and 48 h correlate well with the number of sporozoites added to the hepatocytes in the range of 5×10^3 to 1×10^5, using both the Lumina and the microplate reader (Figure 1C, S2A-C). When using as few as 5×10^3 sporozoites a clear luminescent signal is obtained that is significantly higher than the background signal detected in uninfected wells (p=00,1). We then compared the relative luminescence intensities of cells infected with different sporozoite numbers with the relative amounts of parasite 18S ribosomal RNA using standard qRT-PCR methodologies (Figures 1D, S2D). A good correlation was observed between the

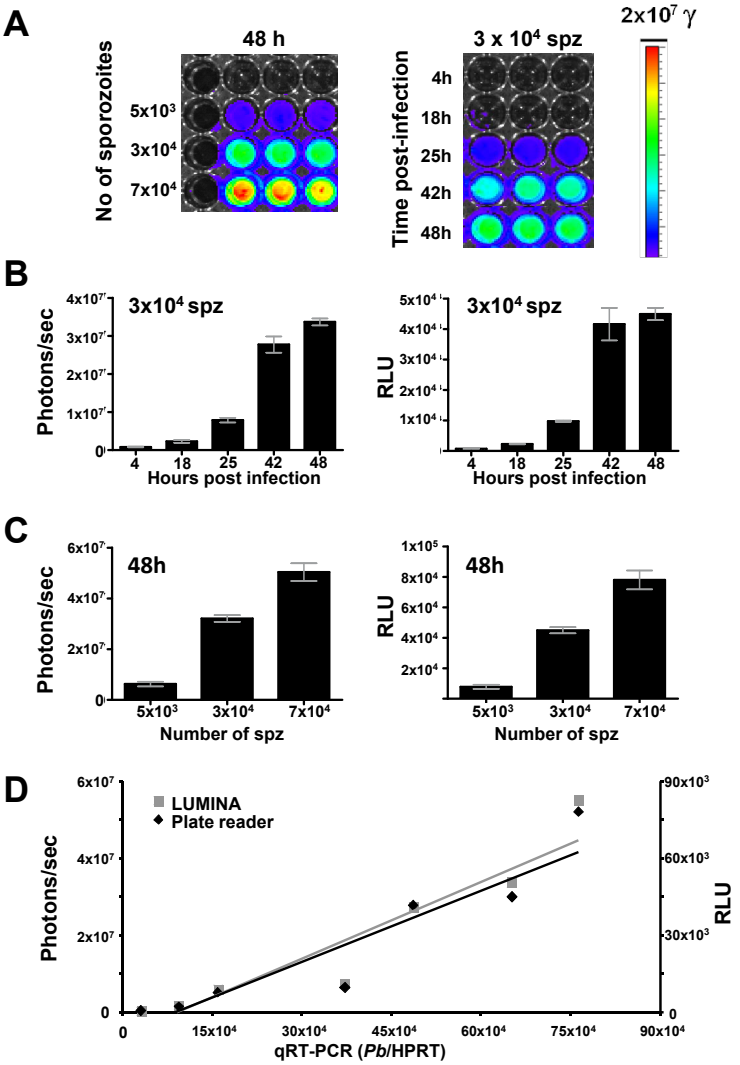

Figure 1: Analysis of *in vitro* liver stage development by determination of luciferase expression.
A) Luminescence levels (photons/sec) during liver stage development of *Pb*GFP-Luc$_{con}$ after infection of Huh7 cells with different numbers of sporozoites at 48 h (left panel) and at different time points after infection with 3×10^4 sporozoites (right panel) determined by direct imaging of samples using the Lumina system. Rainbow images show the relative levels of luminescence ranging from low (blue), to medium (green), to high (yellow/red). **B)** Luminescence levels during development of liver stages at different time points after invasion of Huh7 cells as measured by the Lumina system (Photons/sec) and a Tecan microplate reader (Relative light unit, RLU). **C)** Relationship between the numbers of sporozoites used to infect Huh7 hepatocyte cultures and the luminescence produced by the liver stages at 48 h after infection. Luminescence levels were determined by direct imaging of samples using the Lumina system (Photons/sec) and a Tecan microplate reader (RLU). **D)** Correlation between luminescence values as measured by the Lumina system and the Tecan microplate reader and of *P. berghei* 18S rRNA levels as determined by qRT-PCR of Huh7 cultures that are infected with different numbers of sporozoites. See Table S1 for the correlation coefficient data of the two-tailed Spearman's rho test.

relative luminescence intensities and the relative amounts of parasite 18S rRNA in the same cultures (Spearman correlation coefficient ranging from 0.61–0.94; Table S1).

Analysis of *Pb*GFP-Luc$_{con}$ liver stage development *in vivo*

To determine the timing and level of luminescence during *Pb*GFP-Luc$_{con}$ development in the liver, groups of mice (n=4) were infected intravenously with different numbers of sporozoites ranging from 1×10^3 to 1×10^5. Luciferase activity in animals was visualized through the imaging of whole bodies at 5, 24, 35 and 44 hours after infection. In control, uninfected mice, luminescence values ranged between 1×10^7 and 4×10^7 p/s (sd 1×10^7). In mice infected with the highest dose of sporozoites (i.e. 1×10^5), 3 mice showed luminescence levels above background at 24 h (i.e. 1×10^8 p/s (sd 3×10^7); see Figures 2A&B. Mice infected with 5×10^4 sporozoites showed a signal above background at 35 h. In all infected mice there was a strong increase in bioluminescence signal between 35 and 44 h (Figures 2C, S3), whereas between 44 h and 52 h no further increase was observed and, indeed, in several mice the luminescence signal decreased between these time-points (Figure S4A). After 60 h, luminescence signals could be detected in the whole body, resulting from parasites that had invaded erythrocytes after the rupture of the liver schizonts (Figure S4A). The decrease in luminescence in the liver between 44 and 52 h may either be due to liver schizont rupture and the consequent reduction in the number of infected liver cells or is the results of decrease in luciferase expression in the final stages of schizont maturation. Such a decrease has been previously observed in erythrocytic schizonts where protein expression peaks in mature trophozoites/young schizonts and decreases in maturing schizont when the *eef1a* promoter is used to drive protein expression [36,39] and correlates with destruction of endogenous *eef1a* mRNA in schizonts [46]. Based on these observations, we decided to determine luminescence intensities at 44 h in subsequent experiments. At 44 h, a good correlation was observed between the luminescence intensity and the number of sporozoites initially injected (Figures 2D&E). Specifically, the mean luminescence intensity of mice infected with 1×10^3 sporozoites was 1×10^9 p/s (sd 4×10^8) and increased to 1×10^{10} p/s (sd 7×10^9) in mice infected with 1×10^4 sporozoites.

After the whole body measurements, the livers of several of the mice from each group were dissected and imaged with the IVIS100 system. The luminescence intensity of the extracted livers was significantly lower than that of whole bodies (Figure 2C&D, S3). For example, livers from mice infected with 1×10^5 sporozoites had, on average, a

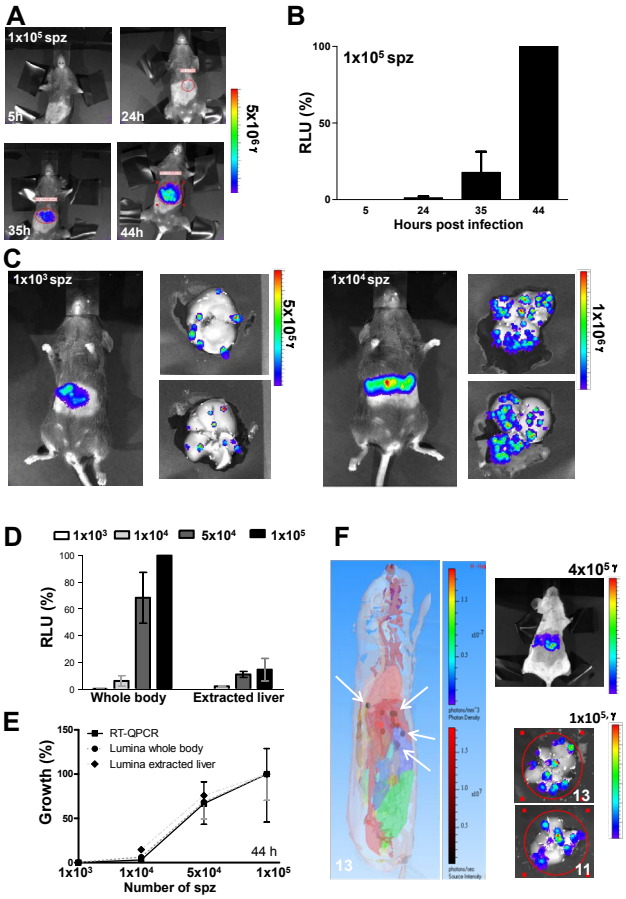

Figure 2: Analysis of *in vivo* liver stage development by determination of luciferase expression.
A) Representative rainbow images of luminescence in livers of live mice at different time points after injection of 1×10^5 sporozoites. Rainbow images show the relative levels of luminescence ranging from low (blue), to medium (green), to high (yellow/red). **B)** Luminescence levels (photons/sec) of livers in whole mice at different time points after infection with 1×10^5 sporozoites (n=4). Photon counts from whole body imaging are expressed as the percentage of the photon counts of mice at 44 h after infection (= RLU %). **C)** Distribution of luminescence signals in the livers of live mice and in extracted livers of the same mice at 44 h after infection with 1×10^3 (left) or 1×10^4 (right) sporozoites. **D)** Luminescence levels (photons/sec) of whole bodies and extracted livers of mice 44 h after inoculation of different numbers of sporozoites. Photon counts are expressed as the percentage of the photon counts of whole body of mice at 44 h infected with 10^5 sporozoites (= RLU %). **E)** Correlation between luminescence values as measured by the Lumina system of whole body and dissected livers and of *P. berghei* 18S rRNA levels as determined by qRT-PCR of dissected livers that are infected with different numbers of sporozoites. The percentage of growth is normalized to the highest reading within each experiment. See Table S2 for the correlation coefficient data of the two-tailed Spearman's rho test. **F)** The left panel shows the 3D-imaging of luminescence signals (3D tomography and source reconstruction) in a mouse at 44 h after infection with 5 to 10 mosquito bites as measured with the IVIS 3D Series system. The brown/red spots (white arrows) indicate the origin of highest luminescence intensity in the body. These spots are located in the liver as shown by overlaying with a digital mouse atlas to obtain anatomical reference points. The right panel shows the same mouse and its extracted liver (imaged at both sides) imaged with the 2D-IVIS100 imaging system. Numbers in the images represent the number of luminescent spots identified.

ten-fold lower luminescence signal compared to whole body imaging (8×10^8 p/s, sd 4×10^8; Figure 2D). The presence of clearly separated luminescent spots in dissected livers of mice infected with low numbers of sporozoites (1×10^3; Figure 2C,S3) indicates that these spots represent individual liver schizonts. Therefore, imaging of dissected livers may provide information on both the number and dissemination of parasites in the liver. When livers containing 3 to 13 individual spots were imaged, both sides often showed a comparable numbers of spots in a similar location (Figures S3B, S4B). However in each liver imaged, one or a few luminescent spots were only visible on one side of the liver, indicating that the imaging of these spots can be influenced by their localization, possibly due to a quenching effect of the liver. To better localize the origin of individual luminescent spots, we used the IVIS 3D Series system (Caliper Life Sciences, USA) to image luminescent signals in live mice in three dimensions. This instrument, in combination with the 3.1 Living Image® software, allows the precise localization of the origin of the luminescent signals in whole bodies in contrast to the more diffuse luminescence signals obtained with the IVIS100 2D-system. 3D-imaging of 4 infected mice in an anatomical context show the presence of clearly separated spots in the liver (Figures 2F and S5). The individual infected hepatocytes can be best visualized in the context of the whole liver when the mice are rotated as visualized in the Supplementary movies S1-S3 (online version of the paper). When the number of luminescent spots was determined by 2D-imaging in livers dissected after the 3D-imaging of the whole mice, a good correlation between the numbers of spots obtained with both methods was found. These observations indicate that 3D-imaging of whole bodies allows the detection of individual liver schizonts in live mice. However, like in 2D-imaging of isolated livers, some luminescent spots may be missed in the 3D-imaging, as shown in mouse 4 Figure S5.

As described for the *in vitro* analysis of liver stage development, we compared the relative luminescence intensities of whole bodies and isolated livers measured at 44 hpi with 18S ribosomal RNA qRT-PCR data derived from RNA extracted from the same livers. The relative luminescence intensities of whole bodies and dissected livers are in good agreement with the 18S rRNA qRT-PCR values (i.e. Spearman correlation coefficient ranging from 0.65 to 0.95; Figure 2E, Table S2). The best correlation is found between qRT-PCR and whole body imaging, possibly because of the decrease of luminescence during extraction of the livers as discussed above.

Rats (e.g. Sprague-Dawley, Wistar etc) as well as mice are frequently used to analyse liver stage development in the *P. berghei* model of malaria. We have performed a

limited number of experiments to investigate whether *in vivo* imaging of liver stage development in Wistar rats generates similar results to the *in vivo* imaging in mice (Figure S4B). In rats luminescence signals were detected at 24 h after infections had been initiated by mosquito bite with rapidly increasing luminescence intensities during the period of 24–30 h. Imaging of dissected livers from these rats also showed the same pattern of clearly separated luminescent spots (on both sides of the liver) as we had observed in extracted mouse livers (Figures 2C, S3).

Analyses of drug-inhibition of *Pb*GFP-Luc$_{con}$ liver stage development by luminescence measurements

Having established that liver stage infection can be accurately and conveniently measured *in vitro* and *in vivo* by assessing the luminescence of *Pb*GFP-Luc$_{con}$-infected cells or mice livers, we decided to investigate the suitability of this method for the evaluation of anti-plasmodial drugs. The inhibition of *in vitro* development by drugs was determined by measurement of luminescence of *Pb*GFP-Luc$_{con}$-infected hepatoma cells maintained in 24-well plates and incubated with serial dilutions of five different drugs known to inhibit liver stage development (Figures 3A&B). Primaquine [47] tafenoquine [48] genistein [25], lopinavir [24] and saquinavir [24] were added to Huh7 cells 1 h before addition of *Pb*-GFP-Luc$_{con}$ sporozoites and luminescence was measured 44 h later with a microplate reader. In samples treated with the highest drug concentrations, known to completely block liver stage development, the luminescence values are low and almost identical to background ranging consistently from 20 to 350 RLU (mean of 104; sd 119). In contrast, in drug-free control samples luminescence values ranged between 4×10^4 to 7×10^4 RLU (mean 5×10^4; sd 9×10^3) in the different experiments (Figures 3A&B). Primaquine's IC50 value as determined by luminescence intensity correlated well with the value obtained by standard qRT-PCR methods (Figure 3A). Complete inhibition with primaquine and tafenoquine was observed at concentrations of 100 μM and 30 μM, respectively, which correspond to inhibitory concentrations reported in the literature for primaquine (2×10^{-7} to 5×10^{-5} M) and tafenoquine 3×10^{-7} M [23,47,49]. Genistein, lopinavir and saquinavir concentrations that inhibited liver stage development, quantified by the decrease in luminescence intensities are also in good agreement with previously reported inhibitory concentrations for these compounds that were determined by direct counting of liver stages or by qRT-PCR (Figure 3B)[24,25].

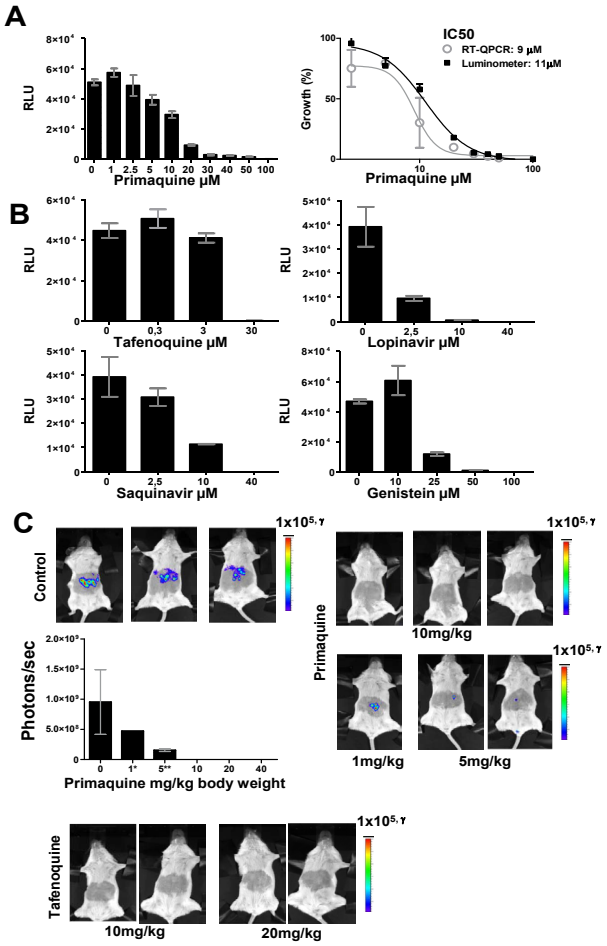

Figure 3: Drug-inhibition of liver stage development determined by measurement of luciferase expression.
A) Inhibition of *in vitro* liver stage development by primaquine (left panel) by measuring luminescence levels (RLU) in samples of Huh7 cells 44 h after infection of the cells with 3×10^4 *Pb*GFP-Luc$_{con}$ sporozoites. The right panel shows the inhibition of liver stage development by primaquine as determined by both luminescence measurements and qRT-qPCR analysis. The percentage of growth is defined by the RLU values and by the amounts of *P. berghei* 18S rRNA levels, respectively. Luminescence levels were measured using a Tecan microplate reader. **B)** Inhibition of *in vitro* liver stage development by tafenoquine, lopinavir, sanquinavir and genistein, as determined by measuring luciferase luminescence levels (RLU) in samples of Huh7-infected cells 44 h after infection of the cells with 3×10^4 *Pb*GFP-Luc$_{con}$ sporozoites. Luminescence levels were measured using a microplate reader. **C)** Inhibition of *in vivo* liver stage development by primaquine and tafenoquine as determined by measuring luminescence levels (photons/sec) in live mice at 44 h after infection of the mice by the bite of 5 infected mosquitoes. Luminescence levels were determined by direct imaging of whole bodies using the IVIS100 system.

Analysis of *in vivo* inhibition of liver stage development by luminescence measurements was performed using primaquine and tafenoquine. Mice were treated 5 times with different doses of these drugs starting one day before infection

with *Pb*GFP-Luc$_{con}$ and the last dose at 29 h after infection. Mice were infected by the bites of 5 infected mosquitoes and luminescence levels were determined 44 h later. Luminescence values of untreated, control mice, ranged between 2×10^8 and 2×10^9 p/s (mean 1×10^9; sd 5×10^8). No detectable luminescence signal was observed in mice treated with 10–40 mg/kg body weight of primaquine, indicating complete inhibition of parasite growth (Figure 3C). Indeed, analysis of these mice 5–9 days after infection showed no detectable parasites in peripheral blood, whereas control mice developed normal blood infections with parasitemias ranging between 0.1 and 3% at day 4 post-infection. In mice treated with 1 and 5 mg/kg body weight of primaquine, 3 out of 6 mice showed a low level of luminescence ranging between 1×10^8 and 5×10^8 p/s (mean 3×10^8; sd 2×10^8) at 44 h while the remaining 3 mice were negative. Five of these mice developed a blood stage parasitemia that was delayed by two days compared to the control mice (parasitemia of 0,5 to 3% at day 6 after infection), indicating a 100-fold inhibition of liver stage development. All mice treated with 10 or 20 mg/kg of tafenoquine were luminescence negative at 44 h and did not develop blood stage infection (Figure 3C). The complete inhibition of liver stage development by primaquine and tafenoquine at doses of 10 mg/kg body weight and higher is in agreement with the inhibitory doses reported in the literature [25,50,51].

Discussion

Rodent malaria parasites are frequently used for the identification and characterization of new anti-malarial drugs [17-20,25,50,52-53]. These parasites are used in initial drug and small molecule inhibitor (SMI) screens in order to determine their *in vivo* anti-malarial activity in cultured cells and in mice. In comparison to the blood-stage parasite SMI screening assays [19] the screening and identification of agents that inhibit *Plasmodium* development in the liver is considerably more complex. Quantitative analysis of liver stage development both in cultured liver cells, *in vitro*, and in small laboratory animals, *in vivo*, is hampered by the low levels of parasite infection as well as the complicated, time consuming and expensive methods required to monitor parasite development, such as qRT-PCR or direct counting of liver stages [21-23,26-27] and RNA hybridization [28-29] We have recently shown that transgenic rodent parasites expressing luciferase are useful reagents to determine parasite load and bio-distribution of blood stages in live mice using in vivo imaging [36,37]. We have also used these parasites to assess the

sensitivity of blood stages to drugs by measuring luminescence using a microplate reader based assay [19]. We now show that luminescence assays can also be used for the quantitative analysis of liver infection and that the results of these assays closely correlate to standard analysis methods (i.e. qRT-PCR). The transgenic parasite used in these assays, *Pb*GFP-Luc$_{con}$, expresses luciferase under the control of the strong and constitutive *eef1a* promoter. This promoter has previously been shown to drive expression of reporter proteins in growing and dividing stages throughout the parasite's life-cycle [39]. The strong increase in reporter gene expression using this promoter from sporozoite-hepatocyte invasion to mature liver schizont is matched with reporter gene expression from merozoite-erythrocyte invasion to schizogony. The significant increase in luminescence 5–10 hours after sporozoite infection of hepatocytes, as compared to cultures incubated with sporozoites whose ability to invade liver cells is impaired (i.e. treated with cytochalasin-D), shows that luciferase production starts rapidly after invasion of the hepatocyte. We reproducibly observed a clear increase in luminescence 48 hours post infection in hepatocyte cultures infected with as few as 5×10^3 sporozoites, compared to uninfected control wells. This sensitivity of the luminescence assays with low sporozoite numbers in combination with the early detection of luciferase expression offers unique possibilities for large scale screenings of inhibitors of parasite liver stage development, with the potential for automation, using microplate assays. The use of such assays would confer the same advantage currently only available to drug screening against blood stage parasites [19].

Despite the expression of luciferase during the early stages of parasite development within hepatocytes, we were not able to detect luminescence signals in live mice during the first 20 hours of infection, even at the highest infection dose of 1×10^5 sporozoites. To investigate whether the sensitivity of detection of the young liver stages could be increased, we analysed a transgenic parasite line (mutant RMgm-152 in www.pberghei.eu) that expresses *Pb*GFP-Luciferase under the control of the promoter of the circumsporozoite protein (CS; PB001026.00.0). The sporozoite stage of these reporter parasites strongly expresses the reporter fusion protein as visualised by GFP-fluorescence intensity; but we were still unable to detect sporozoites in the liver by *in vivo* imaging, although we were able to detect sporozoites in the skin at the site of biting when we measured mice directly after mosquito feeding (data not shown). Although we were not able to detect the young liver stages, the more mature liver stages were readily detected 30 h post infection of the mice, even after infection with a sporozoite dose as low as 1×10^3 sporozoites. The 30–48

h period corresponds to the phase of schizogony during which a single parasite can produce more than 1×10^4 daughter merozoites [54]. It is known that laboratory mice are relatively insensitive to infection with *P. berghei* sporozoites and therefore the sensitivity of *in vivo* imaging might even be higher if the reporter line were made in another rodent malaria parasite, *P. yoelii*, to which mice are more sensitive. When blood stage infections were analysed in mice that resulted from infections initiated with 1×10^3 sporozoites we calculated that the luminescence signal measured at 48 h was the result of only 1–5 schizonts. This is based on the assumption that the parasite multiplication rate in erythrocytes is 10-fold every 24 hours [55] and that each liver schizont contains between 2×10^3 and 1×10^4 merozoites. The detection of localised spots of luminescence in dissected livers indicates that the *in vivo* imaging enables detection to the level of a single infected hepatocyte containing a mature liver schizont. However, the total luminescent intensity of extracted livers was lower than the luminescence intensity of livers determined by imaging of live mice. This was initially surprising because the expected quenching of luminescence by tissues in live mice would be absent when the isolated organ was examined. However, the lower values obtained from dissected livers are most likely the result of the rapid uptake and possibly metabolism of luciferin [56] during the time required to collect the liver.

It has recently been shown that mature liver schizonts produce so called merosomes, packets of 100–200 merozoites surrounded by the host cell membrane [57,58]. The possibility to detect bioluminescence signals of individual liver schizonts might also offer opportunities to analyse the process of merosome formation as well as merosome migration after their release from the infected hepatocyte. Merosomes are released in the blood circulating and appear to specifically accumulate in the lungs whereupon they burst open and merozoites are released and invade red blood cells [58]. It would therefore be interesting to see if the methodologies in this study can be adapted to also image the merosomes in the liver and then in isolated lungs or in lungs of whole bodies of animals to add to our understanding of merosome biology.

The similar numbers of luminescence spots detected in dissected livers and in living mice (analysed by 3D imaging) also supports the notion that *in vivo* imaging can detect an individual mature liver schizont. However, in dissected livers there were several luminescence spots that were detected only on one side of the liver and by combining whole body imaging and imaging of dissected livers we found that a minor fraction of the schizonts was undetectable by either of the two methods. In addition,

a few mice treated with non-curative doses of primaquine showed no luminescence signals but developed a (delayed) blood stage infection. These observations indicate that small numbers of liver schizonts can be missed with whole body imaging, although in the case of primaquine treatment the absence of a luminescence signal might also be due to delayed development of the liver schizonts. To investigate whether we could increase the sensitivity of detection of mature liver schizonts we have separately analysed a different transgenic line which expresses luciferase under the control of the *ama1* promoter (PB000821.01.0) [36]; mutant RMgm-30 in www.pberghei.eu). The *ama1* gene encodes the micronemal protein, AMA1, in merozoites and it was our contention that since very large numbers of merozoites are produced in each liver schizont we could expect a high luciferase signal. Surprisingly, using similar sporozoite numbers as used with our *eef1a* promoter line, we measured a significantly lower luminescence signal, even in measurements that were taken at later time points (48–60 h) after infection (data not shown).

The analysis of drug-inhibition of parasite liver stage development by *in vivo* imaging offers clear advantages over standard qRT-PCR analysis of dissected livers or analysing the dynamics of the blood stage infection subsequent to liver infection. qRT-PCR analysis is both time consuming and expensive whereas the analysis of subsequent blood stage infections cannot easily discriminate the effect of the drugs on liver stage and/or resulting blood stage infections. In contrast, *in vivo* imaging is rapid and simple and allows, within the same animal, to measure both the specific inhibition of liver stage development by an inhibitor or drug and its subsequent effects on the blood stages. The analysis by *in vivo* imaging has the advantage in that analysis does not require sacrificing the experimental animal and thereby reduces the number of animals required for experimentation since multiple measurements can be made in the same animal over time. Moreover, it also has the advantage that it minimizes the biological variation within the study [59,60]. The *in vivo* analysis of drug sensitivity of liver stages to primaquine and tafenoquine was performed with mice that were infected by the bite of only five infected mosquitoes. All the control mice in these experiments (i.e. infections in the absence of drug) show a strong luminescence signal at 48 h after infection. These experiments demonstrate that *in vivo* drug-sensitivity assays are not dependent on the injection of mice with high numbers of sporozoites, which requires time-consuming manual dissection from mosquito salivary glands. The sensitivity of *in vivo* imaging therefore greatly simplifies the procedure of *in vivo* drug-sensitivity testing. An additional feature of the reporter protein luciferase that may be of great benefit is that it has a relatively

short half-life and therefore only allows the detection of live parasites, thereby avoiding errors potentially associated with the counting of dead liver parasites (as may occur with qRT-PCR experiments). The imaging assays described in this paper can also be used for the screening and analysis of parasite mutants for aberrant liver stage development. Moreover, these can be used to analyse liver stage development in challenge studies of mice that are immunized with either subunit vaccines against sporozoites/liver stage molecules or with genetically attenuated sporozoites. In conclusion, quantitative analysis of liver stage development by real-time imaging should greatly aid the validation of drugs and vaccines that act against the liver stages of the *Plasmodium*.

Acknowledgments

We would like to thank Dr Lorraine Bray from GlaxoSmithKline for kindly providing tafenoquine, Hans Kroeze for technical assistance, Dr David Panzarella and Dr. Vivek Shinde Patil from Calipers for technical support. Additionally, we would like to thank Jolanda Klaassen, Laura Pelser-Posthumus, Astrid Pouwelsen and Jacqueline Kuhnen for the breeding of the mosquitoes and technical assistance with the *P. berghei* infections.

References

1. Greenwood BM, Fidock DA, Kyle DE, Kappe SH, Alonso PL, et al. Malaria: progress, perils, and prospects for eradication. J Clin Invest. 2008;118:1266–1276.
2. Waters AP, Mota MM, van Dijk MR, Janse CJ. Parasitology. Malaria vaccines: back to the future? Science. 2005;307:528–530.
3. Craft JC. Challenges facing drug development for malaria. Curr Opin Microbiol. 2008;11:428–433.
4. Cunha-Rodrigues M, Portugal S, Febbraio M, Mota MM. Infection by and protective immune responses against Plasmodium berghei ANKA are not affected in macrophage scavenger receptors A deficient mice. BMC Microbiol. 2006;6:73.
5. Mikolajczak SA, Kappe SH. A clash to conquer: the malaria parasite liver infection. Mol Microbiol. 2006;62:1499–1506.
6. Prudencio M, Rodriguez A, Mota MM. The silent path to thousands of merozoites: the Plasmodium liver stage. Nat Rev Microbiol. 2006;4:849–856.
7. Matuschewski K. Hitting malaria before it hurts: attenuated Plasmodium liver stages. Cell Mol Life Sci. 2007;64:3007–3011.
8. Cui L, Trongnipatt N, Sattabongkot J, Udomsangpetch R. Culture of Exoerythrocytic Stages of the Malaria Parasites Plasmodium falciparum and Plasmodium vivax. Methods Mol Biol. 2009;470:263–273.
9. Baird JK, Schwartz E, Hoffman SL. Prevention and treatment of vivax malaria. Curr Infect Dis Rep. 2007;9:39– 46.
10. Price RN, Tjitra E, Guerra CA, Yeung S, White NJ, et al. Vivax malaria: neglected and not benign. Am J Trop Med Hyg. 2007;77:79–87.
11. Imwong M, Snounou G, Pukrittayakamee S, Tanomsing N, Kim JR, et al. Relapses of Plasmodium vivax infection usually result from activation of heterologous hypnozoites. J Infect Dis. 2007;195:927–933.
12. Adak T, Valecha N, Sharma VP. Plasmodium vivax polymorphism in a clinical drug trial. Clin Diagn Lab

Immunol. 2001;8:891–894.
13. Walsh DS, Eamsila C, Sasiprapha T, Sangkharomya S, Khaewsathien P, et al. Efficacy of monthly tafenoquine for prophylaxis of Plasmodium vivax and multidrug-resistant P. falciparum malaria. J Infect Dis. 2004;190:1456–1463.
14. Lalloo DG, Shingadia D, Pasvol G, Chiodini PL, Whitty CJ, et al. UK malaria treatment guidelines. J Infect. 2007;54:111–121.
15. Sharrock WW, Suwanarusk R, Lek-Uthai U, Edstein MD, Kosaisavee V, et al. Plasmodium vivax trophozoites insensitive to chloroquine. Malar J. 2008;7:94.
16. Lanteri CA, Johnson JD, Waters NC. Recent advances in malaria drug discovery. Recent Pat Antiinfect Drug Discov. 2007;2:95–114.
17. Weisman JL, Liou AP, Shelat AA, Cohen FE, Guy RK, et al. Searching for new antimalarial therapeutics amongst known drugs. Chem Biol Drug Des. 2006;67:409–416.
18. Baniecki ML, Wirth DF, Clardy J. High-throughput Plasmodium falciparum growth assay for malaria drug discovery. Antimicrob Agents Chemother. 2007;51:716–723.
19. Franke-Fayard B, Djokovic D, Dooren MW, Ramesar J, Waters AP, et al. Simple and sensitive antimalarial drug screening in vitro and in vivo using transgenic luciferase expressing Plasmodium berghei parasites. Int J Parasitol. 2008;38:1651–1662.
20. Evers A, Heppner S, Leippe M, Gelhaus C. An efficient fluorimetric method to measure the viability of intraerythrocytic Plasmodium falciparum. Biol Chem. 2008;389:1523–1525.
21. Bruna-Romero O, Hafalla JC, Gonzalez-Aseguinolaza G, Sano G, Tsuji M, et al. Detection of malaria liver-stages in mice infected through the bite of a single Anopheles mosquito using a highly sensitive real-time PCR. Int J Parasitol. 2001;31:1499–1502.
22. Siau A, Silvie O, Franetich JF, Yalaoui S, Marinach C, et al. Temperature shift and host cell contact up-regulate sporozoite expression of Plasmodium falciparum genes involved in hepatocyte infection. PLoS Pathog. 2008;4:e1000121.
23. Li J, Zhu JD, Appiah A, McCutchan TF, Long GW, et al. Plasmodium berghei: quantitation of in vitro effects of antimalarial drugs on exoerythrocytic development by a ribosomal RNA probe. Exp Parasitol. 1991;72:450–458.
24. Hobbs CV, Voza T, Coppi A, Kirmse B, Marsh K, et al. HIV protease inhibitors inhibit the development of preerythrocytic-stage plasmodium parasites. J Infect Dis. 2009;199:134–141.
25. Cunha-Rodrigues M, Portugal S, Prudencio M, Goncalves LA, Casalou C, et al. Genistein-supplemented diet decreases malaria liver infection in mice and constitutes a potential prophylactic strategy. PLoS ONE. 2008;3:e2732.
26. Fisk TL, Millet P, Collins WE, Nguyen-Dinh P. In vitro activity of antimalarial compounds on the exoerythrocytic stages of Plasmodium cynomolgi and P. knowlesi. Am J Trop Med Hyg. 1989;40:235–239.
27. Carraz M, Jossang A, Rasoanaivo P, Mazier D, Frappier F. Isolation and antimalarial activity of new morphinan alkaloids on Plasmodium yoelii liver stage. Bioorg Med Chem. 2008;16:6186–6192.
28. Schofield L, Ferreira A, Altszuler R, Nussenzweig V, Nussenzweig RS. Interferon-gamma inhibits the intrahepatocytic development of malaria parasites in vitro. J Immunol. 1987;139:2020–2025.
29. Gego A, Silvie O, Franetich JF, Farhati K, Hannoun L, et al. New approach for high-throughput screening of drug activity on Plasmodium liver stages. Antimicrob Agents Chemother. 2006;50:1586–1589.
30. Menard R, Amino R, Thiberge S, Gueirard P. [A new view of malaria provided by parasite imaging]. Bull Acad Natl Med. 2007;191:1261–1270.
31. Amino R, Menard R, Frischknecht F. In vivo imaging of malaria parasites—recent advances and future directions. Curr Opin Microbiol. 2005;8:407–414.
32. Thiberge S, Blazquez S, Baldacci P, Renaud O, Shorte S, et al. In vivo imaging of malaria parasites in the murine liver. Nat Protoc. 2007;2:1811–1818.
33. Tarun AS, Baer K, Dumpit RF, Gray S, Lejarcegui N, et al. Quantitative isolation and in vivo imaging of malaria parasite liver stages. Int J Parasitol. 2006;36:1283–1293.
34. Heussler V, Doerig C. In vivo imaging enters parasitology. Trends Parasitol. 2006;22:192–195.
35. Prudencio M, Rodrigues CD, Ataide R, Mota MM. Dissecting in vitro host cell infection by Plasmodium sporozoites using flow cytometry. Cell Microbiol. 2008;10:218–224.
36. Franke-Fayard B, Janse CJ, Cunha-Rodrigues M, Ramesar J, Buscher P, et al. Murine malaria parasite

sequestration: CD36 is the major receptor, but cerebral pathology is unlinked to sequestration. Proc Natl Acad Sci U S A. 2005;102:11468–11473.

37. Franke-Fayard B, Waters AP, Janse CJ. Real-time in vivo imaging of transgenic bioluminescent blood stages of rodent malaria parasites in mice. Nat Protoc. 2006;1:476–485.
38. Janse CJ, Franke-Fayard B, Mair GR, Ramesar J, Thiel C, et al. High efficiency transfection of Plasmodium berghei facilitates novel selection procedures. Mol Biochem Parasitol. 2006;145:60–70.
39. Franke-Fayard B, Trueman H, Ramesar J, Mendoza J, van der KM, et al. A Plasmodium berghei reference line that constitutively expresses GFP at a high level throughout the complete life cycle. Mol Biochem Parasitol. 2004;137:23–33.
40. Silvie O, Greco C, Franetich JF, Dubart-Kupperschmitt A, Hannoun L, et al. Expression of human CD81 differently affects host cell susceptibility to malaria sporozoites depending on the Plasmodium species. Cell Microbiol. 2006;8:1134–1146.
41. Lasonder E, Janse CJ, van Gemert GJ, Mair GR, Vermunt AM, et al. Proteomic profiling of Plasmodium sporozoite maturation identifies new proteins essential for parasite development and infectivity. PLoS Pathog. 2008;4:e1000195.
42. Kumar KA, Oliveira GA, Edelman R, Nardin E, Nussenzweig V. Quantitative Plasmodium sporozoite neutralization assay (TSNA). J Immunol Methods. 2004;292:157–164.
43. Henriquez NV, van Overveld PG, Que I, Buijs JT, Bachelier R, et al. Advances in optical imaging and novel model systems for cancer metastasis research. Clin Exp Metastasis. 2007;24:699–705.
44. Kok P, Dijkstra J, Botha CP, Post FH, Kaijzel EL, et al. Integrated visualization of multi-angle bioluminsecence imaging and micro CT. Proc of SPIE. 2007;6509:1–10.
45. Kuo C, Coquoz O, Troy TL, Xu H, Rice BW. Three-dimensional reconstruction of in vivo bioluminescent sources based on multispectral imaging. J Biomed Opt. 2007;12:024007.
46. Vinkenoog R, Speranca MA, van BO, Ramesar J, Williamson DH, et al. Malaria parasites contain two identical copies of an elongation factor 1 alpha gene. Mol Biochem Parasitol. 1998;94:1–12.
47. Bates MD, Meshnick SR, Sigler CI, Leland P, Hollingdale MR. In vitro effects of primaquine and primaquine metabolites on exoerythrocytic stages of Plasmodium berghei. Am J Trop Med Hyg. 1990;42:532–537.
48. Shanks GD, Oloo AJ, Aleman GM, Ohrt C, Klotz FW, et al. A new primaquine analogue, tafenoquine (WR 238605), for prophylaxis against Plasmodium falciparum malaria. Clin Infect Dis. 2001;33:1968–1974.
49. Francois G, Steenackers T, Timperman G, Ake AL, Haller RD, et al. Retarded development of exoerythrocytic stages of the rodent malaria parasite Plasmodium berghei in human hepatoma cells by extracts from Dioncophyllaceae and Ancistrocladaceae species. Int J Parasitol. 1997;27:29–32.
50. Most H, Montuori WA. Rodent systems (Plasmodium berghei-Anopheles Stephensi) for screening compounds for potential causal prophylaxis. Am J Trop Med Hyg. 1975;24:179–182.
51. Peters W, Robinson BL, Milhous WK. The chemotherapy of rodent malaria. LI. Studies on a new 8-aminoquinoline, WR 238,605. Ann Trop Med Parasitol. 1993;87:547–552.
52. Fidock DA, Rosenthal PJ, Croft SL, Brun R, Nwaka S. Antimalarial drug discovery: efficacy models for compound screening. Nat Rev Drug Discov. 2004;3:509–520.
53. Parvanova I, Epiphanio S, Fauq A, Golde TE, Prudencio M, et al. A small molecule inhibitor of signal Peptide peptidase inhibits Plasmodium development in the liver and decreases malaria severity. PLoS ONE. 2009;4:e5078.
54. Sturm A, Graewe S, Franke-Fayard B, Retzlaff S, Bolte S, et al. Alteration of the parasite plasma membrane and the parasitophorous vacuole membrane during exo-erythrocytic development of malaria parasites. Protist. 2009;160:51–63.
55. Janse CJ, Ramesar J, Waters AP. High-efficiency transfection and drug selection of genetically transformed blood stages of the rodent malaria parasite Plasmodium berghei. Nat Protoc. 2006;1:346–356.
56. Rettig GR, McAnuff M, Liu D, Kim JS, Rice KG. Quantitative bioluminescence imaging of transgene expression in vivo. Anal Biochem. 2006;355:90–94.
57. Sturm A, Amino R, van de SC, Regen T, Retzlaff S, Rennenberg A, et al. Manipulation of host hepatocytes by the malaria parasite for delivery into liver sinusoids. Science. 2006;313:1287–1290.
58. Baer K, Klotz C, Kappe SH, Schnieder T, Frevert U. Release of hepatic Plasmodium yoelii merozoites into the pulmonary microvasculature. PLoS Pathog. 2007;3:e171.
59. Sadikot RT, Blackwell TS. Bioluminescence imaging. Proc Am Thorac Soc. 2005;2:537–2.

60. Welsh DK, Kay SA. Bioluminescence imaging in living organisms. Curr Opin Biotechnol. 2005;16:73–78.
61. Mota MM, Rodriguez A. Invasion of mammalian host cells by Plasmodium sporozoites. Bioessays. 2002;24:149–156.

Supplementary Information

Supplementary Table S1

		RTqPCR	Lumina	Luminometer
		HepG2, Ei: 25K, 50K, 75K spz at 24h		
RTqPCR	ρ	1,00	0,80**	0,52
	N	12	12	12
Lumina	ρ	0,80**	1,00	0,61*
	N	12	12	12
Microplate reader	ρ	0,52	0,61*	1,00
	N	12	12	12
		HepG2, Eii: 25K, 50K, 75K spz at 30h		
RTqPCR	ρ	1,00	0,88**	0,92**
	N	10	10	10
Lumina	ρ	0,88**	1,00	0,85**
	N	10	12	12
Microplate reader	ρ	0,92**	0,85**	1,00
	N	10	12	12
		HepG2, Eiii: 25K, 50K, 75K spz at 48h		
RTqPCR	ρ	1,00	0,83*	0,78
	N	6	6	6
Lumina	ρ	0,83*	1,00	0,93*
	N	6	6	6
Microplate reader	ρ	0,78	0,93*	1,00
	N	6	6	6
		Huh7: 5K, 30K, 75K spz at 48h		
RTqPCR	ρ	1,00	0,83*	0,87**
	N	11	8	11
Lumina	ρ	0,83*	1,00	0,95**
	N	8	9	9
Microplate reader	ρ	0,87**	0,95**	1,00
	N	11	9	12
		Huh7: 4, 18, 25, 42 hpi; 30K spz		
RTqPCR	ρ	1,00	0,94*	0,98*
	N	11	11	11
Lumina	ρ	0,94*	1,00	0,93**
	N	11	12	12
Microplate reader	ρ	0,93*	0,93**	1.00
	N	11	12	12

* Correlation is significant at the 0,05 level (2-tailed)

** Correlation is significant at the 0,01 level (2-tailed)

Supplementary Table S2.
Correlation coefficient data (ρ, two-tailed Spearman's rho test) of the luminescence data (Lumina and Microplate reader) and the RT-qPCR data presented in Figure 2E.

		RTqPCR	Lumina	
			Whole body	Extracted liver
RTqPCR	ρ	1,00	0,95**	0,65*
	N	16	15	11
Lumina whole body	ρ	0,95**	1,00	0,80**
	N	15	15	11
Lumina extracted liver	ρ	0,65*	0,80**	1,00
	N	11	11	11

* Correlation is significant at the 0,05 level (2-tailed)
** Correlation is significant at the 0,01 level (2-tailed)

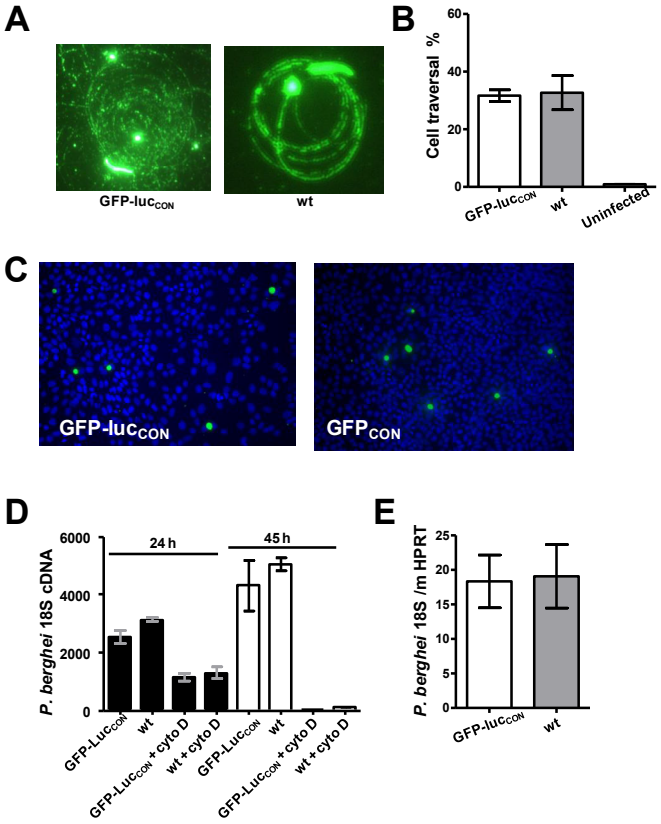

Supplementary Figure S1

Analyis of sporozoite motility, cell traversal and infectivity of *Pb*GFP-Luc$_{con}$ **A)** Representative immunofluorescence staining with anti-*Pb*CSP [61] of the trails produced by *Pb*GFP-Luc$_{con}$ (left) and wildtype sporozoites (right). Characteristic circles of gliding motility are observed in *Pb*GFP-Luc$_{con}$ sporozoites. **B)** Cell traversal ability of wildtype and *Pb*GFP-Luc$_{con}$ sporozoites as determined by FACS counting of Dextran positive Huh7 cells. FACS counting was performed 3 h after infection of Huh7 cells with 6×10^4 sporozoites. Uninfected: hepatocytes cultured in the presence of Dextran but without the addition of sporozoites. **C)** Infection of Huh7 cells on coverslips using 3×10^4 *Pb*GFP-Luc$_{con}$ (left) and *Pb*GFP$_{con}$ [39] (right) sporozoites. After fixing and staining, similar numbers of exoerythrocytic forms are observed at 48 h post infection for both parasites. **D)** qRT-PCR quantification of *in vitro* invasion of HepG2 cells by wild type and *Pb*GFP-Luc$_{con}$ at 24 h (black bars) and at 45 h post invasion (white bars). Cyto D: cultures with cytochalasin-D. **E)** qRT-PCR quantification of liver invasion in mice of wild type and *Pb*GFP-Luc$_{con}$ sporozoites. qRT-PCR was performed on material from livers collected at 43 h after infection of the mice with 3×10^4 sporozoites. The pre-patent period, defined as the days between injection of sporozoites and a blood infection with a parasitemia of 0.5–2%, was 4.2 days (range 4–5 days) for *Pb*GFP-Luc$_{con}$ compared to 4.4 days (range 4–5) for wild type parasites after injection of 1×10^4 sporozoites. After injection of 1×10^4 sporozoites the pre-patent periods were 5.3 days (range 5–6) for *Pb*GFP-Luc$_{con}$ and 5.5 days (range 5–6) for wildtype parasites.

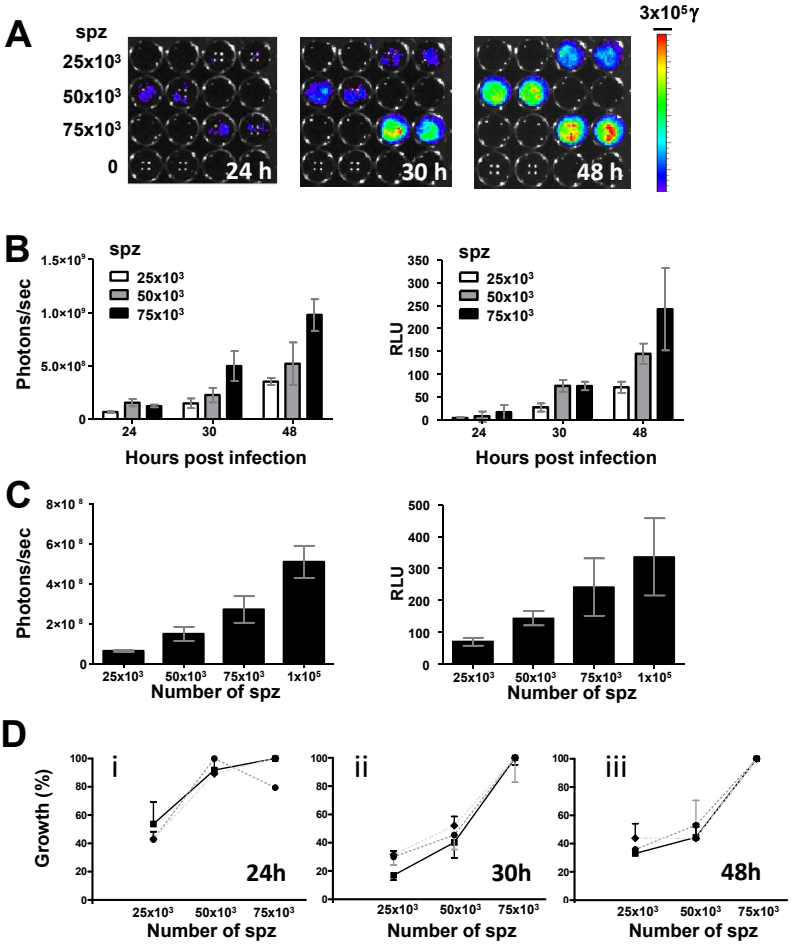

Supplementary Figure S2

Analysis of *in vitro* liver stage development in HepG2 cells by determination of luciferase expression (luminescence). **A)** Relationship between the numbers of sporozoites used to infect hepatocyte cultures and the luminescence produced by the liver stages at 24, 30 and 48 h after infection. Luminescence levels were measured using the Lumina system (Photons/sec). **B)** Relationship between the numbers of sporozoites used to infect hepatocyte cultures and the luminescence produced by the liver stages at 24, 30 h, 48 h after infection. Luminescence levels were measured using the Lumina system (Photons/sec) and a Wallac microplate reader (Relative light units, RLU), respectively. **C)** Relationship between the numbers of sporozoites used to infect hepatocyte cultures and the luminescence produced by the liver stages at 30 after infection. Luminescence levels were measured using the Lumina system (Photons/sec) and a Wallac microplate reader (Relative light unit, RLU), respectively. **D)** Correlation between luminescence values and 18S rRNA levels. Luminescence values were determined using the Lumina system and the Wallac microplate reader (see C). *P. berghei* 18S rRNA levels were determined by qRT-PCR of hepatocyte cultures infected with different numbers of sporozoites. The percentage of growth is normalized to the highest reading within each experiment. See Table S1 for the correlation coefficient data of the two-tailed Spearman's rho test.

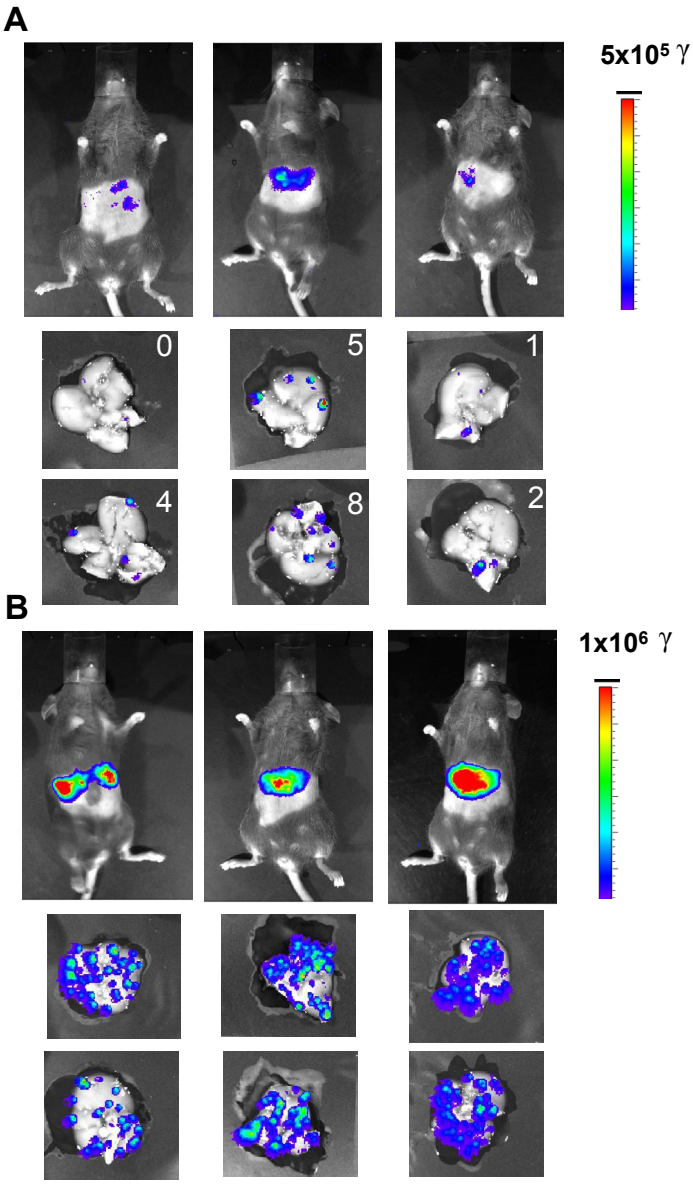

Supplementary Figure S3
Imaging of whole bodies and dissected livers (IVIS100) of mice at 44 h after infection by 1×10^3 **(A)** or 1×10^4 sporozoites **(B)**. Dissected livers were imaged at both sides. Numbers in the pictures of Panel A show the number of luminescent spots identified.

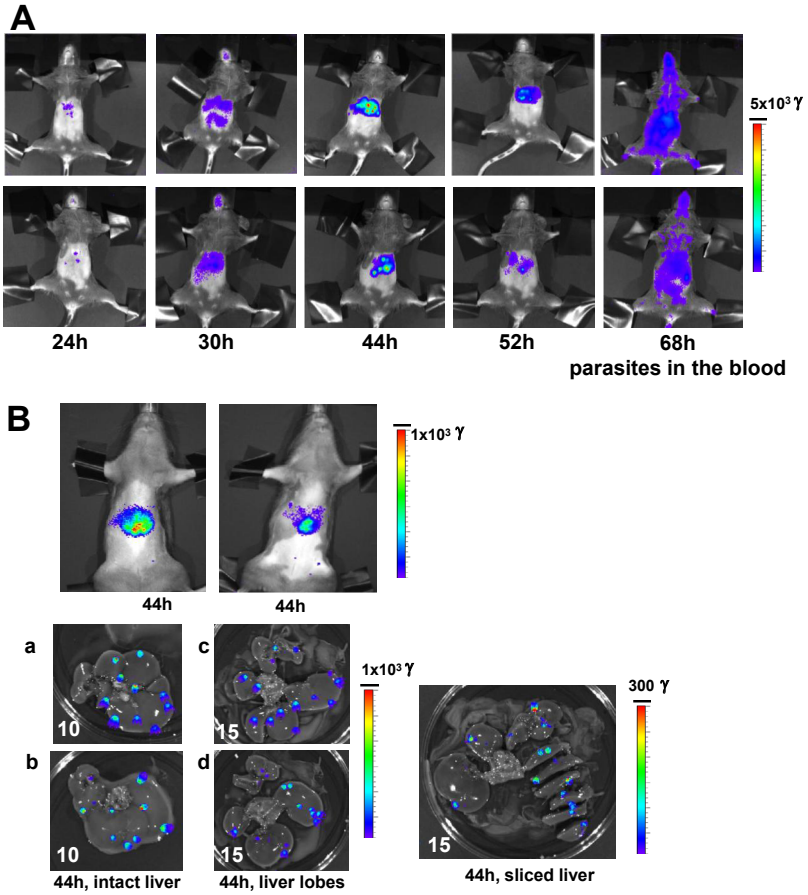

Supplementary Figure S4

A) Whole body imaging (IVIS100) of two representative mice during the period of 24–68 h after infection by bites of 20 infected mosquitoes, showing a strong increase of luminescence intensity of the liver during the period of 30–44 h after infection and a subsequent decrease after 52 h in the liver. The strong increase in luminescence of the whole body at 68 h is the result of the dissemination of the liver merozoites released into the bloodstream and subsequent invasion of erythrocytes. Rainbow images show the relative level of luminescence ranging from low (blue), to medium (green), to high (yellow/red). **B)** Imaging of whole bodies and extracted livers (IVIS100) of Wistar rats at 44 h after infection by bites of 1 or 5 infected mosquitoes. Extracted livers were measured at both sides **(a, b)** and lobes **(c)** and small sliced liver pieces **(d)** were analysed for additional luminescence spots. Numbers in the images represent the number of luminescent spots identified.

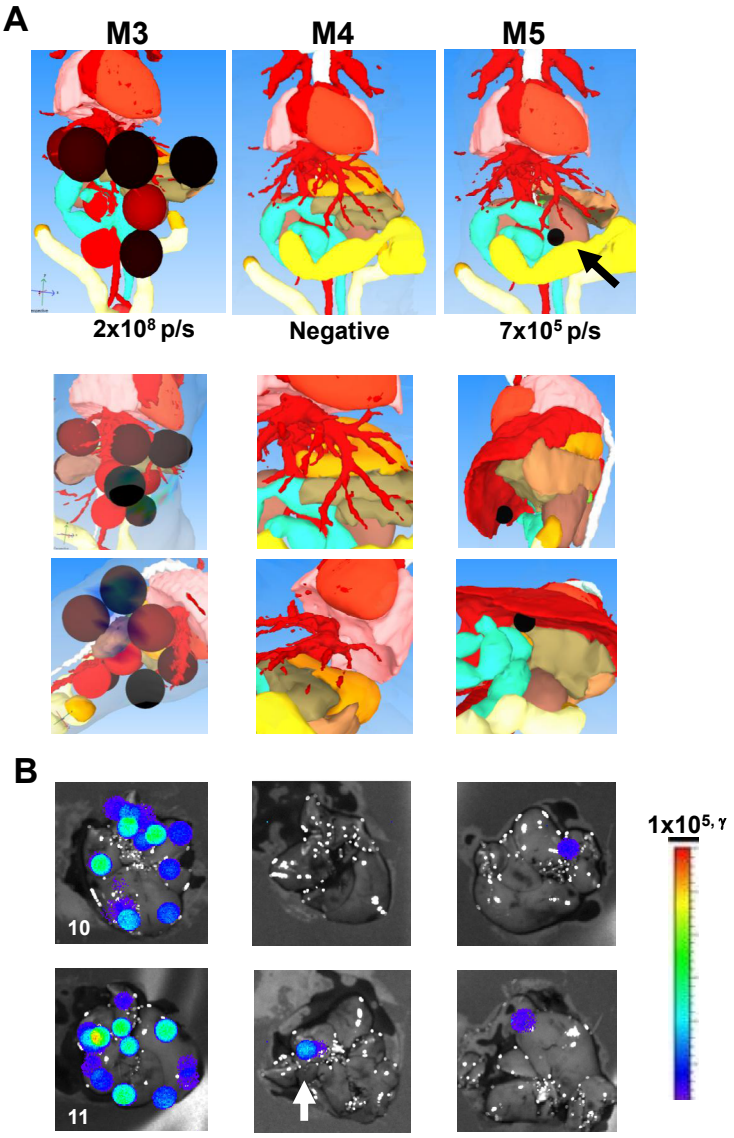

Supplementary Figure S5

A) Source reconstruction of 3D whole body imaging of three mice at 44 h after infection by bites of 5–10 infected mosquitoes. Eleven luminescent sources are detected in mouse 3 (M3), one in mouse 5 (M5) and none in mouse 4 (M4). See also Supplementary Movies 2 and 3 (online version) corresponding to mouse 3 and 5 respectively. **B)** 2D-imaging of the extracted livers of the mice shown in panel A. Livers were imaged at both sides using the IVIS Spectrum system. Numbers in the images represent the number of luminescent spots identified. Rainbow images show the relative level of luminescence ranging from low (blue), to medium (green), to high (yellow/red)

Chapter 3

Evaluation of immunity against malaria using luciferase-expressing *Plasmodium berghei* parasites.

Ivo Ploemen, Marije Behet, Krystelle Nganou-Makamdop, Geert-Jan van Gemert, Else Bijker, Cornelus Hermsen, Robert Sauerwein

Malar Journal 2011 Dec 9;10:350.

Abstract

Measurement of liver stage development is of key interest in malaria biology and vaccine studies. Parasite development in liver cells can be visualized in real-time, both in culture and in live mice, using a transgenic *Plasmodium berghei* parasite, *Pb*GFP-Luc$_{con}$, expressing the bioluminescent reporter luciferase. This study explores the benefit of using these parasites for the evaluation of immunity against malaria, compared to qRT-PCR techniques *in vivo* and *in vitro*. Mice were immunized with either radiation attenuated sporozoites (RAS) or wildtype sporozoites under chloroquine prophylaxis (CPS) and challenged with *Pb*GFP-Luc$_{con.}$ The *in vitro* transgenic sporozoites neutralization assay (TSNA) was adapted by replacing *Pb*CS(Pf) parasites for *Pb*GFP-Luc$_{con}$ parasites. Application of *Pb*GFP-Luc$_{con}$ transgenic parasites provides live quantitative visual information about the relation between parasite liver load and protection. Moreover, fast and reproducible results are obtained by using these parasites in the transgenic sporozoite neutralization assay, measuring functional antibody-mediated immune response. *Pb*GFP-Luc$_{con}$ parasites are a straightforward and valuable tool for comprehension of the biological and immunological principles underlying protection against malaria.

Introduction

Transgenic organisms that express a bioluminescent reporter are increasingly used due to easy handling and visualization. *Plasmodium berghei* parasites, expressing the bioluminescent reporter luciferase (*Pb*GFP-Luc$_{con}$) have been used to visualize and quantify parasite development *in vitro* in hepatic cells and *in vivo* in mice using real-time luminescence imaging [1].

Measurement of liver stage development is of key interest in malaria biology and vaccine studies. Protection against the liver stage is one of the targets to abrogate the infection. Quantification of the number of parasites in hepatocytes is an important read-out to determine inhibitory activity. This quantification of *in vitro* [2] and *in vivo* [3] parasite liver load is usually performed by (qRT)-PCR. This technique, however, is time-consuming and costly, since mice need to be sacrificed at each time point for *in vitro* quantification.

The use of *in vivo* and *in vitro* imaging of luciferase expressing parasites has some requisites. First, it requires that the luciferase expressing parasites are qualitative and quantitative biologically comparable to wildtype in terms of liver and blood infectivity. Second, the *in vivo* and *in vitro* parasite quantification by measurement of luminescence signaling needs to correlate to the established qRT-PCR methods. Previously we showed that the *P. berghei* line 676m1cl1 line (*Pb*GFP-Luc$_{con}$) and wildtype (WT) sporozoites have identical motility, cell traversal and *in vitro* and *in vivo* hepatocyte infectivity. Moreover, detailed examination revealed that luciferase expression correlated tightly with parasite 18S rRNA levels measured by qRT-PCR [1]. Therefore, this transgenic parasite seems suitable for a quantitative analysis of parasite load.

This study aimed to explore the use of *Pb*GFP-Luc$_{con}$ parasites in both *in vivo* and *in vitro* studies evaluating immunity against malaria. For the *in vivo* studies, mice were immunized with either radiation attenuated sporozoites (RAS) or wildtype sporozoites under chloroquine prophylaxis (CPS) and subsequently challenged with *Pb*GFP-Luc$_{con}$. For the *in vitro* studies, the transgenic sporozoites neutralization assay (TSNA) was adapted by replacing *Pb*CS(Pf) parasites for *Pb*GFP-Luc$_{con}$ parasites [2].

Material and Methods

Mice

Female C57BL6/J mice, eight weeks of age, were purchased from Elevage Janvier (France). All studies have been performed according to the regulations of the Dutch "Animal On Experimentation act" and the European guidelines 86/609/EEG. Approval was obtained from the Radboud University Experimental Animal Ethical Committee (RUDEC 2009-019).

Mosquito infection and preparation of sporozoites

The previously described, transgenic *P. berghei* line 676m1cl1 line (*Pb*GFP-Luc$_{con}$) [1] and its reference clone of ANKA strain cl15cy1, were used in this study. *Anopheles stephensi* mosquitoes were infected by feeding on infected mice using standard methods of mosquito infection [4]. On day 21 after infection, the salivary glands of the mosquitoes were collected by hand-dissection. Salivary glands were collected in DMEM (Dulbecco's Modified Eagle Medium from GIBCO) and homogenized in a homemade glass grinder. The free sporozoites were counted in a Bürker-Türk counting chamber using phase-contrast microscopy.

Immunization of mice with radiation attenuated sporozoites (RAS) or sporozoites under chloroquine prophylaxis (CPS)

C57BL/6 mice were immunized with wildtype *P. berghei* radiation attenuated sporozoites (RAS) or sporozoites under chloroquine prophylaxis (CPS). Immunizations were performed by i.v injection with three doses of 1×10^4 (RAS and CPS) or 4×10^3 (CPS) sporozoites, with a 7 day interval between the boosts. For CPS immunization, mice received 800 µg chloroquine base (cq-diphosphate Sigma) in PBS i.p, starting from sporozoite injection up to two weeks after the last immunization. Absence of blood stage parasites was confirmed by examination of Giemsa-stained blood smears of tail blood at the end of the chloroquine treatment period and approximately 1 day before challenge. Mice were challenged two weeks after ending choroquine treatment. Irradiation of sporozoites was performed by exposure of infected *A. stephensi* mosquitoes to 16,000 rad of γ-radiation (Cesium-137 Gammacel 1000).

Challenge and real-time *in vivo* imaging of liver stage development in RAS and CPS immunized mice

Immunized and control C57BL/6 mice were challenged by the bite of 5-11 infectious mosquitoes or by intravenous injection of 1×10^4 *Pb*GFP-Luc$_{con}$ sporozoites in the tail (200 ul). Control mice consisted of two groups, group 1 received chloroquine similar to the CPS immunized mice and group 2 did not receive chloroquine. Giemsa stained bloodsmears were prepared every other day starting from day 3 to day 21 after challenge, to monitor for blood stage parasitaemia. Parasite liver load in animals was visualized through imaging of whole bodies using the *in vivo* imaging system Lumina (Caliper Life Sciences, USA) as described [1], with some small adaptations. Briefly, animals were anesthetized using the isofluorane-anesthesia system, their belly was shaved and D-luciferin dissolved in PBS (100

mg/kg; Caliper Life Science, Belgium) was injected subcutaneously (in the neck). Animals were kept anesthetized during the measurements, performed within 3-5 minutes after the injection of D-luciferin. Bioluminescence imaging was performed with a 10 cm field of view, medium binning factor and an exposure time of 300 seconds. Bioluminescent intensities were expressed in total flux of photons.

Real-time transgenic *Pb*GFP-Luc$_{con}$ sporozoites neutralization assay

The TSNA (transgenic sporozoites neutralization assay) protocol was adapted from Kumar *et al.* (Figure 1). Plasma was obtained from immunized (three doses of 1×10^4;RAS and CPS) and naive C57BL/6 mice, 21 days post challenge by mosquito bite; blood was collected by heart puncture after i.v. injection of 50 i.u. of heparin. Blood samples were centrifuged at 2000 rpm for 5 minutes (RT), plasma was collected and transferred to cryotubes (Nunc) and stored at -80°C for later use. Prior to the TSNA assay, plasma samples were thawed and centrifuged at 13,000 rpm for one minute (RT) to remove protein aggregates. *Pb*GFP-Luc$_{con}$ sporozoites were pre-incubated for 30 minutes on ice with plasma of naive or immunized mice (1:1 ratio). Pre-incubated sporozoites were added to wells containing monolayers of 1×10^5 pre-seeded Huh-7 hepatocyte cultures (1 ml/well in 24 well plates). Huh-7 cells (human liver hepatoma cells) were preferred over standard HepG2 cells [2] since in these cells, luciferase expression correlated slightly better with parasite 18S rRNA levels measured by qRT-PCR [1]. Huh-7 were suspended in 1 ml of 'complete' DMEM (DMEM, Gibco, supplemented with 10% FCS, 1% penicillin/streptomycin and 1% Glutamax) the day prior to infection, seeded in 24 well plates (10^5 cells/well) and incubated overnight. For each plasma sample, 3×10^4 sporozoites each were added to duplicate wells and plates were centrifuged 10 minutes at 1800 × g (Eppendorf centrifuge 5810 R). 40 hours after sporozoite addition, cells were washed once with PBS and lysed in 200 µl of cell culture lysis reagent obtained from the Promega Luciferase Assay System Kit® (Promega, PT). Samples in Promega lysis buffer were either stored at -80°C or processed immediately to measure luminescence intensity with the Lumina system. The *in vivo* imaging system Lumina (Caliper Life Sciences, USA) was used to measure luciferase activity of infected Huh-7 cells. Quantitative analysis was performed by measuring the luminescence signal intensity per well using the ROI settings of the Living Image® 3.0 software. ROI measurements are expressed in total flux of photons. 70 µl of Luciferase Assay Substrate (Promega Luciferase Assay System Kit®) was added to 20 µl of lysed hepatocyte cultures in a white 96-well plate (Dynex Technologies, USA). Bioluminescence images were acquired with a 7 cm FOV, medium binning factor and an exposure time of 10-30 seconds. Percent inhibition was calculated by the following formula; 1 - (average bioluminescence in immune plasma cultures/average bioluminescence in naive plasma cultures) × 100%.

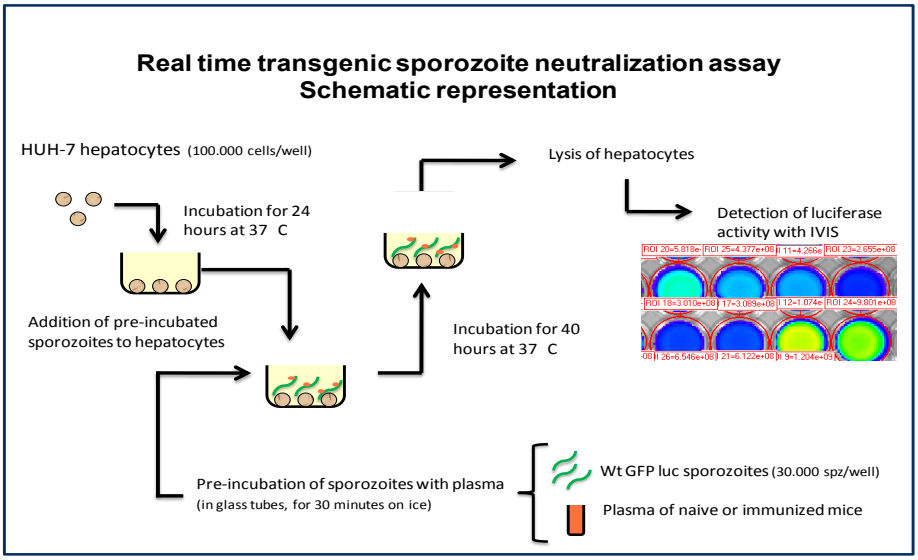

Figure 1. Schematic representation of the adapted transgenic *Pb*GFP-Luc$_{con}$ sporozoite neutralization assay.

Neutralization of hepatocyte invasion by transgenic sporozoites was performed by incubation of naive or immune plasma obtained from (non-) immunized mice with the transgenic sporozoites. Neutralization was performed for 30 minutes on ice before the antibody/sporozoites mix was added to Huh-7 cells containing wells and incubated for 40 h at 37°C. This figure is adapted from figure 1 described by Kumar et al. [2]

Results

Challenge of immunized mice with *Pb*GFP-Luc$_{con}$ sporozoites

Mice immunized with CPS or RAS as well as control mice were challenged by *Pb*GFP-Luc$_{con}$ infected mosquitoes and protection against malaria was evaluated by blood smear reading and real-time *in vivo* imaging. All control challenged mice (n = 10) developed asexual parasitaemia and a positive bioluminescent liver signal by real-time *in vivo* imaging at 44 hours post challenge (Figure 2a). All mice immunized by CPS (n = 10) or RAS (n = 10) with a dose regimen of three times 10^4 sporozoites and challenged by infectious mosquito bites, neither became parasitaemic nor displayed any bioluminescent signal originating from the liver (Figure 2a). Next, the robustness of protective immunity was explored by increasing the challenge level in mice that were immunized with CPS by a lower dose regimen of three times

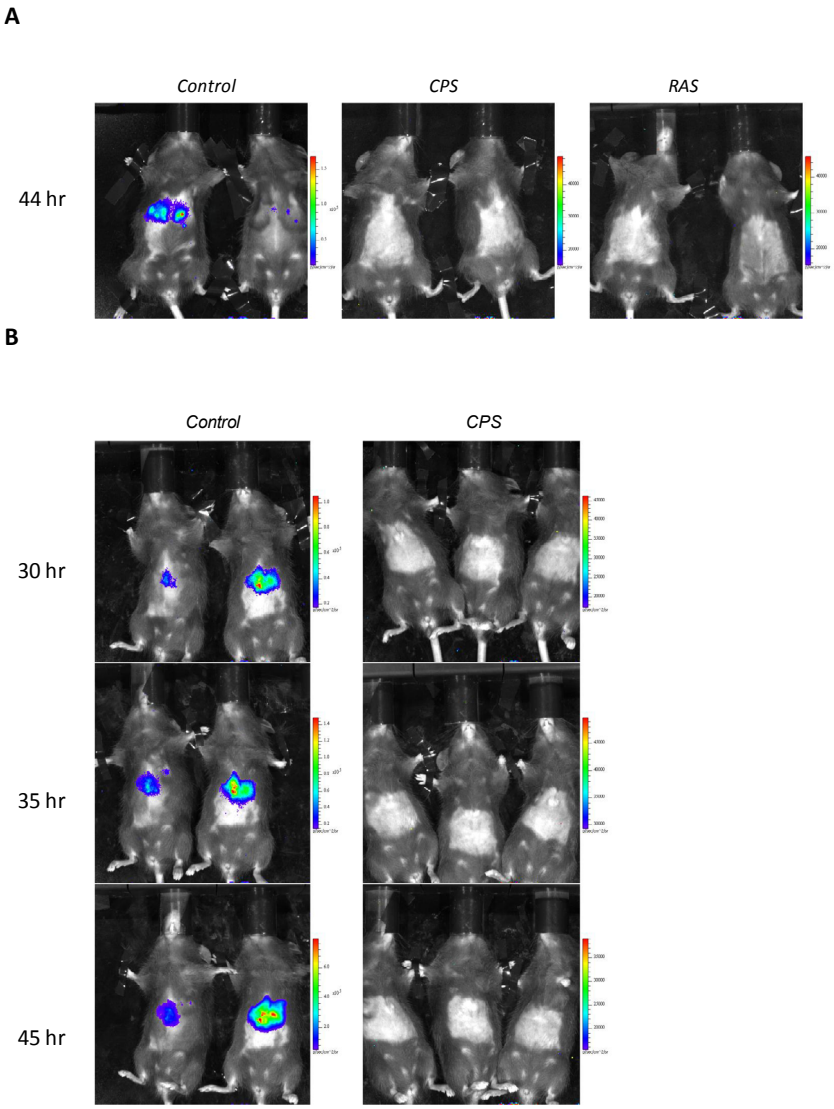

Figure 2. Real-time *in vivo* parasite liver load upon challenge in mice immunized with CPS or RAS.

A) Image (2 representative mice for each group) of the parasite liver load in control (n = 10), CPS (n = 10) and RAS immunized (n = 10) C57BL/6 mice 44 hours post challenge. Mice were immunized i.v with 1×10^4 sporozoites followed by two boosts of 1×10^4 sporozoites. Challenge was performed by infectious mosquito bites. The rainbow image visible in the naive mice represents the total flux of photons (p/sec/cm2) in that area. **B)** Image (2 control mice and 3 immunized mice) of the parasite liver load in control (n = 3) and CPS immunized (n = 5) C57BL/6 mice 30-45 hours post challenge. Mice were immunized with 4×10^3 sporozoites by i.v injection followed by two boosts of 4×10^3 sporozoites. Challenge was performed by injection of 1×10^4 *Pb*GFP-Luc$_{con}$ sporozoites i.v. The rainbow image visible in the control mice represents the total flux of photons (p/sec/cm2) in that area.

4×10^3 sporozoites. Mice were challenged by i.v injection of 1×10^4 *Pb*GFP-Luc$_{con}$ sporozoites and all immunized mice remained negative. These results are in line with the data obtained by *in vivo* imaging; mice immunized with CPS showed no bioluminescent signal, in contrast to control mice, with positive images at 30 to 45 hours post challenge (Figure 2b). Therefore, the use of *Pb*GFP-Luc$_{con}$ in a challenge model, combined with bioluminescent imaging permits determination of protective efficacy in the liver post-immunization.

Real-time transgenic *Pb*GFP-Luc$_{con}$ sporozoites neutralization assay

To evaluate the potential benefits of *Pb*GFP-Luc$_{con}$ for assessment of protection *in vitro*, we adapted the transgenic sporozoite invasion inhibition assay (TSNA) as performed by Kumar *et al.* [2] by replacing the *Pb*CS(Pf) sporozoites with *Pb*GFP-Luc$_{con}$ sporozoites. The use of bioluminescent parasites in the TSNA has some requisites. Recently, Ploemen *et al.* described the highly significant quantitative correlation between parasite 18S rRNA levels measured by qRT-PCR and luminescence intensity for different numbers of *Pb*GFP-Luc$_{con}$ sporozoites invaded into Huh-7 hepatocytes (Spearman rho = 0.83) [1]. As a follow-up of these results, a dose titration with 10 - 50.000 *Pb*GFP-Luc$_{con}$ sporozoites, added to a Huh-7 hepatocyte culture was performed and bioluminescent intensity was measured 40 hrs post invasion (Figure 3a). Luminescent intensities increased linear ($R^2 = 0.97$) with the number of *Pb*GFP-Luc$_{con}$ sporozoites added to a Huh-7 hepatocyte culture. These parasites, therefore, may be used in an adapted TSNA. Plasma from protected C57BL/6 mice was used in the adapted TSNA, after CPS or RAS immunization. Invasion of Huh-7 cells by *Pb*GFP-Luc$_{con}$ sporozoites pre-incubated with plasma of protected mice was significantly inhibited compared to invasion by sporozoites pre-incubated with plasma of naive mice ($p < 0.05$) (Figure 3b). Further, 1:1 diluted plasma (in PBS), showed about half of the inhibition level of the original plasma (data not shown). Inhibition of sporozoites by purified plasma IgG of protected mice resulted in a similar inhibition level as non-purified plasma (data not shown). Although the % inhibition between individual plasma samples differs between mice, the duplicates of one plasma sample diverged at most on average 4% of the mean value of that sample (n = 21). These results show that this adapted TSNA is a more user friendly methodology, allowing identification of antibody-mediated inhibition of parasite liver invasion.

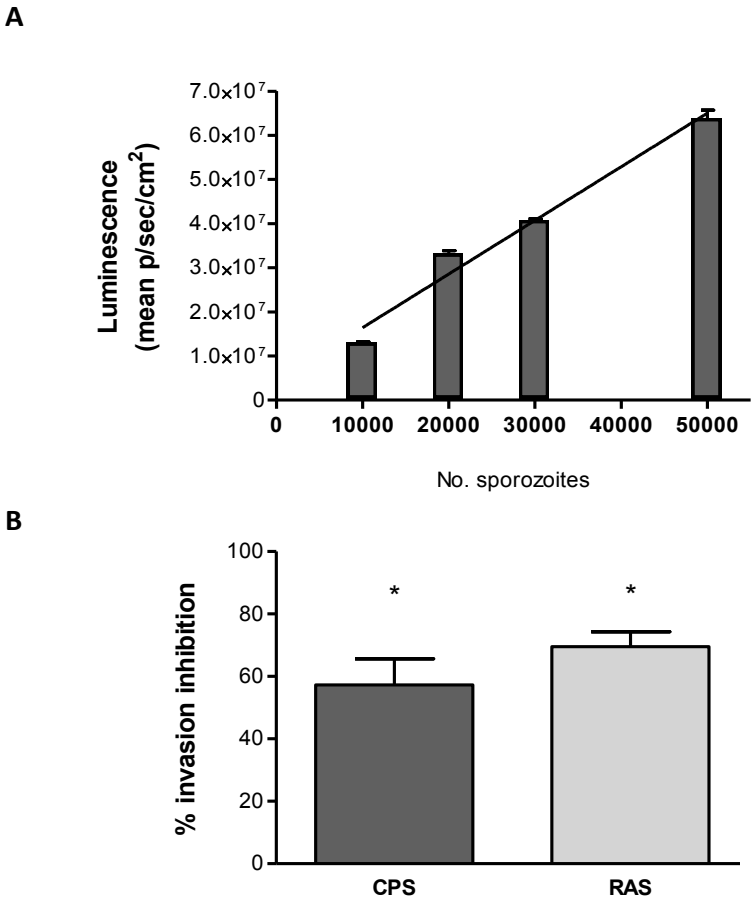

Figure 3. Transgenic *Pb*GFP-Luc$_{con}$ sporozoite hepatocyte invasion inhibition assay.
A) Huh-7 cells were seeded in 24 well plates and were grown to confluency as described in Materials and Methods. Graded numbers of *Pb*GFP-Luc$_{con}$ sporozoites were added to the culture wells in duplicate and incubated for 40 h at 37 C in 5% CO2. Infectivity was quantified by analyzing the luminescent flux (p/sec/cm2) in each well. **B)** Invasion inhibition of sporozoites by plasma from CPS (n = 6) and RAS (n = 7) immunized mice. 30.000 *Pb*GFP-Luc$_{con}$ sporozoites were incubated in plasma of naive or immune mice for 30 min on ice and subsequently added to Huh-7 cells. Infectivity was quantified by analyzing the luminescent flux (p/sec/cm2) in each well. The baseline represents the inhibition level of plasma from naive mice (approximately 4 × 10^7 p/sec/cm^2). Percent inhibition was calculated by the following formula; 1 - (average bioluminescence in immune plasma sample/average bioluminescence in naive plasma sample) × 100%. The level of invasion inhibition in the immunized mice was significantly higher compared to the inhibition from the plasma of naive mice (95% CI CPS 36-79%; 95% CI RAS 58-81%).

Discussion

This study shows that *Pb*GFP-Luc$_{con}$ parasites, can provide real-time quantitative information on the relation between *in vivo* parasite liver load and immunity against malaria. *In vitro* use of these parasites in the adapted TSNA allows for an easy and fast assessment of the functional sporozoite invasion inhibition by antibodies.

Previously, Mwakingwe *et al.* applied bioluminescent imaging and qRT-PCR to analyse parasite prevalence in the liver of immunized mice, using luciferase expressing *P. yoelii* [5]. They did not, however, report on the direct quantitative relation between bioluminescent imaging and parasite (liver) load determined by qRT-PCR and the extent to which the transgenic parasite had similar characteristics as the WT parasite throughout the whole life cycle [5]. In the future, a *Py*-Luc parasite that meets these requisites for assessment of the liver load upon challenge, can be used beside *Pb*GFP-Luc$_{con}$ parasites, allowing for a direct comparison of the characteristics of *P. yoelii* and *P. berghei in vivo*.

Evaluation of immunity against malaria by bioluminescent imaging offers many advantages over conventional qRT-PCR analysis. This analysis technique is more simple, rapid and reduces the amount of mice needed. As an added value, expression of the reporter protein luciferase is restricted to live parasites and therefore allows specific detection of live parasites. This avoids detection of dead liver parasites, as may occur by the qRT-PCR assay [1]. Measurement of parasite liver load upon challenge can be performed *in vivo* without the need for any invasive liver resection or biopsy. It does not require sacrificing animals and thereby reduces the number of animals and costs required for experimentation. Moreover, multiple measurements can be carried out in the same animal over time, linking the parasite liver load with protection and minimizing the effect of biological variation [6,7]. While the use of *Pb*GFP-Luc$_{con}$ over qRT-PCR has its clear benefits, there are limitations. The expression of luciferase in the parasite is relatively low and cannot be visualized earlier than 20 hours post-infection [1]. Moreover, due to limitations in sensitivity, a low number of developing liver parasites may be missed which might mature into asexual parasites [1]. Negative results of *in vivo* imaging of liver stage development can therefore not be used to claim sterile protection, which eventually requires sub-inoculation of blood from challenged mice into naive mice [3]. Nonetheless, challenge of mice with a high number of *Pb*GFP-Luc$_{con}$ sporozoites administered i.v does offer information on the parasite liver load in real-time without sacrifying the mice. In the CPS model the overwhelming majority of the parasites do not develop

in the liver beyond 30 hours. The presence of effector mechanisms that target early developing parasite stages can however, not formally be excluded. At least in this model with complete liver stage development, a high degree of immunity to late liver stage parasites can clearly be inferred.

Finally, the application of *Pb*GFP-Luc$_{con}$ parasites is not restricted to the described assays. In a recent publication describing the host mediated factors regulating the inhibition of liver stage infection upon superinfection, luciferase expressing parasites were used to enable distinction between the parasites from the original infection and the superinfection [8].

Conclusions

With clear benefits over conventional RT-qPCR techniques, *Pb*GFP-Luc$_{con}$ parasites can function as an easy and valuable tool contributing to the comprehension of the immunological principles underlying immunity against malaria. As such, these parasites can be helpful in future studies evaluating protection against malaria.

List of abbreviations

*Pb*GFP-Luc$_{con}$: *Plasmodium berghei* that constitutively express firefly Luciferase and the Green fluorescent protein; *Pb*CS(pf): *Plasmodium berghei* that bears the *Plasmodium falciparum* CS repeats; TSNA: Transgenic sporozoite neutralization assay; RAS: Radiation attenuated sporozoites; CPS: Sporozoites under chloroquine prophylaxis; ROI: Region of interest; q-RTPCR: quantitative real-time polymerase chain reaction; IVIS: in vivo imaging system.

Acknowledgements

We would like to thank Claudia Lagarde for the technical assistance with the mouse infections and Anja Scholzen for critical revision of the manuscript.

References

1. Ploemen IH, Prudencio M, Douradinha BG, Ramesar J, Fonager J, et al. (2009) Visualisation and quantitative analysis of the rodent malaria liver stage by real time imaging. PLoS One 4: e7881.
2. Kumar KA, Oliveira GA, Edelman R, Nardin E, Nussenzweig V (2004) Quantitative Plasmodium sporozoite neutralization assay (TSNA). J Immunol Methods 292: 157-164.
3. Belnoue E, Voza T, Costa FT, Gruner AC, Mauduit M, et al. (2008) Vaccination with live Plasmodium yoelii blood stage parasites under chloroquine cover induces cross-stage immunity against malaria liver stage. J Immunol 181: 8552-8558.
4. Sinden R (1997) Infection of mosquitoes with rodent malaria. In molecular biology of insect disease vectors: a method manual 67-91.

5. Mwakingwe A, Ting LM, Hochman S, Chen J, Sinnis P, et al. (2009) Noninvasive real-time monitoring of liver-stage development of bioluminescent Plasmodium parasites. J Infect Dis 200: 1470-1478.
6. Sadikot RT, Blackwell TS (2005) Bioluminescence imaging. Proc Am Thorac Soc 2: 537-540, 511-532.
7. Welsh DK, Kay SA (2005) Bioluminescence imaging in living organisms. Curr Opin Biotechnol 16: 73-78.
8. Portugal S, Carret C, Recker M, Armitage AE, Goncalves LA, et al. (2011) Host-mediated regulation of superinfection in malaria. Nat Med 17: 732-737.

Chapter 4

Assessing the adequacy of attenuation of genetically modified malaria parasite vaccine candidates.

Takeshi Annoura *, Ivo Ploemen *, Ben van Schaijk *, Mohammed Sajid, Martijn Vos, Geert-Jan van Gemert, Severine Chevalley-Maurela, Blandine Franke-Fayard, Cornelus Hermsen, Audrey Gegoc, Jean-Francois Franetich, Dominique Mazier, Stephen Hoffman, Chris Janse, Robert Sauerwein, Shahid Khan

**these authors contributed equally*

Vaccine 30 (2012) 2662-2670

Abstract

The critical first step in the clinical development of a malaria vaccine, based on live-attenuated *Plasmodium falciparum* sporozoites, is the guarantee of complete arrest in the liver. We report an approach for assessing adequacy of attenuation of genetically attenuated sporozoites *in vivo* using the *P. berghei* model of malaria and *P. falciparum* sporozoites cultured in primary human hepatocytes. We show that two genetically attenuated sporozoite vaccine candidates, *Δp52+p36* and *Δfabb/f*, are not adequately attenuated. Sporozoites infection of mice with both *P. berghei* candidates can result in blood infections. We also provide evidence that *P. falciparum* sporozoites of the leading vaccine candidate that is similarly attenuated through the deletion of the genes encoding the proteins P52 and P36, can develop into replicating liver stages. Therefore, we propose a minimal set of screening criteria to assess adequacy of sporozoite attenuation necessary before advancing into further clinical development and studies in humans.

Introduction

Immunization with live sporozoites that are attenuated by radiation (IrrSpz) induces strong protective immunity both in rodent models of malaria and in humans in experimental clinical studies [1;2]. Recently, the interest in a whole-organism vaccine consisting of live attenuated parasites has been renewed as efforts using recombinant subunit vaccines have still been unable to demonstrate sustained, high level sterile immunity [3-6]. In rodent models of malaria it has been shown that attenuation of sporozoites can also be achieved by reverse-genetic methodologies (genetically attenuated parasites, GAP; [7-9]) or by chemical treatment (chemically attenuated parasites; CAS [10;11]). Importantly, immunization of mice with GAP results in protective immune responses that are similar to those induced by IrrSpz, specifically cell mediated responses, critically involving $CD8^+$ T-cells, which provide a long lasting and sterile protection against infection [12-14]. The use of GAP sporozoites that were shown to be safe (no breakthrough infections) and protective as a whole-organism vaccine could have several advantages over IrrSpz and CAS as they would be a homogeneous population of parasites with the potential for a defined attenuation phenotype. This could remove issues related to the delivery of correct doses of either irradiation or drugs in order to ensure sufficient attenuation without killing the parasites. The conceptual basis of vaccines consisting of IrrSpz or GAP is that after inoculation, sporozoites invade but only partially develop in the liver, as it has been shown that only sporozoites that are able to invade hepatocytes induce protective immune responses [15-17]. This sporozoite growth arrest in the liver needs to be complete, as the appearance of 'breakthrough' parasites in the bloodstream can lead to clinical disease and death [18]. As *P. falciparum* only efficiently infects humans, adequacy of attenuation of *P. falciparum* sporozoites cannot be assessed *in vivo* prior to initiating clinical trials. The murine malaria models *P. berghei* and *P. yoelii* are consequently not only used to identify suitable genes for generating GAPs but also to assess the safety and immunogenicity of GAPs. Thereby, these studies establish a road-map for designing *P. falciparum* GAPs and provide information critical in the decision to proceed with trials in humans.

Several different GAPs have been generated in the rodent malaria parasites *P. berghei* and *P. yoelii* that abort development in the liver [7-9;19;20]. These include GAPs that lack genes essential for the formation and maintenance of a parasitophorous vacuole (*p52*, *p36*, *uis3* and *uis4*; [7-9;21]), genes involved in type II fatty acid synthesis (i.e. *fabb/f* and *fabz*; [22;23] and a gene involved in (post-)transcriptional regulation of sporozoite/early liver stage genes (*sap1/slarp*; [19;20;24]). Immunization of mice

with sporozoites of all these GAPs induces, to varying degrees, protection against challenge with wild type (WT) parasites. Some of these GAPs confer protection against WT challenge after a single dose immunization with as few as 1000–10000 attenuated sporozoites [21;25]. Since unequivocal orthologs for the two rodent *uis*-genes are absent in the *P. falciparum* genome (www.PlasmoDB.org) and *P. berghei* GAP lacking SLARP has been reported to induce limited protective immune responses [20], GAPs lacking *p52* and *p36* or genes involved in type II fatty acid synthesis (FAS II) are considered GAP vaccine candidates for translation into the human malaria parasite, *P. falciparum* [18;22;26].

Occasional breakthrough blood infections in mice after immunization with rodent GAPs lacking *uis4* and *p52* [7;9] emphasize the importance of removing multiple genes in the generation of GAPs that are completely attenuated. Infection of mice with high doses of *P. yoelii* sporozoites of a 'double gene deletion' GAP lacking two genes, *p52* and *p36,* showed no breakthrough blood infections in the *P. yoelii* rodent model [21]. Generation of equivalent *P. falciparum* GAPs lacking these genes [27] have provided evidence that these *P. falciparum* GAPs show a comparable attenuation phenotype to the GAPs of rodent malaria parasites. In cultured human hepatocytes and in mice carrying human hepatocytes, these *P. falciparum* GAP abort development in hepatocytes soon after sporozoite invasion. The observations of the growth arrest of *P. yoelii* and *P. falciparum* GAP has led to the production of a *P. falciparum* GAP lacking expression of both P52 and P36 for use in human clinical trials [18;27].

In this study we have analysed the adequacy of attenuation of two GAPs in the rodent model, *P. berghei*, one lacking expression of both P52 and P36 (Δ*p52+p36)* and the other lacking expression of FabB/F (Δ*fabb/f)*. In addition, we have analysed the development of *P. falciparum* Δ*p52+p36* parasites in cultured primary human hepatocytes. The presence of developing liver stages and the development of breakthrough blood infections in mice immunized with both *P. berghei* GAP show that the sporozoites of these GAP are not completely attenuated. Moreover, we provide evidence that the *P. falciparum* Δ*p52+p36* GAP can produce replicating liver stages, indicating that this GAP is also not adequately attenuated. These results clearly indicate that these GAP vaccine candidates require additional refinement before advancing into clinical studies in humans. The high costs and long time frames associated with clinical trials makes them inefficient methods to screen potential whole-organism vaccines against malaria. We therefore propose a robust and stringent screening approach, using multiple rodent malaria parasites and multiple mice strains, to determine the adequacy of GAP attenuation, as the best

available and providing a stringent safety criterion before advancing with further clinical development and studies in humans.

Material and Methods

Attenuated *P. berghei* and *P. falciparum* parasites were generated using standard genetic modification technologies. Adequacy of attenuation of *P. berghei* sporozoites was determined *in vivo* by infecting Swiss OF1, BALB/c and C57BL/6 mice with live attenuated sporozoites collected from infected *Anopheles stephensi*. Development of attenuated parasites was analysed *in vitro* in either cultured Huh7 hepatocytes (*P. berghei*) or in primary human hepatocytes (*P. falciparum*). Liver stage development in mice was determined by real-time *in vivo* imaging of luciferase-expressing parasites. Details of the generation of attenuated parasite lines, analysis of adequacy of attenuation, *in vivo* imaging of liver stage development and *in vitro* analysis of liver stages can be found in Supplementary Material and Methods.

Results

Generation and characterization of two *P. berghei* GAPs, *Δfabb/f* and *Δp52+p36*

Two *P. berghei* gene-deletion mutants (GAP), Δ*fabb/f* and Δ*p52+p36*, were generated using standard methods of gene targeting by double cross-over integration and for each mutant two independent parasite clones were produced (Fig. S1-3; Table S1). For each GAP, one mutant was generated in the *P. berghei* reference reporter line, *Pb*GFP-Luc$_{con}$, which allows for visualisation and counting of GFP-expressing parasites in hepatocytes, *in vitro*, and analysis of liver-stage development in live mice by real-time *in vivo* imaging [38]. The Δ*fabb/f* mutant lacks expression of elongation condensing enzyme 3-oxoacyl-acyl-carrier protein synthase I/II, FabB/F (Fig. 1B), an enzyme of the bacterial-like type II fatty acid biosynthesis (FAS-II) pathway [39]. For *P. yoelii* it has been demonstrated that enzymes of this pathway are highly expressed in sporozoites and liver-stages and FabB/F was shown to be essential for complete development of liver stages [23;26]. The Δ*p52+p36* mutants lack expression of two 6-cys protein family members [21;40-42], P52 and P36 (Fig. 1A). These genes are expressed in sporozoites and liver stages and appear to be important to the formation and/or maintenance of the parasitophorous vacuole membrane in the infected hepatocyte [9;21;42].

The Δ*fabb/f* and Δ*p52+p36* mutants showed normal blood-stage development

(Table S2) and produced oocyst and sporozoite numbers comparable to those of WT parasites (Fig. 1C). Salivary gland sporozoites demonstrated normal gliding motility, hepatocyte traversal and sporozoites of all mutants were able to invade hepatocytes at WT levels (Fig. 1C and 1D). After *in vitro* invasion of hepatocytes, the Δ*p52*+*p36* mutants showed a greater than 90% reduction in liver stage development at 24 hours after sporozoite invasion as determined by qRT-PCR analysis of parasite ribosomal RNA (Fig. 1E). The early growth-arrest of Δ*p52*+*p36* parasites was confirmed by analysis of infected hepatocytes by immuno-fluorescence microscopy after staining with Hoechst and antibodies against the parasite protein HSP70 (Fig. 2A and 2B). The early arrest of Δ*p52*+*p36* parasites after hepatocyte invasion is similar to the phenotype reported for *P. berghei* mutants lacking expression of only P52 and *P. yoelii* mutants lacking both P52 and P36 [21]. In addition, immunization of BALB/c and C57BL/6 mice with the Δ*p52*+*p36* mutants showed comparable levels of protection against challenge with WT parasites (Table S3) as observed with *P. berghei* mutants lacking *p52* or *P. yoelii* mutants lacking *p52* and *p36* [21]. Full protection was induced in BALB/c mice with a single dose with as few as 1000 sporozoites inoculated intravenously (IV) whereas protection in C57BL/6 mice required 3 immunizations (Table S3).

In contrast to the early growth-arrest phenotype of Δ*p52*+*p36*, liver stages of Δ*fabb/f* developed into mature forms as shown by qRT-PCR analysis and immuno-fluorescence microscopy (Fig. 1E, Fig. 2A). During *in vitro* liver stage development, the Δ*fabb/f* parasites were morphologically similar to WT parasites as judged by immuno-fluorescence microscopy (Fig. 2A). However, schizonts showed a significantly lower level of expression of the merozoite surface protein 1 (MSP1); at 48 hours post infection (hpi) only 18% of the Δ*fabb/f* schizonts strongly expressed MSP1 whereas 39% of WT parasites were MSP1-positive ($p<0.001$) and this increased to 54% in WT and 37% in Δ*fabb/f* at 54hpi ($p=0.01$) as shown in Fig. 2C (and Fig. S5A/B). The normal morphology of maturing Δ*fabb/f* liver stages and expression of MSP1 parasites is different from the phenotype reported for *P. yoelii* parasites lacking expression of FabB/F, where schizonts show clear signs of aberrant nuclear morphology and a complete absence of MSP1 expression [22].

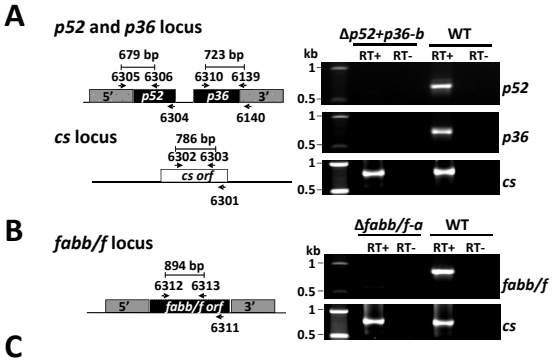

C

Parasite	Oocyst No. Mean ± sd	Spz No. (x10^3) Mean ± sd	Gliding motility No. of circles Mean ± sd	Cell traversal % traversed cells Mean ± sd
WT (cl15cy1)	85 ± 25	102 ± 28	89 ± 3	20.7 ± 3.0
WT (*Pb*GFP-Luc$_{con}$)	63 ± 15	86 ± 24	nd	18.9 ± 2.1
Δp52+p36-a	85 ± 30	133 ± 40	88 ± 3	22.6 ± 1.6
Δfabb/f	46 ± 19	121 ± 31	93 ± 1	22.1 ± 1.6
Δp52+p36-b	49 ± 23	95 ± 8	nd	19.4 ± 0.7
Δp52+p36-a 'breakthrough'	65 ± 17	91 ± 27	nd	18.7± 0.5

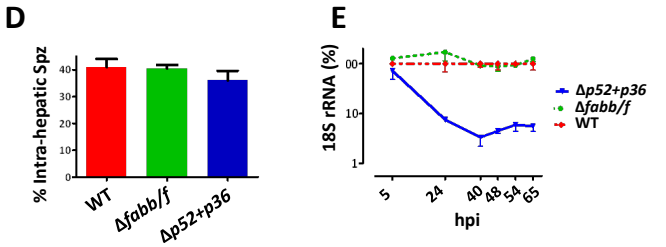

Figure 1: Characterisation of *P. berghei Δp52+p36* and *Δfabb/f* mutant parasites

A) qRT-PCR analysis showing absence of p52 and p36 transcripts in sporozoites of *Δp52+p36-b*. PCR amplification using purified sporozoite RNA was performed either in the presence or absence of reverse transcriptase (RT+ or RT-, respectively) using the primers as shown in the left panel (see Table S1 for the sequence of the primers). The *P. berghei* circumsporozoite protein gene (cs) was used as a positive control. **B)** qRT-PCR analysis showing absence of fabb/f transcripts in sporozoites mutant of *Δp52+p36-b*. PCR amplification using purified sporozoite RNA was performed either in the presence or absence of reverse transcriptase (RT+ or RT-, respectively) using the primers 6312 and 6313 (see Table S1 for the sequence of the primers). The *P. berghei* circumsporozoite protein gene (cs) was used as a positive control. **C)** Table of oocyst and sporozoite production in *A. stephensi* mosquitoes (given as numbers), sporozoite motility (as numbers of anti-CS 'circle' trails) and cell traversal capacity (mean number of cultured hepatocytes, Huh7, traversed) of *P. berghei* wildtype (WT) and mutant parasites. **D)** *In vitro* development 3 hours after sporozoites invasion of hepatocytes (Huh7) by *P. berghei* GAPs is represented as the ratio of extra- and intra-hepatic sporozoites; determined after 3 wash steps to remove sporozoites in suspension (see C). **E)** Growth of *P. berghei* GAPs intra-hepatic stages in culture (in Huh7 cells) at different hours post invasion (hpi) of sporozoites. Growth is determined by qRT-PCR of 18s *P. berghei* rRNA. RNA levels shown are relative to RNA levels of WT liver-stages.

Sporozoites of the *P. berghei* GAPs, *Δfabb/f* and *Δp52+p36*, are not completely attenuated

To examine the adequacy of attenuation of the Δ*fabb/f* and Δ*p52+p36* mutants *in vivo*, we infected mice of two different strains, BALB/c and C57BL/6, with high sporozoite doses. An IV dose of 50K sporozoites did not result in blood infections in BALB/c mice in the two independent Δ*p52+p36* mutants (Table 1). In contrast, IV injection of 50K sporozoites of the two Δ*fabb/f* mutants resulted in breakthrough blood infections in the majority (80-100%) of BALB/c mice (Table 1). Moreover, all C57BL/6 mice developed a blood stage infection when infected with 50K sporozoites of both independent Δ*fabb/f* mutants (Table 1). Genotyping of the breakthrough blood parasites (Δ*fabb/f*$_{br}$) by PCR and Southern analysis of chromosomes showed that these parasites had the Δ*fabb/f* genotype (data not shown). The blood infections show a prolonged prepatency period of 1-2 days as compared to WT parasites. Assuming a *P. berghei* blood stage multiplication rate of 10x per 24 hour this delay to patency indicates a 90-99% reduction in the production and/or infectivity of the Δ*fabb/f* exo-erythrocytic merozoites. Despite the significant reduction in production of infectious merozoites, our results show that *P. berghei* Δ*fabb/f* sporozoites are only weakly attenuated compared to *P. yoelii* sporozoites lacking expression of FabB/F [22].

As infection of BALB/c mice with 50K sporozoites of the Δ*p52+p36* mutants did not result in breakthrough blood infections it was surprising that a low percentage of C57BL/6 mice (10-20%) produced breakthrough blood infections after inoculation with 50K sporozoites (Table 1). The prepatent period of these 'breakthrough' infections was prolonged by 1-2 days compared to WT. Genotyping of the breakthrough blood parasites (Δ*p52+p36*$_{br}$) by PCR and Southern analysis of chromosomes confirmed that these parasites had the Δ*p52+p36* genotype (Fig. S1D). To examine the possibility that parasites can stably switch to an alternative, P52/P36 independent, mechanism of liver stage development we analysed infections in mice after inoculation of 50K sporozoites derived from the Δ*p52+p36*$_{br}$ parasites. Five out of 12 mice did not produce blood infections and those mice that developed a blood infection had a prolonged prepatent period of 1-2 days. Although the percentage of mice with breakthrough blood infections after infection with Δ*p52+p36*$_{br}$ sporozoites is higher (58%) then after infection with Δ*p52+p36* sporozoites (10-20%), these results indicate that the Δ*p52+p36*$_{br}$ are not derived from parasites that had permanently switched to an efficient and P52/P36 independent mechanism of liver stage development.

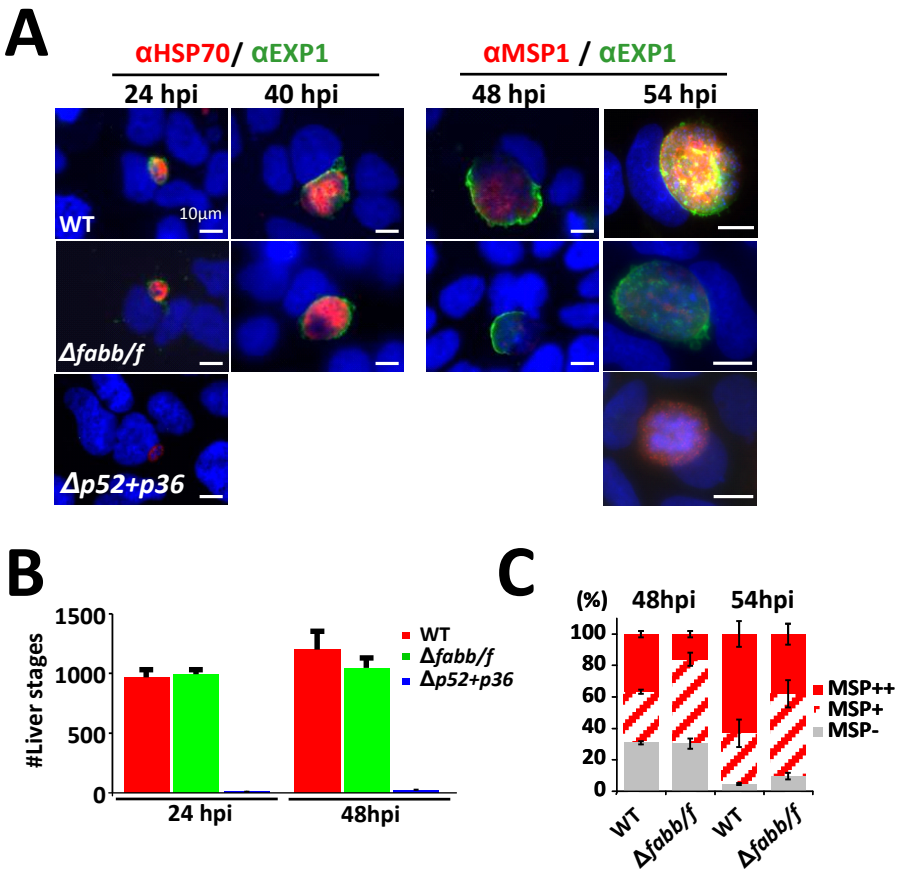

Figure 2: Development of *P. berghei Δp52+p36* and *Δfabb/f* parasites *in vitro*

A) Development of liver-stage parasites of *P. berghei* GAPs in culture as shown by immuno-fluorescence analysis of parasites at different hpi. Staining with anti-PbCSP-antibodies at 3hpi in the invasion assay (see A) distinguishes extracellular (green) from intracellular (yellow/orange) sporozoites; anti-PbEXP1 and anti-HSP70 antibodies recognize the parasitophorous vacuole (green) and the parasite cytoplasm (red), respectively; anti-PbMSP1 antibodies (red) is a marker of PbMSP1 expression during merozoite formation in mature liver-stage parasites. Nuclei are stained with Hoechst-33342. In the Δfabb/f parasites PbMSP1 expression is strongly reduced (see D). While >99% of *Δp52+p36* liver-stage parasites abort development soon after invasion a few, PbEXP1-negative, parasites do mature and are detectable at 54hpi. **B)** Mean number of intra-hepatic (liver stage) WT and *P. berghei* mutant parasites at 24hpi and 48hpi per *in vitro* culture well (4 wells counted per time point for each mutant sporozoite infection). C) Relative PbMSP1 expression in *P. berghei* liver-stages at 48hpi and 54hpi as determined by staining with anti-PbMSP1 antibodies of cultured liver-stages (see A). MSP++: intense staining; MSP+: weak staining; MSP-: MSP negative. See Figure S3 for the relative MSP1 staining of *Δfabb/f* liver stage parasites.

Table 1. Breakthrough blood infections after intravenous injection of different doses of sporozoites of *P. berghei* GAPs

Animals	Parasites	Dose	breakthrough/ infected animals [a]	Pre-patency (days)
BALB/C	WT	$1x10^4$	5/5	5-6
	Δ*fabb/f-a*	$5 x10^4$	12/15	6-7
	Δ*fabb/f-b*	$5 x10^4$	10/10	7-8
	Δ*p52+p36-a*	$5 x10^4$	0/10	n/a
	Δ*p52+p36-b*	$5 x10^4$	0/10	n/a
C57BL6	WT	$1 x10^4$	5/5	5-6
	Δ*fabb/f-a*	$5 x10^4$	15/15	6-7
	Δ*fabb/f-b*	$5 x10^4$	10/10	7-9
	Δ*p52+p36-a*	$5 x10^4$	1/10	6
	Δ*p52+p36-b*	$5 x10^4$	2/10	6-7
	Δ*p52+p36-a 'breakthrough'* [b]	$5 x10^4$	7/12	6-8

[a] Number of mice showing breakthrough infections of the total number of infected mice.

[b] Δ*p52+p36* 'breakthrough' are parasites that were derived from a blood infection in mice after infection with sporozoites of mutant Δ*p52+p36*.

Evidence for complete development of *P. berghei Δp52+36* parasites in hepatocytes *in vitro* and *in vivo*

For *P. berghei* it has been reported that WT sporozoites are not completely restricted to hepatocytes for development but can also develop into infectious merozoites in skin cells, albeit at a very low frequency [43;44]. The Δ*p52+36* breakthrough blood infections may therefore result from development of a low number of sporozoites in cells of other organs where the establishment of a PVM is less critical. To investigate whether *Δp52+36* sporozoites could develop in hepatocytes into maturing liver stages we analysed development of *Δp52+36* sporozoites in cultured hepatocytes and in mice using real-time *in vivo* imaging of liver stage development. Most Δ*p52+p36* parasites rapidly disappear from *in vitro* hepatocyte cultures as shown by quantitative analyses of infected hepatocytes by fluorescence microscopy. However, in-depth analyses whereby all hepatocytes present in the culture wells were analysed by fluorescence microscopy at 48h and 54h after adding sporozoites, showed very low numbers of Δ*p52+p36* liver-schizonts, 1 to 4 per well, that were comparable in size to WT schizonts (Fig. 2A). These liver-schizonts expressed MSP1 as shown

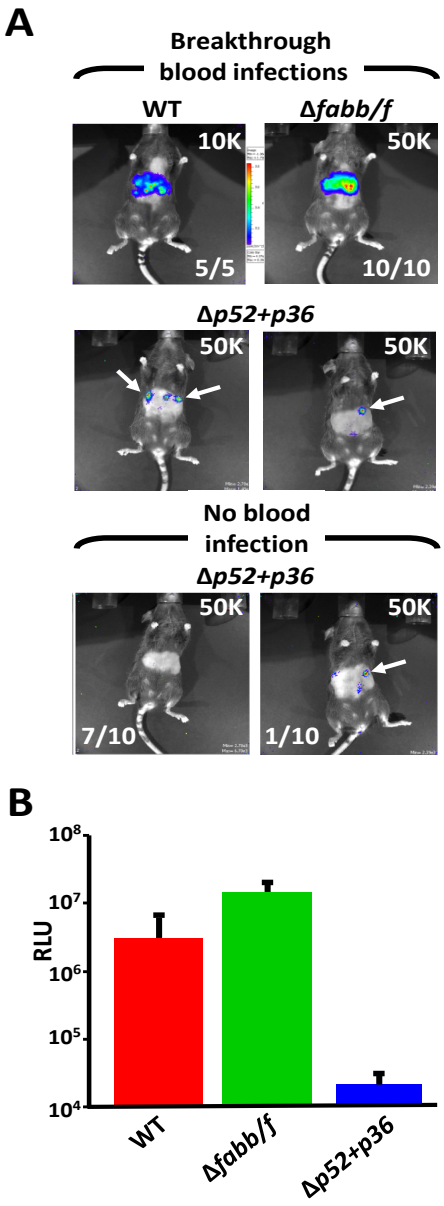

Figure 3: Development of *P. berghei* Δp52+p36 and *Δfabb/f* parasites *in vivo*

A) Development *P. berghei* GAPs in C57BL/6 mice as shown by real-time *in vivo* imaging of luciferase-expressing liver-stage parasites at 40hpi. The upper panels show that all mice infected with 10^3 (10K) WT sporozoites developed a breakthrough infection in the blood (i.e. 5 out of 5 mice), and all mice (10/10) infected with 50K *Δfabb/f* parasites numbers also developed a breakthrough infection. When 10 C57BL/6 mice were infected with 50K *Δp52+p36* sporozoites only 2 produced a breakthrough blood infection, the 2 mice that developed a blood stage infection are shown and individual spots (possibly individual infected hepatocytes) localizing to the liver are clearly visible (see white arrows). 8 of the 10 C57BL/6 mice infected with 50K *Δp52+p36* sporozoites did not develop a blood infection, in 7 of these mice no luciferase expressing parasites were visible. However, 1 mouse did show an individual spot (white arrow) in the liver but did not generate a blood infection. All mice were infected with hand dissected sporozoites injected IV. **B)** Graph showing the measured relative light intensity of C57BL/6 mice infected with 10^3 (10K) WT and $5x10^5$ (50K) *Δp52+p36* and *Δfabb/f* sporozoites IV at 40hpi; as shown in (A) and depicted as relative light units (RLU).

by staining with anti-MSP1 antibodies and contained large numbers of distinct nuclei comparable to mature WT schizonts (Fig. 2A). Interestingly, in contrast to schizonts of WT and Δ*fabb/f*, the Δ*p52+p36* schizonts were negative for staining with antibodies recognizing the PVM-resident protein EXP1, suggesting that the

PVM of these parasites is compromised (Fig. 2A, Fig. S4A). We next examined development of Δ*p52+p36* sporozoites in live mice using real-time *in vivo* imaging of luciferase-expressing parasites [38]. In the liver of mice infected with sporozoites of the reference WT line expressing luciferase, *Pb*GFP-Luc$_{con}$, liver stage luminescence signals can be detected at 24h after infection with sporozoites and imaging between 40h and 60h allows the detection of individual liver schizonts [38]. As expected, based on the Δ*fabb/f* breakthrough blood infections and *in vitro* maturation of Δ*fabb/f* liver schizonts, infected hepatocytes were clearly visible in all mice infected with 50K Δ*fabb/f* sporozoites at 42hpi (Fig. 3A). In contrast, imaging of mice infected with 50K Δ*p52+p36* sporozoites, did not show luminescence signals at 42hpi in 7 out of 10 mice. None of the luminescence-negative mice developed a breakthrough blood stage infection, indicating the absence of developing Δ*p52+p36* sporozoites. Interestingly, in 3 mice we observed a clear luminescence signal in the liver although luciferase signals were confined to a few (1-3) individual spots as compared to the strong luminescence signals of whole livers that were observed in mice infected with WT or Δ*fabb/f* sporozoites (Fig. 3A). Two of the 3 luminescence-positive mice developed a breakthrough blood infection and genotyping of the progeny of the blood parasites confirmed the Δ*p52+p36* genotype (Fig. S1D). Combined these results indicate that the breakthrough blood infections in these mice are associated with the presence of developing Δ*p52+p36* parasites in the liver. The one mouse that was luminescence-positive but did not develop a blood infection may indicate that certain cases Δ*p52+p36* liver sporozoites develop into maturing liver stages but abort development before production of infectious merozoites.

Some *P. falciparum Δp52+36* sporozoites are able to develop into replicating liver stage forms

We next examined if the ability of low numbers of Δ*p52+p36* sporozoites to develop into maturing liver stages was specific for *P. berghei* or that a similar phenotype could also be observed for *P. falciparum* Δ*p52+p36* parasites. Recently it has been reported that *P. falciparum* Δ*p52+p36* sporozoites invaded but did not mature in hepatocytes in culture or in a chimeric mouse harboring human hepatocytes [27]. Using sporozoites derived from two *P. falciparum* Δ*p52+p36* mutants, *Pf*Δ*p52+p36* and *Pf*Δ*p52+p36gfp* [45] we examined their development in cultures of primary human hepatocytes. These *P. falciparum* mutants show normal *in vitro* blood stage development [45] as well as oocyst and sporozoite production (Fig. 4A) and we confirmed by RT-PCR that sporozoites of these mutants are unable to express either *p52* or *p36* (Fig. 4B). In culture, sporozoites showed cell traversal (Fig. 4C) and hepatocyte invasion (Fig.

4D) comparable to WT sporozoites but 24h after invasion the vast majority (>99%) of parasites became arrested as observed by HSP70 antibody-staining on days 2-7 post invasion (Fig. 4D). However, after in-depth analyses whereby all hepatocytes present in the culture wells were analyzed by fluorescence microscopy, we detected very low numbers of *Pf*Δ*p52+p36* parasites (occasionally 1 per well) at day 2, 3 and 4 after sporozoite invasion that were comparable in size to WT parasites. These parasites could be detected in both the *Pf*Δ*p52+p36* and *Pf*Δ*p52+p36gfp* mutant and the parasites present at day 4 clearly demonstrated nuclear division as shown by the presence of multiple, DAPI-stained nuclei (Fig. 4E). Since the *p52* and *p36* genes of both mutants had been deleted by double cross-over homologous recombination, the replicating parasites present at day 4 cannot be due to parasites that have a WT genotype as a result of a 'reversion' event that can occur when genes are deleted by a single cross-over homologous recombination [34]. These observations therefore provide evidence that *P. falciparum* sporozoites can progress into replicating liver stages in the absence of P52 and P36, comparable to *P. berghei* Δ*p52+p36* sporozoites.

Discussion

In this study we report an assessment of the adequacy of attenuation using the *P. berghei* rodent model of two GAPs for which a complete liver stage growth arrest has been previously reported in BALB/c mice infected with the rodent parasite *P. yoelii*. For both *P. berghei* and *P. yoelii* it has been shown that the bacterial like type II fatty acid synthesis (FAS II) pathway plays an important role for liver stage development [22;46]. Deletion of 3 of the 4 genes that encode the key enzymes of this pathway, FabB/F, FabZ and FabI, have no effect on blood stage development but severely affect late liver stage development [22;46]. In *P. yoelii* deletion of either FabB/F or FabZ resulted in a complete growth arrest of liver stages. Moreover, it has been recently reported that *P. yoelii* parasites lacking FabB/F give rise to broader and larger protective CD8 responses in mice, than either IrrSpz or early arresting GAPs, making them promising 'second-generation' GAPs [23]. In contrast to the observations in *P. yoelii*, we found that *P. berghei* GAP lacking expression of FabB/F is not attenuated, in either BALB/c or C57BL/6 mice, although the prolonged prepatent period to a blood infection indicates a significant reduction in the generation of infectious merozoites. This phenotype of partial attenuation is comparable to the phenotype of *P. berghei* mutants lacking expression of FabI [46], which also showed a severe delay in the onset of blood stage patency. Liver schizonts of *P. yoelii* mutants lacking expression of FASII pathway enzymes showed clear features of aberrant nuclear division and

A

Parasite	Oocyst (IQR)	Infected mosquitoes (%)	Sporozoite ($x10^3$) no. Mean ± s.d.
WT (NF54)	47 (17-67)	95	102 (23)
PfΔ*p52+36*	43 (30-60)	95	98 (14)
PfΔ*p52+36gfp*	65 (39-81)	100	136 (36)

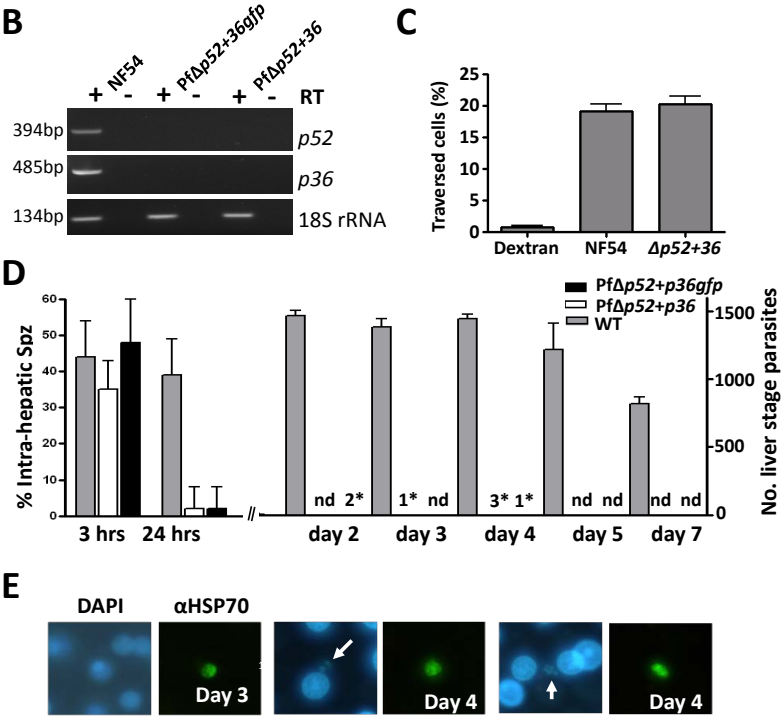

Figure 4: Characterisation of *P. falciparum Δp52+p36* (*PfΔp52+p36* and *PfΔp52+p36gfp*) parasites
A) Oocyst and sporozoite production in *A. stephensi* mosquitoes infected with *P. falciparum* wildtype (WT), *PfΔp52+p36* and *PfΔp52+p36gfp* parasites. **B)** RT-PCR analysis showing absence of p52 and p36 transcripts in *P. falciparum* mutant sporozoites. PCR amplification using purified sporozoite RNA was performed either in the presence or absence of reverse transcriptase (RT+ or RT-, respectively), the positive control was performed by PCR of 18S rRNA using primers 18Sf/18Sr (for primer sequences see Methods). **C)** Cell traversal ability of *P. falciparum* WT (NF54) and mutant sporozoites as determined by FACS counting of Dextran positive hepG2 cells. Dextran: hepatocytes cultured in the presence of Dextran but without the addition of sporozoites. **D)** *In vitro* invasion of *P. falciparum Δp52+p36* sporozoites and development of liver-stages in primary human hepatocytes. Invasion is represented as the ratio of extra- and intracellular sporozoites by double staining at 3 and 24 hpi, determined after 3 wash steps to remove sporozoites in suspension. From day 2 to 7 the number of parasites per 96-well was determined by counting parasites stained with anti-*P. falciparum* HSP70 antibodies. * Total number of liver stages observed in 6 wells, where infected cells were not identified they are indicated as not detected (nd). **E)** At day 4 low numbers of liver stages were detected, possessing multiple nuclei (i.e. replicating) as shown by DAPI staining of their nuclei (white arrows).

an absence of the merozoite specific protein, MSP1, expression. In contrast, the liver schizonts of the *P. berghei* mutants expressed MSP1 although the level of MSP1 expression was clearly delayed in comparison to WT parasites. These observations indicate that differences exist as to the essential nature of the FAS II pathway for *P. berghei* and *P. yoelii* liver stages. To which extent *P. falciparum* liver stages are dependent on the FASII pathways is as yet unknown and awaits investigations on mutant *P. falciparum* liver stages in primary hepatocytes.

P. yoelii and *P. berghei* GAP lacking expression of P52 and P36 show a developmental arrest early after invasion of the hepatocyte [9;21]. These proteins belong to the 6-cys protein family consisting of 10 members, most of which are expressed in a discrete stage-specific manner; in gametocytes, sporozoites or merozoites [41]. P52, a putative GPI-anchored protein and P36, a putative secreted protein, are both expressed in sporozoites and early liver stages [41;42;47]. Despite the early growth-arrest phenotype, C57BL/6 mice inoculated with sporozoites of 'single gene deletion' mutants lacking either P52 or P36 result in breakthrough blood infections in a low number of mice [9]. Since both proteins belong to the same family of proteins and their genes form a paralogous pair in the genome it has been reasoned that they may perform partly redundant functions and that removal of both genes might result in parasites that show a complete growth arrest during development in the liver. Indeed, complete attenuation has been reported for *P. yoelii* sporozoites that lack expression of both P52 and P36 [21] and this attenuation of the 'double gene deletion' mutants was demonstrated by the absence of breakthrough blood infections in BALB/c mice or Wistar rats after IV injection of up to 10^5 sporozoites. In agreement with these studies we found no breakthrough blood infections with *P. berghei* sporozoites lacking both P52 and P36 when tested in BALB/c mice. However, when C57BL/6 mice were injected with similar doses of sporozoites of the *P. berghei* 'double gene deletion' mutants, we observed breakthrough blood infections in a low percentage of mice, showing that these mutants did not completely abort development in the liver. These results indicate that differences may exist between *P. yoelii* and *P. berghei* on their dependence on P36 and P52 for liver stage development comparable to the differences in dependence on the FAS II pathway. For P52 evidence has been presented for a role in establishment and/or maintenance of the parasitophorous vacuole [9;21;42] and the early growth-arrest of sporozoites lacking P52 would suggest that liver stage parasites cannot develop in the absence of a competent PVM. For both *P. berghei* and *P. yoelii* it has recently been reported that WT sporozoites are not completely restricted to hepatocytes for development but can also develop

into infectious merozoites in skin cells, albeit at a very low frequency [43;44]. It may therefore be that the Δ*p52+36* breakthrough blood infections in the C57BL/6 mice arise from sporozoites that have invaded and undergone development in cells other than the liver. However, our observations on maturation of *P. berghei* Δ*p52+36* liver stages both in cultured hepatocytes and as in living mice using *in vivo* imaging provide evidence that breakthrough infections result from merozoites derived from schizonts developing in hepatocytes. Apart from a possible difference in attenuation between *P. yoelii* and *P. berghei* sporozoites lacking P52 and P36, the observed *P. berghei* breakthrough blood infections may also be explained by differences in intracellular survival of attenuated sporozoites inside cells from different mouse strains. Breakthrough blood infections were only observed in C57BL/6 mice and like in *P. yoelii*, infection of BALB/c mice with high doses of *P. berghei* Δ*p52+p36* did not result in 'breakthrough' blood infections. It is known that large difference exist in the dose of sporozoites that is needed to obtain full protective immunity in C57BL/6 and BALB/c mice, where C57BL/6 mice are the more difficult to protect requiring multiple boosting immunizations. It has been suggested that differences in the protective immune responses may be partly attributed to the presence of an immunodominant CD8 +T cell epitope present in the circumsporozoite protein that is H2Kd -restricted [48-50]. Our observations that all Δ*p52+36* infected liver cells are removed in BALB/c mice whereas low numbers of Δ*p52+36* sporozoites are able to complete full liver development in C57BL/6 mice indicate that differences exist between these mouse strains in both the innate and acquired immune responses that are responsible for the recognition and removal of infected hepatocytes. Studies with IrrSpz of *P. yoelii* inoculated into both BALB/c and immunocompromised mice have shown that sufficiently irradiated sporozoites are unable to create breakthrough blood infections, indicating that abortion of development is due to the failure of the parasite to multiply and not the host to eliminate the infection [51]. Interestingly, our observations of breakthrough blood infections of the two rodent GAP provide evidence that the adequacy of sporozoite attenuation is not only dependent on the *Plasmodium* species studied, as in the case of genes encoding enzymes of the FASII pathway, but can also be influenced by host factors. Our results demonstrate that *P. berghei* in C57BL/6 mice is a more stringent model for preclinical testing of these GAPs than *P. yoelii* in BALB/c mice. This observation is emphasized by our analysis of *P. falciparum* Δ*p52+36* GAP in cultured primary human hepatocytes. The observations of low numbers of replicating liver stages demonstrates that maturation of Δ*p52+36* liver stages is not specific for *P. berghei* but can also occur in *P. falciparum* and underscores the incomplete attenuation of *Plasmodium* GAP lacking both P52

and P36. While we were not able to observe replicating *P. falciparum* Δ*p52+p36* liver stages after day 4, we believe that this may result from the drop of 30-40% we observe in cultured primary human hepatocytes between day 5 and day 7, as can be observed with WT infected hepatocytes. Therefore the few Δ*p52+p36* replicating parasites may be below the level of detection in this assay. In a recent clinical trial, where human volunteers were immunized with *P. falciparum* Δ*p52+p36* GAP a breakthrough blood infection was confirmed in one volunteer [52]. Approaches such as the co-administration of anti-Plasmodium drugs with GAP vaccine formulations and/or the creation of genetically modified parasites that have genes introduced into their genome, which when expressed (i.e. in the liver stages) result in the destruction of the parasites, may mitigate the possibility of 'breakthrough' parasites. However, while we are currently exploring these potential solutions, they also raise additional questions both with respect to practical administration of a vaccine requiring prophylactic drugs in an endemic setting, and additional safety concerns related to parasites that 'self-destruct'.

In conclusion, our combined data based on *P. berghei* and *P. falciparum* provides a strong indication that Δ*p52+p36* and Δ*fabb/f* GAP are not sufficiently attenuated to move forward for further clinical development. Multiple genes governing independent cellular process, vital to liver stage development, must be removed such that abortion of liver stage development is complete. Our data underline the need for stringent preclinical testing of GAP before advancing into human vaccine trials. We therefore propose that GAP attenuation evaluation should preferably include, but not be limited to: (i) generation and analysis of equivalent GAPs in both *P. yoelii* and *P. berghei*; (ii) these GAPs should be tested for breakthrough blood infections in different mice strains (e.g. BALB/c, C57BL/6 and outbred mice) with escalating doses of sporozoites; and (iii) analysis of the corresponding *P. falciparum* GAP should be tested for liver stage development in cultured human hepatocytes.

Acknowledgements

This study was performed within the framework of Top Institute Pharma (Netherlands) project: T4-102. The funders had no role in study design, data collection and analysis, decision to publish, or preparation of the manuscript. We would like to thank Prof. Volker Heussler (Institute of Cell Biology, University of Bern, Switzerland) and Prof. Maria Mota (Insituto de Medicina Molecular, University of Lisbon, Portugal) for kindly providing us with the anti-*P. berghei* EXP1 and HSP70 antibodies, respectively. The authors would like to thank Marga van de Vegte-Bolmer for mosquito feeds and Jolanda Klaassen, Astrid Pouwelsen, Laura Pelser-Posthumus and Jacqueline Kuhnen (RUNMC, Nijmegen) for their help with the

maintenance/dissection of mosquitoes and Jai Ramesar, Michel Mulders (LUMC), Claudia Lagarde, Alex Inacio and Iris Lamers-Elemans (RUNMC, Nijmegen) for assistance with the *P. berghei* infections.

References

1. Hoffman SL, Goh LM, Luke TC, et al. Protection of humans against malaria by immunization with radiation-attenuated Plasmodium falciparum sporozoites. J Infect Dis 2002 Apr 15;185(8):1155-64.
2. Nussenzweig R, Vanderberg JP, Most H, Orton C. Protective Immunity Produced by Injection of X-Irradiated Sporozoites of Plasmodium Berghei. Nature 1967;216(5111):160-&.
3. Hoffman SL, Billingsley PF, James E, et al. Development of a metabolically active, non-replicating sporozoite vaccine to prevent Plasmodium falciparum malaria. Hum Vaccin 2010 Jan;6(1):97-106.
4. Kappe SH, Vaughan AM, Boddey JA, Cowman AF. That was then but this is now: malaria research in the time of an eradication agenda. Science 2010 May 14;328(5980):862-6.
5. Pinzon-Charry A, Good MF. Malaria vaccines: the case for a whole-organism approach. Expert Opin Biol Ther 2008 Apr;8(4):441-8.
6. Kester KE, Cummings JF, Ofori-Anyinam O, et al. Randomized, double-blind, phase 2a trial of falciparum malaria vaccines RTS,S/AS01B and RTS,S/AS02A in malaria-naive adults: safety, efficacy, and immunologic associates of protection. J Infect Dis 2009 Aug 1;200(3):337-46.
7. Mueller AK, Camargo N, Kaiser K, et al. Plasmodium liver stage developmental arrest by depletion of a protein at the parasite-host interface. Proc Natl Acad Sci U S A 2005 Feb 22;102(8):3022-7.
8. Mueller AK, Labaied M, Kappe SHI, Matuschewski K. Genetically modified Plasmodium parasites as a protective experimental malaria vaccine. Nature 2005 Jan 13;433(7022):164-7.
9. van Dijk MR, Douradinha B, Franke-Fayard B, et al. Genetically attenuated, P36p-deficient malarial sporozoites induce protective immunity and apoptosis of infected liver cells. Proceedings of the National Academy of Sciences of the United States of America 2005 Aug 23;102(34):12194-9.
10. Purcell LA, Yanow SK, Lee M, Spithill TW, Rodriguez A. Chemical attenuation of Plasmodium berghei sporozoites induces sterile immunity in mice. Infect Immun 2008 Mar;76(3):1193-9.
11. Purcell LA, Wong KA, Yanow SK, Lee M, Spithill TW, Rodriguez A. Chemically attenuated Plasmodium sporozoites induce specific immune responses, sterile immunity and cross-protection against heterologous challenge. Vaccine 2008 Jul 29.
12. Jobe O, Lumsden J, Mueller AK, et al. Genetically attenuated Plasmodium berghei liver stages induce sterile protracted protection that is mediated by major histocompatibility complex Class I-dependent interferon-gamma-producing CD8+ T cells. J Infect Dis 2007 Aug 15;196(4):599-607.
13. Kumar KA, Baxter P, Tarun AS, Kappe SH, Nussenzweig V. Conserved protective mechanisms in radiation and genetically attenuated uis3(-) and uis4(-) Plasmodium sporozoites. PLoS ONE 2009;4(2):e4480.
14. Mueller AK, Deckert M, Heiss K, Goetz K, Matuschewski K, Schluter D. Genetically attenuated Plasmodium berghei liver stages persist and elicit sterile protection primarily via CD8 T cells. Am J Pathol 2007 Jul;171(1):107-15.
15. Hafalla JC, Rai U, Morrot A, Bernal-Rubio D, Zavala F, Rodriguez A. Priming of CD8+ T cell responses following immunization with heat-killed Plasmodium sporozoites. Eur J Immunol 2006 May;36(5):1179-86.
16. Spitalny GL, Nussenzweig RS. Effect of Various Routes of Immunization and Methods of Parasite Attenuation on Development of Protection Against Sporozoite-Induced Rodent Malaria. Proceedings of the Helminthological Society of Washington 1972;39(NOV):506-14.
17. Scheller LF, Stump KC, Azad AF. Plasmodium berghei: production and quantitation of hepatic stages derived from irradiated sporozoites in rats and mice. J Parasitol 1995 Feb;81(1):58-62.
18. Vaughan AM, Wang R, Kappe SH. Genetically engineered, attenuated whole-cell vaccine approaches for malaria. Hum Vaccin 2010 Jan;6(1):107-13.
19. Aly AS, Mikolajczak SA, Rivera HS, et al. Targeted deletion of SAP1 abolishes the expression of infectivity factors necessary for successful malaria parasite liver infection. Mol Microbiol 2008 Jul;69(1):152-63.

20. Silvie O, Goetz K, Matuschewski K. A sporozoite asparagine-rich protein controls initiation of Plasmodium liver stage development. PLoS Pathog 2008 Jun;4(6):e1000086.
21. Labaied M, Harupa A, Dumpit RF, Coppens I, Mikolajczak SA, Kappe SH. Plasmodium yoelii sporozoites with simultaneous deletion of P52 and P36 are completely attenuated and confer sterile immunity against infection. Infect Immun 2007 Aug;75(8):3758-68.
22. Vaughan AM, O'Neill MT, Tarun AS, et al. Type II fatty acid synthesis is essential only for malaria parasite late liver stage development. Cell Microbiol 2009 Mar;11(3):506-20.
23. Butler NS, Schmidt NW, Vaughan AM, Aly AS, Kappe SH, Harty JT. Superior antimalarial immunity after vaccination with late liver stage-arresting genetically attenuated parasites. Cell Host Microbe 2011 Jun 16;9(6):451-62.
24. Aly AS, Lindner SE, MacKellar DC, Peng X, Kappe SH. SAP1 is a critical post-transcriptional regulator of infectivity in malaria parasite sporozoite stages. Mol Microbiol 2011 Feb;79(4):929-39.
25. Douradinha B, van Dijk MR, Ataide R, et al. Genetically attenuated P36p-deficient Plasmodium berghei sporozoites confer long-lasting and partial cross-species protection. Int J Parasitol 2007 May 21;37(13):1511-9.
26. Tarun AS, Vaughan AM, Kappe SH. Redefining the role of de novo fatty acid synthesis in Plasmodium parasites. Trends Parasitol 2009 Dec;25(12):545-50.
27. VanBuskirk KM, O'Neill MT, de l, V, et al. Preerythrocytic, live-attenuated Plasmodium falciparum vaccine candidates by design. Proc Natl Acad Sci U S A 2009 Aug 4;106(31):13004-9.
28. Janse CJ, Ramesar J, Waters AP. High-efficiency transfection and drug selection of genetically transformed blood stages of the rodent malaria parasite Plasmodium berghei. Nat Protoc 2006;1(1):346-56.
29. Franke-Fayard B, Trueman H, Ramesar J, et al. A Plasmodium berghei reference line that constitutively expresses GFP at a high level throughout the complete life cycle. Mol Biochem Parasitol 2004 Sep;137(1):23-33.
30. Janse CJ, Franke-Fayard B, Mair GR, et al. High efficiency transfection of Plasmodium berghei facilitates novel selection procedures. Mol Biochem Parasitol 2006 Jan;145(1):60-70.
31. van Schaijk BC, Vos MW, Janse CJ, Sauerwein RW, Khan SM. Removal of heterologous sequences from Plasmodium falciparum mutants using FLPe-recombinase. PLoS ONE 2010;5(11):e15121.
32. Ifediba T, Vanderberg JP. Complete in vitro maturation of Plasmodium falciparum gametocytes. Nature 1981 Nov 26;294(5839):364-6.
33. Ponnudurai T, Lensen AH, Meis JF, Meuwissen JH. Synchronization of Plasmodium falciparum gametocytes using an automated suspension culture system. Parasitology 1986 Oct;93 (Pt 2):263-74.
34. van Schaijk BC, Janse CJ, van Gemert GJ, et al. Gene disruption of Plasmodium falciparum p52 results in attenuation of malaria liver stage development in cultured primary human hepatocytes. PLoS ONE 2008;3(10):e3549.
35. Sinden R.E. Infection of mosquitoes with rodent malaria. In: Crampton J.M., Beard C.B., Louis C., editors. Molecular biology of insect disease vectors: a method manual.London, United Kingdom, Chapman and Hall, 1997: p. 67-91.
36. Franke-Fayard B, Waters AP, Janse CJ. Real-time in vivo imaging of transgenic bioluminescent blood stages of rodent malaria parasites in mice. Nat Protoc 2006;1(1):476-85.
37. Ploemen IH, Prudencio M, Douradinha BG, et al. Visualisation and quantitative analysis of the rodent malaria liver stage by real time imaging. PLoS ONE 2009;4(11):e7881.
38. Ploemen IH, Prudencio M, Douradinha BG, et al. Visualisation and quantitative analysis of the rodent malaria liver stage by real time imaging. PLoS ONE 2009;4(11):e7881.
39. Sharma S, Sharma SK, Surolia N, Surolia A. Beta-ketoacyl-ACP synthase I/II from Plasmodium falciparum (PfFabB/F)--is it B or F? IUBMB Life 2009 Jun;61(6):658-62.
40. Gerloff DL, Creasey A, Maslau S, Carter R. Structural models for the protein family characterized by gamete surface protein Pfs230 of Plasmodium falciparum. Proc Natl Acad Sci U S A 2005 Sep 20;102(38):13598-603.
41. van Dijk MR, van Schaijk BC, Khan SM, et al. Three members of the 6-cys protein family of Plasmodium play a role in gamete fertility. PLoS Pathog 2010 Apr;6(4):e1000853.
42. Ishino T, Chinzei Y, Yuda M. Two proteins with 6-cys motifs are required for malarial parasites to commit to infection of the hepatocyte. Mol Microbiol 2005 Dec;58(5):1264-75.

43. Gueirard P, Tavares J, Thiberge S, et al. Development of the malaria parasite in the skin of the mammalian host. Proc Natl Acad Sci U S A 2010 Oct 26;107(43):18640-5.
44. Coppi A, Natarajan R, Pradel G, et al. The malaria circumsporozoite protein has two functional domains, each with distinct roles as sporozoites journey from mosquito to mammalian host. J Exp Med 2011 Feb 14;208(2):341-56.
45. van Schaijk BC, Vos MW, Janse CJ, Sauerwein RW, Khan SM. Removal of heterologous sequences from Plasmodium falciparum mutants using FLPe-recombinase. PLoS One 2010;5(11):e15121.
46. Yu M, Kumar TR, Nkrumah LJ, et al. The fatty acid biosynthesis enzyme FabI plays a key role in the development of liver-stage malarial parasites. Cell Host Microbe 2008 Dec 11;4(6):567-78.
47. Matuschewski K, Ross J, Brown SM, Kaiser K, Nussenzweig V, Kappe SHI. Infectivity-associated changes in the transcriptional repertoire of the malaria parasite sporozoite stage. Journal of Biological Chemistry 2002 Nov 1;277(44):41948-53.
48. Kumar KA, Sano G, Boscardin S, et al. The circumsporozoite protein is an immunodominant protective antigen in irradiated sporozoites. Nature 2006 Dec 14;444(7121):937-40.
49. Cockburn IA, Tse SW, Radtke AJ, et al. Dendritic Cells and Hepatocytes Use Distinct Pathways to Process Protective Antigen from Plasmodium in vivo. PLoS Pathog 2011 Mar;7(3):e1001318.
50. Matuschewski K, Hafalla JC, Borrmann S, Friesen J. Arrested Plasmodium liver stages as experimental anti-malaria vaccines. Hum Vaccin 2011 Jan 1;7:16-21.
51. Chattopadhyay R, Conteh S, Li M, James ER, Epstein JE, Hoffman SL. The Effects of radiation on the safety and protective efficacy of an attenuated Plasmodium yoelii sporozoite malaria vaccine. Vaccine 2009 Jun 2;27(27):3675-80.
52. Kappe S. Genetically engineered malaria parasite vaccine approaches: Current status. 2010. Report No.: Symposium 150.

Supplementary Information

Material and Methods

Animals and parasites

Female C57BL/6, BALB/c and Swiss OF1 mice (6-8 weeks old; Charles River/Janvier) were used. All animal experiments were performed after a positive recommendation of the Animal Experiments Committee of the LUMC (ADEC) and RUNMC (RUDEC 2008-123, RUDEC 2008-148) was issued to the licensee. The Animal Experiment Committees are governed by section 18 of the Experiments on Animals Act and are registered by the Dutch Inspectorate for Health, Protection and Veterinary Public Health, which is part of the Ministry of Health, Welfare and Sport. The Dutch Experiments on Animal Act is established under European guidelines (EU directive no. 86/609/EEC regarding the Protection of Animals used for Experimental and Other Scientific Purposes).

The following reference lines of the ANKA strain of *P. berghei* were used: line cl15cy1[1]; line 676m1cl1 (*Pb*GFP-Luc$_{con}$; see RMgm-29 in www.pberghei.eu) and 507cl1 (*Pb*GFP$_{con}$; for details see RMgm-7 in www.pberghei.eu). *Pb*GFP$_{con}$ expresses GFP from the constitutive *eef1a* promoter and *Pb*GFP-Luc$_{con}$ expresses a fusion protein of GFP and Luciferase from the *eef1a* promoter [2;3]. For *P. falciparum* the lines NF54 (wild type; wt) and mutant lines *PfΔ52+36* and *PfΔ52+36gfp* [4] were used. In these mutant lines of the NF54 line the *p52 (*PFD0215c) and *p36* (PFD0210c) genes have been disrupted by double cross-over homologous integration [4]. Blood stages were cultured in a semi-automated culture system using standard *in vitro* culture conditions for *P. falciparum* and induction of gametocyte production in these cultures was performed as previously described[5;6].

Generation of *P. falciparum Δp52+p36* mutants

The generation of two independent *P. falciparum PfΔ52+p36* mutants, *PfΔ52+36* and *Pf**Δ**52+36gfp,* has been previously described in van Schaijk et al [4]. For this study we characterized oocyst and sporozoite production of both clones and the sporozoites were subsequently used for analysis of liver stage development (see below).

RT-PCR analysis of *P. falciparum* WT and *Δp52+p36* mutant sporozoites

Absence of transcripts of the targeted genes in sporozoites was analysed by reverse transcriptase-PCR. Total RNA was isolated using the RNeasy mini Kit (Qiagen) from 10^6 salivary gland sporozoites collected by mosquito dissection of mosquitoes 16 days post feeding with NF54 or *PfΔp52+36* parasites. Remaining DNA was degraded using DNAseI (Invitrogen). cDNA was subsequently synthesized using the First Strand cDNA synthesis Kit for RT-PCR AMV (Roche) (RT+) and as a negative control for the presence of genomic DNA, reactions were also preformed without reverse transcriptase (RT-). PCR amplification was performed for regions of *p52* or *p36* using primers BVS139 (5' gaatgtaaattcagatgaagctcaagaatgc) and BVS140 (5' ag-

gtatattatcaccaaaatcacaaccc) or BVS141 (5' tcataatgtgtatccagttgtgac) and BVS142 (5' catagaatggcatgtaaattcccac) respectively. Positive control was performed by PCR of 18S rRNA using primers 18Sf (5'gtaattggaatgataggaatttacaaggt) and 18Sr (5'tcaactacgaacgttttaactgcaac). PCR products were size fractionated on a 2.0% agarose gel.

Generation of *P. berghei Δp52+p36* and *Δfabb/f mutants*

To disrupt the genes *p36* (PBANKA_100210) and *p52* (PBANKA_100220) a single gene deletion construct was constructed using the standard targeting DNA construct, pL0001 (www.MR4.org) which contains the pyrimethamine resistant (pyr^r) cassette derived from the *Toxoplasma gondii* (*tg*) gene, *tgdhfr/ts*, as a selectable-marker cassette (SM). Target sequences for integration of the construct by double cross-over homologous recombination were PCR amplified from *P. berghei* genomic DNA (cl15cy1) using primers (Table S1) specific for the 5' and 3' end of *p52* and *p36* respectively. The PCR–amplified target sequences were cloned either upstream or downstream of the SM of plasmid pL0001 (Fig. S1). The linear DNA construct, pL1164, used for transfection was obtained after digestion of plasmids with the appropriate restriction enzymes (Table S1). Two independent mutants (*Δp52+p36*-a, -b) were generated that lack expression of both P36 and P52. One mutant (*Δp52+p36*-a; 795cl1) was generated in reference line *Pb*GFP$_{con}$ (Fig. S1) and the other (*Δp52+p36*-b; 1409cl1*)* in the *Pb*GFP-Luc$_{con}$ line (Fig. S2) using standard methods of transfection, drug-selection and parasite cloning [1]. To disrupt the gene *fabb/f* two different DNA constructs were generated. For the first construct, pL1454, the same approach was used as described above for *Δp52+p36* using standard plasmid pL0037 [7]. This plasmid contains the *hdhfr::yfcu* selectable marker which is a fusion of the human *dhfr (hdhfr*) gene and the negative selection marker *yfcu* that confers susceptibility to the pro-drug 5-FC [7]. Target sequences were PCR amplified from *P. berghei* genomic DNA (cl15cy1) using primers (Table S1) specific for the 5' and 3' end of *fabb/f* and cloned either upstream or downstream of the SM (Fig. S3). Using this construct the mutant *Δfabb/f*-a (1345cl1) was generated in the cl15cy1 reference line using standard methods of transfection (Fig. S3). For the second construct, pL1662, we adapted a previously described 'Anchor-tagging' PCR-based method for generation of gene deletion constructs[8]. This method employs a 2-step PCR reaction shown in Figure S4. In the first PCR reaction two-flanking fragments (5'or 3'; 0.8 kb each) of *fabb/f* were amplified using genomic DNA (cl15cy1) as template with the primer pairs 5804/5805 (5'target sequence) and 5806/5807 (3'target sequence). Both primer 5805 and 5806 (Table S1) have 5'-terminal extensions homologues to the *hdhfr* selectable marker cassette. This cassette contains the *hdfr* under control of the *eef1a* promoter region and the 3'UTR *pbdhfr/ts* and is obtained from plasmid pL0040 by digestion with restriction enzymes *Xho*I and *Not*I (pL0040 is available from The Leiden Malaria Research Group). Primers 5804 and 5807 (Table S1) have 5'-terminal overhang with an anchor-tag suitable for the second PCR reaction. In the second PCR reaction the fragments were annealed to either side of the *hdhfr* selectable marker cassette with anchor-tag primers 4661/4662, resulting in the second PCR fragment with the expected size, i.e. 3.2 kb (1.6 kb of the selectable marker cassette + two targeting fragments of 0.8Kb). To remove the anchor-tag from the final DNA

construct, the second PCR fragment was digested with *Asp*718 and *Sca*I as primer 5804 contained an *Asp*718 restriction enzyme site and 5807 contained a *Sca*I site. Following ethanol precipitation, the PCR fragment was re-suspended in water at 1µg/µl and used for transfection. Using this PCR-based targeting construct the mutant *Δfabb/f*-b (1704cl1) was generated in the *Pb*GFP-Luc$_{con}$ reference line using standard methods of transfection (Fig. S4).
Correct integration of the constructs into the genome of mutant parasites was analysed by diagnostic PCR-analysis and Southern analysis of PFG-separated chromosomes[9] as shown in Fig. S1-3. PFG-separated chromosomes were hybridized with a probe recognizing the 3'-UTR *dhfr/ts* of *P. berghei*[1]. Absence of transcripts of the targeted genes in sporozoites was analysed by reverse transcriptase-PCR. Total RNA was purified from salivary gland sporozoites (see below) using TRIzol reagent (Invitrogen) and prepared according to manufactures specifications. Purified RNA was then treated with RQ1 DNase (Promega). Reverse transcription was performed using the Super Script III RT (Invitrogen) as previously described in van Dijk *et al* (2005)[10]. cDNA was used as template for PCR amplification with control and gene specific primers that are listed in Table S1.

Analysis of blood stage and oocyst development of *P. falciparum* and *P. berghei* mutant parasites

P. falciparum blood stages were cultured in a semi-automated culture system using standard *in vitro* culture conditions for *P. falciparum* and induction of gametocyte production in these cultures was performed as previously described [5;6]. Blood stage development and production of gametocytes of PfΔp*52+p36* and PfΔp*52+p36gfp* were analyzed as described [4] and were similar to parasites of the parent line NF54. Feeding of *A. stephensi* mosquitoes and determination of oocyst production was performed as described [11]. Oocyst production of both *pfΔp52+p36* and *pfΔp52+p36gfp* were comparable to the parent line NF54 (Fig. 4A).
The *P. berghei* mutants, *Δp52+p36* and *Δfabb/f,* were maintained in Swiss OF1 mice. The multiplication rate of blood stages and gametocyte production were determined during the cloning procedure [1] and were not different from parasites of the reference ANKA lines. Feeding of *A. stephensi* mosquitoes and determination of oocyst production was performed as described [12].

Analysis of *P. falciparum* and *P. berghei* sporozoite production, motility and hepatocyte traversal

P. berghei sporozoites were collected at day 21 after infection by hand-dissection of the salivary glands. Salivary glands were collected in DMEM (Dulbecco's Modified Eagle Medium from GIBCO) and homogenized in a homemade glass grinder. The number of sporozoites was determined by counting the numbers of sporozoites of 10 salivary glands in duplicate in a Bürker-Türk counting chamber using phase-contrast microscopy. *P. falciparum* sporozoites were collected at day 14-16 after infection by hand-dissection of the salivary glands. These salivary glands were collected in William's E medium supplemented with 10% FCS, 2% penicillin-streptomycin, 1% sodium-pyruvate, 1% L-glutamine, 1% insulin-

transferin-selenium (Gibco) and 10-^{7}M dexamethasone (Sigma) and homogenized in a home made glass grinder. The free sporozoites were counted in a Bürker-Türk counting chamber using phase-contrast microscopy. Sporozoite production of *PfΔ52+36* and *PfΔ52+36gfp* were comparable to the parent line NF54 (Fig. 4A).

Gliding motility of *P. berghei* sporozoites was determined in assays that were performed on anti-*P. berghei* circumsporozoite antibody (3D11, monoclonal mouse antibody 10 µg/ml) pre-coated Labtek slides (Nunc, NL) to which 2×10^{4} sporozoites were added [10]. After 30 minutes of incubation at 37°C sporozoites were fixed with 4% PFA and after washing with PBS, the sporozoites and the trails ('gliding circles') were stained with anti-CSP-antibody (3D11[13]) conjugated to Alexa 488 (Dylight 488 antibody labeling kit; Thermo Scientific, NL). Slides were mounted with Fluoromount-G (SouthernBiotech, NL) and 'gliding circles' were analyzed using a Leica DMR fluorescence microscope at 1000X magnification.

P. berghei sporozoite hepatocyte traversal was determined in assays as described previously[14]. Briefly, human liver hepatoma cells (Huh7) were suspended in 1ml of 'complete' DMEM (DMEM from Gibco, supplemented with 10% FCS, 1% penicillin/streptomycin and 1% Glutamax) and were plated in 24 well plates (10^{5} cells/ml). After the Huh7 monolayers were >80% confluent, 10^{5} sporozoites were added with the addition of FITC- or Alexa-647-labeled dextran (Invitrogen, NL). No sporozoites were added to the negative control wells. FACS analysis of dextran-positive cells was performed on a total 25x10^{3} cells per well (each experiment was performed in triplicate wells) using a FACScalibur flow cytometer (Becton Dickinson, NL). *P. falciparum* sporozoite hepatocyte traversal was determined in assays previously described [11].

Analysis of *P. falciparum* and *P. berghei* sporozoite infectivity and development in hepatocytes in immuno-fluorescence assays

Infectivity of *P. falciparum* sporozoites and development in hepatocytes was analysed in primary human hepatocytes. Primary human hepatocytes were isolated from healthy parts of human liver fragments which were collected during unrelated surgery in agreement with French national ethical regulations as described[15]. Cells were seeded into 96-well plates or 8-chamber Lab-Tec slides (Nalge Nunc) coated with rat tail collagen I (Becton Dickinson, Le Pont de Claix, France) at a density of 8x10^{4} or 21x10^{4} cells per well, respectively. These cells were cultured at 37°C in 5% CO_2 in complete William's E culture medium supplemented with 10% FCS, 2% penicillin-streptomycin, 1% sodium-pyruvate, 1% L-glutamine and 1% insulin-transferin-selenium (reagents for cell culture Gibco, Invitrogen) and 10-^{7}M dexamethasone (Sigma, Saint Quentin Fallavier, France). Sporozoites (5 x10^{4}) were added to the hepatocyte cultures, and 3 hours after addition of sporozoites, the cultures were washed with culture medium to remove mosquito salivary gland material as well as non-invaded and unattached sporozoites, culture medium was added and cultures were incubated overnight at 37°C. The culture medium was replaced with fresh culture medium at 24h and 72h after infection[16]. Cultures were fixed at different time points after adding sporozoites with cold methanol and developing liver schizonts were stained with anti- HSP70 antibodies [17] followed by stain-

ing with goat anti-mouse ALEXA-488 (green, fluorescence; Molecular probes). Nuclei were stained with 1µg/ml diamidino-phenylindole (DAPI).
Invasion of primary human hepatocytes by *P. falciparum* sporozoites was determined as described[18]. Cultures were fixed with 4% paraformaldehyde (PFA) for 20 min at room temperature and extracellular (non-invaded) parasites were stained with anti-CSP antibody (3SP2) followed by staining anti-mouse-ALEXA594 (red fluorescence; Molecular probes). To detect intracellular parasites, the hepatocytes were subsequently permeabilised with 1% Triton-X-100 in PBS for 4 min and stained with with anti-CSP antibody (3SP2) and these were then identified using anti-mouse-ALEXA488 (i.e. green fluorescence; Molecular probes). Nuclei were stained with 1µg/ml DAPI. Analysis and counting of stained intracellular and extracellular parasites were performed using a DM-IRBE Flu Leica fluorescence microscope.
Infectivity of *P. berghei* sporozoites and development was determined in cultures of Huh7 cells (see above). Sporozoites (5×10^4) were added to a monolayer of Huh7 cells on coverslips in 24 well plates (with a confluency of 80-90%) in 'complete' DMEM (see above). At different time points after infection, cells were fixed with paraformaldehyde 4%, permeabilized with Triton-X-100 0.1%, blocked with 10% FCS in PBS, and subsequently stained with a primary and secondary antibody, for 2h and 1h respectively. Primary antibodies used were anti-PbEXP1 (raised in chicken [19]), detecting the PVM-resident protein (PBANKA_092670); anti-PbHSP70 (raised in mouse[10]), detecting the cytoplasmic heat shock protein 70 (PBANKA_081890);, and anti-MSP-1 (mouse; MRA-78 from MR4; www.MR4.org) detecting MSP1 of *P. yoelii* and *P. berghei*. Anti-mouse, -chicken and -rabbit secondary antibodies, conjugated to Alexa-488 and Alexa-594, were used for visualization (Invitrogen). Nuclei were stained with Hoechst-33342. Cells were mounted in Vectashield (Vector Laboratories) and examined using a DM-IRBE Flu Leica fluorescence microscope.
Invasion of hepatocytes *in vitro* by *P. berghei* sporozoites was determined, as described for *P. falciparum* above, specifically by addition of 5×10^4 sporozoites to a monolayer of Huh7 cells. After the addition of sporozoites, cultures were centrifuged for 10 minutes at 1800G (Eppendorf centrifuge 5810 R) and then returned to the 37°C incubator. After 2-3 hours wells were washed 3 times with PBS to remove uninvaded sporozoites. Cells were fixed with 4% paraformaldehyde (PFA) for 10 min and extracellular (non-invaded) parasites were stained with anti-CS-antibody (3D11) and conjugated with Alexa 594 antibody (Dylight 594 antibody labeling kit; Thermo Scientific, NL). After permeabilization with 0.1 % Triton-X-100 for 10 minutes and blocking with 10% FCS in PBS for 20 minutes, intracellular sporozoites were with anti-CS-antibody (3D11) and conjugated with Alexa 488 antibody (Dylight 488 antibody labeling kit; Thermo Scientific, NL). Nuclei were stained with Hoechst-33342. Analysis and counting of stained intracellular and extracellular parasites were performed using a Zeiss Axiophot Fluorescence microscope with Axiocam MRm CCD camera.

Analysis of *P. berghei* sporozoite development in hepatocytes by qRT-PCR

Sporozoites (5×10^4) were added to a monolayer of Huh7 cells, in 24 well plates (seeded the day before with 10^5 hepatocytes) in 'complete' DMEM (see above). At different time points

after adding the sporozoites, culture medium was removed, cells washed once with PBS, and cells were resuspended in 200 µl of RLT buffer (Quiagen's MicroRNeasy kit). RNA from these samples was extracted following the manufacturer's instructions. The transcriptor first-strand cDNA synthesis kit (Roche) was used according to the manufacturer's recommendations to make single-stranded cDNA. Real-time PCR analysis of *P. berghei* 18S rRNA and human β-actin was performed as described [20]. qRT-PCR curves were drawn using the GraphPad Prism software (GraphPad Prism, Inc., US)

Analysis of *P. berghei* sporozoite infectivity in mice and *in vivo* imaging of liver stage development in mice

C57BL/6 mice were inoculated with sporozoites by intravenous injection of different sporozoite numbers, ranging from $1x10^4$ - $5x10^5$. Blood stage infections were monitored by analysis of Giemsa-stained thin smears of tail blood collected on day 4-14 after inoculation of sporozoites. Pre-patency (measured in days after sporozoite inoculation) is defined as the day when parasitemia of 0.5-2%.in the blood is observed.

Liver stage development in live mice was monitored by real-time *in vivo* imaging of liver stages as described [20;21]. Liver stages were visualized by measuring luciferase activity of parasites (expressing luciferase under the *eef1a* promoter) in whole bodies of mice or in dissected livers using the IVIS100 Imaging System (Caliper Life Sciences, USA). Animals were anesthetized using the isofluorane-anesthesia system (XGI-8, Caliper Life Sciences, USA), their belly was shaved and D-luciferin dissolved in PBS (100 mg/kg; Synchem Laborgemeinschaft OHG, Germany) was injected subcutaneously (in the neck). Animals were kept anesthetized during the measurements, which were performed within 3 to 5 minutes after the injection of D-luciferin. Bioluminescence imaging was acquired with a 10 cm FOV, medium binning factor and an exposure time of 10 to 180 seconds. Quantitative analysis of bioluminescence of whole bodies was performed by measuring the luminescence signal intensity using the ROI settings of the Living Image® 3.0 software. The ROI was set to measure the abdominal area at the location of the liver and ROI measurements are expressed in total flux of photons.

Immunizations of mice with *P. berghei* sporozoites

BALB/C and C57BL6 mice were immunized by intravenous injection using different numbers of *Δp52+p36* and Δ*fabb/f* sporozoites collected as described above. Immunized mice were monitored for blood infections by analysis of Giemsa stained films of tail blood at day 4-16 after immunization. Immunized mice were challenged at different time points after immunization by intravenous injection of $1x10^4$ sporozoites from the *P. berghei* ANKA reference lines cl15cy1 or the *Pb*GFP-Luc_{con}. In each experiment, naïve mice were included to verify infectivity of the sporozoite used for challenge. After challenge, mice were monitored for blood infections by analysis of Giemsa stained films. Pre-patent period is defined as the period (days) between sporozoite challenge and the day that mice showed a blood parasitemia of 0.5-2%.

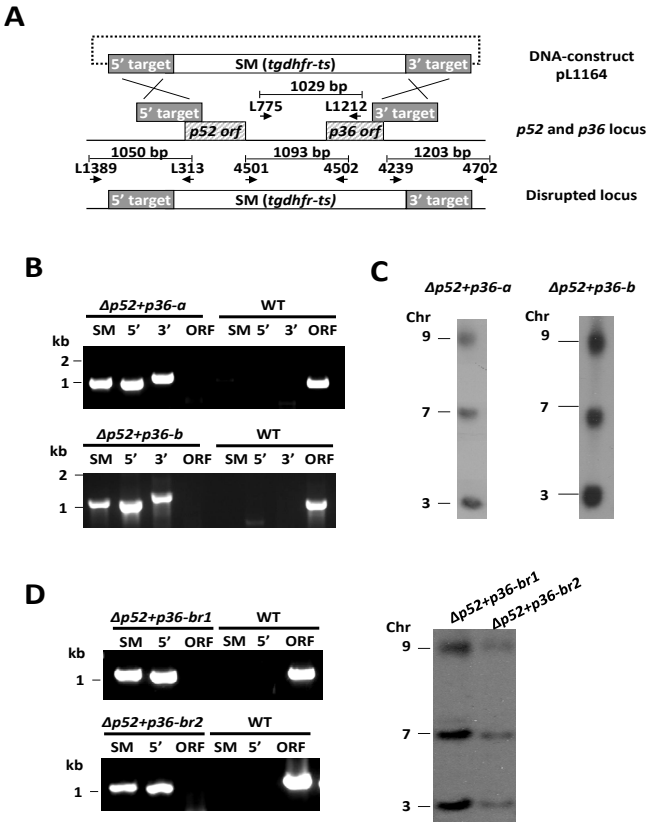

Figure S1: Generation of *P. berghei* mutants *Δp52+p36-a* and *Δp52+p36-b* and genotype analyses of *Δp52+p36-a*

A) Schematic showing the generation of mutants *Δp52+p36-a* (759cl1) and *Δp52+p36-b* (1409cl1). The DNA-construct pL1164 is aimed at disruption of target genes, p52 and p36, by double cross-over homologous recombination. The sequence of the primers to amplify the 5'- and 3'-target regions of the genes are shown in Table S1. Primers for diagnostic PCR (table S1) and size of the PCR DNA fragments are shown. **B)** Diagnostic PCR for confirmation of correct disruption of p52 and p36 in mutant *Δp52+p36-a* and *Δp52+p36-b*. SM: selectable marker (primers 4501/4502); 5'-integration event (primers L1389/ L313); 3'-integration event (primers 4239/47020); ORF (primers L775/L121). See Table S1 for the sequence of the primers. **C)** Southern analysis of Pulse Field Gel (PFG)-separated chromosomes of mutant *Δp52+p36-a* and *Δp52+p36-b*. Mutant *Δp52+p36-a* has been generated in the reference *P. berghei* ANKA line *Pb*GFP$_{con}$ which has a gfp gene integrated into the silent 230p locus (PBANKA_030600) on chromosome 3 (i.e. RMgm-7; http://pberghei.eu/index.php?rmgm=7). Mutant *Δp52+p36-b* has been generated in the reference *P. berghei* ANKA line *Pb*GFP-Luc$_{con}$ which has a gfp-luciferase gene integrated into the silent 230p locus (PBANKA_030600) on chromosome 3 (i.e. RMgm-29; http://pberghei.eu/ index.php?rmgm=29) . Hybridization with the 3'-UTR dhfr/ts probe recognizes the integrated construct on chromosome 9, the reporter GFP-Luc$_{con}$ construct on chromosome 3, and the endogenous dhfr/ts gene located on chromosome 7. **D)** PCR and FIGE confirmation that the *Δp52+p36-b* parasites that produced a breakthrough blood infections in BALB/c mice had the correct, mutant, genotype (see Figure 3).

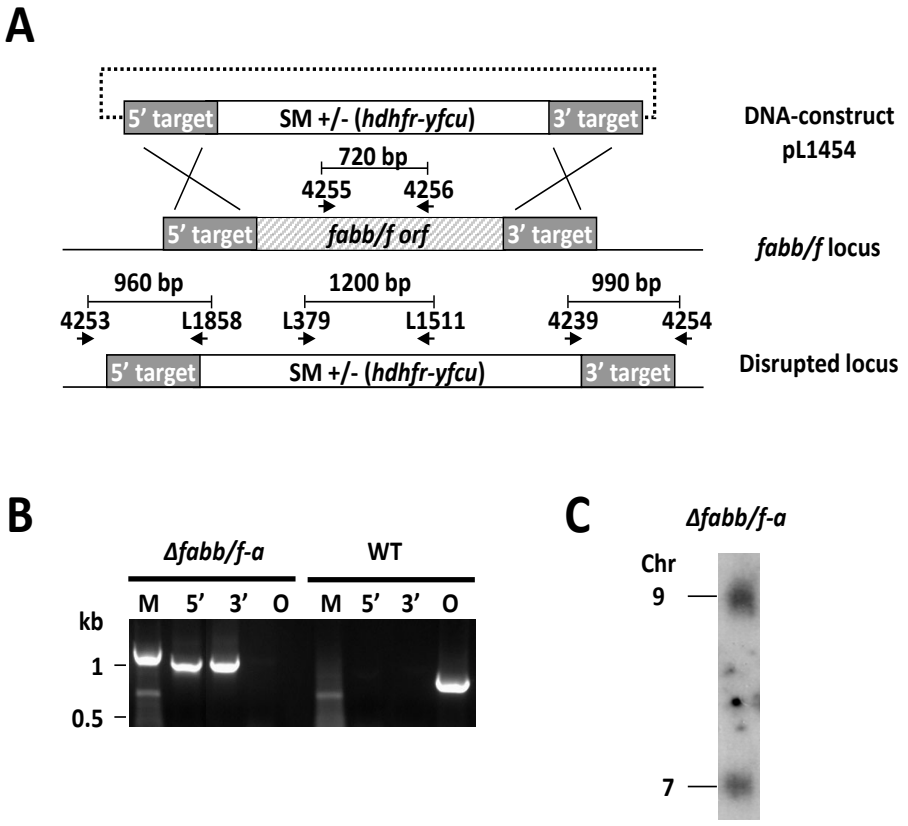

Figure S2: Generation and genotype analyses of *P. berghei* mutant; *Δfabb/f-a*

A) Schematic showing the generation of mutant *Δfabb/f-a* (1345cl1). The DNA-construct pL1454 is aimed at disruption of target gene by double cross-over homologous recombination. The sequence of the primers to amplify the 5'- and 3'-target regions of the genes are shown in Table S1. Primers for diagnostic PCR (Table S1) and size of the PCR DNA fragments are shown. **B)** Diagnostic PCR for confirmation of correct disruption of fabb/f in mutant *Δfabb/f-a*. SM: selectable marker (primers L379/L1511); 5'-integration event (primers 4253/L1858); 3'-interation event (primers 4239/4254); ORF (primers 4255/4256). See Table S1 for the sequence of the primers. **C)** Southern analysis of PFG-separated chromosomes of mutant *Δfabb/f-a*. This mutant has been generated in the reference *P. berghei* ANKA line cl15cy1. Hybridization with the 3'-UTR dhfr/ts probe recognizes the integrated construct on chromosome 9 and the endogenous dhfr/ts gene located on chromosome 7.

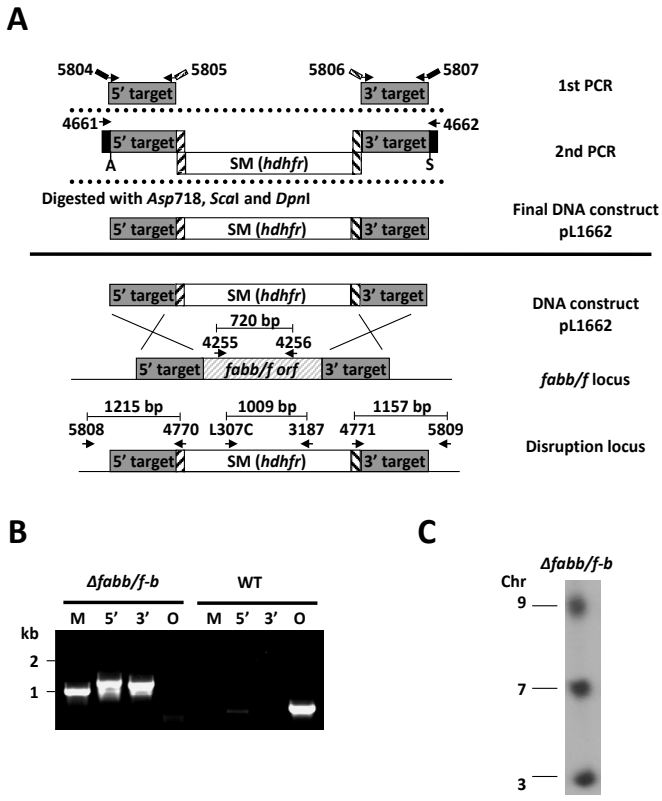

Figure S3: Generation and genotype analyses of *P. berghei* mutant; *Δfabb/f-b*

A) Schematic showing the generation of mutant *Δfabb/f-b* (1704cl1). The DNA-construct pL1662 is aimed at disruption of target gene by double cross-over homologous recombination. The construct was generated by an adapted 'Anchor-tagging' PCR-based method employing a 2-step PCR reaction. In the first PCR step two-flanking fragments of fabb/f were amplified from genomic DNA with the primers 5804/5805 (5') and 5806/5807 (3'). Both primer 5805 and 5806 have 5'-terminal extensions homologues to the hdhfr selectable marker cassette (SM) obtained from plasmid pL0040 by digestion with restriction enzymes XhoI and NotI. Primers 5804 and 5807 have 5'-terminal overhang with an anchor-tag suitable for the second PCR step. In this step the fragments were annealed to either side of the SM with anchor-tag primers 4661/4662, resulting in the second PCR fragment. To remove the 'anchor', the second PCR fragment was digested with Asp718 and ScaI as primer 5804 contained an Asp718 restriction enzyme site and 5807 contained a ScaI site. See Table S1 for the sequence of the primers. **B)** Diagnostic PCR for confirmation of correct disruption of fabb/f in mutant *Δfabb/f*-b. SM: selectable marker (primers L307C/3187); 5'-integration event (primers 5808/4470); 3'-interation event (primers 4471/5809); ORF (primers 4255/4256). See Table S1 for the sequence of the primers. **C)** Southern analysis of PFG-separated chromosomes of mutant *Δfabb/f*-b. This mutant has been generated in the reference *P. berghei* ANKA *Pb*GFP-Luc$_{con}$ which has a gfp-luciferase gene integrated into the silent 230p locus (PBANKA_030600) on chromosome 3. Hybridization with the 3'-UTR dhfr/ts probe recognizes the integrated construct on chromosome 9, the reporter GFP-Luc$_{con}$ construct on chromosome 3, and the endogenous dhfr/ts gene located on chromosome 7.

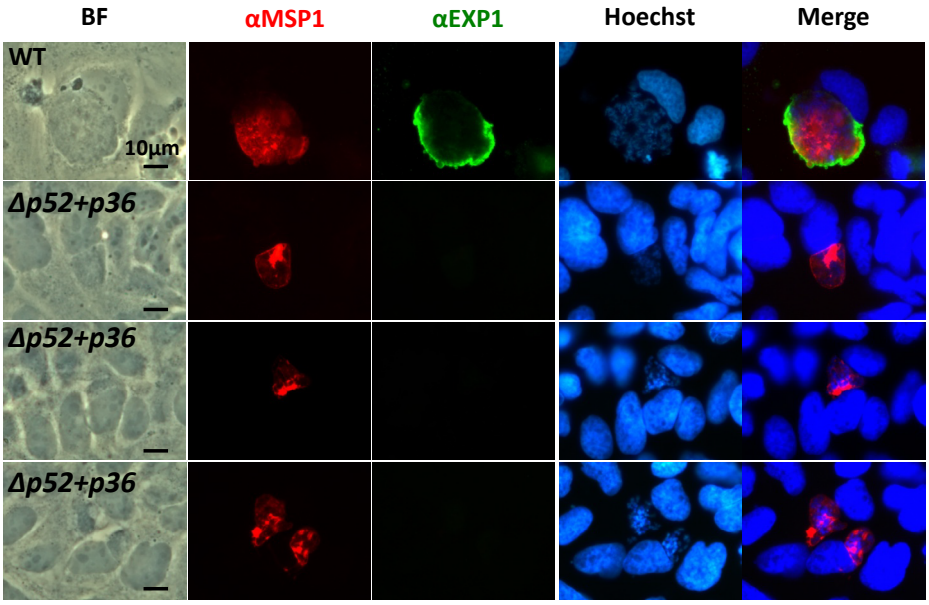

Figure S4: IFA analysis of the few *Δp52+p36* infected hepatocytes (Huh7) visible at 48hpi
Three *Δp52+p36* infected hepatocytes are compared with a control WT infected hepatocytes. Staining with anti-MSP1 antibodies (red) identifies maturing merozoites inside the liver schizont; anti-PbEXP1 recognize the parasitophorous vacuole (green) and is clearly visible around only WT parasites and is absent in all *Δp52+p36* infected cells. Nuclei are stained with Hoechst-33342.

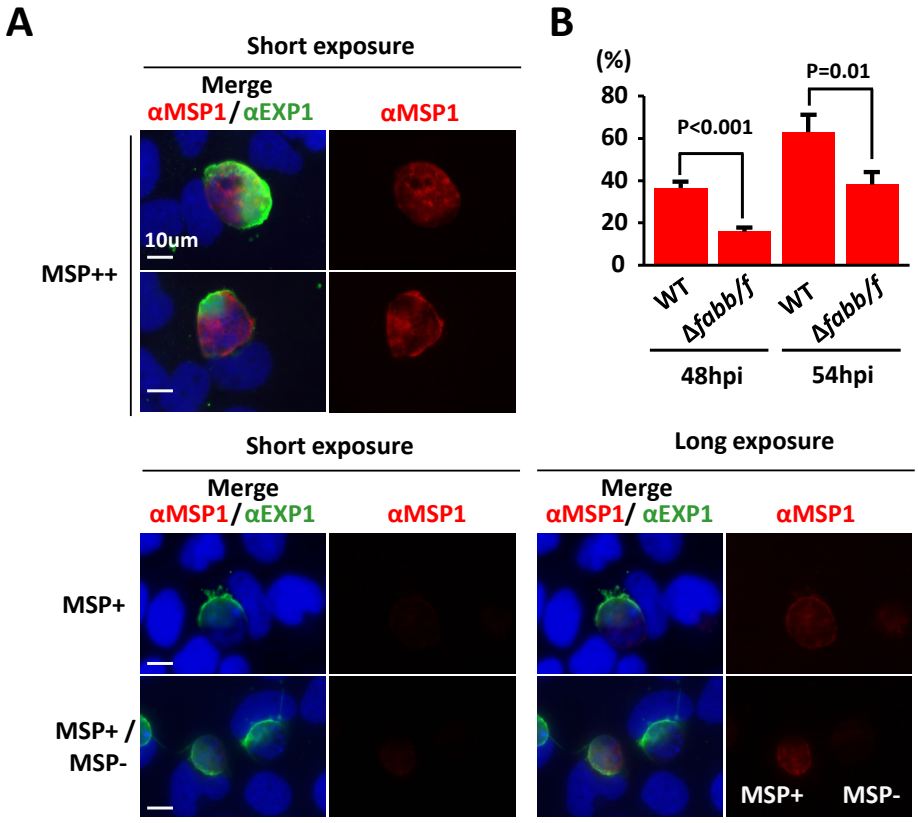

Figure S5

A) MSP1 IFA expression criteria of liver stage parasites at 54hpi. Parasites are stained with anti-MSP1 (red) and anti-EXP1 (green)-antibodies. Nuclei are stained with Hoechst-33342. MSP1++: MSP1 staining visible after short exposure (0.5 sec); MSP +: MSP1 staining only visible after long exposure (4 sec); MSP-: MSP1 staining not visible even after long exposure (4 sec), using a Leica DFC 420C camera and ebq 100 lamp, see Material and Methods for details. **B)** The percentage of (strongly; i.e. MSP++) MSP1 expressing liver stage parasites was determined at 48hpi and 54hpi (see Figure 2C). There are significantly more MSP1++ positive WT infected hepatocytes than MSP++ *Δfabb/f* infected hepatocytes at both 48 and 54hpi (using a paired student t-test; $p<0.001$ at 48hpi and $p=0.01$ at 54hpi; GraphPad Prism 5® software).

Table S1

List of primers and primer sequences used in this study

	Name	Sequence	Restriction site	Description	Gene models
Primers for generation of the Δp52+p36 target regions (for pL1164) (restriction sites are shown in red)					
Δp52+p36	L903	CGATCGATGAATAATAGTAAATGATGAAACGTCG	ClaI	*Δp52+p36* 5' target F	PBANKA_100220 and PBANKA_100210
Δp52+p36	L904	CCCAAGCTTAATTACGTCCCCTGGATATGC	HindIII	*Δp52+p36* 5'target R	PBANKA_100220 and PBANKA_100210
Δp52+p36	L864	GGATATCCGATTTAGCATCTCATCATGG	EcoRV	*Δp52+p36* 3' target F	PBANKA_100220 and PBANKA_100210
Δp52+p36	L865	CGGGGTACCTGGTACTGCGAAAATCACACC	KpnI	*Δp52+p36* 3' target R	PBANKA_100220 and PBANKA_100210
Primers for confirmation PCR of the integration event in *Δp52+p36*					
Δp52+p36	L1389	ATTTTGCAACAATTTTATTCTTGG		*Δp52+p36* 5' integration F	PBANKA_100220 and PBANKA_100210
Δp52+p36	L313	ACGCATTATATGAGTTCATTTTAC		*Δp52+p36* 5' integration R from KO construct pL1164	
Δp52+p36	4239	GATTTTTAAAATGTTTATAATATGATTAGC		*Δp52+p36* 3' integration F from KO construct pL1164	
Δp52+p36	4702	TATTTGGGTATGCCGTGAGG		*Δp52+p36* 3' integration R	PBANKA_100220 and PBANKA_100210
Δp52+p36	L775	GAAACAATATGAGTTCGCACGC		*Δp52+p36* intergenic region F	PBANKA_100220 and PBANKA_100210
Δp52+p36	L1212	TATATTGCTAGTCCTTTGTTCC		*Δp52+p36 p36* orf R	PBANKA_100220 and PBANKA_100210
Δp52+p36	4501	GGACAGATTGAACATCGTCG		*tgdhfr/ts F*	
Δp52+p36	4502	GATCACATTCTTCAGCTGGTC		*tgdhfr/ts R*	
Primers for generation of the *Δfabb/f* target regions (for pL1454) (restriction sites are shown in red)					
Δfabb/f	4194	GCGCGGTACCACATAAATTTGTACAAAACTTAAATGA	KpnI	*Δfabb/f* 5' target F	PBANKA_112510
Δfabb/f	4195	GCGCGGATCCGATATGTATTTATTTCACACACTTTAT	BamHI	*Δfabb/f* 5'target R	PBANKA_112510
Δfabb/f	4196	GCGCGAATTCATTTATTAGTTGATATTATTATTTATA	EcoRI	*Δfabb/f* 3' target F	PBANKA_112510
Δfabb/f	4197	GCGCCCCGGGTTTATATGTATATCTCATATAAATGGT	XmaI	*Δfabb/f* 3' target R	PBANKA_112510
Primers for confirmation PCR of the intergration even in *Δfabb/f*					
Δfabb/f	4253	ATTTCCTCTTTTTCTGCTTTTTGGTTCACC		*Δfabb/f* 5' integration F	PBANKA_112510
Δfabb/f	L1858	ATGCACAAAAAAAAATATGCACAC		*Δfabb/f* 5' integration R from KO construct	
Δfabb/f	4239	GATTTTTAAAATGTTTATAATATGATTAGC		*Δfabb/f* 3' integration F from KO construct	
Δfabb/f	4254	TATATGTATATATGATTAATCCATAACCC		*Δfabb/f* 3' integration R	PBANKA_112510
Δfabb/f	4255	GAGGAATTTCTATTGGTATGTTAAGTGCATGCG		*Δfabb/f* orf F	PBANKA_112510
Δfabb/f	4256	ATTTAATGAAAAATCAATATTCTGTTCTGAGGG		*Δfabb/f* orf R	PBANKA_112510
Δfabb/f	L379	GGCAAGAACGGGGACCTG		*hdhfr F*	
Δfabb/f	L1511	CGATTCACCAGCTCTGAC		*yfcu R*	
Primers for the Anchor-tagging PCR-based method: Generation of *Δfabb/f* target regions (for pL1662) (restriction sites are shown in red; Anchor tags are shown in blue)					
Δfabb/f	5804	GAACTCGTACTCCTTGGTGACGGTACCGGTAATGGATGTGTACACAAAAG	Asp718	*Δfabb/f* 5' target F	PBANKA_112510
Δfabb/f	5805	CATCTACAAGCATCGTCGACCTCCACACTGTATACAGGACACTTG		*Δfabb/f* 5'target R	PBANKA_112510
Δfabb/f	5806	CCTTCAATTTCGGATCCACTAGCATGGCATCTTTCTCGCACAC		*Δfabb/f* 3' target F	PBANKA_112510
Δfabb/f	5807	AGGTTGGTCATTGACACTCAGCAGTACTTGATAACCTATGCACTCAAGG	ScaI	*Δfabb/f* 3' target R	PBANKA_112510
Δfabb/f	4661	GAACTCGTACTCCTTGGTGACG		for 2nd PCR	
Δfabb/f	4662	AGGTTGGTCATTGACACTCAGC		for 2nd PCR	
Primers for confirmation PCR of the integration event in *Δfabb/f* (Anchor tags are shown in blue)					
Δfabb/f	5808	ACTAATGCACACTGCAGTTAC		*Δfabb/f* 5' integration F	PBANKA_112510
Δfabb/f	4770	CATCTACAAGCATCGTCGACCTC		*Δfabb/f* 5' integration R from KO construct	PBANKA_112510
Δfabb/f	5809	GGGTTGTATAATACCTTCTTCG		*Δfabb/f* 3' integration F from KO construct	PBANKA_112510
Δfabb/f	4771	CCTTCAATTTCGGATCCACTAG		*Δfabb/f* 3' integration R	PBANKA_112510
Δfabb/f	L307C	GCTTAATTCTTTTCGAGCTC		*hdhfr F*	
Δfabb/f	3187	GTGTCACTTTCAAAGTCTTGC		*hdhfr R*	
Primers for RT-PCR					
RT-PCR	6301	ATACCAGAACCACATGTTACG		*CS* for RT primer	PBANKA_040320
RT-PCR	6302	CTCTACTTCCAGGATATGGAC		*CS* F for RT-PCR	PBANKA_040320
RT-PCR	6303	CATTGAGACCATTCCTCTGTG		*CS* R for RT-PCR	PBANKA_040320
RT-PCR	6304	CATTTCTTTTGCATGAGCAAC		*p52* for RT primer	PBANKA_100220
RT-PCR	6305	CCTAATACGACCTTAGGACAC		*p52* F for RT-PCR	PBANKA_100220
RT-PCR	6306	AACATCATTACTCGGATCTGG		*p52* R for RT-PCR	PBANKA_100220
RT-PCR	6140	TATTGCTAGTCCTTTGTTCCC		*p36* for RT primer	PBANKA_100210
RT-PCR	6310	TCCAACGGGGAATTGTAGTG		*p36* F for RT-PCR	PBANKA_100210
RT-PCR	6139	GTCCCTTCTATCTCATTAGG		*p36* R for RT-PCR	PBANKA_100210
RT-PCR	6311	GCTCCTATGCAATGACCTGTC		*fabb/f* for RT primer	PBANKA_112510
RT-PCR	6312	GACTTCCAGAGTTGTATGCAC		*fabb/f* F for RT-PCR	PBANKA_112510
RT-PCR	6313	ATCGGATACACTTATGTTGGC		*fabb/f* R for RT-PCR	PBANKA_112510

Table S2
Multiplication rate of asexual blood stages and gametocyte production of different *P. berghei*

Animals	Line number	in vivo multiplication rate[1]	Gametocyte production[2] (% Mean ± SD)
Δ*p52+p36-a*	795cl1	10 (0) n=3	18.4 (1.9)
Δ*p52+p36-b*	1409cl1	10 (0) n=6	19.0 (3.0)
Δ*fabb/f-a*	1354cl1	10 (0) n=3	20.3 (2.3)
Δ*fabb/f-b*	1704cl1	10 (0) n=2	17.9 (2.8)
WT		10 (0) n=10	Range: 15-25

The mean values and standard deviations (between brackets) are shown for the mutant lines. For the wild type parasites the range is shown of values obtained with 10 infections.
[1]The multiplication rate of asexual blood stages per 24h was determined in mice infected with a single parasite; n is the number of mice infected. [2]Gametocyte production is the percentage of blood stage parasites that develop into gametocytes under standardized *in vivo* conditions.

Table S3
Protection of BALB/c and C57BL/6 mice after immunization with *Δp52+p36* GAPs

Mice	GAP	Imm. dose	Challenge after imm[a]. days (re-challenge)	Protected/ infected No. mice (re-challenge)	Pre-patency days
Balb/c	Δp52+p36	50K	10d 90d (180d)	10/10 (10/10) (10/10)	n/a
	Δp52+p36	25K	10d 90d (180d)	10/10 (10/10) (10/10)	n/a
	Δp52+p36	10K	10d 90d (180d)	10/10 (10/10) (10/10)	n/a
	Δp52+p36 gfp::luc	10K	10d 90d (180d)	10/10 (10/10) (10/10)	n/a
	Δp52+p36	5K	10d 90d (180d)	10/10 (10/10) (10/10)	n/a
	Δp52+p36 gfp::luc	5K	10d (180d)	10/10 (10/10)	n/a
	Δp52+p36 gfp::luc	1K	10d (180d)	8/9 (5/5)	6
C57BL/6	Δp52+p36	50K	10d	0/5	6
	Δp52+p36 gfp::luc	50K	10d	0/5	6
	Δp52+p36	50/20/20K[b]	180d	6/7[c]	7[c]

[a]Wt challenge constitutes 10K sporozoites delivered i.v. [b]50K sporozoites i.v. day 0 followed by a boost of 20K sporozoites i.v. at day 7 and day 14. [c]40 mice were exposed to the 50/20/20K immunization regiment, only 7 mice remained blood stage negative and these mice then received their first challenge with WT parasites 6 months later (10K sporozoites i.v), 6/7 mice were protected and 1 mouse developed a patent blood stage infection at day 7.

Chapter 5

Plasmodium berghei Δp52&p36 parasites develop independent of a parasitophorous vacuole membrane in Huh-7 liver cells.

Ivo Ploemen, Huib Croes, Geert-Jan van Gemert, Mietske Wijers-Rouw, Cornelus Hermsen, Robert Sauerwein

PLoS ONE 2012 December 5;7(12): e50772

Abstract

The proteins P52 and P36 are expressed in the sporozoite stage of the murine malaria parasite *Plasmodium berghei*. *Δp52&p36* sporozoites lacking expression of both proteins are severely compromised in their capability to develop into liver stage parasites and abort development soon after invasion; presumably due to the absence of a parasitophorous vacuole membrane (PVM). However, a small proportion of *P. berghei Δp52&p36* parasites is capable to fully mature in hepatocytes causing breakthrough blood stage infections.

We have studied the maturation of replicating *Δp52&p36* parasites in cultured Huh-7 hepatocytes. Approximately 50% of *Δp52&p36* parasites developed inside the nucleus of the hepatocyte but did not complete maturation and failed to produce merosomes. In contrast cytosolic *Δp52&p36* parasites were able to fully mature and produced infectious merozoites. These *Δp52&p36* parasites developed into mature schizonts in the absence of an apparent parasitophorous vacuole membrane as shown by immunofluorescence and electron microscopy. Merozoites derived from these maturing *Δp52&p36* liver stages were infectious for C57BL/6 mice.

Introduction

Plasmodium sporozoites are transmitted to the mammalian host by the bites of infected *Anopheline* mosquitoes. The parasites leave the injection site and make their way to the liver where they invade hepatocytes before commencing the erythrocytic cycle. There are two distinct pathways by which *Plasmodium* sporozoites enter hepatocytes: they either migrate through cells disrupting the host cell membrane, or they invaginate the host cell membrane forming a parasitophorous vacuole (PV) and a parasitophorous vacuole membrane (PVM) [1]. Proper formation and subsequent modification of the PV and PVM are considered crucial for development and survival of intrahepatic parasites [2]. Nonetheless, a small proportion of *Plasmodium* parasites is capable of (partial) intranuclear development [3,4] in the absence of a PVM [4]. After invasion of the hepatocyte the sporozoites multiply and form tens of thousands of merozoites, which are released into the bloodstream as merosomes.
Both the *Plasmodium* genes *p52*, encoding a putative GPI-anchored protein [5,6] and its paralogous gene *p36*, encoding a putative secreted protein [6] are upregulated in sporozoite stages [7] with a putative function in hepatocyte invasion. *P. berghei* and *P. yoelii* parasites, genetically attenuated by the deletion of the *p52* gene or the *p36* gene, lack a PVM upon hepatocyte invasion [5,8]. These mutant parasites are severely compromised in their capability to develop into liver cells and abort development soon after invasion. The developmental arrest of these *Δp52&p36* mutant parasites was confirmed in *P. falciparum* [7]. Infection of mice with high numbers of *P. yoelii Δp52&p36* sporozoites, does not result in a blood stage infection [8]. The developmental arrest of these knock-out parasites is thought to be related to the lack of a PVM, considered critical for intracellular survival in hepatocytes.
Despite the apparent full developmental arrest, we previously showed that a low percentage of *Δp52* [5] and *Δp52&p36* [9]parasites are able to generate a blood stage infection in the *P. berghei* murine model. Moreover, we provided evidence that low numbers of *Δp52&p36 P. falciparum* sporozoites, develop into replicating liver stages [9]. In this study we followed replicating *Δp52&p36* parasites in the course of hepatic maturation and more specifically in relation to intranuclear location and PVM development.

Materials and Methods

Mice and parasites

Female C57BL/6J, eight weeks of age, were purchased from Elevage Janvier (France). All studies in which animals were involved have been performed according to the regulations of the Dutch "Animal On Experimentation act" and the European Directive 2010/63/EU.
The *P. berghei Δp52&p36* and wildtype (*P. berghei* ANKA) parasites used are described elsewhere [9].

Analysis of *in vitro P. berghei* liver stage development by immunofluorescence.

P. berghei sporozoites were collected at day 21 after mosquito infection by hand-dissection of salivary glands. Salivary glands were collected in DMEM (Dulbecco's Modified Eagle Medium from GIBCO) and homogenized in a homemade glass grinder. The number of sporozoites was determined by counting samples in duplicate in a Bürker-Türk counting chamber using phase-contrast microscopy.
Liver stage development of the *P. berghei* mutants and wildtype parasites was determined *in vitro* as described previously [9].Briefly, human liver hepatoma cells (Huh-7 [10]) were suspended in 1 ml of 'complete' DMEM (DMEM, Gibco, supplemented with 10% FCS, 1% penicillin/streptomycin and 1% Glutamax) and were seeded on coverslips in 24-well plates (10^5 cells/well). After Huh-7 monolayers were >80% confluent, $5x10^4$ sporozoites were added per well, and centrifuged 10 minutes at 1800xG (eppendorf centrifuge 5810 R). At different time points after infection, cells were fixed with 4% paraformaldehyde, permeabilized with 0.1% Triton-X-100, blocked with 10% FCS in PBS, and subsequently stained with a primary and secondary antibody at room temperature for 45 and 30 min respectively. Primary antibodies used were anti-*Pb*UIS-4 (raised in rabbit; [11](Mueller *et al.*, 2005), detecting a PVM-resident protein); anti-*Pb*HSP70 (raised in mouse;[5], detecting the parasite cytoplasmic heat-shock protein 70 and anti-*Pb*MSP-1 (raised in mouse; MRA-667 from MR4; www.MR4.org), detecting the merozoite surface protein 1 of *P. berghei*. The anti-UIS-4 antibody were preferred over the earlier described anti-EXP-1 antibody [9]detecting another PVM resident protein because of the intensity and the constitutive expression. Anti-mouse and anti-rabbit secondary antibodies, conjugated to Alexa-488 and Alexa-594, were used for visualization (Invitrogen). Nuclei were stained with DAPI. Analysis of infected hepatocytes was performed using a Zeiss Axiophot Fluorescence microscope with Axiocam MRm CCD camera (Fig. 1C and Fig. S1) or a Olympus FV1000 Confocal Laser Scanning Microscope.

TEM analysis of infected Huh-7 cells

For ultrathin-section transmission electron microscopy, $2x10^5$ wt and $5x10^5$ *p52/p36*-deficient sporozoites were used to infect $3.5x10^5$ sub-confluent Huh-7 cells, seeded the day prior in 35 mm petridishes. Sporozoites were centrifuged for 10 minutes at 1800xG and 32 hours post infection cells were fixed in 2.5% glutaraldehyde (Electron Microscopy Sciences) in 0.1 M sodium cacodylate buffer (pH 7.4) for 1 h at room temperature and subsequently washed

three times for 10 minutes in 0.1 M sodium cacodylate buffer and then post-fixed for 1 h in 1% osmium tetroxide (Electron Microscopy Sciences, Gibbstown, NY) in sodium cacodylate buffer at room temperature. Samples were washed three times 20 minutes in 0.1 M sodium cacodylate buffer and subsequently dehydrated in a graded series (10-50-70-96-100%) of ethanol. Cells were resin infiltrated in a 100% ethanol/EPON (Sigma) mixture (2:1) for 3 hours and subsequently in a 100% ethanol/EPON mixture (1:1) for 5 hours and subsequently in pure EPON overnight. Beem capsules were placed onto the cells perpendicular, filled with EPON, and polymerized overnight at 60 °C. Ultrathin (50–100nm) sections were cut parallel to the cell surface using an Ultracut ultramicrotome (Leica, Germany) and contrasted with 2% uranyl acetate and lead citrate before examination with a JEOL 1010 microscope under 60 kV.

Analysis of infectivity of Huh-7 hepatocyte-derived merozoites.

Assessment of the infectivity of hepatocyte derived merozoites has previously been described for *PbΔlisp1* mutants [12]. The protocol was adapted and Huh-7 cells were seeded in a 24-wells plate at 10^6 cells/ well, overnight. Sporozoites were added to the wells (>80% confluent) at $8x10^4$ sporozoites per well, and centrifuged 10 minutes at 1800xG (eppendorf centrifuge 5810 R). 65 hours post infection 100 µl supernatants were collected from each well, centrifuged for 3 minutes at 12.000 rpm and the cell pellet was re-suspended in 100 µl RPMI. A total of 200 µl re-suspended culture supernatant (from 2 wells) was injected i.v per C57BL/6 mice. Approval was obtained from the Radboud University Experimental Animal Ethical Committee (RUDEC 2009-225). Blood stage infections were monitored by Giemsa staining of blood smears from day 2 up to day 14 post injection. Genotype confirmation of *Δp52&p36* and wildtype parasites was performed as described [9]. The pre-patent period was defined as the period of time (days) between injection and the day that mice showed a blood stage parasitemia of 0.5-2%.

Results

P. berghei Δp52&p36 parasites can partially develop inside the nucleus of the hepatocyte.

In vitro analysis of *P. berghei* infected Huh-7 hepatocyte cultures showed that compared to wildtype (100%), a low proportion of *Δp52&p36* sporozoites, (2±0.6 % ($p<0.01$)) was able to develop into replicating intra-hepatic parasites (Fig. 1a, Table S1). Most knockout parasites (98%) abort development soon after invasion and do not start nuclear replication.

Remarkably, a relatively large proportion of the replicating Δ*p52&p36* parasites, 45% (±0.7%) resided inside the nucleus of hepatocytes, compared to 1.25% (±0.35%) of intranuclear wildtype parasites ($p<0.01$) at 24 hours post invasion (Fig. 1a**,** Table S1). The absolute number of intranuclear mutant parasites matched the number

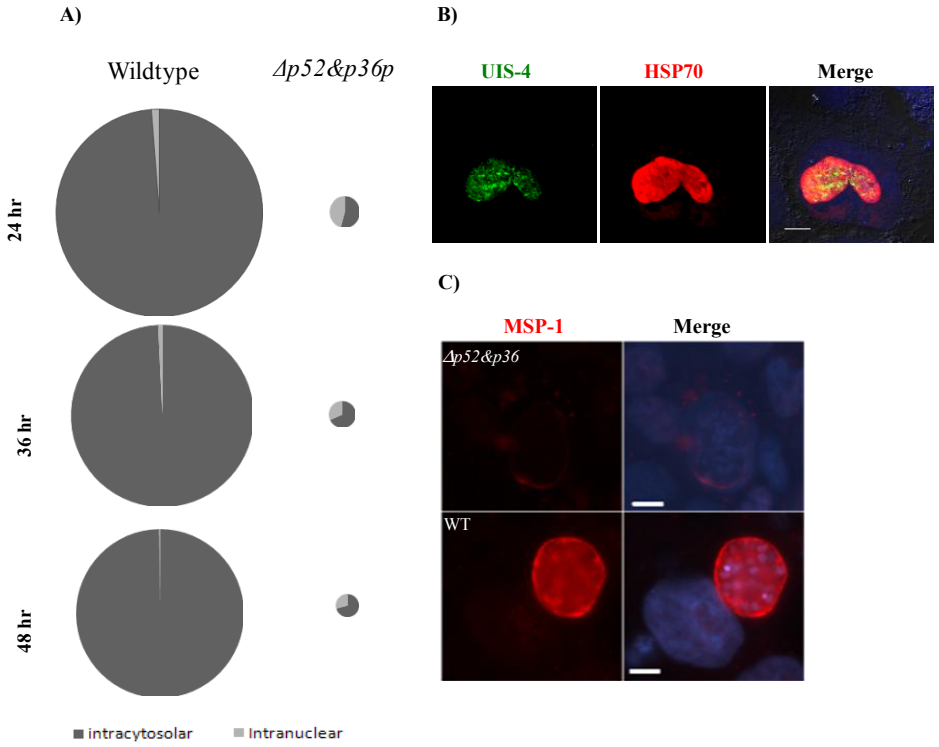

Figure 1: Intranuclear development of *Δp52&p36 P. berghei* parasites.
A)Pie diagrams of intranuclear and cytosolic wildtype and mutant replicating parasites at 24, 36 and 48 hours post invasion in Huh-7 cells. The diameter of the circles represents the relative number of replicating parasites observed per coverslip, where the wildtype circle at 24 hour represent 100% and all other circles are deduced (wildtype = 1300-1500 and *Δp52&p36* = 20-40 replicating parasites per coverslip at 24 hours post infection. Absolute numbers are depicted in Table S1 **B)** UIS-4 and HSP70 expression on an intranuclear *P. berghei* parasite 44 hours post infection (Bar = 10μm). **C)** MSP-1 expression on intranuclear (*Δp52&p36*) and cytocolic (wildtype) *P. berghei* parasites 52 hours post infection (Bar = 10μm).

of wildtype parasites. For both wildtype and mutant parasites, there was a slight decrease in the percentage of intranuclear developing parasites during the course of parasite maturation. At any time point, however, while the absolute number remained the same, the percentage of intranuclear mutant parasites was significantly higher than the percentage of intranuclear wildtype parasites ($p<0.05$) (Fig. 1a).
Intranuclear developing *P. berghei* wildtype and Δ*p52&p36* parasites were negative for UIS-4 peripheral staining, a marker for the presence of a PVM (Fig. 1b) and did not express MSP-1 at 52 hours post infection, as depicted by an intranuclear *Δp52&p36* parasite (Fig. 1c). At time points up to 72 hours post infection, these para-

sites remained negative (data not shown) indicating that the absence of MSP1 staining is not the results of a delay in maturation period . Based on MSP-1 expression, intranuclear parasites are unlikely the cause of Δ*p52&p36* parasite breakthrough in mice.

Cytosolic *Δp52&p36* parasites can produce mature merozoites in the absence of an apparent PVM.

More than half of the replicating *Δp52&p36* parasites resided in the cytosol of Huh-7 hepatocytes (Fig. 1a) expressing MSP-1 and transforming into mature merozoites from 52 hours post invasion onwards. These cytosolic Δ*p52&p36* parasites did not show the typical round shape of wildtype parasites, but were instead characterized by an irregular morphology (Fig. 2a, Fig S1). Individual merosomes were clearly visible budding of from the infected hepatocyte (Fig S1 right box). Replicating cytosolic Δ*p52&p36* parasites (n=498) were negative for peripheral UIS-4 staining at any time point starting from early liver infection onwards (6-52 hour post invasion) (Fig. 2b). Using transmission electron microscopy at 32 hours post infection, we observed cytosolic wildtype parasites demarked by a surrounding PV and PVM, while, in contrast, both PV and PVM could not be detected in Δ*p52&p36* parasites (Fig. 2c). Thus, Δ*p52&p36* parasites replicating in the cytosol expressed MSP-1, but lacked an apparent PVM.

Table 1: *Δp52&p36* merozoites are capable of inducing a blood stage infection

Experiment No.	No. Asexual positive/ No.injected (mean ± sd pre-patency)	
	Δp52&p36	**WT**
1	4/4 (6 ± 0 days)	2/2 (3 ± 0 days)
2	5/5 (5.8 ± 0.4 days)	3/3 (2 ± 0 days)

Huh-7 cells were infected with *Δp52&p36* and WT parasites and cultured for 65 hours. After 65 hours, culture supernatant containing merozoites was collected and injected i.v in C57BL/6 mice. Regular Giemsa staining was performed in all groups, 2-14 days post i.v injection in mice, to control for asexual parasites.

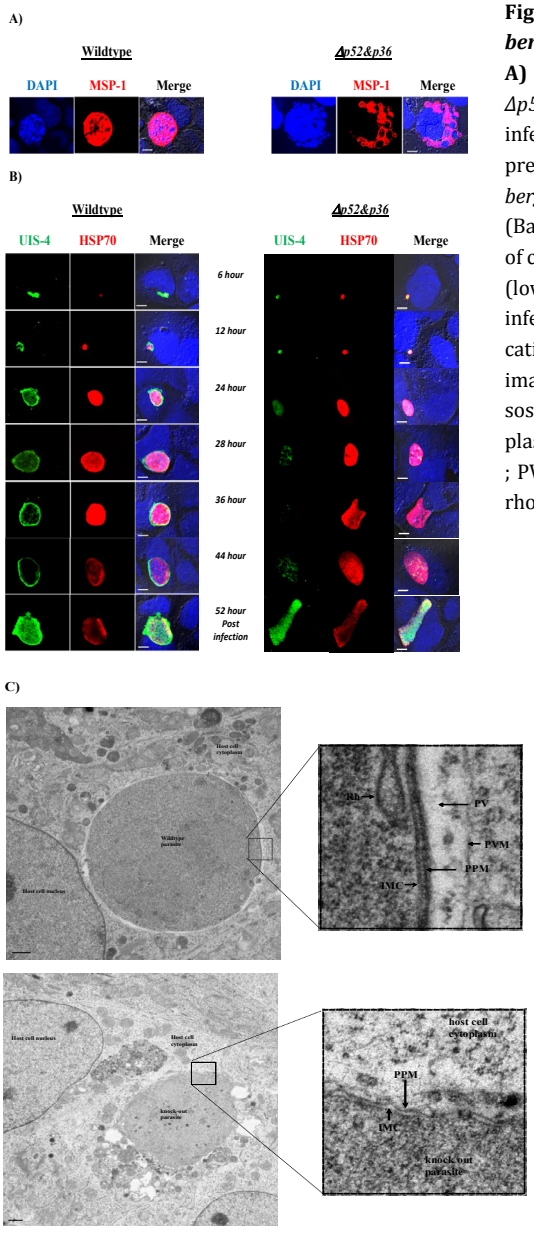

Figure 2: Cytosolic developing *Δp52&p36 P. berghei* parasites lack an apparent PVM.
A) MSP-1 expression on cytosolic wildtype and *Δp52&p36 P. berghei* parasites 52 hours post infection (Bar = 10μm). **B)** UIS-4 and HSP70 expression on cytosolic *Δp52&p36* and wildtype *P. berghei* parasites at 6-52 hours post infection (Bar = 10μm). **C)** Electron microscopic analysis of cytosolic wildtype (upper row) and *Δp52&p36* (lower row) parasites, 32 hours post hepatocyte infection. The inset boxes show higher magnifications of the boxed areas within the overview images. IMC, inner membrane complex; Ly lysosome; NE, Nuclear envelope; PPM, parasite plasma membrane; PV, parasitophorous vacuole ; PVM, parasitophorous vacuole membrane; Rh, rhoptry (Bar = 10μm).

Hepatocyte derived *Δp52&p36* merozoites are able to induce a blood stage infection.

We next tested whether Δ*p52&p36* parasites developing into merozoites were capable of infecting erythrocytes. Therefore, supernatants of Δ*p52&p36* and wildtype infected Huh-7 cells, collected 65 hours post infection, were injected i.v in C57BL/6 mice (Table 1). All mice injected with culture supernatant became patent with blood stage parasitemia as determined by thick smear. Genotyping of blood parasites confirmed the Δ*p52&p36* genotype (Fig. S2). The mean difference in day of patency between Δ*p52&p36* and wildtype parasites i.e. 5.9 versus 2.4 days post injection respectively, likely reflects the difference in number of viable merozoites injected. These data show that Δ*p52&p36* parasites, developing in Huh-7 hepatocytes in the absence of an apparent PVM, are capable of maturing into infectious merozoites.

Discussion

Here we show that a proportion of *P. berghei* Δ*p52&p36* parasites can develop in Huh-7 hepatocytes in the apparent absence of a PVM and fully mature into merozoites. Merozoites derived from an *in vitr*o Δ*p52&p36* hepatocyte culture were infectious and lead to a blood stage infection in mice. Our data question the absolute necessity for the presence of a PVM for intrahepatic *P. berghei* development.

Although all observed replicating Δ*p52&p36* parasites herein (approximately 900 by immunofluorescence) develop free of PVM inside the hepatocytes, one cannot formally exclude the possibility that a small proportion of the *P. berghei* mutants develop with a PVM into infectious merozoites. Nonetheless, the breakthrough blood stage parasites were infectious for mosquitoes and upon re-infection of a hepatocyte culture with sporozoites, all replicating mutants lacked UIS-4 staining (data not shown). This indicates that the infectious merozoites did not arise from a subset of mutant parasites that stably switched to a phenotype of forming a PVM in the absence of P52 or P36.

The relatively high percentage of mutant parasites replicating in the hepatocyte nucleus seems remarkable. However, despite an apparent preference of the mutant parasites to replicate in the nucleus, the absolute number of intranuclear replicating mutants does not differ from wildtype. Thus, mutant parasites do not preferentially invade the nucleus of hepatocytes.

The seemingly preference for intranuclear development merely arises from the de-

velopmental arrest of a major part of the cytosolic mutant parasites. Intranuclear mutants have a developmental advantage over cytosolic mutant parasites and their numbers seem untouched by the absence of a PVM. Possibly, the nuclear envelope acts as a substitute for the PVM.

The intranuclear mutant and wildtype *P. berghei* parasites likely halt inside the nucleus of the hepatocyte upon transmigration, similar to *P. yoelii* and *P. falciparum* [4]. These parasites do probably not play a role in the observed breakthrough infections in mice. Based on MSP-1 expression, cytosolic and not intranuclear parasites are the likely source of infectious merozoites. Nevertheless, we cannot exclude that merozoites may arise from intranuclear developing parasites.

Whereas *Plasmodium* parasites replicating in the nucleus in the apparent absence of a PVM have previously been reported, cytosolic parasites have not. Interestingly, upon close examination of wildtype parasites, a small percentage (± 1.5 % n=27) of the cytosolic wildtype parasites lack peripheral UIS-4 staining at 30 hour post infection, similar to the cytosolic Δ*p52&p36* parasites (data not shown). These data support the possibility of a non-conventional intra-hepatic pathway for *P. berghei* development.

In the absence of an encompassing membrane cytosolic parasites are likely more vulnerable to host defense mechanisms. Genes involved in the evasion of host cell apoptosis [13,14] might be less effective to avert cell death. Possibly, replicating mutant parasites survive in an equilibrium of anti-apoptotic gene expression and host defense mechanism.

It remains to be seen whether these findings in *P. berghei* are representative for other *Plasmodium* species. Fully developing cytosolic parasites absent of a PVM have, to our knowledge, never been reported for any of the other *Plasmodium* species. While *P. yoelii* Δ*p52&p36* breakthrough has not been reported, Labaied *et al.* previously described a multi-nucleated *P. yoelii* 'growth arrested' Δ*p52&p36* parasite in a Hepg2-CD81 cell [4], a human hepatoma cell line that promotes the formation of a PVM by *P. yoelii* [4]. This particular parasite lacked a peripheral UIS-4 expression [8]. Apparently, very low numbers of the mutant *P. yoelii* parasites still replicate inside Hepg2-CD81 cells in the absence of a PVM. Furthermore, it will be interesting to see whether the low numbers of mutant Δ*p52&p36 P. falciparum* parasites that replicate in primary human hepatocytes [9] have a similar phenotype as the *P. berghei* mutants.

Our findings are confined to an *in vitro* Huh-7 *P. berghei* model and the *in vivo* rel-

evance of these findings remains elusive. *In vivo* characterization is hampered by the extremely low number of replicating parasites. Similarly, *P. yoelii* and *P. falciparum* replicating Δ*p52&p36* parasites are extremely rare and at present their mechanism of breakthrough remains unclear. Nevertheless, once confirmed in *P. falciparum*, our findings may have implications for the development of a genetically attenuated malaria vaccine. Based on protective efficacy conferred in mice and apparent full arrest in *P. yoelii* and *P. falciparum* models, genetically attenuated *Δp52&p36* parasites have been considered eligible for clinical development as an attenuated sporozoite vaccine [7]. Given the break-through infections, our data suggest that for a sufficiently attenuated malaria vaccine, multiple genes need to be targeted. Such genes could not only include genes involved in the formation of the PVM, but preferably other *Plasmodium* gene targets with independent functions for liver stage development.

Acknowledgments

We are grateful to Professor Kai Matuschewski for providing the anti-UIS4 antibody. Moreover, we would like to thank Takeshi Annoura for confirmation of Δ*p52+p36* and wildtype genotype after the merosome injection assay. Additionally, we would like to thank Claudia Lagarde for the technical assistance with the *P. berghei* infections, Jolanda Klaassen, Laura Pelser-Posthumus, Astrid Pouwelsen and Jacqueline Kuhnen for the breeding of the mosquitoes and Anja Scholzen and Chris Janse for critical revision of the manuscript.

References

1. Silvie O, Franetich JF, Renia L, Mazier D. Malaria sporozoite: migrating for a living. Trends Mol Med 2004 Mar;10(3):97-100.
2. Vera IM, Beatty WL, Sinnis P, Kim K. Plasmodium protease ROM1 is important for proper formation of the parasitophorous vacuole. PLoS Pathog 2011 Sep;7(9):e1002197.
3. Meis JF, Hollingdale MR, Verhave JP, Aikawa M. Intranuclear localization of Plasmodium berghei sporozoites. Cell Biol Int Rep 1984 Dec;8(12):1016.
4. Silvie O, Greco C, Franetich JF, et al. Expression of human CD81 differently affects host cell susceptibility to malaria sporozoites depending on the Plasmodium species. Cell Microbiol 2006 Jul;8(7):1134-46.
5. van Dijk MR, Douradinha B, Franke-Fayard B, et al. Genetically attenuated, P36p-deficient malarial sporozoites induce protective immunity and apoptosis of infected liver cells. Proc Natl Acad Sci U S A 2005 Aug 23;102(34):12194-9.
6. Ishino T, Chinzei Y, Yuda M. Two proteins with 6-cys motifs are required for malarial parasites to commit to infection of the hepatocyte. Mol Microbiol 2005 Dec;58(5):1264-75.
7. VanBuskirk KM, O'Neill MT, De L, V, et al. Preerythrocytic, live-attenuated Plasmodium falciparum vaccine candidates by design. Proc Natl Acad Sci U S A 2009 Aug 4;106(31):13004-9.
8. Labaied M, Harupa A, Dumpit RF, Coppens I, Mikolajczak SA, Kappe SH. Plasmodium yoelii sporozoites with simultaneous deletion of P52 and P36 are completely attenuated and confer sterile immunity against infection. Infect Immun 2007 Aug;75(8):3758-68.
9. Annoura T, Ploemen IH, van Schaijk BC, et al. Assessing the adequacy of attenuation of genetically modified malaria parasite vaccine candidates. Vaccine 2012 Mar 30;30(16):2662-70.

10. Prudencio M, Rodrigues CD, Ataide R, Mota MM. Dissecting in vitro host cell infection by Plasmodium sporozoites using flow cytometry. Cell Microbiol 2008 Jan;10(1):218-24.
11. Mueller AK, Camargo N, Kaiser K, et al. Plasmodium liver stage developmental arrest by depletion of a protein at the parasite-host interface. Proc Natl Acad Sci U S A 2005 Feb 22;102(8):3022-7.
12. Ishino T, Boisson B, Orito Y, et al. LISP1 is important for the egress of Plasmodium berghei parasites from liver cells. Cell Microbiol 2009 Sep;11(9):1329-39.
13. Rennenberg A, Lehmann C, Heitmann A, et al. Exoerythrocytic Plasmodium parasites secrete a cysteine protease inhibitor involved in sporozoite invasion and capable of blocking cell death of host hepatocytes. PLoS Pathog 2010 Mar;6(3):e1000825.
14. van de SC, Horstmann S, Schmidt A, et al. The liver stage of Plasmodium berghei inhibits host cell apoptosis. Mol Microbiol 2005 Nov;58(3):731-42.

Supplementary Information

Supllementary Table S1

Parasite	Wildtype		Mutant	
24 hr post infection	**Total No. Parasites +/- SD [a]**		**Total No. Parasites +/- SD [a]**	
	1420 +/- 82		27.5 +/- 8	
	% Intranuclear (±SD)	**% Cytosolic (±SD)**	**% Intranuclear (±SD)**	**% Cytosolic (±SD)**
	1.25% (±0.35%)	98.75% (±0.35%)	45.5% (±2.7%)	54.5% (±2.7%)
36 hr post infection	**Total No. Parasites +/- SD [a]**		**Total No. Parasites +/- SD [a]**	
	1099 +/- 58		23 +/- 2	
	% Intranuclear (±SD)	**% Cytosolic (±SD)**	**% Intranuclear (±SD)**	**% Cytosolic (±SD)**
	0.75% (±0.07%)	99.25% (±0.07%)	31.5% (±6.4%)	68.5% (±6.4%)
48 hr post infection	**Total No. Parasites +/- SD [a]**		**Total No. Parasites +/- SD [a]**	
	898 +/- 53		21 +/- 5	
	% Intranuclear (±SD)	**% Cytosolic (±SD)**	**% Intranuclear (±SD)**	**% Cytosolic (±SD)**
	0.15% (±0.07%)	99.85 (±0.07%)	29% (±4.2%)	71% (±4.2%)

[a] Average number of replicating liver stage parasites per coverslip. A total of 3 coverslips was counted per timepoint per parasite.

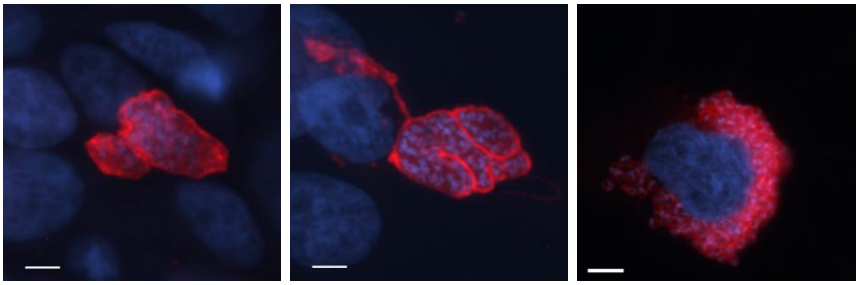

Supplementary Figure S1: Late liver stage intracytosolar *Δp52&p36p* parasites have an irregular shape.

Four representative images of *Δp52&p36p P. berghei* parasites in culture 48 hours post invasion in Huh-7 cells. Msp-1 expression is depicted in red, DAPI in blue (Bar= 10 µm).

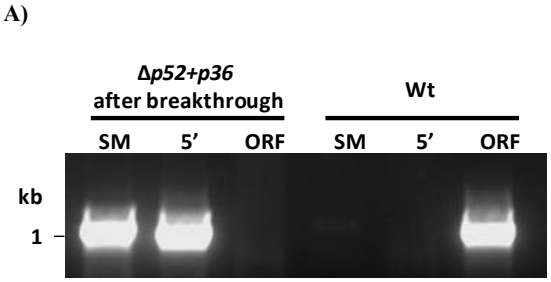

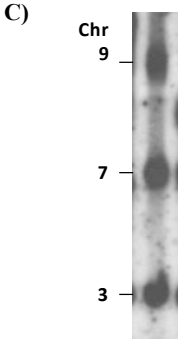

B)

Primers for confirmation PCR of the integration event in *Δp52+p36*				
Δp52+p36	L1389	ATTTTGCAACAATTTTATTCTTGG	*Δp52+p36* 5' integration F	PBANKA_100220 and PBANKA_100210
Δp52+p36	L313	ACGCATTATATGAGTTCATTTTAC	*Δp52+p36* 5' integration R from KO construct pL1164	
Δp52+p36	L775	GAAACAATATGAGTTCGCACGC	*Δp52+p36* intergenic region F	PBANKA_100220 and PBANKA_100210
Δp52+p36	L1212	TATATTGCTAGTCCTTTGTTCC	*Δp52+p36 p36* orf R	PBANKA_100220 and PBANKA_100210
Δp52+p36	4501	GGACAGATTGAACATCGTCG	*tgdhfr/ts F*	
Δp52+p36	4502	GATCACATTCTTCAGCTGGTC	*tgdhfr/ts R*	

Supplementary Figure S2: Confirmation of *Δp52+p36p* and wildtype genotype after merosome injection assay.

A) Diagnostic PCR for confirmation of correct disruption of *p52* and *p36* in mutant *Δp52+p36p* (1409cl1). SM: selectable marker (primers 4501/4502; 1093bp); 5'-integration event (primers L1389/L313; 1050bp); ORF (primers L775/L121; 1029bp). **B)** Sequence of the primers used. **C)** Southern analysis of pulse field gel (PFG)-separated chromosomes of mutant *Δp52+p36p*. Mutant *Δp52+p36p* has been generated in the reference *P. berghei* ANKA line *Pb*GFP-Luc$_{con}$ which has a gfp-luciferase gene integrated into the silent 230p locus (PBANKA_030600) on chromosome 3 (i.e. RMgm-29; http://pberghei.eu/index.php?rmgm=29). Hybridization with the 3'-UTR dhfr/ts probe recognizes the integrated construct on chromosome 9, the reporter GFP-Luc$_{con}$ construct on chromosome 3, and the endogenous dhfr/ts gene located on chromosome 7.

Chapter 6

P. berghei Δb9Δslarp parasites are completely arrested in liver stage development and can confer long-lasting protection against malaria in mice.

Ivo Ploemen

These studies are part of two papers (in preparation); the first paper describes in detail the biology of the B9 protein of P. berghei and P. falciparum (its relationship with other members of the Plasmodium 6-Cys family of proteins, the timing of expression and its cellular location); the second paper reports the generation and characterization of P. berghei and P. falciparum parasites lacking expression of both B9 and SLARP.

Other contributors of this study:

Geert-Jan van Gemert , Martijn Vos, Krystelle Nganou-Makamdop , Cornelus Hermsen, Ben van Schaijk, Robert Sauerwein
Department of Medical Microbiology, Radboud University Nijmegen Medical Center, Nijmegen, The Netherlands.

Takeshi Annoura, Severine Chevalley-Maurel, Blandine M.D. Franke-Fayard, Shahid Khan, Chris Janse
The Leiden Malaria Research Group (Parasitology), Leiden University Medical Center, Leiden, The Netherlands.

Abstract

Over the past decades, many attempts have been made to develop an efficacious malaria vaccine. Protection conferred by the immunization with live whole sporozoites is unequaled by any malaria vaccine attempt, in both animal models and human volunteers. For obvious safety reasons, it is essential to immunize with sporozoites that are 100% unable to develop into the pathogenic blood stage. Genetically attenuated parasites (GAP) that arrest in the liver stage form a high ranked live sporozoite vaccine approach. Both GAP safety (i.e no breakthrough blood infections) and protective efficacy are essential characteristics of a future *P. falciparum* GAP. Here, we report on the generation and characterization of a *P. berghei* GAP consisting of multiple gene deletions: *Δb9Δslarp*. Safety and protective efficacy were assessed by adopting a robust and stringent screening approach. First, single gene deleted *Δb9* GAP were generated and characterized. *P. berghei Δb9* sporozoites abort development soon after hepatocyte invasion. Immunization of mice with *Δb9* parasites confers long-lasting sterile protection. Nonetheless, very low numbers of *P. berghei Δb9* are capable of developing inside the hepatocyte resulting in a blood stage parasitemia. This GAP is therefore not a safe GAP candidate, ready for further clinical development. We subsequently generated a multiply attenuated *Δb9Δslarp* GAP, which was fully safe in our *P. berghei* model. None of the parasites was capable of full liver stage maturation. Moreover, we show that immunization of BALB/c and C57BL/6 mice with low doses of *Δb9Δslarp* confers sterile and long-lasting protection. The *Δb9Δslarp* GAP is now the leading GAP vaccine candidate for further development in *P. falciparum*.

Introduction

Over 40 percent of the world's population is at risk for exposure to malaria. More than 250.000 new clinical malaria cases occur annually resulting in 800.000 to 1.2 million deaths, most of which are children in sub-Saharan Africa suffering from a severe *P. falciparum* infection [1]. Malaria remains a global health crisis and there is a dire need for an effective and potent malaria vaccine.

Preliminary results of a Phase III trial with the most advanced malaria vaccine, a subunit vaccine named RTS,S, show an approximate 55% reduction in the acquisition of clinical malaria and a 35% reduction in the progression into severe malaria for up to 11 months post immunization [2]. While promising, a whole sporozoite vaccine approach might be much more potent in conferring protection, thereby forming the next generation of malaria vaccines. Vaccination with whole life sporozoites is only safe when parasite development is halted before the pathogenic blood stage. For this end, sporozoite immunizations can be performed with, radiation attenuated sporozoites (RAS), genetically attenuated parasites (GAP) and sporozoites administered concomitantly with anti-malarial drugs [chemoprofylactic sporozoites (CPS)]. RAS immunization has a long standing track record of proven efficacy in rodents [3], monkeys [4] and man [5,6,7]. CPS immunization leads to sterile protection in mice [8,9,10] and high (>90%) and sustained (at least 28 months) levels of protection against a controlled homologous human malaria infection in humans [11,12]. At present, the efficacy of the GAP vaccine has not been assessed in human volunteers but in rodent models the protective efficacy conferred by most GAPs is similar to RAS. Both vaccination strategies rely on the complete developmental arrest of the attenuated parasite in the host hepatocyte and subsequent (mainly cellular) immune responses.

There are clear advantages of a GAP vaccine over RAS and CPS in that it is comprised of a homogenous parasite population and its attenuation is not influenced by external (e.g radiation, host drug metabolism) factors. GAPs go into developmental arrest in the hepatocyte at the time point predestined by the specific gene deletion. Most GAPs like *Δp52, Δp36, Δuis3, Δuis4* and *Δslarp/Δsap1* arrest at early liver stage. Other GAPs, like *Δfabb/f* arrest in the late liver stage. Despite this apparent abundance of GAP vaccine candidates it has proved challenging to generate a safe and protective GAP in *P. falciparum*. For instance, unequivocal orthologs of the *P. berghei* and *P. yoelii uis3* and *uis4* genes are absent in the *P. falciparum* genome (www.PlasmoDB.org) and can therefore not be made into a vaccine product. In the *P. berghei* model the arrest of

the *Δp52* [13], the *Δp52&p36* and the *Δfabb/f* [14] parasites was not complete in that they were capable of maturing in the liver in low numbers, resulting in a blood stage infection in mice. Moreover, we observed very low numbers of replicating *Δp52&p36 P. falciparum* parasites in primary human hepatocyte cultures [14].

Based on these low levels of breakthrough GAP parasites, we previously described a set of safety criteria that have to be met by a *P. berghei* GAP prior to further clinical development of the GAP candidate in *P. falciparum* [14]. Adequacy of GAP attenuation can be assessed by testing for breakthrough blood stage infections in different mice strains inoculated with a high number of GAP sporozoites. Moreover, *in vivo* imaging of parasites can be used to further attest the absence of GAP developing in the liver.

In order to find a GAP that completely arrests in the liver stage and following immunization, confers long-lasting protection, one can i) combine known GAP candidates to one multiple attenuated GAP or ii) pursue new GAP candidates. In this study we generate and characterize a new GAP candidate, *Δb9*, which we subsequently multiply attenuate by additional deletion of the *slarp* gene. Both *P. berghei Δslarp* and its orthologue in *P. yoelii Δsap1* mutant parasites completely arrest in the liver and a clear orthologue of the gene is present in *P. falciparum* [15,16]. There is however controversy over the protective efficacy of these parasites upon immunization [17]. Contrary to immunization of mice with *P. yoelii Δsap1*, immunization with *P. berghei Δslarp* did not confer long-lasting sterile protection. Here we show in a *P. berghei* model, using a robust and stringent screening platform [14], the full arrest of the multiply attenuated *Δb9Δslarp* parasite and moreover its potent and long-lived protective efficacy in mice upon immunization.

Material and methods

Experimental animals and parasites

Female C57BL/6J and BALB/c (12 weeks old; Janvier France) and Swiss OF1 (8 weeks old Charles River) were used. All animal experiments were performed after a positive recommendation of the RUNMC (RUDEC 2008-123, RUDEC 2008-148, RUDEC 2010-250, RUDEC 2011-022, RUDEC 2011-208) or the LUMC (ADEC) was issued to the licensee. All studies were performed according to the regulations of the Dutch "Animal On Experimentation act" and the European Directive 2010/63/EU on the protection of animals used for scientific purposes.

The following reference lines of the ANKA strain of *P. berghei* were used: line cl15cy1 [18] and line 676m1cl1 (*Pb*GFP-Luc$_{con}$; see RMgm-29 in www.pberghei.eu). *Pb*GFP-Luc$_{con}$ expresses a

fusion protein of GFP and Luciferase from the *eef1a* promoter [19,20].

Generation of *P. berghei* mutants

To disrupt the *P. berghei b9* gene (PBANKA_080810) two different gene deletion constructs were constructed. The first construct used the standard targeting DNA construct, pL0037 (MR4; www.MR4.org) which contains the positive/negative selectable marker cassette *hdhfr/yfcu*. Target sequences for integration of the construct by double cross-over homologous recombination were PCR amplified from *P. berghei* genomic DNA (cl15cy1) using primers (Table S1) which are specific for the 5' and 3' end of *b9*, respectively. The PCR–amplified target sequences were cloned either upstream or downstream of the SM of plasmid pL0037 resulting in plasmid pL1439 (Fig. S1). Prior to transfection the DNA-construct pL1439 was linearized with *Asp* 718 and *Xma* I. Using this construct the mutant *Δb9-a* (1309cl1) was generated in the cl15cy1 reference line using standard methods of transfection and positive selection with pyrimethamine [18] (Fig. S1).

The second construct for disruption of the *b9* gene, pL1499, was generated using the adapted 'Anchor-tagging' PCR-based method as described [14] (Fig S1). The two targeting fragments (0.8 kb) of *b9* were amplified using genomic DNA (parasite line cl15cy1) as template with the primer pairs 4667/4557 (5'target sequence) and 4558/4668 (3'target sequence). See Table S1 for the sequence of the primers. Using this PCR-based targeting construct the mutant Δ*b9-b* (1481cl4) was generated in the *Pb*GFP-Luc$_{con}$ reference line using standard methods of transfection and positive selection with pyrimethamine (Fig. S1).

To disrupt the *P. berghei slarp* gene (PBANKA_090210) a construct was generated using the adapted 'Anchor-tagging' PCR-based method as described [14] (Fig. S3). The two targeting fragments (1195bp and 823bp) of *slarp* were amplified using genomic DNA (parasite line cl15cy1) as template with the primer pairs 5960/5961 (5'target sequence) and 5962/5963 (3'target sequence). See Table S1 for the sequence of the primers. Using this PCR-based targeting construct (pL1740) the mutant Δ*slarp-a* (1839cl3) was generated in the *Pb*GFP-Luc$_{con}$ reference line using standard methods of transfection and positive selection with pyrimethamine (Fig. S3).

To generate a selectable marker-free mutant PbΔ*b9*Δ*sm* we removed the drug-selectable marker cassette from mutant PbΔ*b9-a* using the standard procedure of negative selection [14] (Fig. S4). The resulting cloned mutant (Δ*b9*Δ*sm*; 1309cl1m0cl2) which contains a disrupted *b9* gene and is drug-selectable marker free was used for deleting the *slarp* (PBANKA_090210) gene. To delete the *slarp* gene the gene deletion construct pL1740 was used as described above. Using this construct the mutant *PbΔb9Δslarp* (line 1844cl1) was generated in the Δ*b9*Δ*sm* line using standard methods of transfection and positive selection with pyrimethamine (Fig. S5).

Correct integration of the constructs into the genome of mutant parasites was analysed by diagnostic PCR-analysis and Southern analysis of PFG-separated chromosomes as shown in Fig. S1+2-5. PFG-separated chromosomes were hybridized with a probe recognizing *hdhfr* or the 3'-UTR *dhfr/ts* of *P. berghei* [18]. Absence of transcripts of the targeted genes in sporozoites was analysed by reverse transcriptase-PCR. Total RNA was purified from

salivary gland sporozoites using TRIzol reagent (Invitrogen) and prepared according to manufactures specifications. Purified RNA was then treated with RQ1 DNase (Promega). Reverse transcription was performed using the Super Script III RT (Invitrogen) as previously described [13]. cDNA was used as template for PCR amplification with control and gene specific primers that are listed in Table S1.

Analysis of blood and mosquito stage development of *P. berghei* mutant parasites

The *P. berghei* mutants were maintained in Swiss mice. The multiplication rate of blood stages and gametocyte production were determined during the cloning procedure [18] and were not different from parasites of the reference ANKA lines. Feeding of *A. stephensi* mosquitoes and determination of oocyst production was performed as described [21]. *P. berghei* sporozoite production was determined by collection of salivary glands at day 21 after infection by hand-dissection. Salivary glands were collected in DMEM (Dulbecco's Modified Eagle Medium from GIBCO) and homogenized in a homemade glass grinder. The number of sporozoites was determined by counting the numbers of sporozoites of 10 salivary glands in triplicate in a Bürker-Türk counting chamber using phase-contrast microscopy.

Analysis of *P. berghei* sporozoite motility, hepatocyte traversal, invasion and development

Gliding motility of *P. berghei* sporozoites was determined in assays that were performed on anti-*P. berghei* circumsporozoite antibody (3D11, monoclonal mouse antibody 10 µg/ml) pre-coated Labtek slides (Nunc, NL) to which 2×10^4 sporozoites were added [13]. After 30 minutes of incubation at 37°C sporozoites were fixed with 4% PFA and after washing with PBS, the sporozoites and the trails ('gliding circles') were stained with anti-CSP-antibody (3D11[22]) conjugated to Alexa 488 (Dylight 488 antibody labeling kit; Thermo Scientific, NL). Slides were mounted with Fluoromount-G (SouthernBiotech, NL) and 'gliding circles' were analyzed using a Leica DMR fluorescence microscope at 1000X magnification.

P. berghei sporozoite hepatocyte traversal was determined in assays as described previously [23]. Briefly, human liver hepatoma cells (Huh7) were suspended in 1ml of 'complete' DMEM (DMEM from Gibco, supplemented with 10% FCS, 1% penicillin/streptomycin and 1% Glutamax) and were plated in 24 well plates (10^5 cells/ml). After the Huh7 monolayers were >80% confluent, 10^5 sporozoites were added with the addition of FITC- or Alexa-647-labeled dextran (Invitrogen, NL). No sporozoites were added to the negative control wells. FACS analysis of dextran-positive cells was performed on a total $25x10^3$ cells per well (each experiment was performed in triplicate wells) using a FACScalibur flow cytometer (Becton Dickinson, NL).

Invasion of hepatocytes *in vitro* by *P. berghei* sporozoites was determined by addition of 5×10^4 sporozoites to a monolayer of Huh7 cells. After the addition of sporozoites, cultures were centrifuged for 10 minutes at 1800G (Eppendorf centrifuge 5810 R) and then returned to the 37°C incubator. After 2-3 hours wells were washed 3 times with PBS to remove uninvaded sporozoites. Cells were fixed with 4% paraformaldehyde (PFA) for 10 min and

extracellular (non-invaded) parasites were stained with anti-CS-antibody (3D11) and conjugated with Alexa 594 antibody (Dylight 594 antibody labeling kit; Thermo Scientific, NL). After permeabilization with 0.1 % Triton-X-100 for 10 minutes and blocking with 10% FCS in PBS for 20 minutes, intracellular sporozoites were stained with anti-CS-antibody (3D11) conjugated with Alexa 488 antibody (Dylight 488 antibody labeling kit; Thermo Scientific, NL). Nuclei were stained with DAPI. Analysis and counting of stained intracellular and extracellular parasites were performed using a Leica DMR fluorescence microscope at 1000X magnification. All quantitative phenotypical assays with *P. berghei* parasite lines were performed in triplo.

P. berghei sporozoites development was determined in cultures of Huh7 cells (see above). Sporozoites (5×10^4) were added to a monolayer of Huh7 cells on coverslips in 24 well plates (with a confluency of 80-90%) in 'complete' DMEM (see above). At different time points after infection, cells were fixed with paraformaldehyde 4%, permeabilized with Triton-X-100 0.1%, blocked with 10% FCS in PBS, and subsequently stained with a primary (anti-*Pb*EXP1 [24]; anti-*Pb*HSP70 [13]; anti-*Pb*UIS-4 and anti-MSP-1 (MRA-78 from MR4;www.MR4.org) and secondary antibody, for 2h and 1h respectively. Anti-mouse, -chicken and -rabbit secondary antibodies, conjugated to Alexa-488 and Alexa-594, were used for visualization (Invitrogen). Nuclei were stained with DAPI. Cells were mounted in Fluoromount-G and examined using a Leica DMR fluorescence microscope at 1000X magnification.

Analysis of *P. berghei* sporozoite infectivity and *in vivo* imaging of liver stage development in mice

C57BL/6 mice were inoculated with sporozoites by intravenous injection of different sporozoite numbers, ranging from $1x10^4$ - $5x10^5$. Blood stage infections were monitored by analysis of Giemsa-stained thin smears of tail blood collected on day 4-18 after inoculation of sporozoites. Pre-patency (measured in days after sporozoite inoculation) is defined as the day when a parasitemia of 0.5-2% is observed in the blood.

Liver stage development in live mice was monitored by real-time *in vivo* imaging of liver stages as described previously [25] with minor adaptations. Briefly, animals were anesthetized using the isoflurane-anesthesia system, their abdomens were shaved and D-luciferin dissolved in PBS (150 mg/kg; Caliper Life Science, Belgium) was injected SC (in the neck). Animals were kept anesthetized during the measurements, which were performed 4 minutes after the injection of D-luciferin. Bioluminescence imaging was acquired with a 10 cm field of view, medium binning factor and an exposure time of 180 seconds. The color scale limits were set automatically and the quantitative analysis of bioluminescence was performed by measuring the luminescence signal intensity using the region of interest (ROI) settings of the Living Image 3.2 software. The ROI was set to measure the abdominal area at the location of the liver. ROI measurements are expressed in total flux of photons.

Immunizations of mice with *P. berghei* sporozoites

Prior to immunization, *P. berghei* sporozoites were collected at day 21-27 after mosquito

infection by hand-dissection. Salivary glands were collected in DMEM (Dulbecco's Modified Eagle Medium from GIBCO) and homogenized in a homemade glass grinder. The number of sporozoites was determined by counting in triplicate in a Bürker-Türk counting chamber using phase-contrast microscopy. BALB/c and C57BL/6J mice were immunized by intravenous injection using different numbers of GAP and γ-irradiated sporozoites (infected mosquitoes were irradiated at 16,000 rad (Gammacel 1000 ^{137}Cs) prior to dissection). BALB/c mice received one immunization and C57BL/6 mice received three immunizations with 7 day intervals. Immunized mice were monitored for blood infections by analysis of Giemsa stained films of tail blood at day 4-16 after immunization. Immunized mice were challenged at different time points after immunization by intravenous injection of $1x10^4$ sporozoites from the *P. berghei* ANKA reference line cl15cy1. In each experiment, age matched naive mice were included to verify infectivity of the sporozoites used for challenge. After challenge, mice were monitored for blood infections by analysis of Giemsa stained films of tail blood at day 4-21. Pre-patency (measured in days after sporozoite inoculation) is defined as the day when a parasitemia of 0.5-2% is observed in the blood.

Mononuclear cell isolation from liver, *ex vivo* stimulation and phenotyping

Immunized C57BL/6 mice were euthanized by isoflurane inhalation after i.v. injection of 50 i.u. of heparin. Livers were collected after perfusion with 10ml of PBS. Cell suspensions of livers were made by pressing the organs through a 70-µm nylon cell strainer (BD Labware). Liver cells were resuspended in 35% Percoll (GE Healthcare) and centrifuged at 800g for 20min. After erythrocyte lysis (5min on ice with ACK lying buffer), hepatic mononuclear cells (HMC) were washed and re-suspended in RPMI medium (Gibco, 1640) for counting. Subsequently, hepatic mononuclear cells were co-cultured in complete RPMI 1640 medium [26] in the presence of cryoconserved sporozoites ($5x10^4$) or salivary glands from uninfected mosquitoes. Cells were stimulated at 37°C/5%CO_2 for 24 hours during which Brefeldin A (Sigma) was added for the last four hours (10µg/ml final concentration). As a positive control to the stimulation, PMA and Ionomycin (Sigma) were added simultaneously with Brefeldin A at a final concentration of 100ng/ml and 1.25µg/ml respectively. Cells were harvested after 24-hours *in vitro* stimulation and stained for 30min at 4°C in cold assay buffer (PBS supplemented with 0.5% bovine serum albumin – Sigma-Aldrich) containing labeled monoclonal antibodies against CD3, CD4 and CD8 (Pacific blue-conjugated anti CD3 (17A2), Peridinin Chlorophyll Protein (PerCP)-conjugated anti CD4 (RM4.5), Alexa fluor 700-conjugated anti CD8a (53-6.7); Biolegend (San Diego, CA)). Cells were fixed for 30min at 4°C with Fix & Perm medium A (Invitrogen) and subsequently stained for 30min at 4°C Fix & Perm medium B (Invitrogen) containing APC-conjugated anti-IFNγ. Flow cytometry was performed on a 9-color Cyan ADP (Beckman Coulter) and data analysis using FlowJo software (version 9.1; Tree Star). Comparisons between groups were performed by a Mann-Whitney U test using PRISM software version 5.0 (Graphpad, San Diego, CA). $p < 0.05$ are considered statistically significant.

Results

Generation and characterization of *P. berghei Δb9* parasites.

The *b9* gene was selected as a potential GAP target based on the presence of b9 transcripts in sporozoites and absence of protein expression in sporozoites. B9 was found to be a member of the 6-Cys family of *Plasmodium* proteins. This family includes P52 and P36, both of which leading GAP candidates. The lack of B9 protein expression in salivary gland sporozoites suggests that the b9 transcripts are translationally repressed and only translated after sporozoites invade hepatocytes (unpublished data). We found that B9 is not expressed during the blood and mosquito stage parasites but is only present as protein during liver stage development (unpublished data).

P. berghei Δb9 mutants were generated, using standard methods of targeted gene-deletion by integrating constructs through double cross-over homologous recombination (Fig. S1). Two independent *b9* mutants were generated in the *P. berghei* ANKA reference lines cl15cy1 and *Pb*GFP-Luc$_{con}$. The latter line is a reporter line which expresses the fusion protein of GFP-Luciferase from the constitutive *eef1a* promoter, thereby allowing analysis of liver stage development in live mice by *in vivo* imaging [25]. Correct deletion of the genes in cloned mutants was confirmed by Southern analysis of FIGE-separated chromosomes and diagnostic PCR (Fig. S1).

The Δ*b9* mutants had normal blood-stage development, and the production of oocysts and sporozoites was comparable to those of wildtype parasites (Table S2). In addition, salivary gland sporozoites exhibited normal levels of gliding motility, hepatocyte traversal and wildtype levels of hepatocyte invasion (Table S2). In WT parasites *b9* transcripts were clearly present in salivary gland sporozoites by RT-PCR analysis whereas *b9* transcripts were, as expected, absent in *Pb*Δ*b9* mutants (Fig. 1A). When Swiss or BALB/c mice were infected by intravenous inoculation of $1x10^4$ or $5x10^4$ Δ*b9* sporozoites none of these mice developed a blood stage infection (Table S3), indicating an important role of b9 in the liver. We next explored whether the *PbΔb9* GAP is capable of eliciting long lasting and sterile protection by immunizing mice with different dosages. Immunization of BALB/c and C57BL/6 mice with *PbΔb9* parasites induced sterile protection against challenge with wildtype parasites (Table 1). A single dose of as few as 1000 sporozoites was sufficient to induce immunity in BALB/c mice. Immunization of C57BL/6 mice by a prime and boost regimen (50K/20K/20K) resulted in sterile protection in approximately 50 % of the mice for up to 1 year post immunization. A 1 year re-challenge of mice that

were already challenged at 6 months increased the level of protection to 100%. The *PbΔb9* thereby elicits at least the same level of protection as observed for mutants lacking either *p52* or *p52&p36* [13,27,28].

Table 1: Protection in BALB/c and C57BL/6 mice following immunization with *P. berghei Δb9*

Mice	Immunization dose Spz x 10^3	Challenge after immunization[a] (re-challenge)	No. protected/ no. challenged -pre-patency-[b] *Δb9*	Control
Balb/c	50	d10 (d90 & d180 & d210 & d365)	20/20 (15/15 & 10/10 & 5/5 & 5/5)	
	25	d10 (d90 & d180)	10/10 (5/5 & 5/5)	
	10	d10 (d90 & d180)	10/10 (5/5 & 5/5)	
	5	d10 (d90 & d180)	8/10 -7.5- (3/3 & 3/3)	
	1	d10 (d90 & d180)	8/10 -7- (3/3 & 3/3)	
	None	d10 & d90 & d180 & d210 & d365		0/5[d] -4.5-
C57BL/6	50/20/20[c]	d10 (d90 & d180)	4/4 (4/4 & 4/4)	
	50/20/20[c]	d90	5/5	
	50/10/20[c]	d180 (d365)	9/9 (4/4)	
	50/20/20[c]	d365	5/11 -7-	
	None	d10 & d90 & d180 & d365		0/4[d] -4-

[a]Challenge was performed by a 10^4 wildtype sporozoite IV injection.

[b]Mean of pre-patent period in days post challenge.

[c]Immunizations were performed with two 7 day intervals.

[d]Representative for challenge of naïve mice at any time point post last immunization

Despite this good protective efficacy, when we infected C57BL/6 mice with a sporozoite dose of $5x10^4$ *PbΔb9* sporozoites, 10-20% of the mice developed breakthrough blood infections (Table S3). In these mice the pre-patent period was delayed with 2-3 days, indicating that blood infections arose from a few infected hepatocytes. Genotyping of parasites derived from the breakthrough blood infections

confirmed the PbΔb9 genotype of these parasites (data not shown).

We next analysed the development of *PbΔb9* parasites in more detail both in cultured hepatocytes and in the liver of infected C57BL/6 mice. Quantitative analyses of *PbΔb9*-infected hepatocytes by fluorescence microscopy demonstrated that Δ*b9* parasites arrest early after invasion of hepatocytes. At 24hpi most parasites had disappeared from the cultures and a few small forms were observed with a size similar to that of liver stages 1-5hpi of hepatocytes (Fig. 1B,C). Analysis of *PbΔb9* parasites in the liver, using real-time *in vivo* imaging of luciferase expressing parasites, confirmed the growth-arrest phenotype observed in cultured hepatocytes. In six out of ten C57BL/6 mice infected $5x10^4$ *PbΔb9* sporozoites we did not observe development of liver stages, as demonstrated by the complete absence of luminescence signals in the liver at 42hpi. At this time point all livers from all control mice infected with luciferase-expressing WT parasites were strongly luminescent (Fig. 1D). None of the luminescent-negative mice developed a blood stage infection. In four *PbΔb9*-infected mice a weak luminescent signal was detected which was confined to only a few (1–2) small spots (Fig. 1D) but only two of these mice developed a blood infection with a pre-patent period of 8 to 9 days (Table S3). Combined, our analyses demonstrate that *PbΔb9* has an important role during early liver stage development. However, in the absence of the B9 protein liver stage development can occur, as shown by the occurrence of breakthrough blood infections in 10-20% of the mice (albeit only after high intravenous *PbΔb9* sporozoite inoculation). On close examination of *in vitro* hepatocyte culture, we found that *P. berghei* Δ*b9* parasites were capable of developing into infectious merozoites in the absence of an apparent PVM, as indicated by the lack of a peripheral EXP-1 and UIS-4 staining (Fig. S2).

Generation and characterization of *P. berghei Δb9Δslarp* parasites.

In our pursued of a fully arresting GAP we next generated a *P. berghei* multiple attenuated *Δb9Δslarp* GAP using standard methods of gene targeting by double cross-over integration (Fig. S5; Table S1). Moreover a Δ*slarp* mutant was generated in the *P. berghei* reference reporter line, *Pb*GFP-Luc_{con} (Fig. S3; Table S1). The *PbΔslarp* and *PbΔb9Δslarp* mutants showed normal blood stage development (data not shown) and produced oocyst and sporozoite numbers comparable to those of WT parasites (Table S4). Salivary gland sporozoites demonstrated normal gliding motility, hepatocyte traversal and sporozoites of all mutants were able to invade hepatocytes at WT levels (Table S4). *PbΔb9Δslarp* parasites had an early growth-arrest in hepatocytes as determined by immunofluorescent microscopy of infected

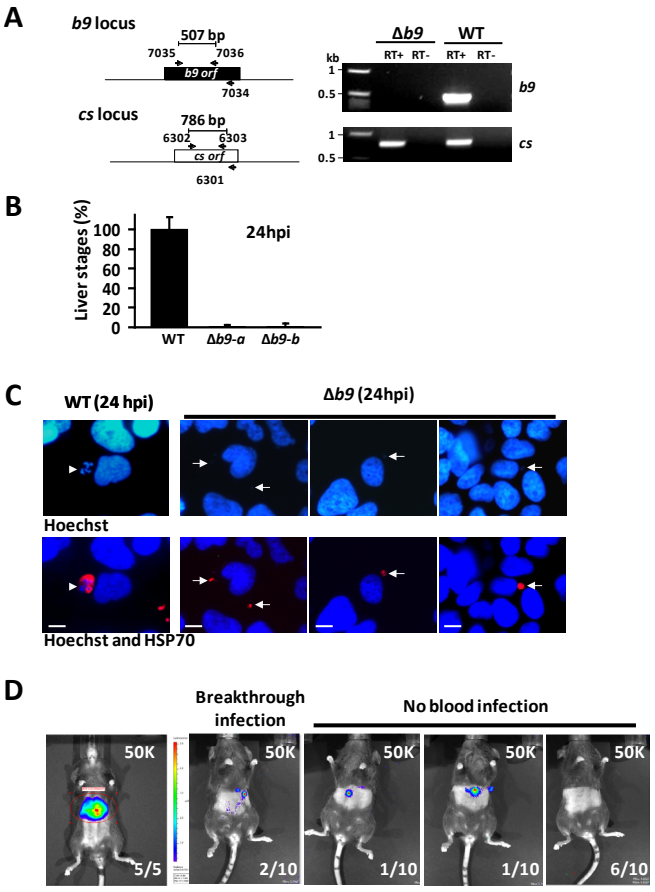

Figure 1: Characterization of *P. berghei Δb9* liver stage development.
A) qRT-PCR analysis showing absence of b9 transcripts in sporozoites of *Δb9* mutants and wildtype. PCR amplification using purified sporozoite RNA was performed either in the presence or absence of reverse transcriptase (RT+ or RT-, respectively) using the primers as shown in the left panel (see Table S1 for the sequence of the primers). The *P. berghei* circumsporozoite protein gene (cs) was used as a positive control. **B)** Number of *Δb9-a* and *Δb9-b* mutant parasites in a Huh-7 infected culture at 24 hours post infection as compared to wildtype. **C)** IFA of wildtype and *Δb9* infected huh-7 cells stained with Hoechst-33342 (upper panel) and anti-HSP70 (red: lower panel) at 24 hours post infection. **D)** Real-time *in vivo* imaging of luciferase-expressing liver stage parasites in C57BL/6 mice at 42hpi. C57BL/6 mice were injected IV with either 5 x10^4 *Pb*-GFPLuc$_{con}$ sporozoites (n=5) resulting in a full liver infection (left figure: representative image of WT infected mice), or with 5 x10^4 *Pb Δb9-b* sporozoites (n=10) (right panel). All mice infected with WT parasites became patent with a blood stage parasitemia. Out of the 10 C57BL/6 mice that were infected with 50K *Δb9-b* sporozoites 6 remained negative for any luminescent signal and did not get infected by a blood stage parasitemia. Out of the other 4 mice, which showed individual spots overlaying the liver (possibly individual infected hepatocytes) 2 became patent with a delayed blood stage infection.

Huh7 cells, similar to the previously reported *PbΔslarp* [15] and that of *PbΔb9* GAP (data not shown). In contrast with *P. berghei Δp52p36* [14] and *Δb9* parasites, not a single *Δb9Δslarp* parasite developed and underwent multiple nuclear replications in the hepatocytes (data not shown). Infection of BALB/c and C57BL/6 mice with high numbers ($5x10^4$ and $5x10^5$ respectively) of *PbΔslarp* and *Δb9Δslarp* sporozoites did not result in a breakthrough blood infection (Table S5). Moreover, infection of C57BL/6 mice with $5x10^5$ *Δslarp* sporozoites did not result in any detectable liver stage development as determined by *in vivo* real-time imaging (Fig. 2).

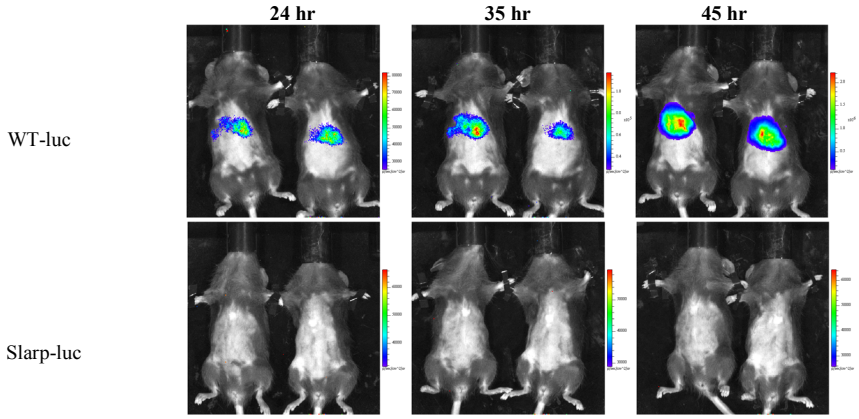

Figure 2: Real-time *in vivo* imaging of *Δslarp*-luc parasite liver development.
Real-time *in vivo* imaging of luciferase-expressing liver stage parasites in C57BL/6 mice at 30, 35 and 44 hours post infection. C57BL/6 mice were injected IV with either $5x10^4$ *Pb*-GFPLuc$_{con}$ sporozoites (n=5) (upper panel: representative image of WT infected mice), or with 5 $x10^4$ *Pb Δslarp-a* sporozoites (n=5) (lower panel: representative image of *Δslarp-a* infected mice).

Immunization of mice with *P. berghei Δb9Δslarp* induces sterile and long-lasting protection.

Having verified that the *PbΔb9Δslarp* GAP cannot develop in mature liver stage parasites we addressed its protective efficacy following immunization. Similar to immunization with *PbΔb9* parasites, *PbΔb9Δslarp* induced sterile protection against challenge with wildtype parasites at low doses in BALB/c mice (Table 2). Moreover, low dose *PbΔb9Δslarp* immunization of C57BL/6 mice resulted in a conferred level of protection, similar to that of γ-irradiated sporozoite immunization (Table 2). These data were affirmed by the cellular immune response in C57BL/6 mice immunized with *Δb9Δslarp* or γ-irradiated sporozoites, at as late as 70 days post challenge (Figure S6). Stimulation of hepatic mononuclear cells from mice immunized with

Table 2: Protection in BALB/c and C57BL/6 mice following immunization with *P. berghei Δb9Δslarp* and irradiated sporozoites.

Mice	Immunization dose Spz x 10^3	Challenge after immunization[a] (re-challenge)	No. protected/ no. challenged -pre-patency-[b] *Δb9Δslarp*	*γ-irradiated*	Control
Balb/c	25	d10	10/10		
	10	d10	20/20		
	5	d10	10/10		
	1	d10	20/20		
	None	d10			0/15 -4.5-
C57BL/6	10/10/10[c]	d10 (d180)	10/10 (5)	10/10 (4/5) -8-	
	1/1/1[c]	d10	6/10 -7-	7/10 -7.3-	
	None	d10			0/6 -4.5-
	50/20/20[c]	d180	6/6	10/10	
	50/10/20[c]	d180	3/3		
	50/20[d]	d180	1/1		
	None	d180			0/4 -4-

[a]Challenge was performed by a 10^4 wildtype sporozoite IV injection.

[b]Mean of pre-patent period in days post challenge.

[c]Immunizations were performed with two 7 day intervals.

[d]Immunizations were performed with a 14 day interval.

a dose regimen of 10K/10K/10K and 1K/1K/1K resulted in significantly higher IFNγ responses of CD8+ T cells, ($p < 0.02$). Within each dose regimen, no significant difference could be observed between mice receiving a *Δb9Δslarp* or γ-irradiated sporozoite immunization.

The majority of mice receiving a low immunization dose (10K/10K/10K spz) were protected upon re-challenge after 180 days. More importantly, mice immunized with *Δb9Δslarp* or with γ-irradiated sporozoites showed high levels of protection after a first time challenge at 180 days post immunization (Table 2). In summary, the multiple attenuated *P. berghei* GAP *Δb9Δslarp* does not develop into mature liver stage parasites and induces long-lasting sterile protection against a wildtype challenge.

Immunization of BALB/c and C57BL/6 mice with the single gene deleted *PbΔslarp*

parasite resulted in sterile and long-lasting protection, not significantly different from immunization with *PbΔb9Δslarp* (Table S6).

Discussion

Here we show that, in the *P. berghei* rodent model, genetic attenuation of the parasite by simultaneous deletion of the *b9* and *slarp* genes, results in a fully arresting (i.e no breakthrough infection) GAP that can induce strong long-lasting immune responses. Deletion of the *b9* gene leads to an arrest of the majority of *P. berghei* parasites early after invasion of hepatocytes by sporozoites. Immunization of mice with *P. berghei Δb9,* leads to long-lived sterile protection, but is not fully safe in that some parasites can develop into blood stage parasites. This early growth-arrested phenotype is very similar to the phenotype described for mutants lacking expression of the P52 protein or lacking the proteins P52 and P36 [13,14]. We previously reported the lack of an apparent PVM in *P. berghei Δp52Δp36* developing in the cytosol of a hepatocyte (*Ploemen et al.* in press). Low numbers of *P. berghei Δb9* parasites seem to avert an arrest in the hepatocyte in a similar fashion. These findings may indicate that B9, P52 and P36 play a similar role in the development of a PVM. Indeed, when we inoculated C57Bl/6 mice with high doses of triple gene deleted *P. berghei* Δ*b9*Δ*p52*Δ*p36* GAP sporozoites, we observed that the multiple gene-deletion mutant Δ*b9*Δ*p52*Δ*p36* shows the same high level of growth arrest as the single gene-deletion mutant Δ*b9* (data not shown). The multiple attenuated *Δb9Δslarp* GAP is absent of the safety concerns from these GAPs.

By adopting a previously proposed robust and stringent screening approach for GAP safety [14], we find that the *Δb9Δslarp* GAP does not induce breakthrough infections. We used amongst others *in vivo* imaging and multiple mice strains, to determine the adequacy of GAP attenuation, before advancement with further clinical development. In fact both *P. berghei Δslarp* and *Δb9Δslarp* parasites meet the screening criteria. Both mutant parasites do not replicate in hepatocytes after invasion. Moreover, both BALB/c and C57BL/6 mice remained negative for blood stage parasitemia after inoculation with high numbers of mutant sporozoites. Although robust, these findings might not be so surprising since it was already observed that inoculation of high numbers of *P. berghei Δslarp* [15] and its *P. yoelii* orthologue *Δsap1* [16] sporozoites, did not result in blood stage infection in mice, albeit in one mouse strain. Still, the multiple attenuated *Δb9Δslarp* GAP has a safety advantage over the single gene deleted *Δslarp* GAP. The full arrest of *Δslarp/Δsap1*

parasites likely results from a depletion of transcripts from a number of various so-called UIS (up-regulated in sporozoites) genes [17]. The combined effect of all these down-regulated UIS genes might very well cause the subsequent full developmental arrest. However, as these UIS genes are down-regulated but not absent there might possibly be a safety concern, which is alleviated by the simultaneous deletion of another gene, *b9*, in one parasite. Thereby forming a multiple genetically attenuated fully arresting safe GAP.

Our results show that immunization of C57BL/6 mice with either *Δslarp* or *Δb9Δslarp* parasites induces long-lived protection. This is remarkable since others have shown that *Δslarp (SL22 cl3)* parasites induce a decreased protective efficacy in C57BL/6 mice from as early as 3 weeks post last immunization [15]. In our present study, we use this exact *Δslarp* parasite and an independently generated mutant to show long-lived protection. Moreover, we observed that a mere prime boost with a two week interval is sufficient to induce long-lived protection in C57BL/6 mice (Table S6). Two immunizations with a one week interval did previously not confer protection in *Δp52* immunized C57BL/6 mice [13]. Possibly, the time interval between the prime and boost immunization is of influence on the conferred level of protection. The discrepancy between the herein and previously reported long-lived protection in *Δslarp* immunized C57BL/6 mice could result from a number of factors. Laboratory differences can possibly influence the outcome of the experiments. Also, the age of the sporozoites at the time of immunization could very well be of influence. When we immunized 10 BALB/c mice with 1000 30-day old *ΔSlarp (Sl22 cl3)* parasites we found a mere 10% protection whereas we observed 80% protection following immunization with 1000 21-day old mutant parasites (Table S6). Late *Δslarp* parasites (30+ days post mosquito infection) showed a strong decrease in gliding motility compared to wildtype (data not shown). Possibly, down-regulation of the *Pumilio-2* gene in the *Δslarp* mutant influences the gliding motility and subsequently the protective efficacy of the sporozoites over time. Previously it was shown that the *pumilio-2* gene is down-regulated in the *P. yoelii Δslarp* orthologue *Δsap1* and in *P. berghei Δpumilio-2* parasites have an impaired gliding motility [17,29]. A possible similar effect on mutant *P. falciparum* parasites could not influence future vaccine efficacy since all parasites will be harvested at the same time early after sporozoite salivary gland infection.

It will be key to determine the phenotype of a *P. falciparum Δb9Δslarp* GAP. These parasites have now been generated (unpublished data Ben van Schaijk). If these multiply attenuated *P. falciparum Δb9Δslarp* parasites make viable sporozoites

which invade primary human hepatocytes prior to a full developmental arrest, these GAP might be ready to go into clinical testing. Subsequently, with the use of the cryopreservation techniques of sporozoites designed by Sanaria Inc. and recent insights in the effective administration of whole sporozoite malaria vaccines by needle and syringe (*Ploemen et al*. in press) the clinical development of a GAP vaccine candidate might be in grasp.

Acknowledgments

We would like to thank Professor Kai Matuschewski and Olivier Silvie for kindly providing *P. berghei Δslarp* (Sl22 cl3). Additionaly we would like to thank Claudia Lagarde, Alex Ignacio and Daniëlle Janssen for the technical assistance with the *P. berghei* immunizations and challenge, Marga van de Vegte-Bolmer for mosquito feeds and Jolanda Klaassen, Laura Pelser-Posthumus, Astrid Pouwelsen and Jacqueline Kuhnen for breeding of mosquitoes.

References

1. WHO (2011) World Malaria Report. (http://www.who.int/malaria/world_malaria_report_2011/9789241564403_eng.pdf)
2. Agnandji ST, Lell B, Soulanoudjingar SS, Fernandes JF, Abossolo BP, et al. (2011) First results of phase 3 trial of RTS,S/AS01 malaria vaccine in African children. N Engl J Med 365: 1863-1875.
3. Nussenzweig RS, Vanderberg J, Most H, Orton C (1967) Protective immunity produced by the injection of x-irradiated sporozoites of plasmodium berghei. Nature 216: 160-162.
4. Gwadz RW, Cochrane AH, Nussenzweig V, Nussenzweig RS (1979) Preliminary studies on vaccination of rhesus monkeys with irradiated sporozoites of Plasmodium knowlesi and characterization of surface antigens of these parasites. Bull World Health Organ 57 Suppl 1: 165-173.
5. Clyde DF, Most H, McCarthy VC, Vanderberg JP (1973) Immunization of man against sporozite-induced falciparum malaria. Am J Med Sci 266: 169-177.
6. Rieckmann KH, Carson PE, Beaudoin RL, Cassells JS, Sell KW (1974) Letter: Sporozoite induced immunity in man against an Ethiopian strain of Plasmodium falciparum. Trans R Soc Trop Med Hyg 68: 258-259.
7. Hoffman SL, Goh LM, Luke TC, Schneider I, Le TP, et al. (2002) Protection of humans against malaria by immunization with radiation-attenuated Plasmodium falciparum sporozoites. J Infect Dis 185: 1155-1164.
8. Belnoue E, Costa FT, Frankenberg T, Vigario AM, Voza T, et al. (2004) Protective T cell immunity against malaria liver stage after vaccination with live sporozoites under chloroquine treatment. J Immunol 172: 2487-2495.
9. Belnoue E, Voza T, Costa FT, Gruner AC, Mauduit M, et al. (2008) Vaccination with live Plasmodium yoelii blood stage parasites under chloroquine cover induces cross-stage immunity against malaria liver stage. J Immunol 181: 8552-8558.
10. Ploemen I, Behet M, Nganou-Makamdop K, van Gemert GJ, Bijker E, et al. (2011) Evaluation of immunity against malaria using luciferase-expressing Plasmodium berghei parasites. Malar J 10: 350.
11. Roestenberg M, McCall M, Hopman J, Wiersma J, Luty AJ, et al. (2009) Protection against a malaria challenge by sporozoite inoculation. N Engl J Med 361: 468-477.
12. Roestenberg M, Teirlinck AC, McCall MB, Teelen K, Makamdop KN, et al. (2011) Long-term protection against malaria after experimental sporozoite inoculation: an open-label follow-up study. Lancet 377: 1770-1776.
13. van Dijk MR, Douradinha B, Franke-Fayard B, Heussler V, van Dooren MW, et al. (2005) Genetically

attenuated, P36p-deficient malarial sporozoites induce protective immunity and apoptosis of infected liver cells. Proc Natl Acad Sci U S A 102: 12194-12199.

14. Annoura T, Ploemen IH, van Schaijk BC, Sajid M, Vos MW, et al. (2012) Assessing the adequacy of attenuation of genetically modified malaria parasite vaccine candidates. Vaccine 30: 2662-2670.
15. Silvie O, Goetz K, Matuschewski K (2008) A sporozoite asparagine-rich protein controls initiation of Plasmodium liver stage development. PLoS Pathog 4: e1000086.
16. Aly AS, Mikolajczak SA, Rivera HS, Camargo N, Jacobs-Lorena V, et al. (2008) Targeted deletion of SAP1 abolishes the expression of infectivity factors necessary for successful malaria parasite liver infection. Mol Microbiol 69: 152-163.
17. Aly AS, Lindner SE, MacKellar DC, Peng X, Kappe SH (2011) SAP1 is a critical post-transcriptional regulator of infectivity in malaria parasite sporozoite stages. Mol Microbiol 79: 929-939.
18. Janse CJ, Ramesar J, Waters AP (2006) High-efficiency transfection and drug selection of genetically transformed blood stages of the rodent malaria parasite Plasmodium berghei. Nat Protoc 1: 346-356.
19. Franke-Fayard B, Trueman H, Ramesar J, Mendoza J, van der Keur M, et al. (2004) A Plasmodium berghei reference line that constitutively expresses GFP at a high level throughout the complete life cycle. Mol Biochem Parasitol 137: 23-33.
20. Janse CJ, Franke-Fayard B, Mair GR, Ramesar J, Thiel C, et al. (2006) High efficiency transfection of Plasmodium berghei facilitates novel selection procedures. Mol Biochem Parasitol 145: 60-70.
21. Sinden RE (1997) Infection of mosquitoes with rodent malaria. 67-91.
22. Yoshida N, Nussenzweig RS, Potocnjak P, Nussenzweig V, Aikawa M (1980) Hybridoma produces protective antibodies directed against the sporozoite stage of malaria parasite. Science 207: 71-73.
23. Mota MM, Pradel G, Vanderberg JP, Hafalla JC, Frevert U, et al. (2001) Migration of Plasmodium sporozoites through cells before infection. Science 291: 141-144.
24. Sturm A, Amino R, van de Sand C, Regen T, Retzlaff S, et al. (2006) Manipulation of host hepatocytes by the malaria parasite for delivery into liver sinusoids. Science 313: 1287-1290.
25. Ploemen IH, Prudencio M, Douradinha BG, Ramesar J, Fonager J, et al. (2009) Visualisation and quantitative analysis of the rodent malaria liver stage by real time imaging. PLoS One 4: e7881.
26. Watarai H, Nakagawa R, Omori-Miyake M, Dashtsoodol N, Taniguchi M (2008) Methods for detection, isolation and culture of mouse and human invariant NKT cells. Nat Protoc 3: 70-78.
27. Douradinha B, van Dijk MR, Ataide R, van Gemert GJ, Thompson J, et al. (2007) Genetically attenuated P36p-deficient Plasmodium berghei sporozoites confer long-lasting and partial cross-species protection. Int J Parasitol 37: 1511-1519.
28. Labaied M, Harupa A, Dumpit RF, Coppens I, Mikolajczak SA, et al. (2007) Plasmodium yoelii sporozoites with simultaneous deletion of P52 and P36 are completely attenuated and confer sterile immunity against infection. Infect Immun 75: 3758-3768.
29. Gomes-Santos CS, Braks J, Prudencio M, Carret C, Gomes AR, et al. (2011) Transition of Plasmodium sporozoites into liver stage-like forms is regulated by the RNA binding protein Pumilio. PLoS Pathog 7: e1002046.

Supplementary Information

Supplementary Table S1: List of primers used in this study.

	Name	Sequence	Restriction site	Description	Gene models
Primers for generation of the ΔB9 target regions (for pL1439) (restriction sites are shown in red)					
Δb9	4096	GGGGTACCTAAATAACATGATGAAACGTCAC	Asp718	*Δb9* 5' target F	PBANKA_080810
Δb9	4097	CCCAAGCTTTCTATGCATTACTTCTACCCTC	HIndIII	*Δb9* 5'target R	PBANKA_080810
Δb9	4098	GGAATTCGATATGCTTGAAATTCCTAGAC	EcoRI	*Δb9* 3' target F	PBANKA_080810
Δb9	4099	TCCCCCCGGGCGCTTGTGGTTGCATACATC	Xmal	*Δb9* 3' target R	PBANKA_080810
Primers for confirmation PCR of the integration event in *ΔB9*					
Δb9	4288	CAAATCCACAGACACTTACTC		*Δb9* 5' integration F	PBANKA_080810
Δb9	L1858	ATGCACAAAAAAAAATATGCACAC		*Δb9* 5' integration R from KO construct pL1439	PBANKA_080810
Δb9	4239	GATTTTTAAAATGTTTATAATATGATTAGC		*Δb9* 3' integration F from KO construct pL1439	PBANKA_080810
Δb9	4289	CAACCTTTTGCCTTGCATG		*Δb9* 3' integration R	PBANKA_080810
Δb9	4437	CGCATTATTCGAGGTAGACC		*Δb9 orf* F	PBANKA_080810
Δb9	4438	ACGGGTTTCACTTACATACTC		*Δb9 orf* R	PBANKA_080810
Δb9	4698	GTTCGCTAAACTGCATCGTC		*hdhfr F*	
Δb9	4699	GTTTGAGGTAGCAAGTAGACG		*yfcu R*	
Δb9	5441	ATGAGCATAAATGTGAGCATGG		*Δb9 negative selection 5' target F*	PBANKA_080810
Δb9	5442	CTTGAACCTAGATTGGGTGTAG		*Δb9 negative selection 3' target R*	PBANKA_080810
Primers for the Anchor-tagging PCR-based method: Generation of ΔB9 target regions (for pL1499) (restriction sites are shown in red; Anchor tags are shown in blue)					
Δb9	4667	GAACTCGTACTCCTTGGTGACGGGTACCTAAATAACATGATGAAACGTCAC	Asp718	*Δb9* 5' target F	PBANKA_080810
Δb9	4557	CATCTACAAGCATCGTCGACCTCTCTATGCATTACTTCTACCCTC		*Δb9* 5'target R	PBANKA_080810
Δb9	4558	CCTTCAATTTCGGATCCACTAGGATATGCTTGAAATTCCTAGAC		*Δb9* 3' target F	PBANKA_080810
Δb9	4668	AGGTTGGTCATTGACACTCAGCAGTACTCGCTTGTGGTTGCATACATC	ScaI	*Δb9* 3' target R	PBANKA_080810
Δb9	4661	GAACTCGTACTCCTTGGTGACG		for 2nd PCR	anchor tag
Δb9	4662	AGGTTGGTCATTGACACTCAGC		for 2nd PCR	anchor tag
Primers for confirmation PCR of the integration event in *ΔB9* (Anchor tags are shown in blue)					
Δb9	4288	CAAATCCACAGACACTTACTC		*Δb9* 5' integration F	
Δb9	4770	CATCTACAAGCATCGTCGACCTC		*Δb9* 5' integration R from KO construct pL1499	anchor tag
Δb9	4771	CCTTCAATTTCGGATCCACTAG		*Δb9* 3' integration F from KO construct pL1499	anchor tag
Δb9	4289	CAACCTTTTGCCTTGCATG		*Δb9* 3' integration R	
Δb9	4437	CGCATTATTCGAGGTAGACC		*Δb9 orf* F	PBANKA_080810
Δb9	4438	ACGGGTTTCACTTACATACTC		*Δb9 orf* R	PBANKA_080810
Δb9	L307C	GCTTAATTCTTTTCGAGCTC		*hdhfr F*	
Δb9	3187	GTGTCACTTTCAAAGTCTTGC		*hdhfr R*	
Primers for RT-PCR					
RT-PCR	6301	ATACCAGAACCACATGTTACG		*CS* for RT primer	PBANKA_040320
RT-PCR	6302	CTCTACTTCCAGGATATGGAC		*CS* F for RT-PCR	PBANKA_040320
RT-PCR	6303	CATTGAGACCATTCCTCTGTG		*CS* R for RT-PCR	PBANKA_040320
RT-PCR	7034	CCATTCTGGGTAGAACAAATGC		*b9* for RT primer	PBANKA_080810
RT-PCR	7035	TATCCCATCACTCATACCTAG		*b9* F for RT-PCR	PBANKA_080810
RT-PCR	7036	ACGGGTTTCACTTACATACTC		*b9* R for RT-PCR	PBANKA_080810
Primers for the Anchor-tagging PCR-based method: Generation of Δslarp target regions (for pL1740) (restriction sites are shown in red; Anchor tags are shown in blue)					
Δslarp	5960	GAACTCGTACTCCTTGGTGACGGGTACCGGGAGTCAAAAACGGTATGC	Asp718	*Δslarp* 5' target F	PBANKA_090210
Δslarp	5961	CATCTACAAGCATCGTCGACCTCTCCTATAGTACATGCCCACG		*Δslarp* 5'target R	PBANKA_090210
Δslarp	5962	CCTTCAATTTCGGATCCACTAGCATGTTAGGAGCACGAAACC		*Δslarp* 3' target F	PBANKA_090210
Δslarp	5963	AGGTTGGTCATTGACACTCAGCAGTACTCTAAAATTGTGGGAATCCACTTG	ScaI	*Δslarp* 3' target R	PBANKA_090210
	4661	GAACTCGTACTCCTTGGTGACG		for 2nd PCR	
	4662	AGGTTGGTCATTGACACTCAGC		for 2nd PCR	
Primers for confirmation PCR of the integration event in *Δslarp* (Anchor tags are shown in blue)					
Δslarp	6125	CATGTCTCTTTGCATGTGGC		*Δslarp* 5' integration F	PBANKA_090210
Δslarp	6349	CTCATCTACAAGCATCGTCG		*Δslarp* 5' integration R from KO construct	
Δslarp	4771	CCTTCAATTTCGGATCCACTAG		*Δslarp* 3' integration F from KO construct	
Δslarp	6126	GTCGTCCTATAGTAAGTTGAGC		*Δslarp* 3' integration R	PBANKA_090210
Δslarp	6127	CCCAAATGATCAAGCACCAG		*slarp orf* F	PBANKA_090210
Δslarp	6128	CAATTTGAATCGGCACAAGGC		*slarp orf R*	PBANKA_090210
	6346	TGGACATTGCCTATGAGGAG		*hdhfr-yfcu F*	
	6347	AACACAGTAGTATCTGTCACC		*hdhfr-yfcu R*	
Δb9	4437	CGCATTATTCGAGGTAGACC		*b9 orf* F	PBANKA_080810
Δb9	4438	ACGGGTTTCACTTACATACTC		*b9 orf R*	PBANKA_080810

Supplementary Table S2: Phenotypic analysis of *P. berghei Δb9* mosquito and liver stages.

Parasite	Oocyst No. Mean ± sd	Spz No. (x 10^3) Mean ± sd	Sporozoite Motility[a]	Cell Traversal[b]	Hepatocyte invasion[c]
WT	85 ± 25	102 ± 28	1.00 ± 0.03	1.00 ± 0.14	1.00 ± 0.12
WT (*Pb*GFP-Luc$_{con}$)	63 ± 15	86 ± 24	Nd	1.0 ± 0.1	0.92 ± 0.16
Δb9-a	89 ± 14	89 ± 28	1.01 ± 0.02	1.11 ± 0.03	1.08 ± 0.28
Δb9-b	55 ± 18	85 ± 25	Nd	0.9 ± 0.08	1.03 ± 0.07

[a]Determined by counting CS protein sporozoite trails.
[b]Sporozoite Traversal through Huh-7 cells.
[c]Sporozoite invasion of Huh-7 cells. Number of intracellular parasites determined at 3h after infection.

Supplementary Table S3: Breakthrough blood infection in Swiss, BALB/c and C57BL/6 after inoculation with *P. berghei Δb9* mutants.

Mouse strain	Parasites	Dose	breakthrough/ infected animals	Pre-patency (days)
Swiss	WT	1x10^4	5/5	5
	PbΔ*b9-a*	1x10^4	0/3	n/a
	PbΔ*b9-b*	1x10^4	0/3	n/a
	PbΔ*b9-b*	5x10^4	0/3	n/a
BALB/c	WT	1 x10^4	5/5	5
	PbΔ*b9-a*	5 x10^4	0/20	n/a
	PbΔ*b9-b*	5 x10^4	0/10	n/a
C57BL/6	WT	1 x10^4	5/5	5
	PbΔ*b9-a*	5 x10^4	2/10	8-9
	PbΔ*b9-b*	5 x10^4	1/10	9
	PbΔ*b9-b*	2 x10^5	2/10	8-9

[a]Inoculation dose of sporozoites administered IV

Supplementary Table S4: Phenotypic analysis of *P. berghei Δslarp* and *Δb9Δslarp* mosquito and liver stages.

Parasite	Oocyst No. Mean ± sd	Spz No. (x 10^3) Mean ± sd	Sporozoite Motility[a]	Cell Traversal[b]	Hepatocyte invasion[c]
WT	119 ± 40	108 ± 23	1.0 ± 0.1	1.00 ± 0.08	1.00 ± 0.06
Δslarp-a	154 ± 17	88 ± 41	1.01 ± 0.13	1.09 ± 0.06	0.97 ± 0.11
Δb9Δslarp	172 ± 5	43 ± 23	1.05 ± 0.03	1.21 ± 0.12	1.02 ± 0.03

[a]Determined by counting CS protein sporozoite trails.
[b]Sporozoite Traversal through Huh-7 cells.
[c]Sporozoite invasion of Huh-7 cells. Number of intracellular parasites determined at 3h after infection.

Supplementary Table S5: No breakthrough blood infection in BALB/c and C57BL/6 after inoculation with *P. berghei Δslarp* and *Δb9Δslarp* sporozoites.

Mouse strain	Parasites	Dose	breakthrough/ infected animals	Pre-patency (days)
BALB/c	WT	$1x10^4$	5/5	4-5
	Δ*slarp-a*	$5\ x10^4$	0/5	n/a
	Δ*slarp-a*	$25\ x10^3$	0/10	n/a
	Δ*b9*Δ*slarp*	$25\ x10^3$	0/10	n/a
C57BL/6	WT	$1\ x10^4$	5/5	4-5
	Δ*slarp-a*	$5\ x10^5$	0/5	n/a
	Δ*slarp-a*	$4\ x10^5$	0/5	n/a
	Δ*slarp-a*	$2\ x10^5$	0/10	n/a
	Δ*b9*Δ*slarp*	$2\ x10^5$	0/10	n/a
	Δ*b9*Δ*slarp*	$15\ x10^4$	0/5	n/a

[a]Inoculation dose of sporozoites administered IV

Supplementary Table S6: Protection in BALB/c and C57BL/6 mice following immunization with *P. berghei Δslarp* sporozoites.

Mice	Immunization dose Spz x 10^3	Challenge after immunization[a] (re-challenge)	No. protected/ no. challenged -pre-patency-[b]		
			Δslarp (1839 cl3)	*Δslarp (SL22 cl3)*[e]	Control[f]
Balb/c	50	d10		14/14	
	25	d10	10/10	14/14	
	10	d10	19/20 -5-	10/10	
	5	d10	10/10	10/10	
	1	d10	20/20	8/10 -8-	
	None	d10			0/15 -4.5-
C57BL/6	10/10/10[c]	d10 (d180)	10/10 (10/10)	10/10 (9/10) -8-	
	1/1/1[c]	d10 (d180)	5/10 -7.2- (4/5) -6-	5/10 -7.8- (5/5)	
	None	d10			0/6 -4.5-
	50/20/20[c]	d180	8/9 -9-		
	50/10/20[c]	d180		6/7 -7-	
	50/20[d]	d180		3/3	
	None	d180			0/4 -4-

[a]Challenge was performed by a 10^4 wildtype sporozoite IV injection.

[b]Mean of pre-patent period in days post challenge.

[c]Immunizations were performed with two 7 day intervals.

[d]Immunizations were performed with a 14 day interval.

[e]This *Δslarp* GAP was previously generated and published [15].

[f]For each mouse strain, immunizations and challenges were conducted in one experiment. Immunizations of mice presented in Table 2 were performed simultaneous with the immunization experiments presented in Table S6; hence only one group of control mice were used per challenge time point.

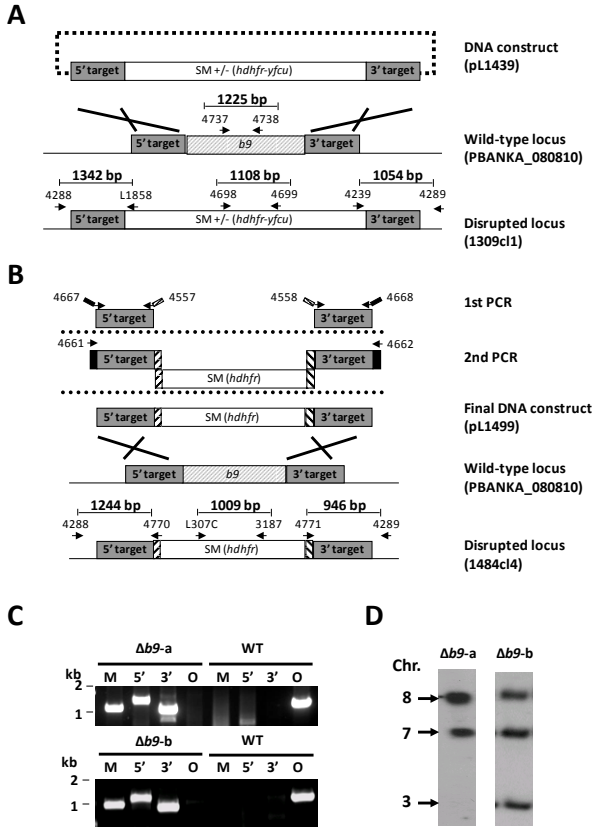

Supplementary Figure S1: Generation and genotype analyses of *P. berghei* mutant; *Δb9*-a and *Δb9*-b.

A) Generation of mutant *Δb9-a* (1309cl1). For *Δb9-a* the DNA-construct pL1439 was generated containing the positive/negative selectable marker cassette *hdhfr/yfcy.* This construct was subsequently used to generate the mutant *Δb9-a* (1309cl1) in the cl15cy1 reference line. See Table S1 for the sequence of the primers. **B)** For the mutant *Δb9-b* (1481cl4) the pL1499 construct was generated which was used for the generation of the mutant in the *Pb*GFP-Luc$_{con}$ reference line. See Table S1 for the sequence of the primers. **C+D)** Diagnostic PCR (**C**) and Southern analysis (**D**) of Pulse Field Gel (PFG)-separated chromosomes of mutant *Δb9*-a and *Δb9*-b confirming correct disruption of the *b9*-locus. See Table S1 for the sequence of the primers used for the selectable marker gene (M); 5'-integration event (5'); 3'-integration event (3') and the *b9*-ORF. Mutant *Δb9*-a has been generated in the reference *P. berghei* ANKA line cl15cy1. Mutant *Δb9*-b has been generated in the reference *P. berghei* ANKA line *Pb*GFP-Luc$_{con}$ which has a gfp-luciferase gene integrated into the silent 230p locus (PBANKA_030600) on chromosome 3 (i.e. RMgm-29; http://pberghei.eu/index.php?rmgm=29). For Southern analysis, PFG-separated chromosome were hybridized using a 3'UTR *pbdhfr* probe that recognizes the construct integrated into *P. berghei b9* locus on chromosome 8, the endogenous locus of *dhfr/ts* on chromosome 7 and in mutant *Δb9*-b the *gfp-luciferase* gene integrated into chromosome 3.

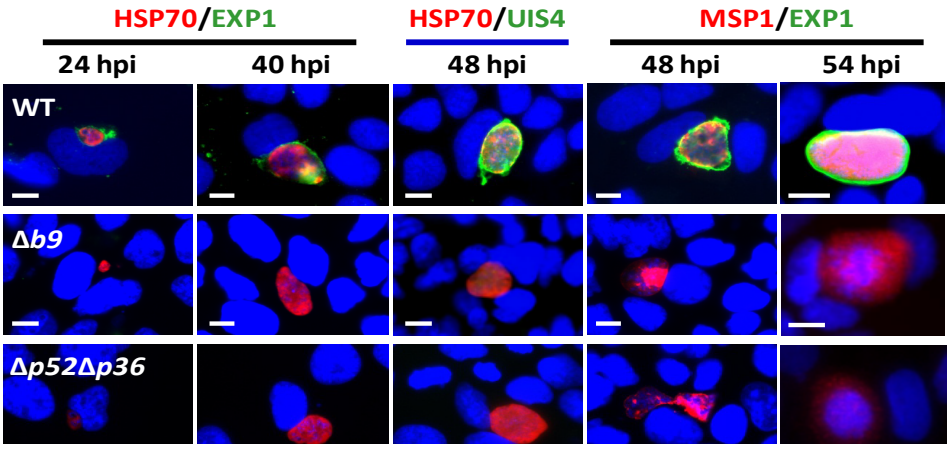

Supplementary Figure S2: Characterization of the PVM in developing *P. berghei Δb9* mutants.
IFA of wildtype and *Δb9* infected hepatocytes stained with anti-HSP70 or anti-MSP1 (red) and anti-EXP1 and anti-UIS4 (green)-antibodies at various time points post infection. Nuclei are stained with Hoechst-33342. Bar represents 10µm.

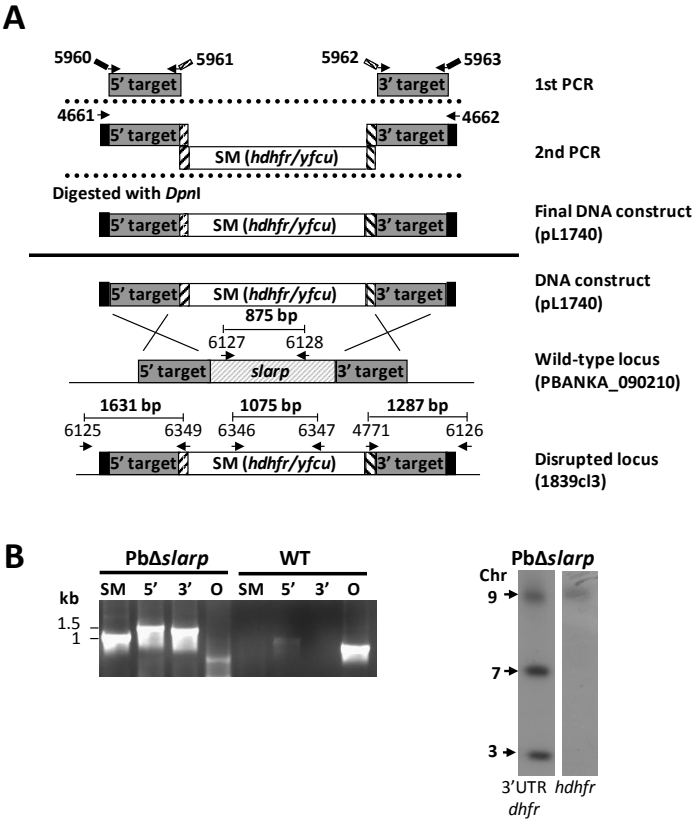

Supplementary Figure S3: Generation and genotype analyses of *P. berghei* mutant; *Δslarp*-a.

A) Generation of mutant *Δslarp*-a (1839cl3) mutant. For *Δslarp*-a the DNA-construct pL1740 was generated containing the positive/negative selectable marker cassette *hdhfr/yfcy.* This construct was subsequently used to generate the mutant *Δslarp*-a (1839cl3) in the *Pb*GFP-Luc$_{con}$ reference line. See Table S1 for the sequence of the primers. **B)** Diagnostic PCR and southern analysis of Pulse Field Gel (PFG)-separated chromosomes of mutant *Δslarp*-a confirming correct disruption of the *slarp*-locus. See Table S1 for the sequence of the primers used for the selectable marker gene (SM); 5'-integration event (5'); 3'-integration event (3') and the slarp ORF. Mutant *Δslarp* has been generated in the reference *P. berghei* ANKA line *Pb*GFP-Luc$_{con}$ which has a *gfp-luciferase* gene integrated into the silent 230p locus (PBANKA_030600) on chromosome 3 (i.e. RMgm-29; http://pberghei.eu/index.php?rmgm=29). For Southern analysis, PFG-separated chromosomes were hybridized using a 3'UTR *pbdhfr* probe that recognizes the construct integrated into *P. berghei slarp* locus on chromosome 9, the endogenous locus of *dhfr/ts* on chromosome 7 and the *gfp-luciferase* gene integrated into chromosome 3. In addition, the chromosomes were hybridized with the *hdhfr* probe recognizing the integrated construct into the slarp locus on chromosome 9.

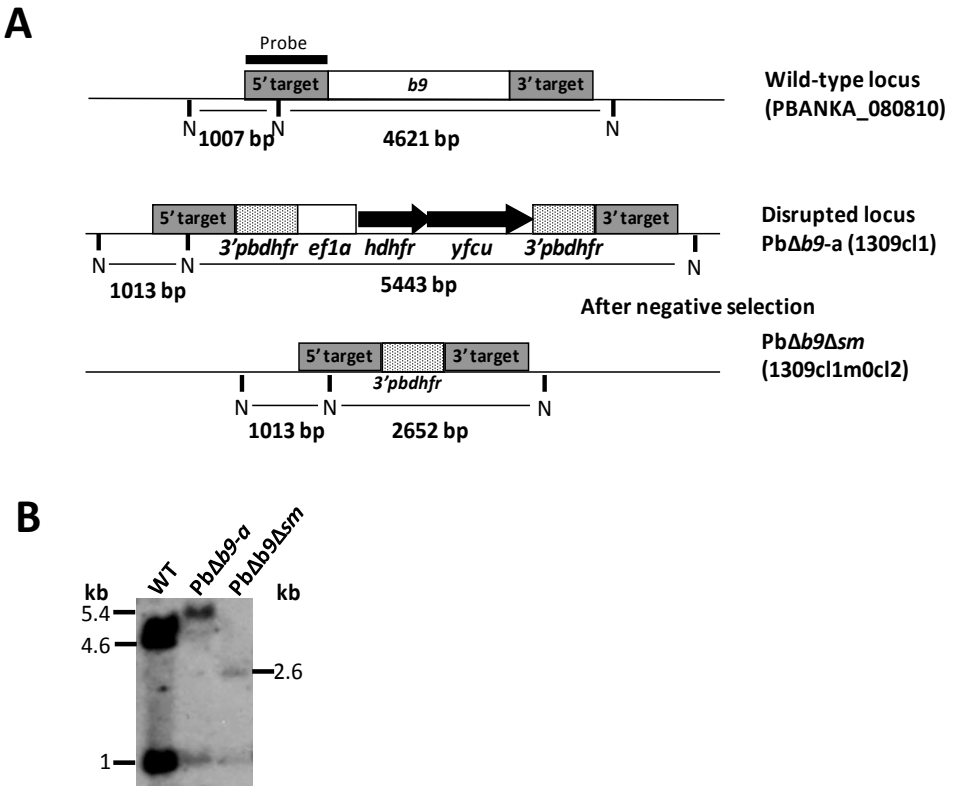

Supplementary Figure S4: Generation and genotype analyses of *P. berghei* mutant; *Δb9Δsm*.
A) Schematic representation of the generation of a selectable marker free *Δb9* mutant using the marker-recycling method. The b9 disruption construct containing the *hdhfr::yfcu* selectable marker (black arrows) flanked by the recombination sequences (3'*pbdhfr*, shaded boxes) targets the 230p locus by double cross-over homologous recombination at specific target regions (gray boxes). The *Δb9*-a mutant is obtained after transfection, using positive selection with pyrimethamine and then cloning. Subsequently, the marker-free *Δb9*(*Δsm*) mutant is selected by negative selection using 5-FC. Only mutant parasites that have 'spontaneously' lost the *hdhfr::yfcu* marker from their genome, achieved by a homologous recombination/excision, survive the negative selection. **B)** Southern blot analysis was hybridized with a 5' UTR *b9* probe (i.e. 5' targeting region). The localization of the restriction enzyme site (N; Nde I) and the expected size of the fragments are shown in Wt (wild type); *Δb9*-a (*b9* deletion mutant) and *Δb9Δsm* (*b9* deletion mutant free of selectable-marker).

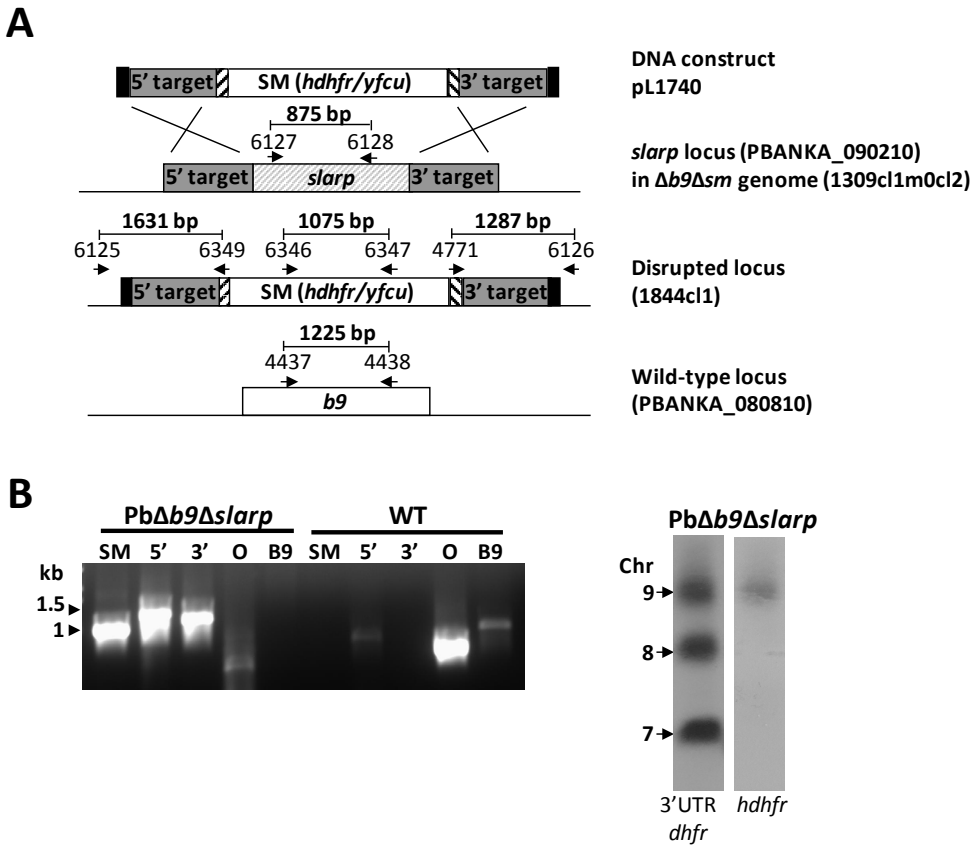

Supplementary Figure S5: Generation and genotype analyses of *P. berghei* mutant; *Δb9Δslarp*.
A) Generation of mutant *Δb9Δslarp*. For *Δb9Δslarp* the DNA-construct pL1740 was generated containing the positive/negative selectable marker cassette *hdhfr/yfcy.* This construct was subsequently used to generate the mutant *Δb9Δslarp* in the *Δb9Δsm* mutant. See Table S1 for the sequence of the primers. **B)** Diagnostic PCR and southern analysis of Pulse Field Gel (PFG)-separated chromosomes of mutant *Δb9Δslarp* confirming correct disruption of the *slarp*-locus and the *b9* locus. See Table S1 for the sequence of the primers used for the selectable marker gene (SM); 5'-integration event (5'); 3'-integration event (3') and the *slarp* and the *b9* ORF. For Southern analysis, PFG-separated chromosomes were hybridized using a 3'UTR *pbdhfr* probe that recognizes the construct integrated into *P. berghei slarp* locus on chromosome 9, the endogenous locus of *dhfr/ts* on chromosome 7 and a 3'UTR *pbdhfr* probe that recognizes the construct integrated into *P. berghei b9* locus on chromosome 8. In addition, the chromosomes were hybridized with the *hdhfr* probe recognizing the integrated construct into the *slarp* locus on chromosome 9.

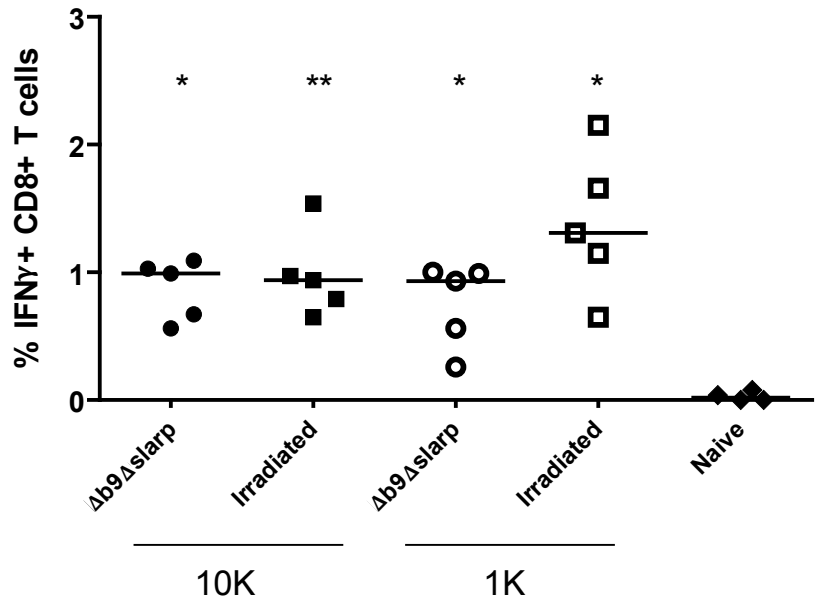

Figure S6: Liver CD8+ T cells with IFNγ response after immunization with *Δb9Δslarp* or γ-irradiated sporozoites. Sporozoite specific CD8+ T cell response in the liver of naïve or immunized C57BL/6j mice at C+70 post a *Δb9Δslarp* or irradiated sporozoites immunization with a 10K/10K/10K or a 1K/1K/1K dose regimen. Intracellular IFNγ production was measured by flow cytometry before challenge in liver. Immunized groups and naive mice responded equally to a polyclonal (PMA/Ionomycine) stimulation (data not shown). * $P < 0.02$; ** $P < 0.001$ compared to naïve mice.

Chapter 7

Reduced *Plasmodium berghei* sporozoite liver load associates with low protective efficacy after intradermal immunization.

Krystelle Nganou-Makamdop *, Ivo Ploemen *, Marije Behet, Geert-Jan van Gemert, Cornelus Hermsen, Meta Roestenberg, Robert Sauerwein

*these authors contributed equally

Parasite Immunol. 2012 Dec;34(12):562-9.

Abstract

Studies in animal models suggest that protection against malaria induced by intradermal (ID) administration of sporozoites is less effective compared to intravenous injection (IV). We investigated in a murine model the protective efficacy and immune responses after ID or IV immunization of sporozoites. Mice were immunized via either IV or ID route with *P. berghei* sporozoites in combination with chloroquine treatment (CPS) (allowing full liver stage development) or by γ-radiation attenuated sporozoites (RAS) (early liver stage arrest). While IV immunization with both RAS and CPS generated 90-100% protection, ID immunization resulted in reduced levels of protection with either immunization strategy in both Balb/cByJ (50%) and C57BL/6j mice (7-13%). Lower protection by ID routing associated with a 30-fold lower parasite liver load ($p<0.001$ ($\chi^2= 49.08$, (df 1)) assessed by real-time *in vivo* imaging of bioluminescent *P. berghei* parasites. Unlike IV, ID immunization did not result in expansion of CD8+ T-cells with effector memory phenotype and showed lower IFNγ responses irrespective of the immunization regime. In conclusion, protection against sporozoite infection is likely dependent on parasite liver infection and subsequently generated cellular immune responses.

Introduction

Attenuated whole malaria parasites are considered eligible candidates for a potentially successful vaccine [1,2]. The approach is based on disruption of the *Plasmodium* parasite life cycle allowing the host to develop protective immunity in the absence of overt clinical disease [3]. Whole parasite immunizations with sporozoites attenuated by radiation (RAS), or with sporozoites in combination with chloroquine chemo-prophylaxis (CPS), have been successfully conducted in mice and men resulting in complete protection [4,5,6]. RAS arrest early in liver stage development [7] whereas CPS undergo full liver stage maturation releasing blood stage parasites that are subsequently killed by chloroquine [4]. While murine immunizations are generally performed by intravenous (IV) routing, alternative routes are required for sustainable clinical applications in humans. Immunity to malaria is known to comprise cellular and humoral responses [8]. Various studies have report antibody responses during sporozoite immunization in mice, including RAS and CPS [9,10,11]. Moreover, protective efficacy following IV immunizations in mice is attributed to liver CD8+ effector memory T cells and high levels of IFNγ production [12,13,14,15]. However lower levels of protection are induced following intradermal (ID) sporozoite immunization with either *P. berghei* genetically attenuated parasites (GAP) [16] or *P. yoelii* RAS [17]. In a recent clinical study, subcutaneous or ID immunization with irradiated *P. falciparum* sporozoites also showed suboptimal immune responses and protective efficacy in humans [18]. These data corroborated with findings in a murine model, showing that protective efficacy following ID immunization requires a higher sporozoite inoculation compared to IV immunization, and suggesting that differences in protective efficacy may be related to the number of sporozoites reaching the liver.

Using bioluminescent parasites, we studied the relation between parasite liver load following IV or ID sporozoite infection and protective immunity following IV or ID immunizations by *P. berghei* RAS or CPS protocols.

Material and Methods

Mice and parasites

Female BALB/cByJ and C57BL/6J, eight weeks of age, were purchased from Elevage Janvier (France). All studies were performed according to the regulations of the Dutch "Animal On Experimentation act" and the European guidelines 86/609/EEG. Approval was obtained from

the Radboud University Experimental Animal Ethical Committee (RUDEC 2009-019, RUDEC 2009-225). *P. berghei* (ANKA) sporozoites (spz) were obtained by dissection of the salivary glands of infected female *Anopheles stephensi* mosquitoes 21-28 days after infected blood meal. For radiation attenuated sporozoites (RAS), infected mosquitoes were irradiated at 16,000 rad (Gammacel 1000 ^{137}Cs) prior to dissection.

Intravenous and intradermal immunization by RAS and CPS

All immunizations were performed with freshly isolated sporozoites. BALB/cByJ mice were immunized once with 50.000 *P. berghei* sporozoites. C57BL/6J mice received three injections of 10,000 sporozoites with 7 day intervals. Different immunization protocols were used given that in contrast to BALB/c mice, multiple sporozoite inoculations are required to induce protection in C57BL/6 mice [19,20]. In both mouse strains, the choice for specific immunization dose was made based on a suspected (sub)optimal level of conferred protection. All immunizations were performed by IV injection (200 µl in the tail vein) or ID injection (50 µl in the proximal part of each hind leg). For the chloroquine prophylactic sporozoites (CPS) immunizations, mice received a daily i.p. injection of 800µg of chloroquine base starting simultaneously with the first sporozoite inoculation up to two weeks after the last sporozoite inoculation. Chloroquine diphosphate (CQ, Sigma-aldrich) was diluted in PBS and administered to mice. At the end of the chloroquine treatment and one day before challenge, absence of parasitemia was confirmed by examination of Giemsa-stained slides of tail blood.

Challenge of immunized mice by mosquito bite

Groups of BALB/cByJ and C57BL/6J mice, immunized with either irradiated sporozoites or sporozoites under chloroquine cover, were challenged by *Pb*GFP-Luc$_{con}$ infectious mosquito bites (5-11 mosquitoes) two weeks after the chloroquine treatment. Salivary glands of all blood-engorged mosquitoes were dissected to confirm the presence of sporozoites. Giemsa stained bloodsmears were prepared every other day starting from day 3 to day 21 after mosquito bite challenge, to monitor for blood stage parasitemia. The pre-patent period was defined as the period of time between challenge and the first appearance of blood stage parasites (0.5-2% blood smear positive).

Real-time *in vivo* imaging of liver stage development in C57BL/6 mice

Since *in vivo* visualization of parasites during particularly RAS immunization is not possible, we performed a separate infection experiment with *Pb*GFP-Luc$_{con}$. *Pb*GFP-Luc$_{con}$ sporozoites ($50x10^3$) were administered to C57BL/6 mice by IV injection in the tail (200 µl) or by ID injection in the proximal part of each hind leg (50 µl per leg). C57BL/6 mice were preferred over BALB/c mice based on a higher susceptibility for *P. berghei* infection [21], which enables a more sensitive visualization of the parasite load. Each group consisted of 5 mice. Luciferase activity in animals was visualized through imaging of whole bodies using the *in vivo* imaging system Lumina (Caliper Life Sciences, USA) as described previously [22] with minor adaptations. Briefly, animals were anesthetized using the isoflurane-anesthesia

system, their abdomen was shaved and D-luciferin dissolved in PBS (100 mg/kg; Caliper Life Science, Belgium) was injected subcutaneously (in the neck). Animals were kept anesthetized during the measurements, which were performed within 3-5 minutes after the injection of D-luciferin. Bioluminescence imaging was acquired with a 10 cm FOV, medium binning factor and an exposure time of 300 seconds. Quantitative analysis of bioluminescence was performed by measuring the luminescence signal intensity using the ROI settings of the Living Image 3.0 software. The ROI was set to measure the abdominal area at the location of the liver. ROI measurements are expressed in total flux of photons.

Mononuclear cell isolation from blood, spleen and liver

Before and after challenge, C57BL/6J mice were euthanized by isoflurane inhalation after i.v. injection of 50 i.u. of heparin. Blood, spleen and livers were collected after perfusion of the livers with 10ml of PBS. Cell suspensions of livers and spleen were made by pressing the organs through a 70-µm nylon cell strainer (BD Labware). Liver cells were resuspended in 35% Persoll (GE Healthcare) and centrifuged at 800g for 20min. Liver and spleen erythrocytes were lysed by a 5 min incubation of the cells on ice in ACK lysing buffer. After erythrocyte lysis, hepatic mononuclear cells (HMC) and splenocytes were resuspended in RPMI medium (Gibco, 1640). Isolation of peripheral blood mononuclear cells (PBMC) was performed using Histopaque-1077 (Sigma-Aldrich) according to the manufacturer's recommendation.

Phenotyping CD8+ effector and memory T cells

Five-color staining of PBMC, HMC and splenocytes was performed using the following monoclonal anti-mouse antibodies: Pacific blue-conjugated anti CD3 (17A2), Peridinin Chlorophyll Protein (PerCP)-conjugated anti CD4 (RM4.5), Alexa fluor 700-conjugated anti CD8a (53-6.7), fluorescein isothiocyanate (FITC)–conjugated anti-CD44, allophycocyanin (APC)– or phycoerythrin-Cy7 (PE-Cy7)-conjugated anti-CD62L (MEL-14). All antibodies were purchased from Biolegend (San Diego, CA). Briefly, 10^6 cells were resuspended in cold assay buffer (PBS supplemented with 0.5% bovine serum albumin – Sigma-Aldrich) and incubated for 30min at 4°C with monoclonal antibodies. Cells were fixed with Fix & Perm medium A (Invitrogen) and resuspended in assay buffer for measurement. Flow cytometry was performed on a 9-color Cyan ADP (Beckman Coulter) and data analysis using FlowJo software (version 9.1 ; Tree Star).

***Ex vivo* sporozoite stimulation and intracellular IFNγ staining**

HMC and splenocytes in complete RPMI 1640 culture medium [23] were co-cultured in presence of cryoconserved sporozoites or salivary glands from uninfected mosquitoes. Cells were stimulated at 37°C/5%CO_2 for 24 hours during which Brefeldin A (Sigma) was added for the last four hours (10µg/ml final concentration). As a positive control to the stimulation, PMA and Ionomycin (Sigma) were added simultaneously with Brefeldin A at a final concentration of 100ng/ml and 1.25µg/ml respectively. Cells were harvested after 24-hours *in vitro* stimulation and stained with labeled monoclonal antibodies against CD3,

CD4, CD8a and CD44 as cited above. Fixed cells were stained with APC-conjugated anti- IFNγ for 30min at 4°C with Fix & Perm medium B (Invitrogen). Flow cytometry was performed on a 9-color Cyan ADP (Beckman Coulter) and data analysis using FlowJo software (version 9.1 ; Tree Star). For the analysis of cytokine production, background responses to salivary glands was subtracted from PbSPZ responses respectively for each individual mouse.

Transgenic *Pb*GFP-Luc$_{con}$ sporozoites neutralization assay

The transgenic sporozoite neutralization assay (TSNA) was performed as described [24]. Mice were sacrificed and plasma was collected 1 day before challenge. *Pb*GFP-Luc$_{con}$ sporozoites ($9x10^4$ in 30 µl RPMI) were pre-incubated for 30 minutes on ice with 30µl (1:1 ratio) plasma of naive or immunized mice. Pre-incubated freshly isolated sporozoites were added to wells containing monolayers of $1x10^5$ pre-seeded Huh-7 hepatocyte cultures (1 ml/well in 24 well plates). Human liver hepatoma cells (Huh-7) were suspended in 1ml of 'complete' DMEM (DMEM, Gibco, supplemented with 10% FCS, 1% penicillin/streptomycin and 1% Glutamax) the day prior to infection and were seeded overnight in 24 well plates (10^5 cells/well). For each plasma sample, duplicates of $3x10^4$ sporozoites were added per well and plates were centrifuged 10 minutes at 1800 G (eppendorf centrifuge 5810 R).

At 40 hours post sporozoite addition, cells were washed and lysed in 200 µl of cell culture lysis reagent obtained from the Promega Luciferase Assay System Kit® (Promega, PT). Samples in Promega lysis buffer were measured for luminescence intensity with the Lumina system. 70 µl of Luciferase Assay Substrate (Promega Luciferase Assay System Kit®) was added to 20 µl of lysed hepatocyte cultures in a white 96-well plate. Bioluminescence images were acquired with a 7 cm FOV, medium binning factor and exposure time of 10-30 seconds. Quantitative analysis was performed by measuring the luminescence signal intensity per well using the ROI settings of the Living Image 3.0 software. ROI measurements are expressed in total flux of photons. Percent inhibition was calculated by the following formula; 1 – (average bioluminescence in immune plasma sample/average bioluminescence in naive plasma sample) * 100%.

Statistical analysis

In all experiments and assays, comparisons between two groups were performed by a Mann-Whitney U test using PRISM software version 5.0 (Graphpad, San Diego, CA). $p < 0.05$ are considered statistically significant. Overall comparisons over three groups or more was performed by Kruskas-Wallis test. Calculations of sample sizes were performed (power 0.85; $\alpha = 0.05$) by estimation of differences between IV and ID groups.

Results

RAS and CPS ID immunization induce less protection compared to the IV route

To compare protective efficacy conferred by ID or IV immunization, mice immunized by either RAS or CPS protocols were challenged by infectious mosquito bites.

Irrespective of the immunization protocol, ID immunization induced lower protection in BALB/cByJ (50%) and C57BL/6J (7-13%) mice as compared to 90-100% protection after IV immunization (Table 1). Development of blood stage parasites in unprotected ID immunized mice showed no significant delay compared to control mice.

Table 1. Protection by intravenous and intradermal immunizations

	No. protected/ No. challenged (% protection) pre-patency (days)			
	BALB/c 50K		C57BL6/j 10k/10k/10k	
	Intravenous	Intradermal	Intravenous	Intradermal
RAS	9/10 (90) 7	5/10 (50) 6	15/15 (100)	1/15 (7) 6
CPS	10/10 (100)	5/10 (50) 6	15/15 (100)	2/15 (13) 6
Naive	0/9 (0) 5.5		1/11 (9) 5	

C57BL/6j and BALB/cByJ mice were immunized with RAS or CPS by IV or ID. Challenged by bites of 5-11 infected mosquitoes was performed 3 to 4 weeks after the last immunization (two weeks after chloroquine treatment). Parasitaemia was monitored by Giemsa staining of tail-vein blood slides up to 21 days after challenge.

ID injection of *Pb*GFP-Luc$_{con}$ sporozoites results in lower parasite liver load

To evaluate whether infection by IV or ID routes resulted in different magnitude of liver infection, we measured *in vivo* parasite liver loads in C57BL/6 mice by real-time imaging after IV or ID injection of identical doses of fresh *Pb*GFP-Luc$_{con}$ sporozoites. Mice that received IV injection showed a clear bioluminescent signal originating from the site of the liver as from 30 hours post infection onwards. This signal subsequently further increased covering the whole liver area at 44 hours post infection (Figure 1A). In contrast, ID injection did not result in a bioluminescent signal distinct from background at 30 and 35 hours post infection while a weak signal was visible at 44 hours. After ID injection, mice showed approximately a 30 fold lower parasite liver load ($p < 0.0001$) compared to IV injected mice (Figure 1B). These data show a strong association ($p<0.001$ ($\chi 2 = 49.08$, (df 1)) between the number of parasites reaching the liver in this experiment and the level of protection conferred by different routes of sporozoite administration as shown in preceding immunization experiments.

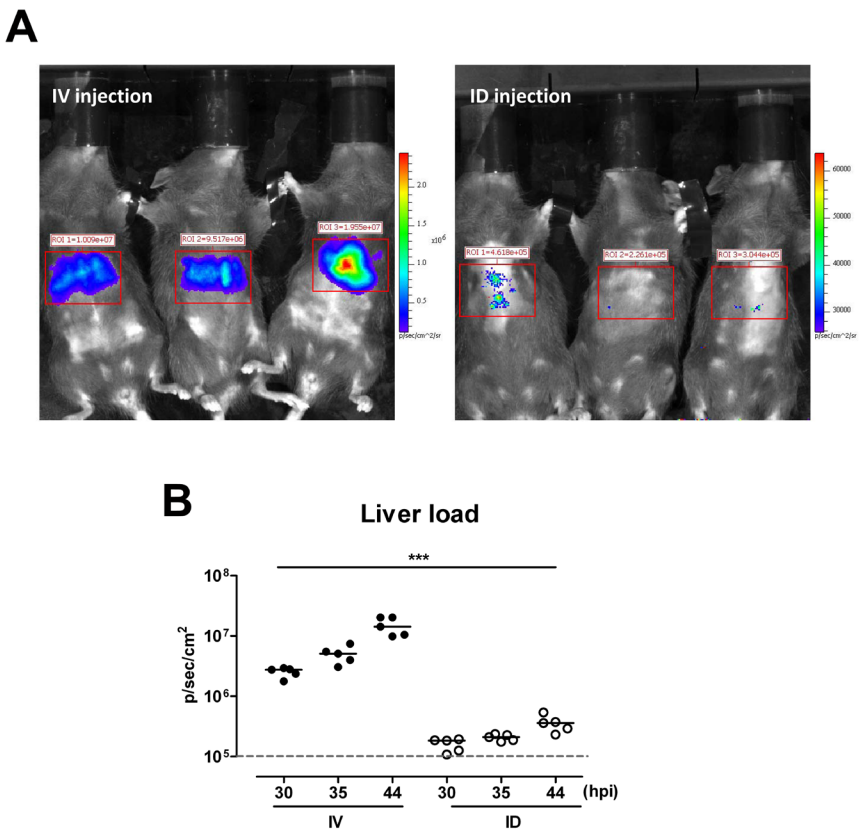

Figure 1. Liver stage development of *Pb*GFP-Luc$_{con}$ sporozoites after IV or ID injection.
A) Representative rainbow images of luminescence (photons/sec/cm^2) in livers of live C57BL/6 mice at 44 h after infection. Mice were injected with 5x10^4 sporozoites by intravenous (left) or intradermal (right) inoculation. **B)** Real-time measurement of the parasite liver load in mice injected with 5x10^4 sporozoites by IV (n=5) or ID (n=5) inoculation, at different time points (30, 35 and 44 hours post infection). Dots represent the luminescent intensity (photons/sec/cm^2) of the Regions of interest (ROI's) overlaying the livers, as depicted in A. The dotted line represents the threshold of luminescent signaling. *** p ≤ 0.0001.

Expansion of CD8+ effector memory T cells and sustained sporozoite-specific IFNγ responses in IV but not in ID immunized mice.

We next assessed cellular immune responses after IV or ID immunization of C57BL/6j mice. Following RAS or CPS IV immunization, proportions of CD8+ T cells with effector memory phenotype (Tem) were significantly increased in both liver (p = 0.008) and spleen (p = 0.008). With the exception of one CPS mouse, this

expansion of CD8+ Tem cells was not observed in any of the ID immunized mice, remaining at baseline levels similar to naïve mice (Figure 2A). Because IFNγ has been shown to play an essential role in protection against liver stages [12,15] we studied IFNγ responses of T cells in liver and spleen of IV or ID immunized mice. Overall, RAS or CPS immunizations resulted in sporozoite specific IFNγ responses in the liver ($p = 0.03$) and spleen ($p = 0.008$). Although not reaching statistical significance, there was a tendency of higher sporozoite specific IFNγ response by T cells with memory phenotype (CD44hi) in liver and spleen (Figure 2B) cells from IV immunized compared to ID immunized C57BL/6J mice. Within the T cell population, similar observations were made for CD8+CD44hi T cells. Furthermore, the levels of CD8+ Tem cells in both IV and ID groups correlated with the IFNγ response in liver ($R= 0.63$, $p = 0.003$) and spleen ($R= 0.54$, $p=0.01$). Three weeks after challenge, the observed high levels of liver CD8+ Tem cells (Figure 2C) and increased IFNγ responses (Figure 2D) were sustained in IV immunized mice. No data were obtained from ID immunized mice as these did not survive challenge infection (Table 1).

Both IV and ID immunization induce antibodies blocking sporozoite hepatocyte invasion

Finally, functionality of RAS and CPS induced antibodies was tested in the sporozoite neutralization assay, testing their capacity to invade and subsequently develop in liver cells [24]. Sporozoite invasion was strongly reduced in the presence of plasma from both RAS and CPS immunized mice ($p\leq0.05$) with, stronger inhibition by IV immunized mice within the RAS group ($p <0.01$) (Figure 3). Since CPS ID immunized mice showed similar blocking activity compared to IV immunized mice, antibodies may contribute but are by themselves likely not sufficient to induce complete protection.

Discussion

Our findings show that ID immunization with whole live malaria parasites confers a far lower protective efficacy when compared to IV immunization. The reduced protective efficacy clearly associates with a lower number of sporozoites reaching the liver. Lower protective efficacy by ID immunization was observed in both BALB/c and C57BL6/j mice using two independent immunization protocols; i.e. sporozoite liver cell invasion only with early developmental arrest (RAS) or full completion of liver maturation and early abrogation of blood stage multiplication (CPS). Moreover,

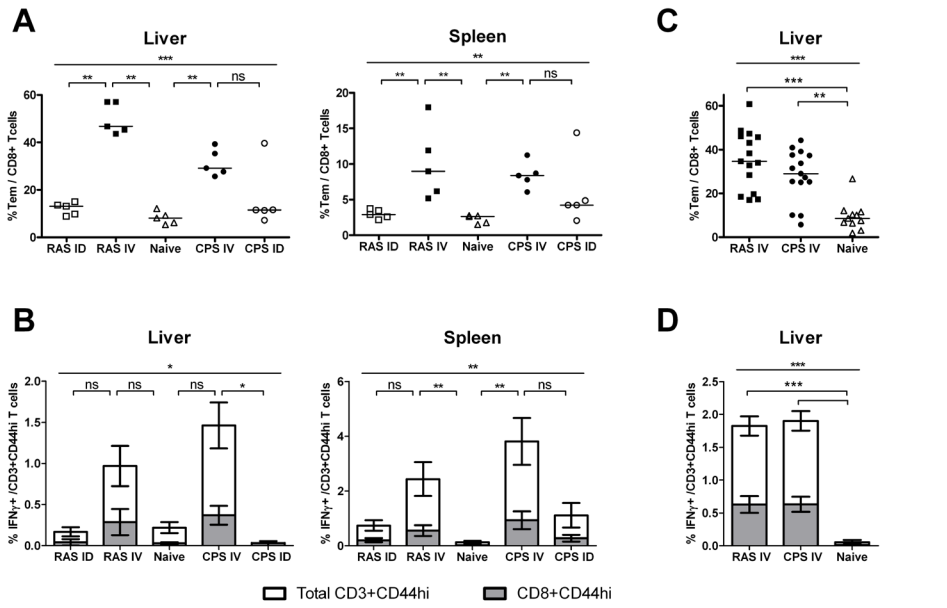

Figure 2. Liver and spleen CD8+ T cells with effector memory phenotype and IFNγ responses after intravenous or intradermal immunizations.

A) Percentages of cells with effector memory phenotype (Tem: CD44hiCD62L-) per total CD8+ T cells were measured *ex vivo* in liver and spleen of C57BL/6j mice on day 39 after RAS and CPS IV or ID immunization. **B)** Percentages of IFNγ producing T cells or CD8+ T cells with memory phenotype (CD44hi) were measured by intracellular staining after stimulation of liver and spleen cells from RAS and CPS immunized mice with cryoconserved sporozoites. Total salivary gland background responses were similar between groups (mean(SD): 0.42% (0.18) in the liver and 0.29% (0.16) in the spleen). Three weeks after challenge, IV immunized mice showed **C)** sustained levels of liver CD8+ Tem cells and **D)** higher anti-sporozoite IFNγ responses in the liver. In the spleen, measured responses were similar to pre-challenge results (data not shown). A and C: Individual values and median are presented. B and D: Error bars represent standard error of the mean. * $p \leq 0.04$, ** $p \leq 0.008$, *** $p \leq 0.0001$.

both RAS and CPS IV immunizations induce higher cellular immune responses compared to ID.

Our data confirm the earlier formulated hypothesis by Epstein *et al.*: based on low hepatic immune responses in ID immunized animals and low protection level in a clinical trial, the authors suggest that the degree of parasite liver load following sporozoite administration associates with protective efficacy [18]. However, ID immunization can induce high levels of protection provided that sufficiently high numbers of sporozoites (i.e. $9x10^4$ *P. yoelii*) are injected [17]. The necessity of high numbers of sporozoites for ID induced protection supports the notion that liver

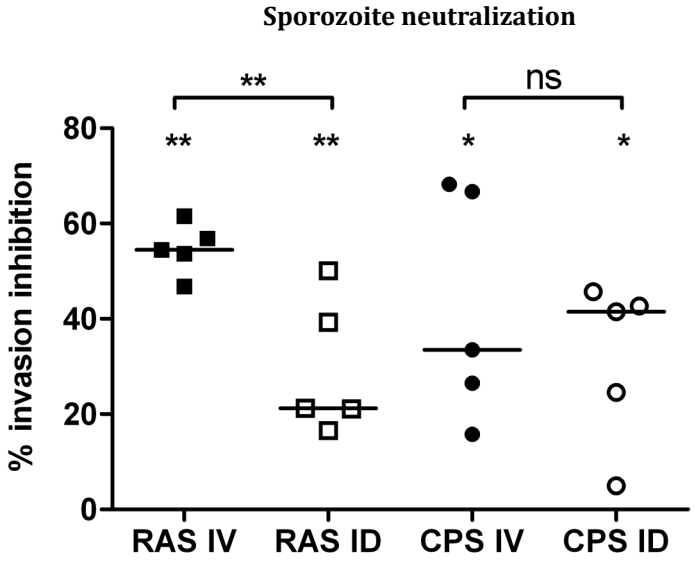

Figure 3. Transgenic *Pb*GFP-Luc$_{con}$ sporozoite neutralization assay
Sporozoite invasion inhibition (mean ± sd) in Huh-7 liver cells of *Pb*GFP- Luc$_{con}$ sporozoites pre-incubated with plasma from CPS or RAS immunized C57BL/6 mice by either IV or ID route. The baseline represents the mean invasion inhibition by plasma from naive mice. P-values represent significance in invasion inhibition between plasma from immunized mice and baseline values or between groups of immunized mice. Infectivity was quantified by analyzing the luminescent flux (p/sec/cm^2) in each well. * $p \leq 0.05$, ** $p \leq 0.01$.

parasite load might be important for protective efficacy of whole sporozoite immunization. ID injection of *P. yoelii* sporozoites results in a 10-20 fold lower parasite liver load compared to IV injection as determined by q-RTPCR analysis of parasite 18S rRNA [25], possibly related to a slower or inefficient migration of sporozoites to the liver. IV inoculated parasites reach the liver within minutes [26], whereas sporozoites inoculated into the skin slowly trickle out of the inoculation site over a period of one to three hours [27]. Our results indicate that the lower parasite liver load after ID inoculation is unlikely to be explained by a delayed arrival of sporozoites in the liver. Comparison of the parasite liver load at 35 hours post ID injection was still ±15 times lower compared to the parasite liver load at 30 hours post IV injection (Figure 2). Despite differences between parasites species, including among others infectivity [28] or host cell preference [29,30,31], our data in *P. berghei* parallel previous results in *P. yoelii* studies [25]. Therefore, the relatively low level of parasites capable of reaching the liver after ID injection is likely a common feature among *Plasmodium* species.

CD8+ T cell responses are known to be essential for protection induced by attenuated live sporozoite immunization in rodent models. Our data corroborate previous studies on *P. berghei* RAS-induced immunity showing expansion of CD8+ memory T cells, mainly in the liver, together with high IFNγ production in IV immunized mice [12,13,14,15][8-11]. The low immune responses observed after ID immunization likely follow the low parasite liver load. RAS ID and subcutaneous immunization of human volunteers also show low protection levels, and in non-human primates and mice subcutaneous or ID immunization lead to lower IFNγ responses compared to IV sporozoite immunization [18]. Despite differences in phenotyping and gating strategy, CD8+ effector (memory) T cells (CD44hi CD62L-) and not central memory T cells (CD44hi CD62L+) are identified as induced T-cell subset. In another study using the *P. yoelii* model, major CD8+ T cell responses were generated in the draining lymph nodes after infected mosquito bites or ID inoculation of sporozoites. Although parasite liver load was reduced, complete protection defined as impediment of blood stage infection was not evaluated [32]. We did not test the regional lymph nodes response and cannot exclude a possible contribution but our data clearly demonstrate that ID inoculation is inefficient in inducing protection. In addition, a measure of sporozoite load in regional lymph nodes following ID inoculation would have been informative. Unfortunately, *in viv*o visualization of *Pb*GFP-Luc$_{con}$ is not possible due to a relatively low luciferase expression at the sporozoite stage [22]. Next to cellular components, antibody responses can contribute to protection by whole sporozoite immunization [8]. Our data suggest that induced functional antibodies may contribute to protection but are more likely related to exposure. CPS-induced antibodies do not show significant functional differences in *in vitro* sporozoite invasion inhibition between plasma of mice immunized by IV or ID inoculations. On the contrary, RAS induced antibodies after IV injection compared to ID immunization are more potent and also more predominant as determined by IFA titration (data not shown). However, others have previously shown that RAS and GAP protection does not rely on induced sporozoite-specific antibodies. In B-cell deficient RAS or GAP immunized mice, protection upon challenge was unaffected [33,34]. Moreover, GAP immunized IFNγ -/- mice produced sporozoite-specific antibodies but were not protected against a WT challenge [34]. Overall, our findings corroborate the conclusions of a meta-analysis by Guilbride et al., emphasizing the poor capacity to induce protective efficacy after sporozoite inoculation via the skin as compared to the IV route [35].

Although in human volunteers whole parasite immunization by bite of infected

mosquitoes can induce complete protection [6,36,37,38], mosquito bites are obviously not a practical route of immunization. Further studies with luciferase expressing *P. berghei* parasites are in progress, evaluating various administration routes, injection volumes and doses as well as numbers of injections. By a stepwise selection process we aim to find the best regimen to achieve maximal parasite liver loads and subsequently protection. Such regimen may form a critical element in the future for a successful immunization strategy in humans with attenuated whole-sporozoites.

Acknowledgments

We would like to thank Claudia Lagarde, Alex Ignacio, Iris Lamers-Elemans and Nynke Tichelaar for the technical assistance with the *P. berghei* immunizations and Jolanda Klaassen, Laura Pelser-Posthumus, Astrid Pouwelsen and Jacqueline Kuhnen for breeding of mosquitoes and assistance with the *P. berghei* challenge.

References

1. Vaughan AM, Wang R, Kappe SH (2010) Genetically engineered, attenuated whole-cell vaccine approaches for malaria. HumVaccin 6: 107-113.
2. Wykes M, Good MF (2007) A case for whole-parasite malaria vaccines. IntJParasitol 37: 705-712.
3. Hafalla JC, Silvie O, Matuschewski K (2011) Cell biology and immunology of malaria. ImmunolRev 240: 297-316.
4. Belnoue E, Costa FT, Frankenberg T, Vigario AM, Voza T, et al. (2004) Protective T cell immunity against malaria liver stage after vaccination with live sporozoites under chloroquine treatment. JImmunol 172: 2487-2495.
5. Luke TC, Hoffman SL (2003) Rationale and plans for developing a non-replicating, metabolically active, radiation-attenuated Plasmodium falciparum sporozoite vaccine. JExpBiol 206: 3803-3808.
6. Roestenberg M, McCall M, Hopman J, Wiersma J, Luty AJ, et al. (2009) Protection against a malaria challenge by sporozoite inoculation. NEnglJMed 361: 468-477.
7. Scheller LF, Stump KC, Azad AF (1995) Plasmodium berghei: production and quantitation of hepatic stages derived from irradiated sporozoites in rats and mice. JParasitol 81: 58-62.
8. Good MF, Doolan DL (2010) Malaria vaccine design: immunological considerations. Immunity 33: 555-566.
9. Golenser J, Heeren J, Verhave JP, Kaay HJ, Meuwissen JH (1977) Crossreactivity with sporozoites, exoerythrocytic forms and blood schizonts of Plasmodium berghei in indirect fluorescent antibody tests with sera of rats immunized with sporozoites or infected blood. Clin Exp Immunol 29: 43-51.
10. Orjih AU, Nussenzweig RS (1979) Plasmodium berghei: suppression of antibody response to sporozoite stage by acute blood stage infection. Clin Exp Immunol 38: 1-8.
11. Schofield L, Villaquiran J, Ferreira A, Schellekens H, Nussenzweig R, et al. (1987) Gamma interferon, CD8+ T cells and antibodies required for immunity to malaria sporozoites. Nature 330: 664-666.
12. Berenzon D, Schwenk RJ, Letellier L, Guebre-Xabier M, Williams J, et al. (2003) Protracted protection to Plasmodium berghei malaria is linked to functionally and phenotypically heterogeneous liver memory CD8+ T cells. JImmunol 171: 2024-2034.
13. Guebre-Xabier M, Schwenk R, Krzych U (1999) Memory phenotype CD8(+) T cells persist in livers of mice protected against malaria by immunization with attenuated Plasmodium berghei sporozoites. EurJImmunol 29: 3978-3986.

14. Jobe O, Donofrio G, Sun G, Liepinsh D, Schwenk R, et al. (2009) Immunization with radiation-attenuated Plasmodium berghei sporozoites induces liver cCD8alpha+DC that activate CD8+T cells against liver-stage malaria. PLoSOne 4: e5075.
15. Jobe O, Lumsden J, Mueller AK, Williams J, Silva-Rivera H, et al. (2007) Genetically attenuated Plasmodium berghei liver stages induce sterile protracted protection that is mediated by major histocompatibility complex Class I-dependent interferon-gamma-producing CD8+ T cells. JInfectDis 196: 599-607.
16. Douradinha B, van Dijk MR, Ataide R, van Gemert GJ, Thompson J, et al. (2007) Genetically attenuated P36p-deficient Plasmodium berghei sporozoites confer long-lasting and partial cross-species protection. IntJParasitol 37: 1511-1519.
17. Voza T, Kebaier C, Vanderberg JP (2010) Intradermal immunization of mice with radiation-attenuated sporozoites of Plasmodium yoelii induces effective protective immunity. MalarJ 9: 362.
18. Epstein JE, Tewari K, Lyke KE, Sim BK, Billingsley PF, et al. (2011) Live Attenuated Malaria Vaccine Designed to Protect through Hepatic CD8+ T Cell Immunity. Science.
19. Schmidt NW, Butler NS, Badovinac VP, Harty JT (2010) Extreme CD8 T cell requirements for anti-malarial liver-stage immunity following immunization with radiation attenuated sporozoites. PLoSPathog 6: e1000998.
20. van Dijk MR, Douradinha B, Franke-Fayard B, Heussler V, van Dooren MW, et al. (2005) Genetically attenuated, P36p-deficient malarial sporozoites induce protective immunity and apoptosis of infected liver cells. ProcNatlAcadSciUSA 102: 12194-12199.
21. Scheller LF, Wirtz RA, Azad AF (1994) Susceptibility of different strains of mice to hepatic infection with Plasmodium berghei. Infect Immun 62: 4844-4847.
22. Ploemen IH, Prudencio M, Douradinha BG, Ramesar J, Fonager J, et al. (2009) Visualisation and quantitative analysis of the rodent malaria liver stage by real time imaging. PLoSOne 4: e7881.
23. Watarai H, Nakagawa R, Omori-Miyake M, Dashtsoodol N, Taniguchi M (2008) Methods for detection, isolation and culture of mouse and human invariant NKT cells. NatProtoc 3: 70-78.
24. Ploemen I, Behet M, Nganou-Makamdop K, van Gemert GJ, Bijker E, et al. (2011) Evaluation of immunity against malaria using luciferase-expressing Plasmodium berghei parasites. Malar J 10: 350.
25. Inoue M, Culleton RL (2011) The intradermal route for inoculation of sporozoites of rodent malaria parasites for immunological studies. Parasite Immunol 33: 137-142.
26. Shin SC, Vanderberg JP, Terzakis JA (1982) Direct infection of hepatocytes by sporozoites of Plasmodium berghei. J Protozool 29: 448-454.
27. Yamauchi LM, Coppi A, Snounou G, Sinnis P (2007) Plasmodium sporozoites trickle out of the injection site. Cell Microbiol 9: 1215-1222.
28. Vanderberg JP (1991) Rodent malaria models. Parasitol Today 7: 340; author reply 340-341.
29. Gueirard P, Tavares J, Thiberge S, Bernex F, Ishino T, et al. (2010) Development of the malaria parasite in the skin of the mammalian host. Proc Natl Acad Sci U S A 107: 18640-18645.
30. Hollingdale MR, Leef JL, McCullough M, Beaudoin RL (1981) In vitro cultivation of the exoerythrocytic stage of Plasmodium berghei from sporozoites. Science 213: 1021-1022.
31. Silvie O, Franetich JF, Boucheix C, Rubinstein E, Mazier D (2007) Alternative invasion pathways for Plasmodium berghei sporozoites. Int J Parasitol 37: 173-182.
32. Chakravarty S, Cockburn IA, Kuk S, Overstreet MG, Sacci JB, et al. (2007) CD8+ T lymphocytes protective against malaria liver stages are primed in skin-draining lymph nodes. NatMed 13: 1035-1041.
33. Chen DH, Tigelaar RE, Weinbaum FI (1977) Immunity to sporozoite-induced malaria infeciton in mice. I. The effect of immunization of T and B cell-deficient mice. JImmunol 118: 1322-1327.
34. Mueller AK, Deckert M, Heiss K, Goetz K, Matuschewski K, et al. (2007) Genetically attenuated Plasmodium berghei liver stages persist and elicit sterile protection primarily via CD8 T cells. AmJPathol 171: 107-115.
35. Guilbride DL, Gawlinski P, Guilbride PD (2010) Why functional pre-erythrocytic and bloodstage malaria vaccines fail: a meta-analysis of fully protective immunizations and novel immunological model. PLoSOne 5: e10685.
36. Clyde DF, Most H, McCarthy VC, Vanderberg JP (1973) Immunization of man against sporozite-induced falciparum malaria. AmJMedSci 266: 169-177.
37. Hoffman SL, Goh LM, Luke TC, Schneider I, Le TP, et al. (2002) Protection of humans against malaria by immunization with radiation-attenuated Plasmodium falciparum sporozoites. JInfectDis 185: 1155-1164.

38. Vanderberg JP, Nussenzweig RS, Most H, Orton CG (1968) Protective immunity produced by the injection of x-irradiated sporozoites of Plasmodium berghei. II. Effects of radiation on sporozoites. JParasitol 54: 1175-1180.

Chapter 8

Plasmodium liver load following parenteral sporozoite administration in rodents.

Ivo Ploemen, Sumana Chakravarty, Geert-Jan van Gemert, Takeshi Annoura, Shahid Khan, Chris Janse, Cornelus Hermsen, Stephen Hoffman, Robert Sauerwein

Vaccine, in press

Abstract

One of the bottlenecks in the development of a whole sporozoite malaria vaccine is the route and method of sporozoite administration. Immunization and challenge of human volunteers by mosquito bites is effective, but cannot be used as a vaccine. Intravenous immunization with sporozoites is effective in rodents and non-human primates, and being studied in humans, but is not yet used for licensed vaccines for infectious diseases. Intradermal and subcutaneous immunization regimens show a strong decrease in protective efficacy, which in rodents, is associated with a decreased degree of parasite liver infection during immunization. The objective of this study was to explore alternative routes of sporozoite administration to increase efficiency of liver infection. Using *in vivo* imaging, we found that IM injection of sporozoites resulted in a greater parasite liver load compared to ID and SC injection. The use of small inoculation volumes and multiple injections further increased the subsequent liver load. These observations were corroborated in a *P. yoelii* model using cryopreserved sporozoites administered ID. Our findings provide a rationale for the design of clinical trials to optimize needle and syringe administration of *P. falciparum* sporozoites.

Introduction

A considerable effort is now being made to develop a malaria vaccine based on live *Plasmodium falciparum* sporozoites [1,2]. This initiative is based on the fact that immunization of volunteers by bites of mosquitoes infected with irradiated or live *P. falciparum* sporozoites induces sterile and sustained protection [3,4,5,6,7]. One of the challenges to translate this successful protection into a practically applicable technology is replacement of mosquitoes by needle and syringe. Overcoming this challenge will require optimization of the route and method of sporozoite administration to ensure successful infection and protection [2].

In the first clinical trial with radiation attenuated purified, cryopreserved *P. falciparum* sporozoites, the PfSPZ Vaccine was administered intradermally (ID) or subcutenuously (SC) and immunogenicity and protective efficacy were sub-optimal [2]. Parallel and other studies in mice and non human primates (NHPs) demonstrated that intravenous (IV) inoculation of sporozoites was significantly more efficient in inducing antibody and T cell responses and/or protective immunity than ID or SC administration of fresh or purified, cryopreserved sporozoites [2,8]. Based on these results a clinical trial of the PfSPZ Vaccine administered IV is underway.

However, it is clearly preferable if non-IV administration could be made as efficient as IV administration. Comparing ID and IV immunizations using bioluminescent *P. berghei* sporozoites and *in vivo* imaging in mice, we recently demonstrated a clear association between the capacity to induce protective efficacy and the degree of liver infection with increased protective efficacy with higher liver loads [9]. In this study, we used this *in vivo* imaging model as a fast-track technical platform to pursue a systematic and stepwise selection process to study the effects of route of administration, number of injections and location and volume of sporozoite injection on subsequent parasite liver infection. The results were corroborated by infection studies using blood stage parasitaemia as the outcome variable.

Material and Methods

Experiments with bioluminescent *P. berghei* and *P. yoelii* sporozoites

Mice and parasites

Female C57BL/6J and BALB/c mice, eight weeks of age, were purchased from Elevage Janvier (France). All studies were performed according to the regulations of the Dutch "Animal On Experimentation act" and the European Directive 2010/63/EU. Mice were housed in the presence (except experiment in Fig. 2) of a treadmill. Approval was obtained from the Radboud University Experimental Animal Ethical Committee (RUDEC 2010-229). In this study we used the previously described transgenic *P. berghei* line 676m1cl1 line (*Pb*GFP-Luc$_{con}$) [10,11] and the transgenic *P. yoelii* line 1971 cl1 (*Py*GFP-Luc$_{con}$) [12].

Mosquito infection and preparation of sporozoites

Sporozoites were obtained by hand-dissection of the salivary glands of infected female *A. stephensi* mosquitoes 21 days (*P. berghei* at 21 °C) or 17 days (*P. yoelii* at 24 °C) after infected blood meal feeding. Salivary glands were collected in DMEM supplemented with 1% human serum albumin (Albuman) and homogenized in a homemade glass grinder. The free sporozoites were counted in a Bürker-Türk counting chamber using phase-contrast microscopy.

Injection of sporozoites

Prior to administration of sporozoites, mice were anesthetized using isoflurane and the site of injection was shaved (SC, ID, IM) in order to optimize the precision of administration. Sporozoites were administered by IV injection (200 µL in the tail vein), or by SC, ID or IM injection in various volumes and at distinct locations. All groups of mice (5 mice per group) were infected with a total of $5x10^4$ *P. berghei* or 1-2 $x10^4$ *P. yoelii* sporozoites. SC, ID and IM injections were administered in a single or multiple (4 times) injections at both lateral sites (e.g both thighs). The volume per injection site ranged from 50 to 1 µL. Injection of high volumes (50 µL) was performed using a 27 gauge needle and 1 ml syringe (BD); low volumes (10-1 µL) were injected using a 35 beveled gauge needle and a NanoFil syringe (World Precision Instruments).

Real-time *in vivo* imaging of liver stage development

At various time points post injection of sporozoites, luciferase activity was visualized through imaging of whole bodies using the *in vivo* imaging system Lumina (Caliper Life Sciences, USA) as described previously [11] with minor adaptations. Briefly, animals were anesthetized using the isoflurane-anesthesia system, their abdomens were shaved and D-luciferin dissolved in PBS (150 mg/kg; Caliper Life Science, Belgium) was injected SC (in the neck). Animals were kept anesthetized during the measurements, which were performed 4 minutes after the injection of D-luciferin. Bioluminescence imaging was acquired with a 10 cm field of view,

medium binning factor and an exposure time of 180 or 300 seconds (based on the number of mice per experiment). The color scale limits were set automatically and the quantitative analysis of bioluminescence was performed by measuring the luminescence signal intensity using the region of interest (ROI) settings of the Living Image 3.2 software. The ROI was set to measure the abdominal area at the location of the liver. ROI measurements are expressed in total flux of photons. Statistical analysis was performed by Kruskal-Wallis and subsequent individual comparisons were performed by a Dunn's multiple comparisons test using the GraphPad Prism 5.0 software.

Experiments with wildtype cryopreserved *P. yoelii* sporozoites

Mice and parasites

Four to six week-old HSD:ICR (CD-1®) mice (Harlan Bioproducts, Indianapolis, IN) infected with *P. yoelii* (clone 1.1) [13] were used to infect five day-old heat-selected female *A. stephensi* mosquitoes. Six to eight week old BALB/c mice were used for assessment of sporozoite infectivity. The IACUC committee of the University of Maryland (UMD), (College Park, Maryland) approved experiments with mice used to generate stocks of cryopreserved *P. yoelii* sporozoites and assessment of their infectivity described in this study. UMD's animal facility at Rockville was used to house the mice and all experiments were conducted at UMD.

Preparation of sporozoites

After a 15 minute feed on infected HSD:ICR mice, mosquitoes were maintained for 14–17 days at 24 °C to allow for sporozoite development. Infected mosquito salivary glands were hand dissected into M-199 medium supplemented with 1% human serum albumin (HSA). PySPZ were released from salivary glands by multiple passages through a 1 mL syringe fitted with a 26½ gauge needle and purified by a proprietary method used in purification of the PfSPZ in the PfSPZ Vaccine [1]. PySPZ were cryopreserved as for the PfSPZ Vaccine [2], and stored in liquid nitrogen vapor phase until use. All experiments were performed with cryopreserved PySPZ from one lot.

Injection of sporozoites

Mice were injected ID in the upper thigh either at a single or multiple sites with cryopreserved PySPZ reconstituted in volumes as indicated in the description of results. Infections in mice were determined by examining Giemsa-stained thin blood smears (at 1000× magnification) for the presence of blood stage parasites on days 7 and 14 after infection.

Results

Comparison of parasite liver load following IV, IM, SC, and ID administration of *P. berghei* sporozoites.

First, we studied the effect of different routes of administration on parasite liver load. Mice were injected with *Pb*GFP-Luc$_{con}$ sporozoites by IV injection (200µL) in the tail, or by IM, ID and SC injection (50µL) in each thigh. IV injection resulted in significantly higher (approximately 50 fold) liver loads compared to ID and SC injection. IM injection gave 2-3 fold higher liver loads compared to ID or SC injection ($p<0.05$) at each time point (Fig. 1). The liver load after IM injection was approximately 5% ($p<0.01$) of the liver load post IV injection. Thus, IV injection resulted in a 20-fold increase in liver load as compared to IM and 40-60 fold increase in liver load as compared to ID or SC administration.

We next explored the effect of the location of sporozoite injection on sporozoite invasion and development in the liver. Sporozoites were injected IM or ID at two and four different locations, respectively. Since SC and ID injection of sporozoites showed similar results , SC administration was not further included in subsequent experiments. The location of sporozoite injection was of minor influence on the parasite liver load (Fig. S1). ID administration always resulted in lower parasite liver loads as compared to IM administration.

Effect of injection volume on parasite liver load.

To next assess the influence of injection volume, mice were inoculated IM and ID with sporozoites delivered in different volumes (50µL, 10µL and 1µL). A decrease of injection volume increased the liver load after IM and ID sporozoite injection (Fig. 2A-C). Although there was a tendency to higher infection rates, the differences in parasite liver loads following IM injection in various volumes did not reach statistical significance ($p=0.10$). In contrast, ID injection in a low (1µL) injection volume resulted in a significantly higher liver load compared to a high (50µL) injection volume administered in both the upper front leg ($p<0.01$) and the ear ($p<0.05$). In this particular experiment, IM injection did not result in higher parasite liver loads compared to ID injection; possibly due to the omission of a treadmill in the cage.

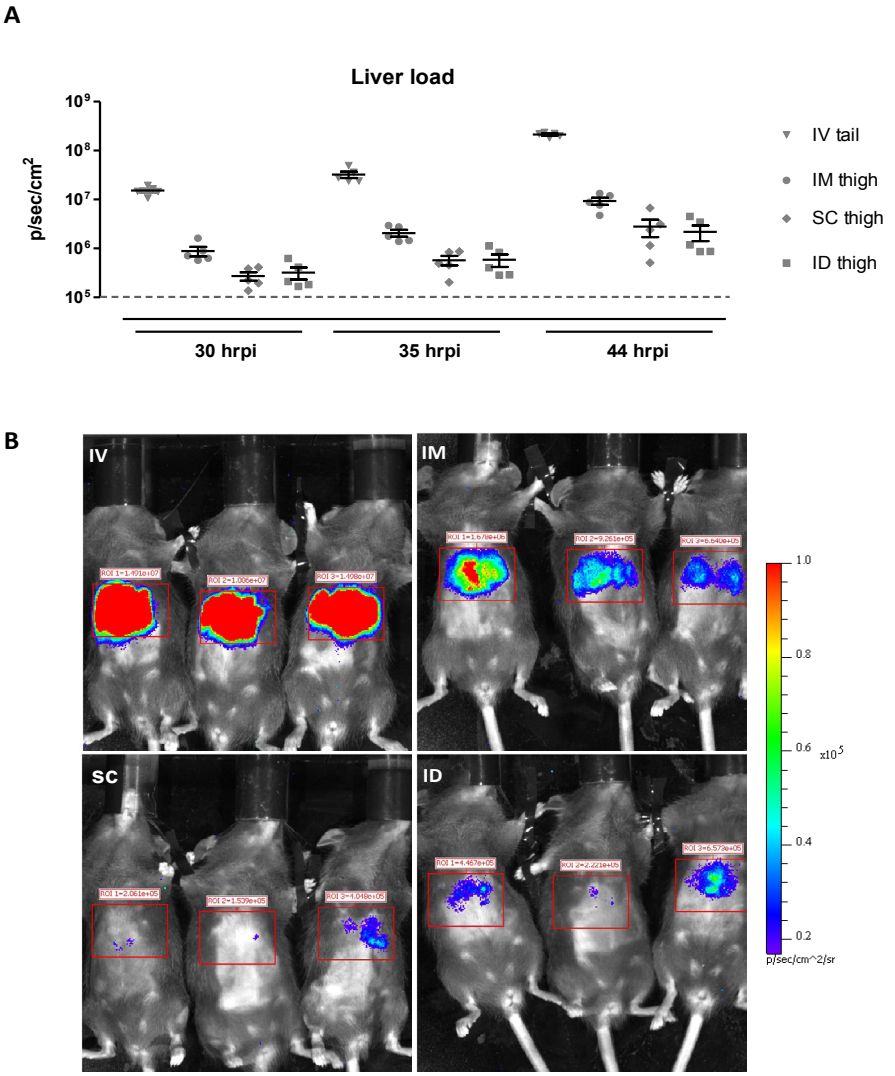

Figure 1: Liver loads following IV, IM, SC and ID administration of *P. berghei* sporozoites.
Liver loads in C57Bl/6 mice were determined by real-time *in vivo* imaging of luminescence signals in mice injected with 5x10^4 *Pb*GFP-Luc$_{con}$ sporozoites by IV injection (200µL) in the tail or IM, SC, or ID injection (50µL) in the thigh (n=5 per group). Measurements were performed at 30, 35 and 44 hours post infection and liver loads are presented as luminescent intensities (photons/sec/cm2) of the ROI's overlaying the livers from individual mice measured for 300 seconds. The dotted line represents the mean (threshold) luminescent signal of uninfected mice. In **A** the liver loads are shown and in **B** representative rainbow images of luminescence signals in C57BL/6 mice at 30 hours post infection. Mice received an IV (upper left corner), IM (upper right corner), SC (lower left corner) or ID (lower right corner) injection. Luminescence scales are set to match the scale in ID injected mice.

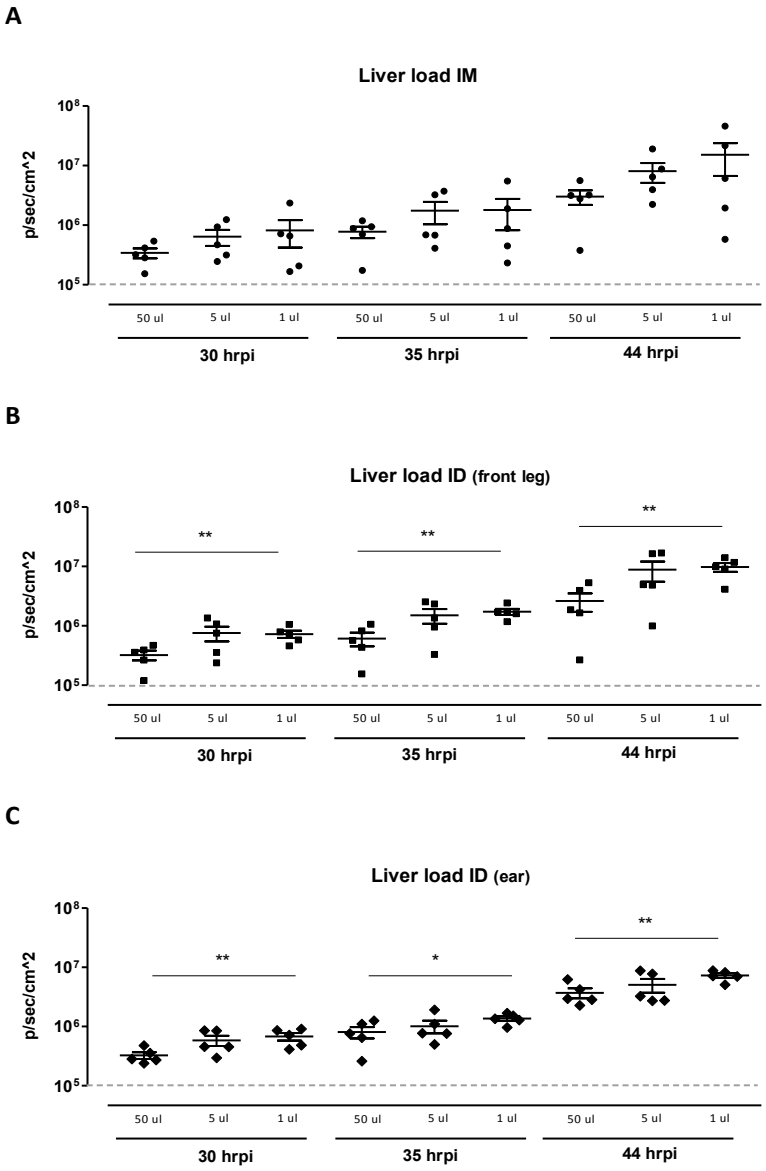

Figure 2: Liver loads following IM and ID injection of different volumes of sporozoite suspensions.

Liver loads in C57Bl/6 mice were determined by real-time *in vivo* imaging of luminescence signals in mice injected with 5x10^4 *Pb*GFP-Luc$_{con}$ sporozoites in different volumes (50, 5 and 1µL) by **A)** IM or **B+C)** ID injection (n=5 per group), at 30, 35 and 44 hours post infection. Liver loads are presented as luminescent intensities (photons/sec/cm2) of the ROI's overlaying the livers from the individual mice measured for 180 seconds. The dotted line represents the mean (threshold) luminescent signal of uninfected mice. *P <0.05, ** P<0.01

Effect of number of injections on parasite liver load.

Next, mice were IM inoculated with sporozoites delivered by a single or multiple (4 in each upper front leg) injections of 1µL or 10µL. Multiple 1µL injections resulted in a higher liver load compared to multiple 10 µL injections ($p<0.05$) but not to a single 1µL injection ($p=0.10$). For all administration regimens (1 or 10µL in multiple or single injections), the liver load following IM administration was significantly higher compared to ID administration in multiple 1µL volumes ($p<0.05$).

To ensure that the observed differences in parasite liver load at 44 hours were not due to a delay of sporozoites reaching the liver [13] following different routes of administration, parasite distribution in the liver and blood was determined in mice 60 and 75 hours post IV, IM and ID injection (Fig. S2). After IV injection parasites were observed in the blood at 60 and 75hpi and we did not observe an unexpected increase in luminescence signals in livers at these time points after IM and ID injection. These results indicate that the route of injection is of minor influence on the time it takes for sporozoites to reach the liver and therefore quantitative differences in parasite liver load measured at 44 hour after injection do not result from a delayed liver invasion.

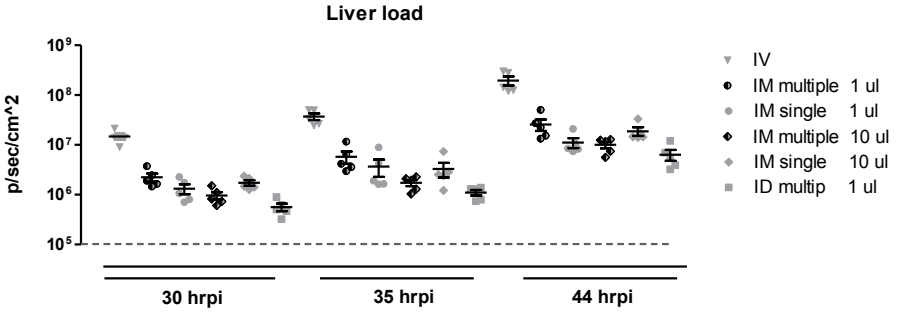

Figure 3: Liver loads following IM and ID injection of sporozoites; single injection versus multiple injections.

Liver loads in C57Bl/6 mice were determined by real-time *in vivo* imaging of luminescence signals in mice injected with $5x10^4$ *Pb*GFP-Luc_{con} sporozoites by IV injection in the tail (200µL), IM in the upper front leg by single or multiple injections of 1 or 10µL and ID injection in the upper front leg by multiple injections of 1µL (n=5 per group). Measurements were performed at 30, 35 and 44 hours post infection. Liver loads are presented as luminescent intensities (photons/sec/cm2) of the ROI's overlaying the livers from mice measured for 180 seconds. The dotted line represents the mean (threshold) luminescent signal of uninfected mice.

Parasite liver load following *P. yoelii* infection.

To further study the effects of different sporozoite administration regimes, *P. yoelii* sensitive BALB/c mice were inoculated by IV, IM and ID with *Py*GFP-Luc$_{con}$ sporozoites (Fig. 4). Similar to *P. berghei*, multiple injections of *P. yoelii* sporozoites in small volumes, administered IM led to a significantly increased parasite liver load compared to ID administration ($p<0.05$). Application of a topical vasodilator (Midalgan) did not increase the parasite liver load following ID injection. IM administration of $2x10^4$ sporozoites approximated the parasite liver load of mice receiving $1x10^4$ sporozoites IV, whereas for *P. berghei*, the parasite liver load after IM administration of sporozoites did not exceed 15-20% of IV (Fig. 3).

Infectivity experiments with purified, cryopreserved PySPZ.

The cryopreserved sporozoites were obtained from a wildtype *P. yoelii* XNL line which does not express a luminescent reporter protein. Therefore, infectivity of these sporozoites and effect of administration was not determined by imaging, but by measuring parasitaemia in mice injected with sporozoites. Infectivity was defined as the percentage of mice that developed a patent parasitaemia. The process of cryopreservation decreases the viability of sporozoites as compared to freshly isolated sporozoites. Although approximately 70% of the *P. yoelii* sporozoites shows membrane integrity after cryopreservation, it takes approximately 7 times as many cryopreserved sporozoites, compared to fresh sporozoites to induce a similar blood stage infection in mice after i.v. injection (Roestenberg, M, Bijker, E *et al*, in press).

At the outset we determined that infection of mice with cryo PySPZ followed a dose response with 100% of mice infected with a total of 30K cryo PySPZ injected in two sites on the thigh in a volume of 50µL each (Fig. 5 dark grey bars). The volume of 50µL and number-of-sites combination was the baseline against which all other inoculation variables were then compared. We showed that inoculation of 5,000 or 10,000 cryo PySPZ in two sites in 50µL each gave between 20% and 70% infection rates (Fig. 5, dark grey bars). In all experiments, either decreasing the volume or increasing the number of sites increased the infectivity, but only once did we achieve 100% (10,000 cryo PySPZ in four 5 µL injections), and in no case were the differences statistically significant.

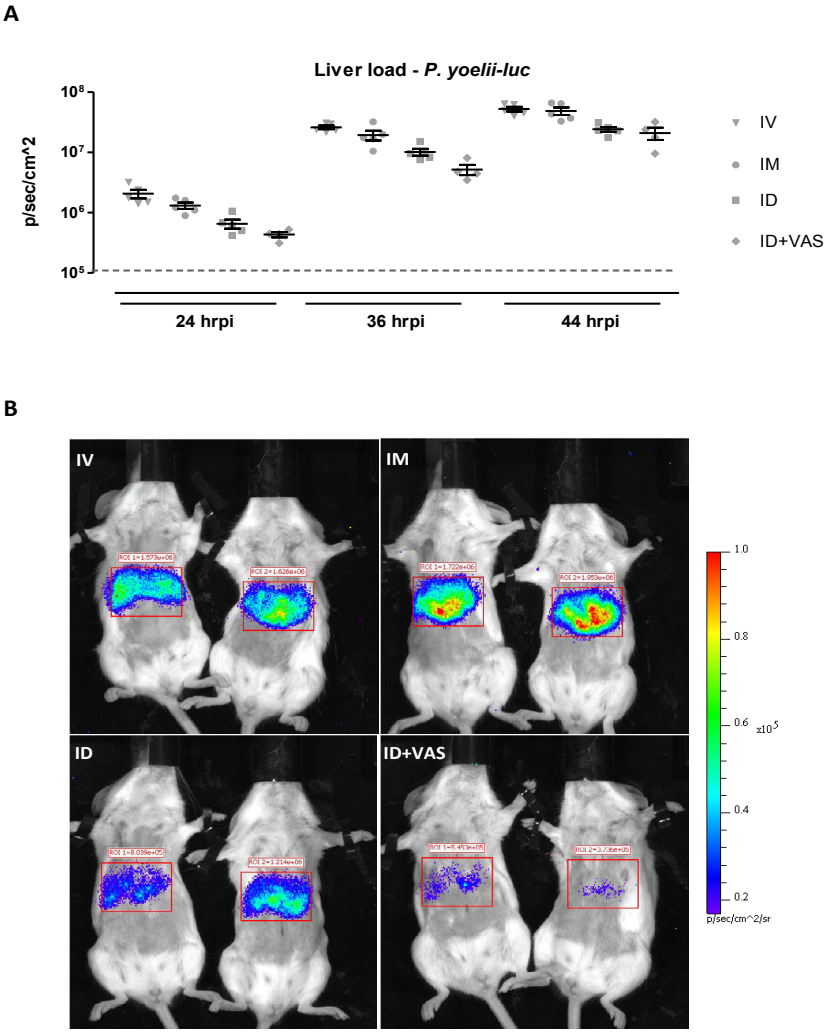

Figure 4: Liver loads following IV, IM and ID administration of *P. yoelii* sporozoites.
Liver loads in BALB/c mice were determined by real-time *in vivo* imaging of luminescence signals in mice injected with 1x10^4 *Py*GFP-Luc$_{con}$ sporozoites by IV injection in the tail (200µL) or 2x10^4 *Py*GFP-Luc$_{con}$ sporozoites by IM or ID injection in the upper front leg (n=5 per group), at 24, 36 and 44 hours post infection. IM or ID inoculation was by multiple (4 in each upper front leg) 1µL injections. Liver loads are presented as luminescent intensities (photons/sec/cm2) of the ROI's overlaying the livers from mice measured for 180 seconds. The dotted line represents the mean (threshold) luminescent signal of uninfected mice. In **A** the liver loads are shown. One group of mice (ID+VAS) received a topical vasodilator (Midalgan) prior to the ID injection. In **B** representative rainbow images of luminescence signals are shown in live BALB/c mice at 24 hours post infection. Mice received an IV (upper left corner), IM (upper right corner), ID (lower left corner) or ID+VAS (lower right corner) injection. Luminescence scales are set to match the scale in ID+VAS injected mice.

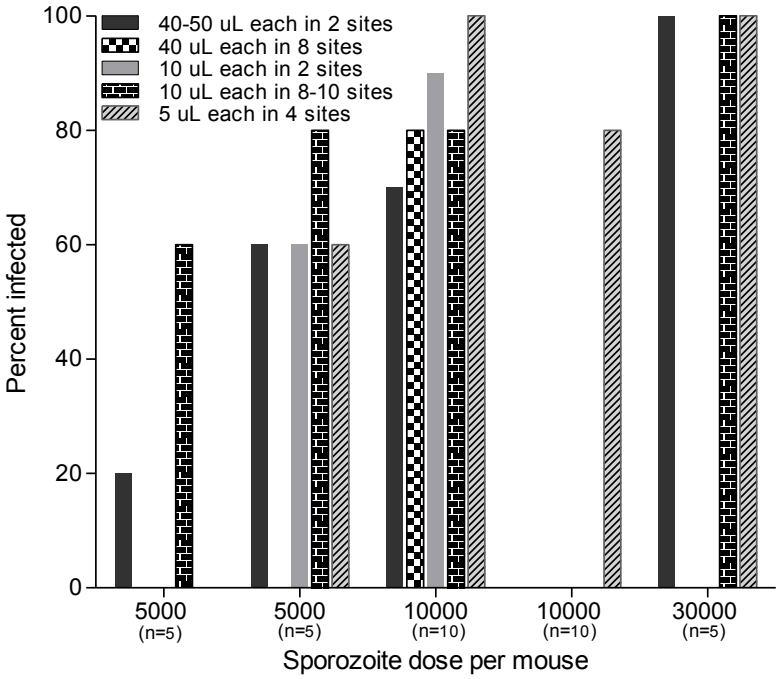

Figure 5: Effect of volume of inoculum and multiplicity of injection sites on infectivity of cryopreserved *P. yoelii* sporozoites (cryo PySPZ) in BALB/c mice.

Mice were infected with cryo PySPZ suspensions, in several volume/numbers of site combinations. A single batch of cryo PySPZ was used for all experiments. Infectivity is defined as the percentage of mice that developed a patent blood parasitemia. Dark grey = 50 µL each in 2 sites, checkerboard = 40 µL each in 8 sites, light grey = 10 µL each in 2 sites, brick stone = 10 µL each in 8-10 sites, diagonal hatch = 5 µL in 4 sites. Due to biological variability in infectivity readouts each single experiment is denoted as a distinct group of data, with all points within a group being directly comparable. All experiments did not include all tested volume/number of injection sites combinations. Group 1 and group 2 were two independent experiments both using 5000 cryo PySPZ per mouse, and likewise group 3 and group 4 both used 10000 cryo PySPZ per mouse. The number of animals per treatment in each experiment are denoted below the x-axis labels.

The effect of increasing the number of inoculation sites from 2 to 8 while keeping the volume constant (40µL) resulted in a marginal increase in infectivity from 70% to 80% with 10K cryo PySPZ (Fig. 5 checkerboard bar). Decreasing the volume alone (from 50µL to 10µL), while injecting in 2 sites showed no difference with 5K cryo PySPZ, but resulted in more mice being infected with 10K cryo PySPZ (90% compared to 70%, light grey bars). While decreasing volume or increasing the number of inoculations independently gave better outcomes, combining the two variables (10µL injections in 8-10 sites, brick stone bars) consistently improved

infectivity of mice compared to a 50µL x 2 regimen across all dose ranges. Using 5µL injections in 4 sites gave the best outcome with 10K cryo PySPZ (100% infection, diagonal hatch bars), but was not as good as the 10µL x 8 regimen with 5K PySPZ. In summary, the highest infectivity was obtained with cryo PySPZ inoculated in 5-10 µL volumes over 4 – 10 sites. To be able to show significant differences we may have to decrease the number of cryo PySPZ further.

Discussion

In *P. berghei* and *P. yoelii* models our data demonstrate that multiple variables significantly influence parasite liver loads after administration of sporozoites by needle and syringe. Firstly, IM administration of sporozoites resulted in higher parasite liver loads compared to either ID or SC administration. Secondly, the use of smaller inoculation volumes of sporozoite suspensions increased efficiency of infection that was further improved when the sporozoite suspensions were applied as multiple injections over multiple sites.

As previously reported, IM immunization with attenuated *P. berghei* sporozoites induces stronger protective immune responses compared to SC [8,14], IP [15] and ID immunizations [8,15]. Protection was, however, always less than 50% and inferior to IV immunizations. These combined results corroborate our previous notion that higher parasite liver loads while dependent on the route of sporozoite immunization are associated with superior protection [9]; after IV administration, the IM route results both in the highest parasite liver loads and strongest protective immune responses. The relative contribution of sporozoites that have not invaded the liver, but are cleared in the skin, lymph nodes or spleen, to total protective immunity remains to be determined. Following ID injection many sporozoites likely remain in the dermis and in *P. yoelii* these sporozoites can prime the first cohort of CD8+ T cell responses in the draining lymph nodes [16]. The role in immune priming/suppression mediated by sporozoites in the skin, remains to be elucidated and will have considerable impact on studies on anti-*Plasmodium* vaccines based on attenuated sporozoite. However, it is quite clear that it requires far fewer sporozoites to achieve high level protective immunity when the sporozoites are injected IV as compared to ID or SC [2]. Thus, regardless of what immunity may be induced in the skin and draining lymph nodes it is not as potent as that induced in the central compartment, which include liver, spleen and draining lymph nodes.

Density of the vascular bed in the skin or muscle may well influence the exit of sporozoites [17] and may explain the higher liver loads observed after IM compared

to ID injection. Interestingly, the effect of vasodilatation and increased blood flow was illustrated in one experiment in which the treadmill was omitted from the mice cage; in that latter case parasite liver load following IM injection was not superior to ID injection. This suggests that muscle exercise and subsequent increased blood flow may have a positive effect on sporozoite egress from the IM injected site. Nevertheless, application of a topical vasodilator (Midalgan) did not increase the parasite liver load subsequent to ID sporozoite injection.

The relationship among IV, IM, and ID infections was similar for *P. yoelii* and *P. berghei*. Nonetheless, IM and ID injection of *P. yoelii* parasites more closely approximated the liver load following IV injection compared to *P. berghei*, indicating that *P. yoelii* sporozoites are more efficient in establishing liver infections. The infectivity of *P. yoelii* sporozoites might more closely resemble that of *P. falciparum* than *P. berghei* [18]. While one cannot directly compare the infectivity of *P. yoelii* and *P. falciparum*, our preliminary data from human studies (Roestenberg, M, Bijker, E *et al*, in press) indicate that when administered by the intradermal route, *P. yoelii* and *P. falciparum* have similar infectivity. Therefore, our findings suggest that *P. yoelii* may be good indicators for clinical *P. falciparum* sporozoite administration studies.

Future (pre-) clinical studies with needles, and indeed with newly developed devices, delivering sporozoites at the various sites at the best formulation (e.g. multiple injections, low injection volume) will be important to further optimize the infection rates that then engender the greatest protective immunity.

Different injection volumes and number of sites did not show such distinct outcomes on asexual erythrocytic stage infections as on liver loads. This is likely due to the reduced sensitivity to detect differences in blood stage infections between study groups, since one sporozoite can lead to an asexual stage infection. However, in general these experiments also suggest that decreasing volume and increasing the number of sites will increase infection rates.

P. falciparum sporozoites are the only immunogens that have ever been shown to induce sustained (at least 28 months), high level (>90%) protection against controlled human malaria infection in humans [6,7]. Thus, there is now a major effort to develop whole *P. falciparum* sporozoite vaccines. The first challenge addressed was how to manufacture the aseptic, purified, cryopreserved, potent *P. falciparum* sporozoites (PfSPZ) required for such vaccines [19]. This challenge has been overcome [1,2]. The second major challenge is to determine how to optimally administer such sporozoites [19]. There is no question that IV administration of

P. falciparum sporozoites is the best route and thus far non-IV administration has been far less efficient and effective [2]. Recently, the first clinical trial demonstrated that human volunteers can be successfully infected with graded numbers of aseptic, purified, cryopreserved PfSPZ, a product called PfSPZ Challenge, by ID administration (Roestenberg, M, Bijker, E *et al*, in press). However, the administration strategy needs to be further optimized. Our rodent malaria model system developed to quantify *in vivo* the magnitude of the effects of varying administration variables on *in vivo* liver stage infection, will be used to guide the clinical development plan of PfSPZ Challenge. Clinical trials are now planned to assess the effect of route, volume, and number of sites on infection rates in humans, and thereby accelerate whole sporozoite vaccine development against malaria.

Acknowledgments

We would like to thank Claudia Lagarde, Alex Inacio, Iris Lamers-Elemans, Nynke Tichelaar and Séverine Chevalley for the technical assistance with the *P. berghei* and *P. yoelii* infections and Jolanda Klaassen, Laura Pelser-Posthumus, Astrid Pouwelsen and Jacqueline Kuhnen for the breeding of the mosquitoes. In addition we thank Aderonke Awe for her technical assistance with experiments involving cryopreserved *P. yoelii* parasites, Meta Roestenberg for helpful discussions and Anja Scholzen for critical revision of the manuscript.

References

1. Hoffman SL, Billingsley PF, James E, Richman A, Loyevsky M, et al. (2010) Development of a metabolically active, non-replicating sporozoite vaccine to prevent Plasmodium falciparum malaria. Hum Vaccin 6: 97-106.
2. Epstein JE, Tewari K, Lyke KE, Sim BK, Billingsley PF, et al. (2011) Live attenuated malaria vaccine designed to protect through hepatic CD8 T cell immunity. Science 334: 475-480.
3. Rieckmann KH, Carson PE, Beaudoin RL, Cassells JS, Sell KW (1974) Letter: Sporozoite induced immunity in man against an Ethiopian strain of Plasmodium falciparum. Trans R Soc Trop Med Hyg 68: 258-259.
4. Hoffman SL, Goh LM, Luke TC, Schneider I, Le TP, et al. (2002) Protection of humans against malaria by immunization with radiation-attenuated Plasmodium falciparum sporozoites. J Infect Dis 185: 1155-1164.
5. Clyde DF, Most H, McCarthy VC, Vanderberg JP (1973) Immunization of man against sporozite-induced falciparum malaria. Am J Med Sci 266: 169-177.
6. Roestenberg M, McCall M, Hopman J, Wiersma J, Luty AJ, et al. (2009) Protection against a malaria challenge by sporozoite inoculation. N Engl J Med 361: 468-477.
7. Roestenberg M, Teirlinck AC, McCall MB, Teelen K, Makamdop KN, et al. (2011) Long-term protection against malaria after experimental sporozoite inoculation: an open-label follow-up study. Lancet 377: 1770-1776.
8. Douradinha B, van Dijk MR, Ataide R, van Gemert GJ, Thompson J, et al. (2007) Genetically attenuated P36p-deficient Plasmodium berghei sporozoites confer long-lasting and partial cross-species protection. Int J Parasitol 37: 1511-1519.
9. Nganou-Makamdop K, Ploemen I, Behet M, van Gemert GJ, Hermsen C, et al. (2012) Reduced Plasmodium berghei sporozoite liver load associates with low protective efficacy after intradermal immunization. Parasite Immunol.
10. Janse CJ, Franke-Fayard B, Mair GR, Ramesar J, Thiel C, et al. (2006) High efficiency transfection of

Plasmodium berghei facilitates novel selection procedures. Mol Biochem Parasitol 145: 60-70.
11. Ploemen IH, Prudencio M, Douradinha BG, Ramesar J, Fonager J, et al. (2009) Visualisation and quantitative analysis of the rodent malaria liver stage by real time imaging. PLoS One 4: e7881.
12. Lin JW, Annoura T, Sajid M, Chevalley-Maurel S, Ramesar J, et al. (2011) A novel 'gene insertion/marker out' (GIMO) method for transgene expression and gene complementation in rodent malaria parasites. PLoS One 6: e29289.
13. Weiss WR, Good MF, Hollingdale MR, Miller LH, Berzofsky JA (1989) Genetic control of immunity to Plasmodium yoelii sporozoites. J Immunol 143: 4263-4266.
14. Kramer LD, Vanderberg JP (1975) Intramuscular immunization of mice with irradiated Plasmodium berghei sporozoites. Enhancement of protection with albumin. Am J Trop Med Hyg 24: 913-916.
15. Spitalny GL NR (1972) Effects of various routes of immunization and methods of parasite attenuation on the development of protection against sporozoite-induced rodent malaria. . Mil med 39: 506-514.
16. Chakravarty S, Cockburn IA, Kuk S, Overstreet MG, Sacci JB, et al. (2007) CD8+ T lymphocytes protective against malaria liver stages are primed in skin-draining lymph nodes. Nat Med 13: 1035-1041.
17. Yamauchi LM, Coppi A, Snounou G, Sinnis P (2007) Plasmodium sporozoites trickle out of the injection site. Cell Microbiol 9: 1215-1222.
18. Doolan DL, Hoffman SL (2000) The complexity of protective immunity against liver-stage malaria. J Immunol 165: 1453-1462.
19. Luke TC, Hoffman SL (2003) Rationale and plans for developing a non-replicating, metabolically active, radiation-attenuated Plasmodium falciparum sporozoite vaccine. J Exp Biol 206: 3803-3808.

Supplementary Information

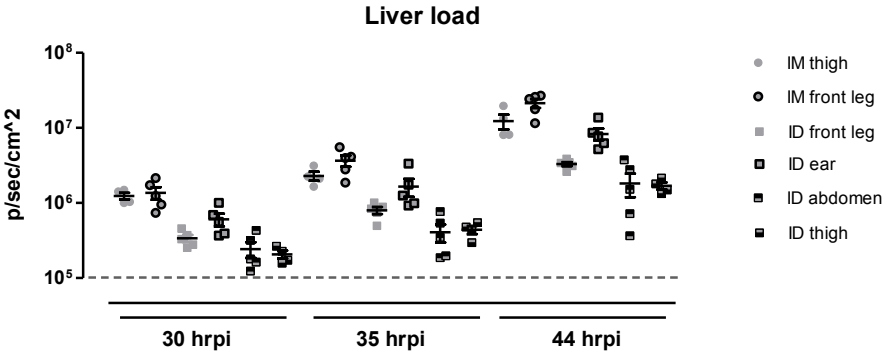

Supplementary Figure 1: Influence of location of sporozoite injection on liver infection.
Liver loads in C57Bl/6 mice were determined by real-time *in vivo* imaging of luminescence signals in mice injected with $5*10^4$ *Pb*GFP-Luc_{con} by IM or ID injection at different locations (n=5 per group). Measurements were performed at 30, 35 and 44 hours post infection. Liver loads are presented as luminescent intensities (photons/sec/cm2) of the ROI's overlaying the livers from mice measured for 300 seconds. The dotted line represents the mean (threshold) luminescent signal of uninfected mice.

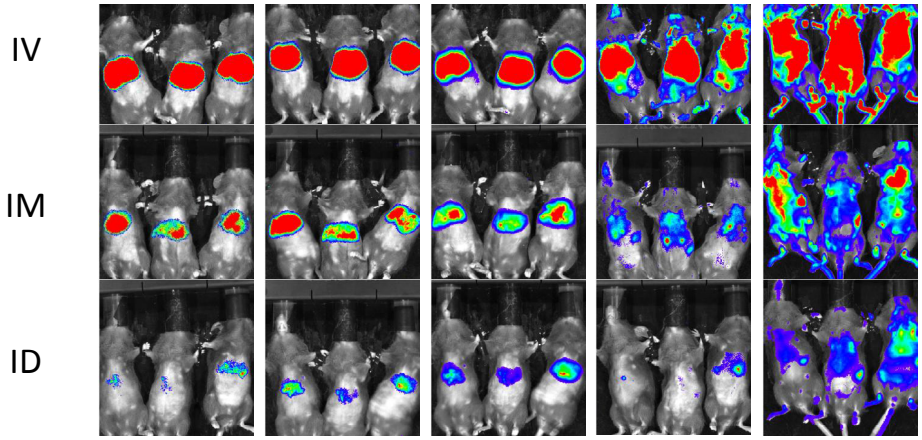

Supplementary Figure 2: Parasite development overview (IV, IM and ID).
Rainbow images of luminescence signals in C57BL/6 mice at various time points post administration of sporozoites by IV, IM (multiple injections, 1µL volume) and ID (multiple injections, 1µL volume) routes. Luminescence scales in figures representing IV and IM injected mice are set to match the scale in ID injected mice for each time point.

Chapter 9

General Discussion

A vaccine against malaria and specifically against P. falciparum infection is pressingly needed. In human volunteers, life sporozoites are the only immunogens that, by immunization with mosquito bites, have ever been shown to induce sustained and high levels of protection against a malaria infection. The GAP vaccine approach is considered the safest and best option for a life sporozoite vaccine. At the outset of this thesis we aimed at developing tools for the quantification of liver stage murine malaria parasites that could be used to address two essential criteria for the development of a GAP vaccine; GAP safety and efficacious delivery of sporozoites. We have created and characterized luminescent P. berghei parasites to test the safety of various GAPs, which eventuated in the development and characterization of a fully safe murine GAP with multiple gene deletions, full protective efficacy and an ortholgue in P. falciparum. The safety of the P. falciparum GAP is currently assessed. Efficacious vaccination of human volunteers with future GAP will be dependent on the protective effect of the sporozoite inoculum. With the aid of luminescent murine malaria sporozoites we studied the effect of varying administration variables on in vivo liver stage infection. The results are now used to guide the clinical development plan of whole sporozoite vaccination.

Assessment of parasite liver load by luciferase expressing parasites.

A quantitative analysis of the liver stage of *Plasmodium* parasites has long been subject to time-consuming and costly techniques with low sensitivity. Malaria parasites expressing bioluminescent reporters have greatly simplified the quantification of the parasite liver stage. In this thesis we have made extensive use of a transgenic *P. berghei* parasite, *Pb*GFP-Luc$_{con}$ expressing the bioluminescent reporter protein luciferase, allowing for a direct quantification and visualization of the parasites in both *in vitro* hepatocyte cultures and whole bodies of live mice **(Chapter 2)**.The impact of this transgenic parasite and the novel possibilities it offers malaria research are broad. *Pb*GFP-Luc$_{con}$ parasites can be used to evaluate the immunity against malaria in both *in vitro* and *in vivo* models **(Chapter 3).** Incorporated in the genome of a GAP the bioluminescent reporter can be used to provide *in vivo* real-time information on the (lack of) parasite liver stage development **(Chapter 4, 6 and 7)**. Moreover, these transgenic parasites were used to study the liver load following sporozoite administration by different routes and injection variables **(Chapter 8 and 9)**. Others have used *Pb*GFP-Luc$_{con}$ parasites to characterize important features of the parasite such as the development of *P. berghei* in the skin at ultra low frequencies [1] and the preclusion of a liver stage superinfection in the presence of an asexual parasitemia [2].

The *Pb*GFP-Luc$_{con}$ parasites can be used to assess the effects of anti-malarial drugs on the parasite liver stage. With an increasing resistance of *Plasmodium* for the currently available anti-malarials directed [3] there is a pressing need for replacement drugs [4]. New drugs against the liver stage have a tactical advantage over blood stage drugs as the relatively low number of parasites in the liver stage might delay the development of resistance [5]. Moreover, new drugs directed against the liver stage might also kill the hypnozoites of *P. vivax*, responsible for recurrent blood stage infections. At present, the only drug that is known to act on these hypnozoites is primaquine, which unfortunately causes hemolytic anemia in patients with glucose-6-phospate dehydrogenase deficiency [6] attesting yet again the need for new liver stage drugs. Already, the *Pb*GFP-Luc$_{con}$ parasite has been used in high throughput drug screens [7] and was instrumental in the characterization of potential new anti-malarial drugs like Primaquine-Artemisinin hybrids [8], Halofuginone [9] and Decoquinate [10].

Notwithstanding these applications, the *in vivo* visualization of parasites in the liver can be further optimized. Both the transgenic *P. berghei* and *P. yoelii* parasites used in this thesis (*Pb*GFP-Luc$_{con}$ and *Py*GFP-Luc$_{con}$ respectively) express the bioluminescent

reporter under control of the eef1α promoter [11,12], which allows for the *in vivo* visualization of mature liver schizonts. Transgenic parasites which express luciferase under the control of other promoters might facilitate *in vivo* parasite visualization throughout the whole liver stage. Analysis of a transgenic *P. berghei* parasite that expresses luciferase under the control of the promoter of the circumsporozoite protein, enabled the *in vivo* detection of sporozoites in the skin at the site of mosquito bite measured directly after mosquito feeding. Nonetheless, we were unable to detect sporozoites in the liver by *in vivo* imaging [11]. Next generation transgenic parasites that express (a stronger) luciferase under the control of for instance the HSP70 promoter, might allow for a more continuous visualization throughout the liver stage.

While the application of luciferase expressing rodent malaria parasites has been broadly assessed, a transgenic luminescent *P. falciparum* parasite (*Pf-luc*) has not yet been described. *Pf-luc* can possibly enable the visualization of the liver stage in humanized mice engrafted with human hepatocytes [13]. This could open up new opportunities to study the effect of anti-malarial drugs. Moreover, *Pf-luc* could be used in the evaluation of immunity against a *P. falciparum* infection. Most of the broadly used immunological techniques in clinical malaria research are descriptive and do not provide functional information. Routinely used sporozoite ELISA's and IFATs cannot make a distinction between antibody binding and functional neutralizing responses. Similarly, assessment of cellular responses in immunized human volunteers is most often descriptive and a functional characterization of for instance the cytotoxic effect of CD8 T cells on infected hepatocytes is lacking. A transgenic sporozoite neutralization assay (**Chapter 3**) could be easily adapted to meet the perquisites for *Pf-luc* parasites. Hepatocytes derived from the Rhesus macaque can be infected with [14] and allow full development (unpublished data) of *P. falciparum* parasites. Following pre-incubation with plasma from immunized human volunteers developing *Pf-luc* sporozoites can be easily quantified in (frozen) rhesus hepatocytes. In the future, adoptive transfer of immune cells from immunized volunteers into an immunodeficient humanized mice, infected with *Pf-luc*, would possibly allow for a direct quantification of the cytotoxic effect of these immune cells on the infected hepatocytes. Near-infrared fluorescent imaging of the adoptively transferred immune cells can possibly allow for a live visualization of infected human hepatocyte killing.

The hunt for a Genetically Attenuated Parasite malaria vaccine.

In this dissertation the *P. berghei* GAP *Δp52+p36, Δb9, Δfabb/f* and *Δ(b9)slarp* are

thoroughly tested for their safety and conferred protective efficacy following immunization. Based on a complete arrest of *P. yoelii* and *P. falciparum Δp52+p36* GAP in the liver [15,16], it was considered the leading GAP vaccine candidate. In **chapter 4** we show that in the *P. berghei* model *Δp52+p36* are able to generate a blood stage infection. Moreover, we provide evidence that low numbers of *Δp52&p36 P. falciparum* sporozoites, develop into replicating liver stages. *Δb9* parasites arrest in the liver stage at a nearly similar time point and, alike *Δp52&p36* these parasites are capable of developing into replicating *P. berghei* liver schizonts in very low numbers **(Chapter 6)**. As described for *P. berghei Δp52&p36* GAP **(Chapter 5)**, *P. berghei Δb9* liver schizonts develop in the absence of an apparent PVM **(Chapter 6)**. The exact mechanism by which *P. berghei Δp52&p36* and *Δb9* enter the hepatocyte and start replicating in the absence of an apparent PVM remains elusive. Supposedly, these parasites develop by means of an undisclosed non-conventional pathway which is present in wildtype parasite. Just like intranuclear replicating *P. yoelii* and *P. falciparum* parasites which are deprived of a PVM [17], cytosolic replicating *P. berghei Δp52&p36* might arise from sporozoites that start developing following an arrest after hepatocyte transmigration. Nevertheless, the difference between a sporozoite that invades the hepatocyte in the absence of a PVM and one that arrests in the hepatocyte upon transmigration might be a matter of semantics.

Despite a reported discrepancy in *P. berghei* and *P. yoelii* GAP breakthrough [15,18], it was observed that high inoculations of *P. yoelii Δp52+p36* sporozoites can result in a breakthrough infection in BALB/c mice, depending on the subtype of BALB/c mice [19]. In *P. berghei*, C57BL/6 mice were more susceptible for a *Δp52* blood stage infection compared to BALB/c mice [20]. These results, yet again, attest the importance of GAP safety assessment in multiple malaria models (i.e *P. berghei* and *P. yoelii*) and multiple mice strains before advancing into further clinical development of a GAP vaccine candidate. Corresponding the observed replicating *Δp52&p36 P. falciparum* parasite in a primary human hepatocyte culture, in a recent clinical trial others observed a blood infection in one volunteer, immunized with *Δp52+p36 P. falciparum* [19].

The late liver stage arresting GAP *Δfabb/f* completely aborts development in the *P. yoelii* model while a considerable number of mutant *P. berghei* parasites develops into a blood stage parasitemia **(Chapter 4)**. The (partial) arrest of the *Δfabb/f* GAP results from an impaired *de novo* fatty acid synthesis, which is of particular importance in late liver stage development (i.e membrane formation of merosomes) [21]. Possibly,

the discrepancy in GAP phenotype results from a difference in the length and speed of parasite liver stage maturation between the two models. The capacity to infect hepatocytes is similar for both *P. berghei* and *P. yoelii*, but the efficiency to amplify in hepatocytes is markedly different. In BALB/c mice, the *P. berghei* parasite liver load increases approximately 35 fold whereas the *P. yoelii* liver load increases over 400 fold, from 20 to 40 hours post sporozoite injection [22]. Likely, *Δfabb/f P. yoelii* parasites replicate relatively fast and fully arrest due to a complete dependence on the *de novo* fatty acid synthesis whereas *P. berghei* parasites develop somewhat slower and are less dependent on this pathway.

Our hunt for a genetically attenuated malaria vaccine has lead to the development and characterization of the *Δb9Δslarp* GAP. In *P. berghei* these mutants fully arrest in the liver stage and none develops into a mature liver schizont **(Chapter 6)**. Moreover, immunization of mice with *P. berghei Δb9Δslarp* leads to a longlived protection in mice. There is no clear advantage of using a *b9* gene deletion instead of a *p52+p36* gene deletion in the multiple attenuated GAP, other than that deletion of *b9* might result in a slightly better protection in mice **(Chapter 4 and 6)**. The generation of a quadruple attenuated *Δp52+p36Δb9Δslarp* GAP is not sensible since both *Δp52+p36* and *Δb9* parasites incidentally develop in the hepatocyte, likely by the same mechanism and there is no additive safety of a quadruple GAP over *Δb9Δslarp.* The multiple attenuated *Δb9Δslarp* GAP arrests in early liver stage and it has been argued that late liver stage arresting GAP induce superior anti-malarial immunity [23]. This superior immunity supposedly result from a more diverse set of antigens that are recognized by CD8 T cells, and potentially additional arms of the immune system reacting with multi-stage expressed antigens [23]. However, immunization of both BALB/c and C57BL/6 mice with *P. berghei* sporozoites under azithromycin or chloroquine profylaxis, which allows for full development of parasites in the liver, does not result in a superior immune response compared to immunization with RAS sporozoites [24,25], or *Δb9* sporozoites (unpublished data, Ploemen I). If results in rodents, comparing the efficacy of GAP, RAS and CPS immunization **(Chapter 6 and 7),** are in any way predictive for the outcome of future clinical trials we can rest assure; the protective efficacy conferred by CPS immunization in human volunteers is unprecedented by any malaria vaccination approach. Regardless, as long as a fully arresting late liver stage *P. falciparum* GAP is absent these considerations are of little use.

Clinical administration of a whole sporozoite vaccine

Immunization with irradiated sporozoites has since long been the point of reference for the development of an efficacious malaria vaccine. In spite of a track record of proven efficacy in rodents [26], monkeys [27]and man [28,29,30] the pursuit of a whole sporozoite malaria vaccine was largely abandoned, mainly because it was thought impractical to vaccinate people with live sporozoites. Recent progress in i) the cryopreservation of sporozoites by Sanaria Inc. [31], and ii) the development of tailor-made genetically attenuated parasites that fail to complete the liver stage [20,32] have renewed the interest in a whole sporozoite vaccine. The successful immunization of human volunteers by the bites of a mere three rounds of 15 *P. falciparum*-infected mosquitoes under chloroquine prophylaxis gave further momentum [33].

Once the phenotype of the *P. berghei Δb9Δslarp* GAP has been confirmed in the orthologue *P. falciparum* mutant, this GAP is ready to go into clinical testing. Ultimately, these sporozoites could be successfully cryopreserved [31] for later administration into humans, albeit that the efficiency of cryopreservation might be a bit low. The major challenge will be to determine how to optimally administer these sporozoites in human volunteers. Administration of *P. falciparum* sporozoites by mosquito bites and IV injection are likely effective, but these techniques are not suitable for vaccination campaigns in Sub-Saharan Africa. In a recent clinical study, SC or ID immunization with irradiated *P. falciparum* sporozoites showed suboptimal immune responses and protective efficacy [14]. In **Chapter 7** we show that the protective immunity following IV and ID *P. berghei* RAS and CPS immunization associates with an increase in parasite liver loads following sporozoite administration. These findings encouraged us to determine which variables, associated with sporozoite inoculation, could influence the parasite liver load **(Chapter 8)**. As assessed in our *Pb*GFP-Luc$_{con}$ and *Py*GFP-Luc$_{con}$ *in vivo* imaging models, multiple variables significantly influence the parasite liver loads after administration of sporozoites by needle and syringe. Multiple intramuscular injections of sporozoites in small volumes resulted in the highest parasite liver load, thereby most likely comprising the most optimal non-IV sporozoite administration. Our studies in rodent models provide rational guidance for the development of clinical trials, which are now planned to assess the effect of route, volume, and number of sites on infection rates in humans. These studies will accelerate the development of a whole sporozoite vaccine against malaria.

Future outlook and directions

Less than a decade ago, the first GAP vaccine candidates were characterized in rodent models [20,32]. Now, we have generated and characterized in a *P. berghei* model a fully arresting and protective GAP with multiple gene deletions. The phenotype of the orthologue mutant in *P. falciparum* is presently studied in primary human hepatocytes (Unpublished data Ben van Schaijk). Results from the *P. yoelii* model indicate that the development of the mutant is fully aborted in the liver [34]. Potential future immunization trials in human volunteers with *P. falciparum Δb9Δslarp* GAP will be key in determining the potential of this vaccine approach. Considering the efficiency of CPS and RAS immunization in human volunteers the prospects for a GAP immunization good. While travelers and military personal can possibly be immunized by IV inoculation with sporozoites in a clinical setting, large GAP vaccination campaigns in Africa will require non-IV delivery. There is a need for a device that is capable of delivering the sporozoites at the right perquisites. Injection systems such as needle free jet-injectors and hollow microneedle arrays might be up for the task; alternatively a device might need to be newly designed. The success of the sporozoite inoculation will largely determine the speed by which the GAP vaccine approach further evolves. Other advancements in the GAP approach can possibly be made by optimization of the sporozoite cryopreservation process.

It will require a major effort to implement a whole sporozoite vaccine strategy in the field. However, there is no time to falter since, as explained by the philosopher Thomas Pogge [35], the development of an effective malaria vaccine is not a matter of scientific bonhomie, rather is it a moral obligation.

References

1. Gueirard P, Tavares J, Thiberge S, Bernex F, Ishino T, et al. (2010) Development of the malaria parasite in the skin of the mammalian host. Proc Natl Acad Sci U S A 107: 18640-18645.
2. Portugal S, Carret C, Recker M, Armitage AE, Goncalves LA, et al. (2011) Host-mediated regulation of superinfection in malaria. Nat Med 17: 732-737.
3. White NJ (2004) Antimalarial drug resistance. J Clin Invest 113: 1084-1092.
4. Derbyshire ER, Mota MM, Clardy J (2011) The next opportunity in anti-malaria drug discovery: the liver stage. PLoS Pathog 7: e1002178.
5. Mazier D, Renia L, Snounou G (2009) A pre-emptive strike against malaria's stealthy hepatic forms. Nat Rev Drug Discov 8: 854-864.
6. Cappellini MD, Fiorelli G (2008) Glucose-6-phosphate dehydrogenase deficiency. Lancet 371: 64-74.
7. Derbyshire ER, Prudencio M, Mota MM, Clardy J (2012) Liver-stage malaria parasites vulnerable to diverse chemical scaffolds. Proc Natl Acad Sci U S A 109: 8511-8516.
8. Capela R, Cabal GG, Rosenthal PJ, Gut J, Mota MM, et al. (2011) Design and evaluation of primaquine-artemisinin hybrids as a multistage antimalarial strategy. Antimicrob Agents Chemother 55: 4698-4706.

9. Derbyshire ER, Mazitschek R, Clardy J (2012) Characterization of Plasmodium liver stage inhibition by halofuginone. ChemMedChem 7: 844-849.
10. da Cruz FP, Martin C, Buchholz K, Lafuente-Monasterio MJ, Rodrigues T, et al. (2012) Drug screen targeted at Plasmodium liver stages identifies a potent multistage antimalarial drug. J Infect Dis 205: 1278-1286.
11. Ploemen IH, Prudencio M, Douradinha BG, Ramesar J, Fonager J, et al. (2009) Visualisation and quantitative analysis of the rodent malaria liver stage by real time imaging. PLoS One 4: e7881.
12. Lin JW, Annoura T, Sajid M, Chevalley-Maurel S, Ramesar J, et al. (2011) A novel 'gene insertion/marker out' (GIMO) method for transgene expression and gene complementation in rodent malaria parasites. PLoS One 6: e29289.
13. Vaughan AM, Kappe SH, Ploss A, Mikolajczak SA (2012) Development of humanized mouse models to study human malaria parasite infection. Future Microbiol 7: 657-665.
14. Epstein JE, Tewari K, Lyke KE, Sim BK, Billingsley PF, et al. (2011) Live attenuated malaria vaccine designed to protect through hepatic CD8(+) T cell immunity. Science 334: 475-480.
15. Labaied M, Harupa A, Dumpit RF, Coppens I, Mikolajczak SA, et al. (2007) Plasmodium yoelii sporozoites with simultaneous deletion of P52 and P36 are completely attenuated and confer sterile immunity against infection. Infect Immun 75: 3758-3768.
16. VanBuskirk KM, O'Neill MT, De La Vega P, Maier AG, Krzych U, et al. (2009) Preerythrocytic, live-attenuated Plasmodium falciparum vaccine candidates by design. Proc Natl Acad Sci U S A 106: 13004-13009.
17. Silvie O, Greco C, Franetich JF, Dubart-Kupperschmitt A, Hannoun L, et al. (2006) Expression of human CD81 differently affects host cell susceptibility to malaria sporozoites depending on the Plasmodium species. Cell Microbiol 8: 1134-1146.
18. Annoura T, Ploemen IH, van Schaijk BC, Sajid M, Vos MW, et al. (2012) Assessing the adequacy of attenuation of genetically modified malaria parasite vaccine candidates. Vaccine.
19. Kappe SH (2010) Genetically engineered malaria parasite vaccine approaches: Current status. American Society of Tropical Medicine and Hygiene Meeting: Report No.: Symposium 150.
20. van Dijk MR, Douradinha B, Franke-Fayard B, Heussler V, van Dooren MW, et al. (2005) Genetically attenuated, P36p-deficient malarial sporozoites induce protective immunity and apoptosis of infected liver cells. Proc Natl Acad Sci U S A 102: 12194-12199.
21. Vaughan AM, O'Neill MT, Tarun AS, Camargo N, Phuong TM, et al. (2009) Type II fatty acid synthesis is essential only for malaria parasite late liver stage development. Cell Microbiol 11: 506-520.
22. Schmidt NW, Butler NS, Harty JT (2011) Plasmodium-host interactions directly influence the threshold of memory CD8 T cells required for protective immunity. J Immunol 186: 5873-5884.
23. Butler NS, Schmidt NW, Vaughan AM, Aly AS, Kappe SH, et al. (2011) Superior antimalarial immunity after vaccination with late liver stage-arresting genetically attenuated parasites. Cell Host Microbe 9: 451-462.
24. Friesen J, Matuschewski K (2011) Comparative efficacy of pre-erythrocytic whole organism vaccine strategies against the malaria parasite. Vaccine 29: 7002-7008.
25. Nganou-Makamdop K, van Gemert GJ, Arens T, Hermsen CC, Sauerwein RW (2012) Long term protection after immunization with P. berghei sporozoites correlates with sustained IFNgamma responses of hepatic CD8+ memory T cells. PLoS One 7: e36508.
26. Nussenzweig RS, Vanderberg J, Most H, Orton C (1967) Protective immunity produced by the injection of x-irradiated sporozoites of plasmodium berghei. Nature 216: 160-162.
27. Gwadz RW, Cochrane AH, Nussenzweig V, Nussenzweig RS (1979) Preliminary studies on vaccination of rhesus monkeys with irradiated sporozoites of Plasmodium knowlesi and characterization of surface antigens of these parasites. Bull World Health Organ 57 Suppl 1: 165-173.
28. Clyde DF, Most H, McCarthy VC, Vanderberg JP (1973) Immunization of man against sporozite-induced falciparum malaria. Am J Med Sci 266: 169-177.
29. Rieckmann KH, Carson PE, Beaudoin RL, Cassells JS, Sell KW (1974) Letter: Sporozoite induced immunity in man against an Ethiopian strain of Plasmodium falciparum. Trans R Soc Trop Med Hyg 68: 258-259.
30. Hoffman SL, Goh LM, Luke TC, Schneider I, Le TP, et al. (2002) Protection of humans against malaria by immunization with radiation-attenuated Plasmodium falciparum sporozoites. J Infect Dis 185: 1155-1164.
31. Hoffman SL, Billingsley PF, James E, Richman A, Loyevsky M, et al. (2010) Development of a metabolically active, non-replicating sporozoite vaccine to prevent Plasmodium falciparum malaria. Hum Vaccin 6: 97-106.

32. Mueller AK, Labaied M, Kappe SH, Matuschewski K (2005) Genetically modified Plasmodium parasites as a protective experimental malaria vaccine. Nature 433: 164-167.
33. Roestenberg M, McCall M, Hopman J, Wiersma J, Luty AJ, et al. (2009) Protection against a malaria challenge by sporozoite inoculation. N Engl J Med 361: 468-477.
34. Aly AS, Mikolajczak SA, Rivera HS, Camargo N, Jacobs-Lorena V, et al. (2008) Targeted deletion of SAP1 abolishes the expression of infectivity factors necessary for successful malaria parasite liver infection. Mol Microbiol 69: 152-163.
35. Pogge T (2002) World Poverty and Human Rights: Cosmopolitan Responsibilities and Reforms. Chapter 9.

Chapter 10

Summary
Samenvatting
List of publications
Dankwoord - Acknowledgments
Curriculum vitae

Summary

Malaria remains one of the most devastating infectious diseases responsible for approximately 225 million clinical cases and 750.000 deaths annually. A vaccine against malaria and specifically against *P. falciparum* infection, is pressingly needed. An infection with the malaria parasite originates from the bite of an infected mosquito, which deposits malaria sporozoites in the skin. In a controlled clinical setting, immunization with live sporozoites proved to induce sustained and high levels of protection against a homologous *P. falciparum* infection in human volunteers. This vaccine approach requires a full cessation of parasite development in the host, before the onset of a pathogenic blood stage parasitemia. By genetic modification, sporozoites can be tailor made to arrest in the liver stage. Immunization of mice with these so called genetically attenuated parasites (GAP) can lead to protection.

Work described in this thesis aimed to develop and characterize a GAP that

i) fully arrests in the liver stage with

ii) full protective efficacy in a murine *P. berghei* malaria model and

iii) a clear orthologue in *P. falciparum*

Once a GAP candidate has been developed that meets these perquisites it is essential to characterize the best route for human GAP vaccination.

This thesis additionally aimed to

iv) determine which factors are predictive for the protective efficacy conferred by different routes of sporozoite immunization

v) determine by which parameters sporozoites can best be administered in order to optimize the efficiency of human immunization.

Prior to addressing these aims, it was essential to develop and validate new tools for the quantification of liver stage parasites. In **Chapter 2** we describe a transgenic *P. berghei* parasite, *Pb*GFP-Luc$_{con}$ expressing the bioluminescent reporter protein luciferase, allowing for a direct quantification and visualization of the parasites in both *in vitro* hepatocyte cultures and whole bodies of live mice. These transgenic parasites are powerful research tools for the studies performed in subsequent chapters. In **Chapter 3** we describe the use of *Pb*GFP-Luc$_{con}$ in the evaluation of immunity against malaria, both in live mice and cultured hepatocytes. In live mice, *Pb*GFP-Luc$_{con}$ can provide quantitative information about the relation between the parasite liver load and protection against malaria in real-time. Moreover in

a cultured hepatocyte model, fast and reproducible results were obtained by introducing a transgenic sporozoites neutralization assay, measuring functional antibody-mediated immune responses.

One of the most important requisites of a GAP vaccine candidate is that it is safe; i.e does not lead to a pathogenic blood stage malaria infection. In **Chapter 4** we describe the lack of complete attenuation of two leading GAP, *Δp52+p36* and *Δfabb/f* parasites. At low frequencies, these mutant parasites fully developed inside hepatocytes leading to a blood stage infection in the murine *P. berghei* model. Moreover, replicating *Δp52+p36 P. falciparum* parasites were observed in a primary hepatocyte culture. These GAPs are therefore not safe and we proposed a minimal set of screening criteria to assess adequacy of GAP sporozoite attenuation necessary before advancing into further clinical development and studies in humans. In **Chapter 5** we studied the phenotype of developing intrahepatic *Δp52+p36 P. berghei* parasites and describe a non-conventional pathway, by which these parasites are likely capable of maturing into blood stage parasites. These *P. berghei* GAP apparently lack the need for a parasitophorous vacuole membrane (PVM) for full liver stage development. The PVM has been considered essential for parasite development and normally shields the parasite from the interior of the hepatocyte. Our findings might have implications for the development of a GAP vaccine insofar that GAPs with a gene deletion involved in the formation or maintenance of the PVM are likely unsafe. **Chapter 6** describes the development and characterization of the *Δb9* GAP. This GAP conferred sterile protection in mice and abrogated development soon after hepatocyte invasion, associated with a compromised PVM. Again however, low numbers of *P. berghei Δb9* matured in the absence of an apparent PVM. We therefore developed and characterized the multiple gene deleted *Δb9Δslarp* GAP. Immunization of both BALB/c and C57BL/6 mice with *P. berghei Δb9Δslarp* resulted in sterile and sustained protection. Also, the *Δb9Δslarp* GAP fully abrogated liver stage development in various mice strains and none of the parasites developed into the pathogenic blood stage. The orthologue mutant in *P. falciparum* has been generated and its development inside the hepatocyte will need to be assessed. If the *P. falciparum Δb9Δslarp* GAP indeed arrests in the hepatocyte alike the *P. berghei* GAP, it will likely constitute the leading GAP vaccine candidate.

In **Chapter 7** we describe the relation between the parasite liver load following sporozoite immunization and the level of protection conferred in mice. Intravenous sporozoite immunizations of both BALB/c and C57BL/6 mice resulted in a superior protection compared to intradermal immunization. The decrease in protection

was associated with a decreased parasite liver load following sporozoite injection. However, IV injection is not the preferred immunization route for large scale application in Sub-Saharan Africa. In **Chapter 8**, we therefore determined which variables, associated with sporozoite injection, influence the parasite liver load. As assessed in our *Pb*GFP-Luc$_{con}$ and *Py*GFP-Luc$_{con}$ *in vivo* imaging models, multiple variables significantly influenced the parasite liver loads after administration of sporozoites by needle and syringe. Multiple intramuscular injections of sporozoites in small volumes resulted in the highest parasite liver load, thereby most likely comprising the most optimal non-IV sporozoite administration. These data provide rational guidance for the development of clinical trials, in search of the most optimal method for sporozoite immunization and hopefully the development of a whole sporozoite vaccine against malaria.

Samenvatting

Malaria is tot op heden een van de meest verwoestende infectieziektes ter wereld. Jaarlijks worden om en nabij de 225 miljoen mensen klinisch ziek, waarbij ongeveer 750.000 mensen sterven aan de gevolgen van de ziekte. Een vaccin tegen malaria, en dan vooral tegen *P. falciparum* infecties, is daarom ook hard nodig. Een infectie met de malariaparasiet begint met de beet van een geïnfecteerde mug die malaria sporozoieten in de huid brengt. In een gecontroleerde klinische setting is het mogelijk om vrijwilligers met intacte levende sporozoieten te immuniseren. Dit zorgt voor langdurige bescherming tegen een homologe *P. falciparum* infectie in een hoog percentage van de vrijwilligers. Deze vaccinstrategie vereist een volledig tot stilstand komen van de ontwikkeling van de parasiet in de gastheer, voorafgaand aan het pathogene bloedstadium. Middels genetische modificatie kunnen sporozoieten worden gecreëerd die specifiek in de lever tot stilstand komen. Immunisatie met genetisch geattenueerde parasieten (GAP) kan leiden tot bescherming tegen malaria in muizen.

Het werk beschreven in deze thesis had tot doel een GAP te ontwikkelen en te karakteriseren welke

i) volledig tot stilstand komt in de lever

ii) volledige bescherming biedt in een muizen malariamodel (*P. berghei*)

iii) een duidelijke ortholoog heeft in *P. falciparum*.

Wanneer er een GAP kandidaat is ontwikkeld, die aan deze eisen voldoet, is het essentieel om de meest optimale route voor humane GAP immunisatie te karakteriseren.

Deze thesis doelde daarbij tevens op

iv) het bepalen van de factoren die voorspellend zijn voor de protectieve effectiviteit geïnduceerd door de verschillende routes van sporozoiet immunisatie en

v) het bepalen van de manier waarop sporozoieten het best toegediend kunnen worden teneinde de efficiëntie van de uiteindelijke immunisatie van mensen te optimaliseren.

Voordat wij ons op deze doelstellingen konden richten was het essentieel om nieuwe technieken te ontwikkelen en te valideren voor de kwantificatie van parasieten in het leverstadium. In **Hoofdstuk 2** beschrijven we een transgene *P. berghei* para-

siet, *Pb*GFP-Luc$_{con}$ welke het bioluminescente reporter eiwit luciferase tot expressie brengt. *Pb*GFP-Luc$_{con}$ maakt een directe kwantificatie en visualisatie van parasieten mogelijk in zowel een *in vitro* levercelkweek als in levende muizen. Deze transgene parasieten zijn essentieel voor de studies in de volgende hoofdstukken. In **Hoofdstuk 3** beschrijven we het gebruik van *Pb*GFP-Luc$_{con}$ in de evaluatie van immuniteit tegen malaria, zowel in levende muizen als in een *in vitro* levercelmodel. In levende muizen, kan *Pb*GFP-Luc$_{con}$ live kwantitatieve informatie verschaffen over de relatie tussen de hoeveelheid parasieten in de lever (parasieten lever load) en de bescherming tegen malaria. Deze parasieten kunnen tevens in een *in vitro* levercelmodel worden gebruikt, waarbij er snel reproduceerbare resultaten worden verkregen door de introductie van de zogenaamde transgene sporozoiet neutralisatie test, welke de functionele antilichaam-gemedieerde immuunrespons meet.

Een van de belangrijkste vereisten van een GAP vaccinkandidaat is veiligheid; d.w.z. dat de parasieten zich niet kunnen ontwikkelen tot het pathogene bloedstadium. In **Hoofdstuk 4** beschrijven we het gebrek aan veiligheid van twee GAPs, *Δp52+p36* en Δ*fabb/f* parasieten. Deze GAPs kunnen zich in zeer lage frequenties volledig ontwikkelen in de levercel en daarbij een bloedstadiuminfectie veroorzaken in het *P. berghei* muizenmodel. Tevens werden er replicerende *Δp52+p36 P. falciparum* parasieten gevonden in een kweek van primaire humane levercellen. Deze GAPs zijn klaarblijkelijk niet veilig en we stelden daarom een aantal screening criteria op voor het bepalen van de veiligheid van GAP kandidaten, voorafgaand aan verdere klinische ontwikkeling en studies in mensen. In **Hoofdstuk 5** bestuderen we het fenotype van *Δp52+p36 P. berghei* parasieten die zich in de lever ontwikkelen. Deze parasieten blijken zich op onconventionele wijze te kunnen ontwikkelen tot bloedstadium parasieten. Het parasitophorous vacuole membraan (PVM) schermt de parasiet normaal gesproken af voor herkenning door de levercel en wordt als essentieel beschouwd voor de ontwikkeling van de parasiet. We lieten zien dat *Δp52+p36 P. berghei* parasieten zich zonder het PVM volledig kunnen ontwikkelen in de levercel. Deze bevindingen kunnen implicaties hebben voor de ontwikkeling van een GAP vaccin, aangezien GAPs met een gen deletie betrokken bij de formatie of het onderhouden van het PVM waarschijnlijk onveilig zijn. **Hoofdstuk 6** beschrijft de ontwikkeling en karakterisatie van de Δ*b9* GAP. Deze GAP kan steriele bescherming induceren in muizen. De afgebroken ontwikkeling van de parasiet, vlak na de invasie in de levercel, lijkt samen te hangen met een gecompromitteerde PVM. Een laag aantal *P. berghei Δb9* GAP bleek zich te kunnen ontwikkelen in de afwezigheid van een PVM. We ontwikkelden vervolgens een *P. berghei* Δ*b9*Δ*slarp* GAP, bestaande uit een para-

siet met meerdere gen deleties. Deze meervoudig geattenueerde GAP komt volledig tot stilstand in de lever van muizen en ontwikkelt zich nooit tot het pathogene bloed stadium. Immunisatie van BALB/c en C57BL/6 muizen met *P. berghei* Δ*b9*Δ*slarp* GAP resulteerde in steriele en langdurige bescherming. De ortholoog mutant in *P. falciparum* is reeds gegenereerd en de ontwikkeling van deze GAP in de levercel zal moeten worden bestudeerd. Als de *P. falciparum* Δ*b9*Δ*slarp* GAP inderdaad volledig tot stilstand komt in de levercel, evenals de *P. berghei* GAP, zal het zeer waarschijnlijk de meest veelbelovende GAP vaccinkandidaat vormen.

In **Hoofdstuk 7** beschrijven we de relatie tussen de parasieten lever load als gevolg van sporozoieten immunisatie en de mate van bescherming in muizen. Intraveneuze sporozoieten immunisatie van zowel BALB/c als C57BL/6 muizen resulteerde in een hogere mate van bescherming in vergelijking met intradermale immunisatie. De afname in bescherming na intradermale immunisatie bleek samen te hangen met een relatief laag aantal parasieten dat de lever wist te bereiken. Hoewel hoogstwaarschijnlijk zeer effectief, vormt IV injectie niet de meest preferente immunisatie methode voor grootschalige toepassing in Sub-Sahara Afrika. In **Hoofdstuk 8** bestuderen we derhalve welke variabelen, betrokken bij sporozoiet injectie, de parasieten lever load beïnvloeden. Met behulp van luminescente *Pb*GFP-Luc$_{con}$ en *Py*GFP-Luc$_{con}$ parasieten bepaalden we in muizen welke toedieningsvariabelen (bijvoorbeeld locatie van injectie, injectie volume) de parasieten lever load beïnvloeden. Meervoudige intramusculaire injecties van sporozoieten in kleine volumina resulteerde in de hoogste parasieten lever load en vormt daarmee hoogstwaarschijnlijk de meest optimale route van non-IV sporozoieten immunisatie. Deze data verschaffen een richtlijn voor toekomstige klinische trials, op zoek naar de meest optimale methode van sporozoieten immunisatie en hopelijk voor de ontwikkeling van een sporozoietenvaccin tegen malaria.

List of Publications

Ploemen IH, Croes HJ, van Gemert GJ, Wijers-Rouw M, Hermsen CC, Sauerwein RW. Plasmodium berghei Δp52&p36 Parasites Develop Independent of a Parasitophorous Vacuole Membrane in Huh-7 Liver Cells. *PLoS One* 2012, 7:e50772.

Ploemen IH, Chakravarty S, van Gemert GJ, Annoura T, Khan SM, Janse CJ, Hermsen CC, Hoffman SL, Sauerwein RW. Plasmodium liver load following parenteral sporozoite administration in rodents. *Vaccine in press*

Nganou-Makamdop K*, **Ploemen I***, Behet M, van Gemert GJ, Hermsen C, Roestenberg M,Sauerwein RW. Reduced Plasmodium berghei sporozoite liver load associates with low protective efficacy after intradermal immunization. *Parasite Immunol* 2012, 34:562-569.

Annoura T*, **Ploemen IH***, van Schaijk BC*, Sajid M, Vos MW, van Gemert GJ, Chevalley-Maurel S, Franke-Fayard BM, Hermsen CC, Gego A, et al: Assessing the adequacy of attenuation of genetically modified malaria parasite vaccine candidates. *Vaccine* 2012, 30:2662-2670.

Ploemen I, Behet M, Nganou-Makamdop K, van Gemert GJ, Bijker E, Hermsen C, Sauerwein R. Evaluation of immunity against malaria using luciferase-expressing Plasmodium berghei parasites. *Malar J* 2011, 10:350.

McCall MB*, Ferwerda B*, Hopman J, **Ploemen I**, Maiga B, Daou M, Dolo A, Hermsen CC, Doumbo OK, Bedu-Addo G, van der Meer JW, Troye-Blomberg M, van der Ven AJ, Schumann RR, Sauerwein RW, Mockenhaupt FP, Netea MG. Persistence of full-length caspase-12 and its relation to malaria in West and Central African populations. *Eur Cytokine Netw* 2010, 21:77-83.

McCall MB*, Hopman J*, Daou M, Maiga B, Dara V, **Ploemen I**, Nganou-Makamdop K, Niangaly A, Tolo Y, Arama C, Bousema JT, ban der Meer JW, van der Ven AJ, Troye-Blomberg M, Dolo A, Doumbo OK, Sauerwein RW. Early interferon-gamma response against Plasmodium falciparum correlates with interethnic differences in susceptibility to parasitemia between sympatric Fulani and Dogon in Mali. *J Infect Dis* 2010, 201:142-152.

McCall MB, Roestenberg M, **Ploemen I**, Teirlinck A, Hopman J, de Mast Q, Dolo A, Doumbo OK, Luty A, van der Ven AJ, Hermsen CC, Sauerwein RW. Memory-like IFN-gamma response by NK cells following malaria infection reveals the crucial role of T cells in NK cell activation by P. falciparum. *Eur J Immunol* 2010, 40:3472-3477.

Ploemen IH*, Prudencio M*, Douradinha BG, Ramesar J, Fonager J, van Gemert GJ, Luty AJ, Hermsen CC, Sauerwein RW, Baptista FG, Mota MM, Waters AP, Que I, Lowik CW, Khan SM, Janse CJ, Franke-Fayard BM. Visualisation and quantitative analysis of the rodent malaria liver stage by real time imaging. *PLoS One* 2009, 4:e7881.

van Drongelen J, **Ploemen IH**, Pertijs J, Gooi JH, Sweep FC, Lotgering FK, Spaanderman ME, Smits P: Agingattenuates the vasodilator response to relaxin. *Am J Physiol Heart Circ Physiol* 2011, 300:H1609-1615.

*These authors contributed equally.

Dankwoord - Acknowledgments

Met een ogenschijnlijk gemak (met de nadruk op ogenschijnlijk) is het nu af. Althans….bijna af. Ik begon mijn promotie met het doel een bijdrage te leveren aan de ontwikkeling van een malaria vaccin. Zoals zo veel promovendi raakte ik al snel verknocht aan mijn onderwerp en werd het een echte jacht op de ultieme GAP. Nu, een aantal jaartjes later en wijzer hoop ik dat ik mijn eigen steentje bij heb kunnen dragen.. Time will tell! Het was in ieder geval nooit gelukt zonder de hulp van een groot aantal mensen.

Robert, als eerste wil ik graag jou bedanken. Jij gaf me de kans om aan een fantastisch mooi promotieproject te werken. De outline van het project was simpel 'zorg ervoor dat er over 4 jaar een GAP kandidaat klaarligt'. Daarbinnen was er heel veel mogelijk. Ik wil je enorm bedanken voor het vertrouwen dat je me de afgelopen jaren hebt gegeven, de (soms) noodzakelijke nuances die je in mijn stukken aanbracht en de ruimte die je me gaf me steeds verder te ontwikkelen. Experimenten verzinnen en uitvoeren lukte meestal wel; jij leerde me de reultaten in duidelijke taal te vervatten. Waar het vinden van een goede GAP 4 jaar geleden een grote uitdaging was, lijkt dat nu overgenomen te worden door de route van immunisatie. Graag wil ik ook deze 'hobbel' in de toekomst samen met jou en het team tackelen.

Chris, al heel vroeg in mijn promotie betrok je me bij het werk dat in Leiden wordt uitgevoerd. Samen met **Blandine** gaf je met de *pb*-luc parasieten een kick-start aan mijn promotie. Ik kan niet genoeg benadrukken hoe belangrijk deze parasieten zijn geweest voor mijn boekje. Als de GAP *P. berghei* expert was je via skype altijd beschikbaar voor vragen en overleg. Je had altijd wel even een minuutje. Dank daarvoor! Waar het gebruik van de *pb*-luc parasieten aan de voet stond voor de ene helft van dit boekje, staan de Knock-outs dit voor de andere helft. **Shahid**, **Takeshi, Severine** and **Saj** thanks for all the GAP lines. While the word breakthrough has a whole new connotation in my dictionary I am glad we were able to close the deal in the end.

I would very much like to thank the collaborators from **Sanaria**. It has been a privilege to work in a consortium with such a strong commitment to one goal. **Steve**, thank you for your inspirational 'just do it' mentality**.** I hope that in the future, our roads will cross and I can continue the work with you and your team on the development of a 'sporoject'. **Sumana**, **Peter**, **Eric**, **Kim Lee** and **Judy** (U.S Military Malaria

Vaccine Program) thanks for all the helpful discussions.

Mijn dank gaat ook zeker uit naar **TIPharma**. Dankzij jullie funding heb ik niet alleen mijn promotieonderzoek kunnen uivoeren maar heb ik ook allerlei nuttige cursussen kunnen volgen die me in staat hebben gesteld mijn kennis te verbreden en carrière te ontwikkelen. Het concept van public private partnership werkt zeker!

Geert-jan, ik kan me geen betere compagnon hebben gewenst voor het muggen en muizenwerk. Vijf parasietenlijnen tegelijk opwerken, 'ff' sporozoieten verzamelen voor de immunisatie van 180 muizen, 'ff' samen met de Volvo op en neer naar Leiden om muggen te dissecteren, niets was jou te gek… Bedankt, je inzet was ongekend! **Jolanda**, **Laura**, **Astrid** en **Jacqueline**, ontzettend bedankt voor het vele kweekwerk wat jullie hebben verricht. **Claudia**, **Alex**, **Iris**, **Danielle**, **Michael**, **Marieke**, **Kitty**, **Bianca** en **Debby**, bedankt voor alle biotechnische ondersteuning. Zonder jullie hulp was dit nooit gelukt.

Rob, bedankt voor de goede start. Als laboudste wist je me altijd van goede raad te voorzien. Ook wist je me, waar de expertise binnen het lab begrensd was, altijd wel met iemand in contact te brengen die me verder kon helpen. Daarnaast heb ik dankzij jou nooit een horloge hoeven dragen: jij vertelde me elke morgen hoe laat het was. Bedankt! **Miguel** and **Maria**, thanks a lot for teaching me the gliding and liver stage assays. I really enjoyed the (short) stay in Lisbon. **Huib** en **Mietske**, bedankt voor alle hulp bij de electronenmicroscopie. Een speld in een hooiberg was wellicht makkelijker te vinden geweest. **Conor** and **Anne**, thank you for your expertise and insights in the use of microneedles, let's hope the HM do the trick!

Een van de leukste dingen van het promoveren is zeker wel het begeleiden van studenten. **Marije**, je bent tijdens jou stage enorm gegroeid en het is dan ook zeer terecht dat je de stageprijs biomedische wetenschappen 2012 hebt mogen ontvangen. Ontzettend bedankt voor je inzet en je enthousiasme. Zet hem op en dan komen de mooie resultaten vanzelf! **Moniek**, je hebt een sterk verhaal afgeleverd dat zeker heeft bijgedragen aan de totstandkoming van dit boekje, bedankt.

Ben, we hebben hard gelachen! Het was tof om al die jaren een U-tje met je te delen. Die glijbaan naar het dak is er helaas nooit van gekomen. Een tip… zoals reeds aangetoond bij het kerststallenmailtje, indien er sprake is van twijfel: SEND!
Martijn, de man met de gouden handjes. Het *P. berghei* team zette hem voor, en jij

speelde hem (samen met Ben) de andere helft van het veld over. Bovenal een goede mtb-maat. We blijven zeker biken! **Amrish**, ineens zat je daar aan mijn labtafel. Nu viel het pas echt op hoeveel praktisch werk ik nog deed… thanks mate! ik ben aan het sparen voor Suriname en ik verheug me op doldwaze whiskyavondjes. Binnenkort gaan we op jouw promotie toosten!

Matthew, jij stond aan de wieg van mijn malaria avontuur. Een onvergetelijke tijd in Mali samen met jou en **Joost** zorgde er mede voor dat ik na een omzwerving terug ben gekeerd naar de afdeling. **Teun**, eerder nog wakkerde het blok outbreak epidemiology de al aanwezige voorliefde voor infectieziektes verder aan. Bedankt voor je hulp bij de moeilijke statistiek, je goede whisky en je 'goede' grappen. **Meta**, **Else** en **Guido**, bedankt voor de klinische input bij de zoektocht naar de route van inoculatie. Op naar een immunisatie die echt goed werkt! **Maurits**, als je door de microneedles het bos niet meer ziet, bedenk dan… als je maar hard genoeg drukt raak je vanzelf een bloedvat. **Annemieke**, bedankt voor alle carrièretips! **Anja**, zsonder jou souden mijn teksten er zo uit heppen gezien… bedankt! **Anne**, bijna gelijk gestart, bijna gelijk klaar, heel veel succes met de laatste lootjes! Dat fietje hou je van me tegoed! **Maarten**, voor jou duurt het nog ff, als je straks afleiding zoekt van het schrijven moet je gewoon weer mee gaan fietsen. **Mayke**, heel veel geluk met de kleine en... Tot borrels! **Marga**, **Will, Wouter**, **Theo**, **Pieter, Adrian, Karina, Krystelle, Rianne**, **Koen**, **Martijn**, **Helmi, Sanna**, **Kjerstin** and **Stone** bedankt voor alle gezelligheid bij de koffie tafel, bieravondjes, pokeravondjes en labuitjes.

Hans, samen rotsen beklimmen, samen thuiswerken, biertjes drinken, gezellige etentjes. Binnenkort weer in dezelfde stad! Ik ben trots de 27e April achter jou en Mirte te mogen staan. **Sten,** nog ff doorbijten en dan ben je er ook… wie had dat ooit gedacht?! Libië schijnt weer veilig te zijn… what do thou say? **Koen,** als een van de weinige van groepje wit ging jij ook in Nijmegen promoveren. Bedankt voor je vriendschap, onvergetelijke tijgermomenten en OMB3! Als ik in de States ben kom ik zeker langs! Een promotie zonder vakantie is overigens als spaghetti zonder saus…. erg saai. Gelukkig waren er de snowboard vakanties om het hoofd ff leeg te boarden: **groepje WIT...** Bedankt! Maar ook als er geen sneeuw lag was er altijd wel een manier om wat kilometers te maken: **Bram**, **Jasper**, **Joep & Stijn** bedankt voor onvergetelijke wielren/mtb weekendjes; ik zeg een barbecue, een steengril, een zwavelhuisje een midgetgolfbaan en een paar flessen Erdinger...**Pap** en **mam**, **Juud** en **Alex** bedankt voor alles. Binnenkort kunnen jullie ook bij ons komen logeren!

Lieve **Pien**, jou steun en begrip zijn onbegrensd. Je bent een held en mijn weirdo! Nu, na twee jaar dan eindelijk saampjes het avontuur tegemoet, een nieuwe stad, een nieuwe plek, heel veel chille weekendjes met het busje aan kabbelende beekjes en nog vele memory boeken die we samen gaan vullen. Je maakt dat ik een beter mens ben en ik hou van je!

Ivo

Curriculum Vitae

Ivo Henry Johannes Ploemen, de schrijver van dit proefschrift, werd op 2 februari 1984 geboren te Heerlen. In 2002 behaalde hij zijn gymnasiumdiploma aan het Trevianum in Sittard. Aansluitend begon hij aan de studie biomedische wetenschappen in Nijmegen waar hij in 2005 zijn bachelordiploma behaalde. Voorts startte hij in 2004 met het 2-jarige extra-curriculaire Honours Programma van de Radboud Universiteit, waarbij hij zich o.a. verdiepte in de elementaire deeltjesfysica en het evolutionaire denken. In 2005 begon hij aan de masteropleiding biomedische wetenschappen waarbij hij de Pathobiologie als hoofdrichting verkoos. Tijdens deze 2-jarige opleiding doorliep hij 2 stages. In 2006, hetzelfde jaar waarin hij zijn Honoursdegree behaalde, voerde hij zijn hoofdonderzoek uit bij de afdeling Medische Microbiologie/Parasitologie aan het UMC St Radboud Nijmegen onder leiding van dr. Matthew McCall. Deze stage betrof onderzoek naar de relatie tussen NK cel activiteit en susceptibiliteit tegen *P. falciparum* binnen twee etnische stammen en werd gedeeltelijk uitgevoerd in Mali. Een tweede stage naar het effect van relaxine resistentie in een pre-klinisch model werd uitgevoerd binnen de afdeling Toxicologie aan het UMC St. Radboud Nijmegen.

Na het behalen van zijn Master of Science in 2007 startte hij met een studie filosofie waarvoor hij een beurs van de Radboudstichting (thans Stichting Thomas Moore) verkreeg. In het kader van deze studie schreef hij een scriptie getiteld: 'Het verbeteren van de gezondheidssituatie in de derde wereld; een ethische beschouwing.' Vervolgens keerde hij in mei 2008 als promovendus terug naar de afdeling Medische Microbiologie van het UMC St Radboud Nijmegen, waar hij onder leiding van Prof. dr. Robert Sauerwein werkte aan de zoektocht naar een genetisch geattenueerd malariavaccin. Binnen dit promotietraject, dat gefinancierd werd door Top Institute Pharma (TI Pharma), werkte hij in een consortium zeer nauw samen met Sanaria Inc. uit Rockville, Maryland (Verenigde Staten van Amerika) onder leiding van Dr. Stephen Hoffman en de Leiden Malaria Research Group van het LUMC onder leiding van Dr. Chris Janse. De voornaamste resultaten van dit traject zijn vervat in dit proefschrift. Mede op basis van de in dit traject behaalde resultaten werd – wederom door TI Pharma - een nieuwe subsidie toegekend voor een vervolgtraject, waarbij hij van mei tot november 2012 betrokken was bij de uitvoering en de coördinatie van translationeel vaccinonderzoek. Vanaf januari 2013 is hij als scientist vaccine delivery werkzaam bij Intravacc, voorheen onderdeel van het Rijksinstituut voor Voorlichting en Milieu (het RIVM) te Bilthoven.

Hij hoopt in de toekomst middels innovatief vaccinonderzoek bij te kunnen dragen aan het verlichten van de ziektelast in de derde wereld.